STUDIES ON CELLULAR RESPONSES TO DNA DAMAGE IN HUMAN CELLS EXPOSED TO LOW DOSE IONIZING RADIATION

By

Vinay Jain

LIFE 01201004001

BHABHA ATOMIC RESEARCH CENTRE

A thesis submitted to the

Board of Studies in Life Sciences

In partial fulfillment of requirements for the

Degree of

DOCTOR OF PHILOSOPHY

Of

HOMI BHABHA NATIONAL INSTITUTE

December 2015

Homi Bhabha National Institute[1]

Recommendations of the Viva Voce Committee

As members of the Viva Voce Committee, we certify that we have read the dissertation prepared by **Mr.Vinay Jain** entitled **"Studies on cellular responses to DNA damage in human cells exposed to low dose ionizing radiation"** and recommend that it may be accepted as fulfilling the thesis requirement for the award of Degree of Doctor of Philosophy.

Chairman - Dr. R. Sarin — **Date:** 6.04.16

Guide / Convener - Dr. Birajalaxmi Das — **Date:** 06/04/2016

Co-guide - — **Date:**

Examiner – Prof. Mayurika Lahiri — **Date:** 6/4/16

Member 1- Dr. S. Chattopadhyay — **Date:** 6/4/16

Member 2- Dr. H.S. Misra — **Date:** 6/4/16

Final approval and acceptance of this thesis is contingent upon the candidate's submission of the final copies of the thesis to HBNI.

I/We hereby certify that I/we have read this thesis prepared under my/our direction and recommend that it may be accepted as fulfilling the thesis requirement.

Date: 06/04/2016

Place: BARC, Trombay

Co-guide (if applicable)

Guide 06/04/2016

[1] This page is to be included only for final submission after successful completion of viva voce.

STATEMENT BY AUTHOR

This dissertation has been submitted in partial fulfillment of requirements for an advanced degree at Homi Bhabha National Institute (HBNI) and is deposited in the Library to be made available to borrowers under rules of the HBNI.

Brief quotations from this dissertation are allowable without special permission, provided that accurate acknowledgement of source is made. Requests for permission for extended quotation from or reproduction of this manuscript in whole or in part may be granted by the Competent Authority of HBNI when in his or her judgment the proposed use of the material is in the interests of scholarship. In all other instances, however, permission must be obtained from the author.

Vinay Jain

DECLARATION

I, hereby declare that the investigation presented in the thesis has been carried out by me. The work is original and has not been submitted earlier as a whole or in part for a degree / diploma at this or any other Institution / University.

Vinay Jain

List of Publications arising from the thesis

Journal

1. Lack of increased DNA double strand breaks in peripheral blood mononuclear cells of individuals from high level natural radiation areas of Kerala coast in India (2016). **Vinay Jain**, P.R.Vivek Kumar, P.K.M. Koya, G. Jaikrishan and Birajalaxmi Das. Mutation Research, Fundamental and Molecular Mechanisms of Mutagenesis. http://dx.doi.org/10.1016/j.mrfmmm.2016.03.002 (in press).
2. Radiation induced conformational changes in chromatin structure in resting human peripheral blood mononuclear cells (2014). **Vinay Jain**, P.A Hassan and Birajalaxmi Das. International Journal of Radiation Biology, 90 (12): 1143-1151.
3. Transcription profile of DNA damage response genes at G_0 lymphocytes exposed to gamma radiation (2012). Divyalakshmi Saini, Shridevi Shelke, A. Mani Vannan, Sneh Toprani, **Vinay Jain**, Birajalaxmi Das, M.Seshadri. Molecular and Cellular Biochemistry, 364: 271-281.
4. Transcriptional expression of H2B, CTP synthase & PLK3 genes in whole blood exposed to ^{60}Co gamma radiation (2011). **Vinay Jain**, Birajalaxmi Das and M. Seshadri. International Journal of Low Radiation, 8 (1): 55-65.
5. Efficient repair of DNA double strand breaks in individuals from high level natural radiation areas of Kerala coast, south-west India. **Vinay Jain**, Divyalakshmi Saini, P. R. Vivek Kumar, G. Jaikrishan and Birajalaxmi Das. Scientific Reports (under revision).

Conferences

1. Role of chromatin structure in the detection and repair of double strand breaks induced by low dose radiation. **Vinay Jain**, Birajalaxmi Das; 38th Annual Conference of Environmental Mutagen Society of India and National Conference on ―Current Perspectives on Environmental Mutagenesis and Human Health; Mumbai 28-30 January, 2013, pp-85.
2. Transcriptome profile of human adults living in high background radiation areas of Kerala coast, south west India. **Vinay Jain**, Birajalaxmi Das, M.Seshadri; International Conference on Genes, Genetics & Genomics: Today & Tomorrow- Human Concerns and Annual Conference of The Indian Society of Human Genetics, Chandigarh; March 03-05, 2012, pp 143.
3. Conformational Changes in the Chromatin Structure of Human Peripheral Blood Mononuclear Cells Exposed to Low Dose Radiation; **Vinay Jain**, P.A Hassan, Birajalaxmi Das and M.Seshadri; 7th International Conference on High Levels of Natural Radiation and Radon Areas. (7HLNRRA), Navi Mumbai, Nov 24-26, 2010. pp-151-152. ***(Adjudged as the best poster award)***

Others

1. Conformational changes in the chromatin structure of human peripheral blood mononuclear cells exposed to low dose radiation (2011). **Vinay Jain**, P.A Hassan, Birajalaxmi Das and M.Seshadri. BARC Newsletter Founder‘s Day Special Issue, 368-370.

Vinay Jain

Dedicated to
my
Parents

Acknowledgements

Every ending leads to a fresh beginning. This holds true with this journey too. This thesis has been a great journey which was full of new learning and experiences. Many people have contributed either directly or indirectly to bring this thesis to this shape. First and foremost, I thank my parents and sisters for motivating me throughout my life. No words would be enough to express my gratitude towards my mentor and guide *Dr. Birajalaxmi Das* for her unparallel support, encouragement and guidance at every step of this thesis. I thank *Dr. M. Seshadri* (Former Head, RB&HSD) for his encouragement and guidance during the initial phase of the work. I express my heartfelt gratitude towards *Dr. S. Chattopadhyay* (Associate Director 'B', Bioscience Group) for his constant support and encouragement.

It has been a privilege to be guided by distinguished doctoral committee members during the thesis. I thank *Dr. R. Sarin, Dr. S. Chattopadhyay, Dr. H. S. Misra, Dr. J. R. Bandekar, Dr. K. B. Sainis, Dr. M. Seshadri* and *Dr. Rita Mulherkar* for their critical views and suggestions during the doctoral committee meetings. I also thank *Dr. S.K Apte* and *Dr. Hema Rajaram* for their timely guidance in HBNI related matters.

This thesis would not have been possible without the unconditional support of all my colleagues of LLRRS, Mumbai and LLRRL, Kollam. They have been a great strength at every step. I also thank *Dr. Bhavani Shankar, Dr. Shilpa Sawant, Dr. P.A Hassan* and *Dr. Sandhya.P* for their help and inputs during different experiments. I would like to thank *Ms.J. Prabhu* and *Mr. Sangram* for helping in collection of blood samples. I also thank *Mr. Prayag Amin, Mr. Manjoor Ali* and *Ms. Vasumathy* for their technical help.

Nothing is possible without the unrelenting support from family and friends. I thank my biggest strengths, my wife (*Shmilona*) and daughter (*Anshika*) for bearing with long working

hours and my absences on holidays. I extend my gratitude to all my teachers and friends who have directly or indirectly influenced me to be a better person and achieve this milestone.

Last but not the least, I extend my biggest gratitude to all the volunteers who participated in the studies and gave their precious blood samples.

Vinay Jain

CONTENTS

LIST OF TABLES

CHAPTER DETAILS

List of Abbreviations

µg/ml	Microgram per millilitre	**ATRIP**	ATM And Rad3-Related-Interacting Protein
µR/ h	Microroentgen per hour	**ATXN1**	Ataxin 1
53BP1	Protein p53 binding protein1	**BARC**	Bhabha Atomic Research Centre
^{60}Co	Cobalt-60	**BBS10**	Bardet-Biedl syndrome 10
AFM	Atomic force microscopy	**BCAT1**	Branched chain amino-acid transaminase 1
AKT2	v-akt murine thymoma viral oncogene homolog 2	**BCL10**	B-cell CLL/lymphoma 10
ANOVA	Analysis of variance	**BCL6**	B-cell CLL/lymphoma 6
AP	Apurinic/Apyrimidinic	**BEIR**	Biological Effects Of Ionizing Radiation
AP1	Activating Protein 1	**BER**	Base excision repair
APAF1	Apoptotic peptidase activating factor 1	**BET1**	Blocked early in transport 1 homolog (*S. cerevisiae*)-like
APE1	Apurinic/apyrimidinic endonuclease 1	**BP**	Base pair
APEX	Apurinic-Apyrimidinic Endonuclease	**BRCA1**	Breast cancer 1
APEX2	Apurinic/Apyrimidinic endonuclease 2	**BRCA2**	Breast cancer 2
aRNA	Amplified RNA	**BTG1**	B-cell translocation gene 1, anti-proliferative
ARRB1	Arrestin, beta 1	**CCR2**	Chemokine receptor 2
ATF2	Activating transcription factor 2	**CD38**	CD38 molecule
ATF3	Activating transcription factor 3	**CDC42**	Cell division cycle 42
ATM	Ataxia Telangiectasia Mutated	**cDNA**	Complementary DNA
ATR	Ataxia telangiectasia and Rad3 related	**cGy**	Centigray

CHK1	Checkpoint Kinase 1	**DNA-PKcs**	DNA Dependent Protein Kinase Catalytic Subunit
CHK2	Checkpoint Kinase 2	**DS**	Down syndrome
CO_2	Carbon dioxide	**DSB**	Double strand break
CREB	cAMP responsive element binding protein	**DUSP1**	Dual specificity phosphatase 1
CREBZF	CREB/ATF bZIP transcription factor	**DUSP10**	Dual specificity phosphatase 10
CSA	Cockayne syndrome A	**DUSP5**	Dual specificity phosphatase 5
CSB	Cockayne syndrome B	**EDTA**	Ethylenediamine tetra acetic acid
CSNK1A1	Casein kinase 1, alpha 1	**EIF1**	Eukaryotic translation initiation factor 1
CSRNP1	Cysteine-serine-rich nuclear protein 1	**EIF4G3**	Eukaryotic translation initiation factor 4 gamma, 3
CT	Computed tomography	**ERCC1**	Excision repair cross-complementing group 1
CXCR1	Chemokine (C-X-C motif) receptor 1	**EXO1**	Exonuclease 1
DAPI	4',6-diamidino-2-phenylindole	**FANCE**	Fanconi anemia, complementation group E
DCLRE1C	DNA cross-link repair 1C	**FANCF**	Fanconi anemia, complementation group F
DDB2	Damage-specific DNA binding protein 2	**FBS**	Fetal bovine serum
DDIT3	DNA-damage-inducible transcript 3	**FDR**	False discovery rate
DDR	DNA Damage Response	**FEN1**	Flap Endonuclease
DHFRL1	Dihydrofolate reductase-like 1	**FOS**	FBJ murine osteosarcoma viral oncogene homolog
DLS	Dynamic Light Scattering	**FOXO3**	Forkhead box O3
DNA	Deoxyribonucleic acid	**FUSIP1**	Serine/arginine-rich splicing factor 10 (SRSF10)
DNA-PK	Deoxyribonucleic Acid-Protein Kinase	**GADD45A**	Growth arrest and DNA-damage-inducible, alpha

GADD45B	Growth arrest and DNA-damage-inducible, beta	**HIPK1**	Homeodomain interacting protein kinase 1
GAPDH	Glyceraldehyde-3-phosphate dehydrogenase	**HLA-DRB4**	Major histocompatibility complex, class II, DR beta 1
GCOS	GeneChip operating software	**HLNRA**	High level natural radiation area
GFRAL	GDNF family receptor alpha like	**HLTF**	Helicase-like transcription factor
GG-NER	Global genome- Nucleotide excision repair	**HNRNPM**	Heterogeneous nuclear ribonucleoprotein M
GIMAP4	GTPase, IMAP family member 4	**HP1BP3**	Heterochromatin protein 1, binding protein 3
GIMAP8	GTPase, IMAP family member 8	**HR**	Homologous recombination repair
GM	Geiger Muller	**ICRP**	International commission on radiological protection
GNAS	GNAS complex locus	**IDLs**	Insertion/deletion loops
GO	Gene ontology	**IGHG**	Immunoglobulin heavy constant gamma 1
GTF2E1	General transcription factor IIE, polypeptide 1	**IL1A**	Interleukin 1, alpha
GTF2H1	General transcription factor II H, polypeptide 1	**IL8**	Interleukin 8
Gy	Gray	**ING3**	Inhibitor of growth family, member 3
H2AX	H2A histone family, member X	**IR**	Ionizing radiation
H3F3B	H3 histone, family 3B	**IRIF**	Ionizing radiation induced foci
HDG	High dose group	**IVT**	In vitro transcription
HEY1	Hairy/enhancer-of-split related with YRPW motif 1	**JUN**	jun oncogene
HG	Human genome	**JUND**	Jun D proto-oncogene
HIST1H1E	Histone cluster 1, H1e	**KCl**	Potassium chloride
HIST1H2B	Histone cluster 1, H2b	**KDM6B**	Lysine (K)-specific demethylase 6B

KEGG	Kyoto encyclopedia of genes and genomes	**MRE11**	Meiotic recombination 11
KIR3DS1	Killer cell immunoglobulin-like receptor, three domains, short cytoplasmic tail, 1	**MRN**	MRE 11-RAD50-NBS1
KLF6	Kruppel-like factor 6	**mRNA**	Messenger RNA
LDG	Low dose group	**MSH2**	MutS homolog 2
LDIR	Low dose ionizing radiation	**MSH3**	MutS homolog 3
LET	Linear energy transfer	**MSH6**	MutS homolog 6
LIG4	Ligase IV	**mSv**	Millisievert
LNT	Linear no threshold	**mSv/y**	Millisievert per year
MAPK	Mitogen-activated protein kinase	**MXD1**	MAX dimerization protein 1
MDC1	Mediator of DNA damage checkpoint 1	**MN**	Micronuclei
MDM2	Mouse double minute 2 homolog	**NAMPT**	Nicotinamide phosphoribosyltransferase
METTL13	Methyltransferase like 13	**NBS1**	Nijmegen Breakage Syndrome 1
MgCl2	Magnesium chloride	**NEIL1**	Nei endonuclease VIII-like 1
mGy	Milligray	**NER**	Nucleotide Excision Repair
mGy/y	Milligray per year	**NF-kB**	Nuclear factor of kappa light B-cells
MLH1	MutL homolog 1	**NFKB2**	Nuclear factor of kappa light B-cells 2
MLH3	MutL homolog 3	**NHEJ**	Non homologous end joining
MMR	Mis-match Repair	**NLNRA**	Normal level natural radiation area
MNase	Micrococcal nuclease	**NLRC4**	NLR family, CARD domain containing 4
MPG	N-methylpurine-DNA glycosylase	**nm**	Nanometre

NR4A2	Nuclear receptor subfamily 4, group A, member 2	**PRKDC**	Protein kinase, DNA-activated, catalytic peptide
NT5E	5'-nucleotidase, ecto (CD73)	**POLB**	Polymerase (DNA directed), beta
OGG1	8-oxoguanine DNA glycosylase	**QC**	Quality check
P53	protein p53	**RAD18**	RAD18 homolog
PAPB2	Polyadenylate-binding protein 2	**RAD21**	RAD21 homolog (*S. pombe*)
PAPD4	PAP associated domain containing 4	**RAD23B**	RAD23 homolog B
PBMCs	Peripheral blood mononuclear cells	**RAD50**	RAD50 homolog (*S. cerevisiae*)
PBS	Phosphate buffered saline	**RAD51**	RAD51 recombinase.
PCNA	Proliferating cell nuclear antigen	**RAD52**	RAD52 homolog (*S. cerevisiae*)
PDK4	Pyruvate dehydrogenase kinase, isozyme 4	**RAD54**	RAD54 homolog (*S. cerevisiae*)
PET	Positron emission tomography	**REV3L**	REV3-like, catalytic subunit of DNA polymerase zeta
PIKK	Phosphatidylinositol 3-Kinase-Related Kinase	**RIN**	RNA integrity number
PLK3	Polo-like kinase 3	**RMA**	Robust multichip analysis
PMAIP1	Phorbol-12-myristate-13-acetate-induced protein 1	**RMI1**	RMI1, RecQ mediated genome instability 1,
PMS1	Postmeiotic segregation 1	**RNA**	Ribonucleic acid
PMS2	Postmeiotic segregation 2	**ROS**	Reactive oxygen species
PMSF	Phenylmethylsulfonyl fluoride	**RPMI**	Roswell Park Memorial Institute
POLH	Polymerase (DNA directed), eta	**RPA**	Replication Protein A
PPIF	Peptidylprolyl isomerase F	**rpm**	Revolution per minute
PPP1R15A	Protein phosphatase 1, regulatory subunit 15A	**rRNA**	Ribosomal RNA

RT q-PCR	Real time quantitative polymerase chain reaction	**TNFα**	Tumor necrosis factor, alpha
S.D	Standard deviation	**TRAF4**	TNF receptor-associated factor 4
SAR1B	SAR1 homolog B	**TSC22D2**	TSC22 domain family, member 2
SCN1A	Sodium channel, voltage-gated, type I, alpha subunit	**THAP2**	THAP domain with apoptosis protein 2
SEM	Scanning electron microscopy	**UBE2B**	Ubiquitin-conjugating enzyme E2B
SEM	Standard error of mean	**UBE2T**	Ubiquitin-conjugating enzyme E2T
SETDB2	SET domain, bifurcated 2	**UNG**	Uracil DNA glycosylase
SFRS3	Splicing factor, arginine/serine-rich 3	**UNSCEAR**	United Nations Scientific Committee on the Effects of Atomic Radiation
SFRS5	Splicing factor, arginine/serine-rich 5	**UPL**	Universal probe library
SLC2A3	Solute carrier family 2, member 3	**UV**	Ultra violet
SNRPA1	small nuclear ribo-nucleoprotein peptide A'	**XPB**	Xeroderma pigmentosum, complementation group B
SP1	Specificity Protein 1	**XPC**	Xeroderma pigmentosum, complementation group C
SSB	Single Strand Break	**XPD**	Xeroderma pigmentosum, complementation group D
ssDNA	Deoxyribonucleic Acid-Protein Kinase	**XPF**	Xeroderma pigmentosum, complementation group F
Sv	Sievert	**XPG**	Xeroderma pigmentosum, complementation group G
TC-NER	Transcription coupled-Nucleotide Excision Repair	**XRCC4**	X-ray repair complementing defective repair in Chinese hamster cells 4
TF	Transcription factor	**XRCC5 (KU80)**	X-ray repair complementing defective repair in Chinese hamster cells 5
TNFRSF10B	Tumor necrosis factor receptor superfamily, 10b	**XRCC6 (KU70)**	X-ray repair complementing defective repair in Chinese hamster cells 6

ZBTB1	Zinc finger and BTB domain containing 1	**α -particle**	Alpha- particle
ZBTB24	Zinc finger and BTB domain containing 24	**β-actin**	Beta actin
ZNF167	Zinc finger protein 167	**γ - ray**	Gamma-ray

Synopsis

Homi Bhabha National Institute

SYNOPSIS OF Ph. D. THESIS

1. **Name of the Student:** Vinay Jain
2. **Name of the Constituent Institution:** RB&HSD, BARC
3. **Enrolment No. :** LIFE01201004001/ January 1, 2010
4. **Title of the Thesis**: Studies on cellular responses to DNA damage in human cells exposed to low dose ionizing radiation.
5. **Board of Studies:** Life Sciences

SYNOPSIS (Limited to 10 pages in double spacing)

Human beings are continuously exposed to low levels of ionizing radiation (IR) through various man-made and natural sources. Natural radiation exposures are mainly from terrestrial and cosmic sources whereas man-made low level exposure varies from medical exposures (diagnostic and therapeutic) to accidental exposures such as Chernobyl and Fukushima Daiichi nuclear disasters. IR induces a variety of isolated and clustered DNA damages such as base damages, single strand breaks (SSBs) and double strand breaks (DSBs). DSBs are most deleterious and if remain unrepaired or misrepaired may lead to consequences like lethal mutations, genome instability and carcinogenesis. However, cells possess efficient surveillance systems, termed as the DNA damage response (DDR). DDR is a complex phenomenon, which involves all major cellular activities such as damage recognition, DNA repair, cell cycle progression, transcriptional changes, and chromatin modification.

Biological effects of high doses of IR in humans are well documented. However, data at low dose and low dose rate exposures are inconsistent and inconclusive. The current paradigm of radiation protection supports the linear no threshold (LNT) hypothesis, although it lacks scientific evidence of experimental data (1). The data for low dose radiation exposure has been extrapolated from high acute exposures. Efforts have been made worldwide to generate radio-biological data at low dose exposures in human cells, tissues, organs and organisms. Recent studies have shown that biological effect of low and high dose exposures are quantitatively and qualitatively different especially at the level of DNA damage and gene expression (2-4). Biological and health effects at low dose exposures below 100 mSv have important implications in radiation protection science. High level natural radiation areas (HLNRA) provide unique opportunity to study the biological and health effects of low dose/dose rate radiation directly on humans. The HLNRA of Kerala coast is a 55 km long and 0.5 km wide strip extending from Neendakara in south to Purakkadu in north. Due to non-uniform distribution of monazite in the beach sand, a great deal of variation is observed at the level of background radiation, which varies from <1.0 mGy to 45 mGy/y. Areas with a background dose ≥ 1.5 mGy/y are considered as HLNRA and ≤ 1.5 mGy/y are considered as normal level natural radiation area (NLNRA). The human population inhabiting this area has been investigated using various biological end points such as chromosome aberrations, micronuclei frequency, DNA strand breaks and telomere length. None of the above parameters showed significant difference between NLNRA and HLNRA population. Epidemiological data such as incidence of cancer and congenital malformations did not show any statistical difference at the level of phenotype (5-9). Further new high throughput techniques might throw some new insights to understand the biological effect of low dose and low dose IR.

The rationale of the present thesis is to understand cellular and molecular effects of low dose radiation, which might provide a better understanding of the underlying biological processes occurring in human cells exposed to low dose radiation.

Objectives of the thesis: The aim is to understand the molecular basis of the DNA damage response in human cells on exposure to low dose IRs. The objectives are:

1. To study DNA damage and repair using gamma-H2AX as a biomarker
2. Transcriptome analysis of human population residing in normal and high level natural radiation areas:
    - To find out the differentially expressed genes (up/down regulated), if any.
    - Bioinformatic analysis to understand the molecular networks of differentially expressed genes and their involvement in various pathways.
    - To carry out validation of selected differentially expressed genes using real time q-PCR.
3. Evaluation of the changes in chromatin structure/conformation on exposure to low dose radiation.

Outline of the Thesis: The work embodied in this thesis is divided into five chapters:

1) Introduction 2) Materials and Methods 3) Results 4) Discussion 5) Summary and Conclusions.

1. Introduction:

IR challenges the integrity of the genome by causing several types of lesions in DNA, of which DSBs are most deleterious. Cells possess inherent surveillance systems which monitor and maintain the integrity of genome and termed as the DNA-damage response (DDR). DDR is a complex phenomenon, which involves all major cellular activities such as damage recognition, cell cycle progression, transcriptional changes, DNA repair, apoptosis and chromatin

modification. Alteration in the global pattern of gene expression is an important aspect of cellular response which plays an essential role in orchestrating a variety of cellular events including growth arrest, apoptosis and DNA repair. Along with transcriptional changes cells respond to radiation stress by activating and modifying various regulatory proteins which in turn leads to changes in chromatin structure. Post translational modification of histone proteins might be playing a crucial role in radiation induced damage recognition as well as recruitment of repair proteins for efficient DNA repair. Phosphorylated H2AX or gamma-H2AX is one of the important biomarker to study radiation exposure in terms of double strand break detection. Studies have shown that gene expression profile is different in high dose and low dose exposure. Although, a lot of studies deal with the effect of acute doses of radiation in human cells, limited data is available at chronic radiation exposure. High Level Natural Radiation Areas (HLNRA) offer unique opportunities to study DNA damage and its cellular responses at chronic low dose exposures on human population.

2. Materials and Methods:

In the present study, venous blood samples from random and healthy male individuals belonging to Kerala coast (NLNRA and HLNRA) and Mumbai were collected in EDTA vacutainers with written informed consent approved by Medical ethic committee, BARC. PBMCs were separated and divided into different aliquots for each study. For acute dose studies, PBMCs were irradiated with gamma radiation using cobalt-60 source at room temperature. DNA damage quantitation study using gamma- H2AX was carried out using two approaches: Basal frequency of DSBs were measured using fluorescence microscopy and induced DSBs and their repair kinetics was studied using flow cytometry. Gene expression study was carried out by two approaches: 1) Transcriptome study was carried out using Human HG U133 plus 2 microarray chip (Affymetrix,

USA). 2) Validation of microarray data and transcriptional changes at acute doses was carried out using hydrolysis probe based quantitative real time PCR (RT q-PCR). Chromatin conformational changes at acute low doses were studied using Dynamic Light Scattering (DLS). ***Statistical analysis*:** Statistical analysis was done using SPSS software. Student t-test, ANOVA (Analysis of Variance) and regression analysis were used for all the experiments. The level of significance was set at $p \leq 0.05$ for all statistical analysis. The materials and methods section will be discussed in detail in the thesis.

3. Results:

The results are discussed under the three headings. These include: DNA damage and repair using gamma-H2AX as a biomarker, gene expression studies at both acute as well as chronic exposure and radiation induced chromatin changes at acute doses.

3.1 DNA damage and repair kinetics study using gamma H2AX biomarker:

3.1.1 Evaluation of basal level frequency of DNA DSBs in NLNRA and HLNRA individuals: The basal level frequency of DNA DSBs was estimated among 91 individuals from NLNRA (≤ 1.5 mGy/y, N=30) and two dose groups of HLNRA {Low dose group, LDG (1.51-5.0 mGy/y, N=20) and High dose group, HDG (>5.0 mGy/y, N=41)}. The mean frequency of gamma-H2AX foci in NLNRA, LDG and HDG was observed to be 0.095 ± 0.009, 0.096 ± 0.008 and 0.078 ± 0.004 per cell respectively. A marginal reduction in frequency of gamma H2AX foci, though not significant (P= 0.1) was observed in the HDG individuals as compared to the LDG and NLNRA individuals.

3.1.2 Induced damage in HLNRA and NLNRA individuals: Induced damage in terms of gamma H2AX positive cells (DSBs) was studied in 78 individuals {NLNRA, N=23 and HLNRA (LDG, N=21 and HDG, N=34)}. Our results revealed a decreasing trend in the mean gamma-

H2AX positive cells at 1.0 Gy and 2.0 Gy in LDG and HDG individuals as compared to NLNRA. However, at 0.25 Gy, a statistically significant reduction ($p \leq 0.05$) of DSBs was observed in HDG individuals as compared to LDG and NLNRA individuals.

3.1.3 Repair Kinetics of DSBs in HLNRA and NLNRA individuals: Repair kinetics of DSBs was studied in 30 individuals {NLNRA, N=8 and HLNRA (LDG, N=7 and HDG, N=15)} at different post irradiation time points (0.5 to 24 h) at low (0.25 Gy) and high dose (2.0 Gy) exposures. Repair kinetics of DSBs followed a biphasic curve consisting of a rapid phase of foci formation for which peak was obtained at 2.0 h followed by an exponential phase of DSB repair in terms of decrease in gamma H2AX intensity. Fast and efficient repair of DSBs were observed at 4 to 6 h post irradiation time points. The percentage of DSB repaired at 6 h in NLNRA, LDG, and HDG were 51.3, 51.0, 59.1 and 44.9, 59.2, 62.9 at 0.25 Gy and 2.0 Gy respectively. The residual damage at the end of 24 h was approximately 15-20%. .

3.2 Gene expression studies at chronic and acute exposure:

3.2.1 Global gene expression profile (Transcriptome analysis) in HLNRA and NLNRA individuals using microarray: Transcriptome analysis was carried out on 36 individuals from NLNRA and HLNRA. The individuals belonged to NLNRA ($\leq$ 1.5 mGy/y, Group I) and three HLNRA groups {(1.51-5.0 mGy/y, Group II), (5.1-15 mGy/y, Group III) and (> 15.0 mGy/y, Group IV)}. A total of 6 (3 up and 3 down), 24 (15 up and 9 down), 97 (72 up and 25 down) genes were differentially expressed at a threshold of 2 fold ($p \leq 0.05$) in Group II, III and IV respectively. At a threshold of 1.3 fold ($p \leq 0.05$), 138 (39 up and 99 down), 1361 (611 up and 750 down), 2427 (889 up and 1538 down) were differentially expressed in Group II, III and IV respectively. Among these 82 genes (13 up and 69 down) were observed to be common in all

HLNRA groups. The above results indicated background dose dependent increase in number of differentially expressed genes.

3.2.2 Gene ontology analysis of differentially expressed genes: Analysis have shown that the majority of genes in higher HLNRA dose groups (> 5.0 mGy/y) are involved in DNA repair, cell cycle, stress response, immune response, RNA processing and histone/chromatin modification. Some of the important DDR and repair genes were *XRCC4, LIGASE4, RAD23B, ERCC4, GADD45B, CDKN1A* etc. Some of the important transcription factors such as, *c-JUN, ATF2, CREBZF* were over expressed in HLNRA individuals. We have also observed few dose responsive genes with respect to background doses which included *DDIT3, GADD45B, PMAIP1, DUSP1, PAPD4, DUSP10* etc. Important signaling pathways such as MAPK pathway, p53 pathways etc. were also overrepresented in HLNRA groups. In summary, an important finding of this study is the abundance of DNA damage response and repair genes in high dose groups of HLNRA (>5mGy/y) in response to chronic low dose rate radiation.

3.2.3 Validation of selected genes form microarray data: Thirty genes selected from transcriptome data were validated using RT q-PCR in two sets of individuals: the first set of 30 individuals was from microarray experiment and the second set of 24 individuals was completely a new group of individuals. Data showed similar trend and good correlation between microarray analysis and RT q-PCR. We observed few of the genes showing dose related changes in transcriptome analysis also showed similar changes in q-RT PCR suggesting them to be possible signatures of low dose exposure.

3.2.4 Expression profile of genes involved in DNA repair pathway after a challenging dose in NLNRA and HLNRA individuals: Radio-adaptive response of six genes *(KU70, KU80, DCLRE1C, XRCC4, PRKDC* and *LIGASE4*) involved in DSB repair was studied at 4 h after

giving the challenging dose of 2 Gy in 20 individuals (HLNRA, N=10 and NLNRA, N=10). We observed *XRCC4, DCLRE1C* and *KU80* genes showed significant upregulation in HLNRA individuals as compared to NLNRA indicating the involvement of NHEJ pathway in efficient repair of DSBs in HLNRA individuals.

3.2.5 Gene expression profile of selected genes after exposure to acute doses of IR. Transcription profile of a set of genes (*HISTH2B, PLK3, DDIT3, JUN, DUSP10, PAPD4, BTG1, PMAIP1* etc) was studied in PBMCs of 10 individuals. A significant up regulation was observed in the transcription profile of *DDIT3, PMAIP1, HISTH2B, PLK3, DUSP10* genes at 4 h post irradiation.

3.3 Radiation induced chromatin conformational changes at acute doses:

Conformational changes in terms of hydrodynamic diameter of chromatin fiber at different doses were analyzed using DLS. Our study revealed significant changes in hydrodynamic diameter in PBMCs exposed to low level gamma radiation (0.25 Gy and 0.50 Gy) followed by 2 h post-irradiation recovery period. Inter-individual variation was clearly observed. The study will be extended to HLNRA population in future.

4. Discussion

Biological effect of low dose radiation in humans has important implications to human health. Human population residing in HLNRA provides an opportunity to study the biological effects of chronic low dose radiation *in vivo*. In the present study, quantitation of spontaneous or basal level frequency of DNA DSBs showed a marginally reduced frequency of DSBs in HDG of HLNRA (> 5.0 mGy/y). Gamma H2AX assay is specific to DSBs and has been shown to have sensitivity to detect DSBs at doses as low as 1 mGy. The basal level frequency obtained in our study are comparable to the results obtained in other studies (10,11). A significant reduction in

DSBs was observed at 0.25 Gy in HDG individuals as compared to LDG and NLNRA individuals. At higher doses (1.0 and 2.0 Gy), a decreasing trend of DSBs was observed in HDG and LDG as compared to NLNRA suggesting that induction of damage at low and high doses are different. Repair kinetics study at 2.0 Gy revealed that there is biphasic repair kinetics with a peak at 2h. Significantly efficient repair of DSBs at 4 to 6 h post irradiation time point indicated radioadaptive response *in vivo*. The residual damage did not show much variation and it was 15-20 % at the end of 24h for low and high doses. Our results indicated that HLNRA individuals are repairing DSBs more efficiently as compared to NLNRA individuals. Transcriptome analysis revealed background dose dependent increase in the number of differentially expressed genes in HLNRA individuals as compared to NLNRA. Over representation of genes involved in response to DNA damage and repair, cell cycle regulation, RNA processing, stress response, chromatin modification, apoptosis and immune response in high dose groups of HLNRA (> 5.0 mGy/y). Some of the important pathways such as p53 pathway, MAPK pathways were activated at higher background dose group. Our results indicated abundance of DDR and repair genes in HLNRA individuals belonging to HDG (≥ 5.0 mGy). This could be the reason of reduced frequency of basal level DSBs observed in HDG of HLNRA individuals that might have influenced faster and efficient repair of DSBs observed in HLNRA individuals. Alteration in chromatin structure is another important aspect of cellular response to DNA damage. Relaxation of chromatin fiber at damage site plays crucial role in initiating DNA damage response in human cells. In the present study, using DLS, changes in the hydrodynamic diameter of chromatin fibers were observed at low doses (0.25 and 0.5 Gy) indicating qualitative difference between high and low dose exposures.

5. Summary and Conclusions:

In the present thesis, the cellular responses to chronic low level radiation exposure were investigated in human individuals residing in HLNRA and NLNRA. The basal frequency of DNA DSBs was evaluated using gamma H2AX marker in NLNRA and HLNRA individuals exposed to ≤ 5.0 mGy/y (LDG) and > 5.0 mGy/y (HDG). Radio-adaptive response was studied in terms of induced level of DSBs after giving challenging dose to the PBMCs of individuals from HLNRA (LDG and HDG) and NLNRA. DNA repair kinetics was studied at different post-irradiation time points in HLNRA (LDG and HDG) and NLNRA individuals. Transcriptome analysis was carried out to find out differentially expressed genes and involvement of different pathways in response to chronic radiation exposure. Selected genes from transcriptome analysis were validated by q-RT PCR. Radio-adaptive response of NHEJ repair pathway genes was studied after giving a challenging dose in HLNRA and NLNRA individuals. Chromatin conformational changes were studied in PBMCs exposed to acute doses of IR in terms of hydrodynamic diameter. This thesis leads to the following conclusions.

- A marginal reduction in basal level frequency of DNA DSBs was observed in HLNRA individuals (> 5.0 mGy/y) as compared to NLNRA.
- A significant reduction of induced DSBs observed at 0.25 Gy. However, a decreasing trend in gamma-H2AX positive cells was observed at 1.0 Gy and 2.0 Gy in LDG and HDG individuals as compared to NLNRA.
- Significantly increased repair of DSBs was observed at 4 h and 6 h in HLNRA individuals as compared to NLNRA individuals at 0.25 and 2.0 Gy challenging doses. Repair kinetics of DSBs showed a biphasic pattern. A residual damage of 15-20 % observed at the end of 24 h.

- ❖ Significant upregulation of genes involved in NHEJ repair pathway genes was observed in HLNRA individuals after giving challenging dose of 2.0 Gy indicating their role in *in vivo* adaptation.
- ❖ Transcriptome analysis revealed a dose dependent increase in the number of differentially expressed genes in different background dose groups of HLNRA individuals as compared to NLNRA individuals.
- ❖ An over-representation of DNA damage response and repair, cell cycle regulation, apoptosis and histone modification genes was observed in HLNRA individuals (>5.0 mGy/y).
- ❖ DLS may be useful in studying the radiation induced changes in chromatin structure at low dose exposures.

References:

1. W.F. Morgan, W.J. Blair, Radiat Res, 179 (2013) 501-510.
2. S.A. Amundson, R.A. Lee, C.A. Koch-Paiz, M.L. Bittner, P. Meltzer et al, Mol Cancer Res, 1 (2003) 445-452.
3. L.H. Ding, M. Shingyoji, F. Chen, J.J. Hwang, S. Burma et al, Radiat Res, 164 (2005) 17-26.
4. S. Grudzenski, A. Raths, S. Conrad, C.E. Rube, M. Lobrich, Proc Natl Acad Sci U S A, 107 (2010) 14205-14210.
5. R.R. Nair, B. Rajan, S. Akiba, P. Jayalekshmi, M.K. Nair et al, Health Phys, 96 (2009) 55-66.
6. G. Jaikrishan, K.R. Sudheer, V.J. Andrews, P.K. Koya, M. Madhusoodhanan et al, J Community Genet, 4 (2013) 21-31.
7. E.N. Ramachandran, C.V. Karuppasamy, V.D. Cheriyan, D.C. Soren, B. Das et al, Int J Radiat Biol, 89 (2013) 259-267.
8. B. Das, C.V. Karuppasamy, Int J Radiat Biol, 85 (2009) 272-280.
9. P.R. Kumar, V.D. Cheriyan, M. Seshadri, Radiat Res, 177 (2012) 643-650.
10. S. Roch-Lefevre, T. Mandina, P. Voisin, G. Gaetan, J.E. Mesa et al, Radiat Res, 174 (2010) 185-194.
11. C.S. Djuzenova, I. Elsner, A. Katzer, E. Worschech, L.V. Distel, M. Flentje, B. Polat, Radiat Oncol, 8 (2013) 98.

Publications in Refereed Journal:

a. Published:

1. Lack of increased DNA double strand breaks in peripheral blood mononuclear cells of individuals from high level natural radiation areas of Kerala coast in India (2016). **Vinay Jain**, P.R.Vivek Kumar, P.K.M. Koya, G. Jaikrishan and Birajalaxmi Das. Mutation Research, Fundamental and Molecular Mechanisms of Mutagenesis.
   http://dx.doi.org/10.1016/j.mrfmmm.2016.03.002 (in press).
2. Radiation induced conformational changes in chromatin structure in resting human peripheral blood mononuclear cells (2014). **Vinay Jain**, P.A Hassan and Birajalaxmi Das. International Journal of Radiation Biology, 90 (12): 1143-1151.
3. Transcription profile of DNA damage response genes at G_0 lymphocytes exposed to gamma radiation (2012). Divyalakshmi Saini, Shridevi Shelke, A. Mani Vannan, Sneh Toprani, **Vinay Jain**, Birajalaxmi Das, M.Seshadri. Molecular and Cellular Biochemistry, 364: 271-281.
4. Transcriptional expression of H2B, CTP synthase & PLK3 genes in whole blood exposed to ^{60}Co gamma radiation (2011). **Vinay Jain**, Birajalaxmi Das and M. Seshadri. International Journal of Low Radiation, 8 (1): 55-65.

b. Accepted: Nil

c. Communicated:

1. Efficient repair of DNA double strand breaks in individuals from high level natural radiation areas of Kerala coast, south-west India. **Vinay Jain**, Divyalakshmi Saini, P. R. Vivek Kumar, G. Jaikrishan and Birajalaxmi Das. Scientific Reports (under revision).

d. Other Publications:

1. Conformational changes in the chromatin structure of human peripheral blood mononuclear cells exposed to low dose radiation (2011). **Vinay Jain**, P.A Hassan, Birajalaxmi Das and M.Seshadri. BARC Newsletter Founder's Day Special Issue, 368-370.

Signature of Student:

Date:

Doctoral Committee

S. N.	Name	Designation	Signature	Date
1.	Dr R. Sarin	Chairman		
2.	Dr Birajalaxmi Das	Convener & Guide		
3.	Dr H.S Misra	Member		
4.	Dr J. R Bandekar	Member		

Chapter 1

Introduction

Human beings are exposed to various types of physical and chemical mutagens in their daily lives. Exposure to physical mutagens such as ionizing radiation (IR) comes from various natural as well as man-made sources. Natural radiation exposures are mainly from terrestrial and cosmic sources whereas the sources of man-made exposure may vary from medical (diagnostic and therapeutic) to accidental exposures such as Chernobyl and Fukushima Daiichi incidents. The global average of annual background exposure to radiation due to natural sources is around 2.4 millisievert/year (mSv/y) (*1*). Contribution from natural background radiation is substantial. However, man-made exposures which include radio-diagnostic examinations such as angiographic procedures, computed tomography, occupational exposure as well as exposures from nuclear accidents may expose a large population to the level of radiations which are higher than the annual exposure through natural sources.

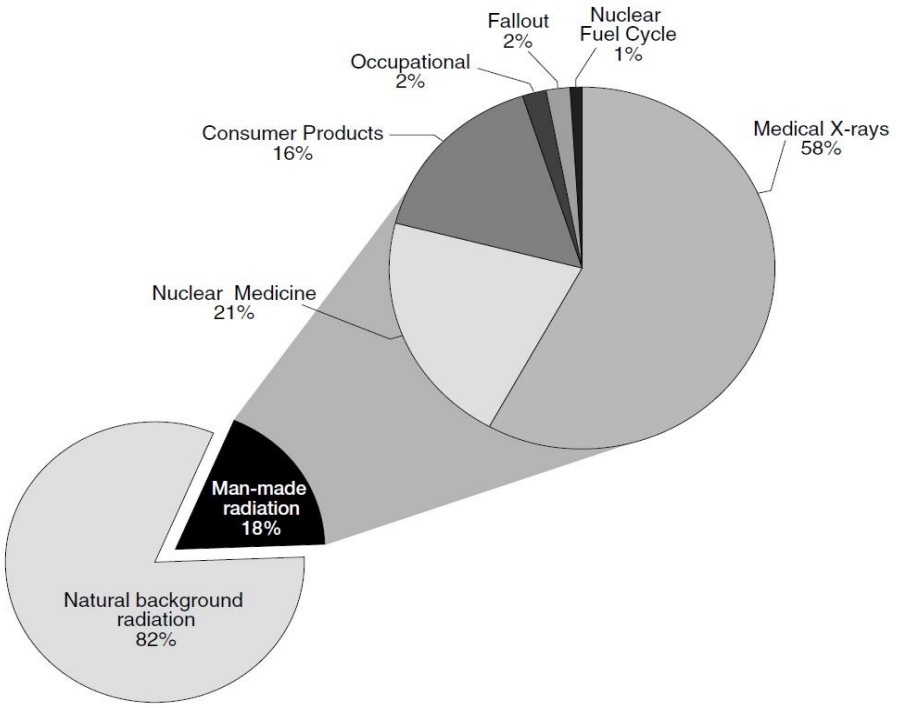

Figure 1.1: Different sources of low level radiation exposure to human beings. (Source: Health Risks from Exposure to Low Levels of IR: BEIR VII – Phase 2 report)

1.1 Health risks and low dose radiation

Biological effects of IR in human cells/tissues may vary with type and quality of radiation, dose and dose rate as well as duration of exposure (acute or chronic). The biological and health effects of high doses of IRs are well documented which especially came from data of atomic bomb survivors. However, limited information is available on biological effects of IR at low dose and low dose rate. In general, low dose and low dose rate exposures are considered to be below 100mSv (*2-3*). Understanding the biological and health effects of very low dose and dose rate {in the order of few milligray (mGy)} of IR on human beings is of utmost importance as the data is very inconsistent in this region of dose response curve. Additionally, in recent years, studies pertaining to low dose and low dose rate radiation exposure have gained importance as it poses concern among the public due to accidental exposure situations such as Chernobyl and Fukushima Daiichi and the increasing use of medical radiation in health care. Hence, it has become a thrust area of research in radiation biology today. For the last few years, epidemiological information at low dose exposures has improved and plenty of data has been generated in human population on cancer incidences and heritable changes (*4-12*). However, epidemiological studies are not conclusive enough due to the low statistical power. At the same time, it needs a larger population or cohort to be studied to draw firm conclusions. It is also important to understand the biological mechanisms at low dose and low dose rates to understand the effect of IR at low doses occurring in human cells. Therefore, efforts have been made worldwide to study the biological effect of IR at low dose and low dose rates using various biological end points (*13*).

Due to lack of sufficient and conclusive radio-biological and epidemiological data at low dose exposures, the current paradigm of radiation protection support the linear no threshold

(LNT) hypothesis to estimate the risk at low dose radiation exposures. LNT model is based on the fact that, smallest radiation dose has the potential to cause an increase in health risk to humans and the effects at low dose exposures are extrapolated from the data of high dose exposures. It implies that the radiation risk is directly proportional to the dose. The risks from radiation have been largely derived from atomic bomb survivor studies (Life span study cohort). The LNT model assumes that cancer incidence as it relates to radiation dose behaves in the same way at low doses as at higher doses (*14*). However, use of LNT hypothesis as the basis of radiation protection and the potential health effects at low dose exposures has been under debate and discussion within the scientific community (*15-21*). LNT hypothesis assumes that DNA damage and repair processes function with equal efficiency at low doses as well as high doses. It has not taken into account the processes like scavenging of reactive oxygen species (ROS) and programmed cell death in human cells. In the recent years, several studies have shown the occurrence of mechanisms like low dose hypersensitivity, adaptive response, hormesis and bystander effects in human cells exposed to low dose IR (*18, 22-30*).

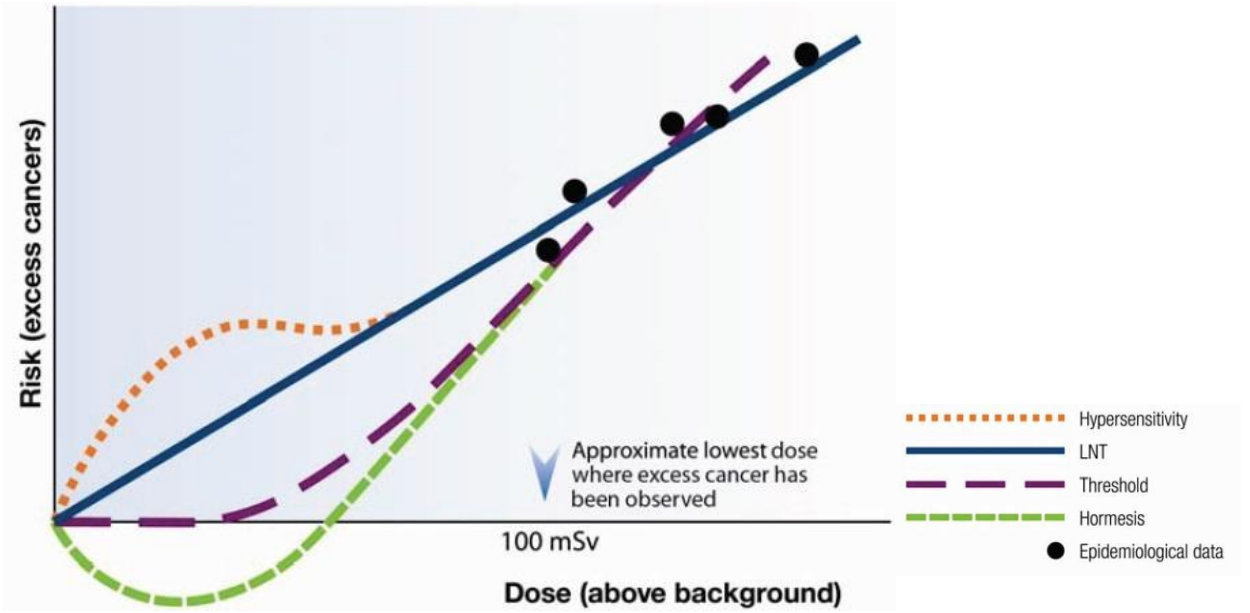

Figure 1.2: Different models for the health risks from exposure to low levels of IR. (Source: Canadian union safety commission, 2013, www.nuclearsafety.gc.ca)

Keeping these studies in mind, several alternate theories have been proposed to explain the relationship between low radiation exposure and cancer risk. The shapes of the dose response curve have been proposed in four different models (figure 1.2). These models have been proposed as alternate models based on cellular and sub-cellular responses to radiation at very low doses to address findings of studies that do not follow the LNT model. Figure 1.2 illustrates different radiation risk models that estimate the risk of cancer below the lowest dose where excess cancers have been observed (~ 100 mSv). The hypersensitivity model suggests a greater risk at lower doses, whereas the threshold model implies that no risk is associated with radiation dose below a certain dose. Another model called hormesis suggests that low doses of radiation exposure may even be protective or beneficial.

United Nations Scientific Committee on the Effects of Atomic Radiation (UNSCEAR) has evaluated health effects of exposure to IR at low doses and dose rates and has recognized the limits to the statistical power of epidemiological studies. However, phenotypic effect is the most

important consequence of the effect of radiation exposure. Interpolating the dose response between data from epidemiological investigations and incremental doses above background exposures requires knowledge of the mechanisms of radiation action and post-irradiation processes that specifically relate to health effects (*3*). Therefore, it is essential to focus on understanding the biological effects of low dose radiation as it will provide better insights into the mechanistic understanding and its potential risk to human health.

1.2 High level natural radiation areas

There are many areas in the world, where the level of natural background radiation is high (sometimes 10 -100 times the normal levels) either due to high levels of radioactivity in soils, rocks and hot springs or due to high levels of indoor radon and its decay products. These areas are known as High Level Natural Radiation Areas (HLNRA). Some of the prominent areas around the world are Ramsar (Iran), Yangjiang (China), Guarapari (Brazil) and Kerala (India). The level of background radiation dose in these areas varies from < 1.0 mGy/y to 260 mGy/y. The background radiation is elevated due to radioactive thorium containing monazite sand in Kerala (India), Yangjiang (China) and Guarapari (Brazil) and due to radium content in the hot springs in Ramsar (Iran). The HLNRAs offer ample opportunities to study the biological and health effects of chronic low dose and low dose rate exposure directly on humans at all stages of development.

The HLNRA of Kerala is about 55 km long and 0.5 km wide strip, extending from Neendakara (Kollam district) in south to Purakkadu (Alapuzha district) in north Kerala (*31*) (figure 1.3). The radioactive component of this beach sand is monazite, which contains thorium (8-10%, highest in the World) and its radioactive daughter products. This area is thickly populated with an approximate population size of 4,00, 000 inhabitants. This area is inhabited

for around 1000 years and population has been living here for many generations. Due to non-uniform distribution of monazite sand, the level of background radiation in this area varies from <1.0 mGy to 45 mGy per year. The areas with a dose range of ≤ 1.5 mGy/y are considered as Normal Level Natural Radiation Areas (NLNRA), whereas dose range of >1.5mGy/y is considered as HLNRA. (*6-7, 32-35*).

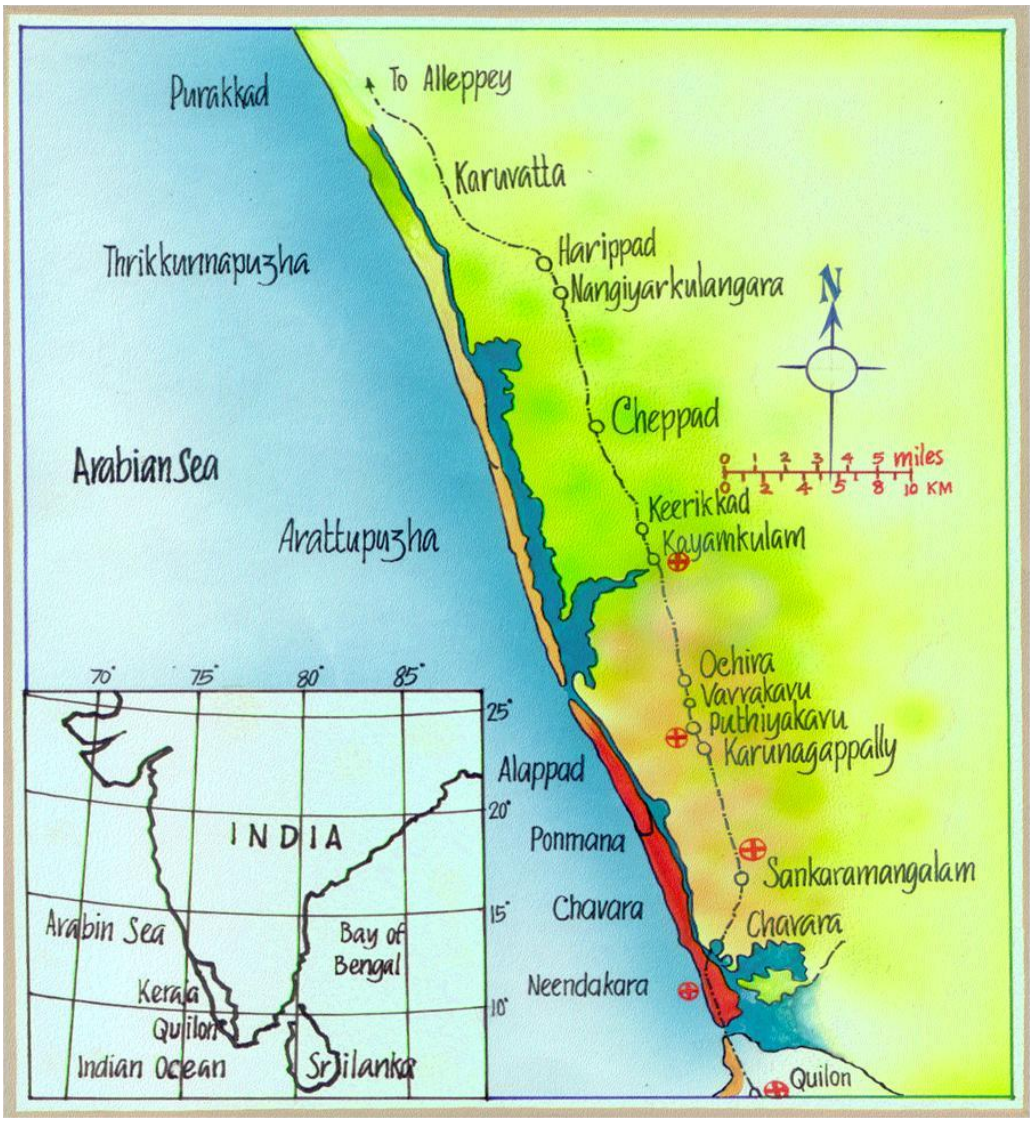

Figure 1.3: The High level Natural Radiation Areas of Kerala coast in south India (Source: Das, B., 2010, BARC Newsletter, pp 28-37)

It is a difficult task to delineate the effect of natural background radiation, if any, on humans as there are many confounding factors such as age, gender, habits, diet, life style etc. in a population. This area is unique as compared to other HLNRAs of the world because it exhibits a great deal of variation in the level of background dose exposures, which is ideal to study *in vivo* dose response. Since, the population is residing in this area for many generations, the accumulated dose could play an important factor.

Studies on biological and health effects of the human population living in HLNRAs provide an important source of information on the effects of chronic low dose rate exposures to IR. The human population inhabiting this area has been investigated using various biological end points. Several studies have been conducted to delineate the effect of low dose and low dose rate chronic exposure on human population residing in this area. These include demographic characterization of approximately 70,000 population which did not show any significant differences in reproductive parameters, infant mortality etc between the high and normal level radiation areas (*36*). In addition to humans, cytogenetic studies of native plants belonging to different genera and species (*37-38*) and genetic studies on dental and skeletal characterization of wild rats have been carried out in this area (*39-40*). These studies did not reveal any significant difference between control and exposed population. However, a higher prevalence of Down Syndrome (DS) among the population from HLNRA was reported (*41*) but there were few shortcomings in the study design (*42*). An increased frequency of mitochondrial germ line point mutation was reported in a study with saliva samples from residents of the high radiation area of Kerala compared to a nearby control area (*43*). Similarly, an increase in Y chromosome mutations was reported in this area (*44*). However, both the above studies did not have dosimetric information and were therefore highly criticized.

In recent years, epidemiological studies on cancer incidence conducted in this area on a cohort of 69,958 individuals did not reveal any significant difference in the incidence of any of the cancers in this area. Moreover, the relative risk remained flat with negative correlation values (*10*). A large scale monitoring of the newborns from a hospital based study covering over 1,50,000 newborns did not show any significant difference in the incidence of congenital malformations, still births and down syndrome between HLNRA and NLNRA population (*7-8*). The data indicates that there is no significant effect of background radiation exposure at the level of phenotype in this area. A case control study on cleft lip/palate and mental retardation was also carried out in this area. The results obtained did not show any significant association of these two diseases with radiation levels (*9*). Recently, a study on sex ratio at birth did not show influence of high background radiation on the frequencies of male and female newborns (*12*).

Apart from epidemiology, biological studies conducted in this area include cytogenetic investigation of karyotype anomalies (numerical and structural) of over 27,000 newborns. Cytogenetic analysis included both stable (translocation and inversions) and unstable (dicentrics and rings) type of chromosomal aberrations. No significant difference between control and exposed population was observed. No dose response was observed when analysis was carried out with different background dose groups (*32, 45*). The frequency of micronuclei (MN) was determined among the newborns and was comparable between these two populations. Telomere length analysis was carried out in newborns and adults (*46-48*). No attrition of telomere length was observed with respect to different background dose groups. DNA mutation rate using microsatellites and mini-satellites also did not show any significant change in the mutation rate based on approximately 200 families from this area (*49-50*). DNA damage quantitation was done using alkaline comet assay, where the frequency of strand breaks, oxidized purines and

pyrimidines were quantitated (*51*). No significant difference was observed in all these parameters in NLNRA and HLNRA individuals. However, reduction of DNA strand breaks was observed among the individuals with higher age groups in HLNRA as compared to NLNRA (*30*).

Recently, DNA damage and repair study using alkaline comet assay revealed better repair capacity among the individuals from HLNRA at early time point of fast repair process. Additionally, challenging doses of 2.0 Gy and 4.0 Gy showed significant reduction of DNA strand breaks in HLNRA groups with a background dose of > 5.0mGy/y (*30*). These results further warrant a deeper understanding of cellular and molecular effects of chronic low dose radiation in this population with newer molecular biological techniques.

1.3 Biological effects of ionizing radiation

IR interacts randomly with the important bio-molecules (DNA, RNA and Lipids) in the cell. DNA is one of the most important target as it contains the hereditary material. IR damages DNA molecule either through direct deposition of energy (ionization and excitation) or through indirect mechanisms mediated by ROS produced by radiolysis of water (*21*). The interaction of IR with human cells is complex. At high doses, human cells are typically hit by many tracks of radiation, but at low doses most cells are typically hit by a single track of radiation. At very low doses proportionately fewer cells are hit, mostly by single track of radiation (*52*). IR induces a variety of isolated and clustered DNA damages such as base damages, single strand breaks (SSBs) and double strand breaks (DSBs). It also produces clustered DNA damage which includes DNA DSBs and non-DSB clusters. Clustered DNA damage, which is defined as two or more of such lesions within one to two helical turns of DNA induced by a single radiation track which is considered to be a unique feature of ionizing radiation. (*53-55*). Double strand break is a type of clustered DNA damage, in which single strand breaks are formed on opposite strands in

close proximity, also DSB cluster may have associated base lesions and AP sites (*53-54, 56-60*). The induction of radiation induced cluster damage has been reported in mammalian cells (*55, 61-63*). The yield of non-DSB clusters has been reported to be 4-8 times greater than that of DSB lesion. Also, it has been reported that life span of clustered damage (DSB or non-DSB) in mammalian cells is considerably longer than isolated lesions (*53, 57, 64-65*) as they are hard to repair. Exposure to 1 Gy of low linear energy transfer (LET) IR is known to produce about 1000 SSBs, 500 base damages, approximately 40 DSBs and 150 DNA-protein cross-links (*1*). At a typical radio-therapeutic dose of around 2 Gy/fraction of sparsely ionizing radiation, about 3000 DNA lesions are produced per cell exposed which is far lower than approximately 50 000 lesions produced daily through ROS (*66*).

1.4 Cellular responses to DNA damage in human cells

DSBs are most deleterious and if remain unrepaired or misrepaired may lead to consequences like lethal mutations, genome instability and carcinogenesis. However, to monitor and maintain the integrity of genome, cells possess surveillance systems, termed as the DNA damage response (DDR). DDR is a complex phenomenon which includes all major cellular activities such as damage detection, cell cycle progression, transcriptional changes, DNA repair, apoptosis and chromatin modification (figure 1.4)(*67-72*).

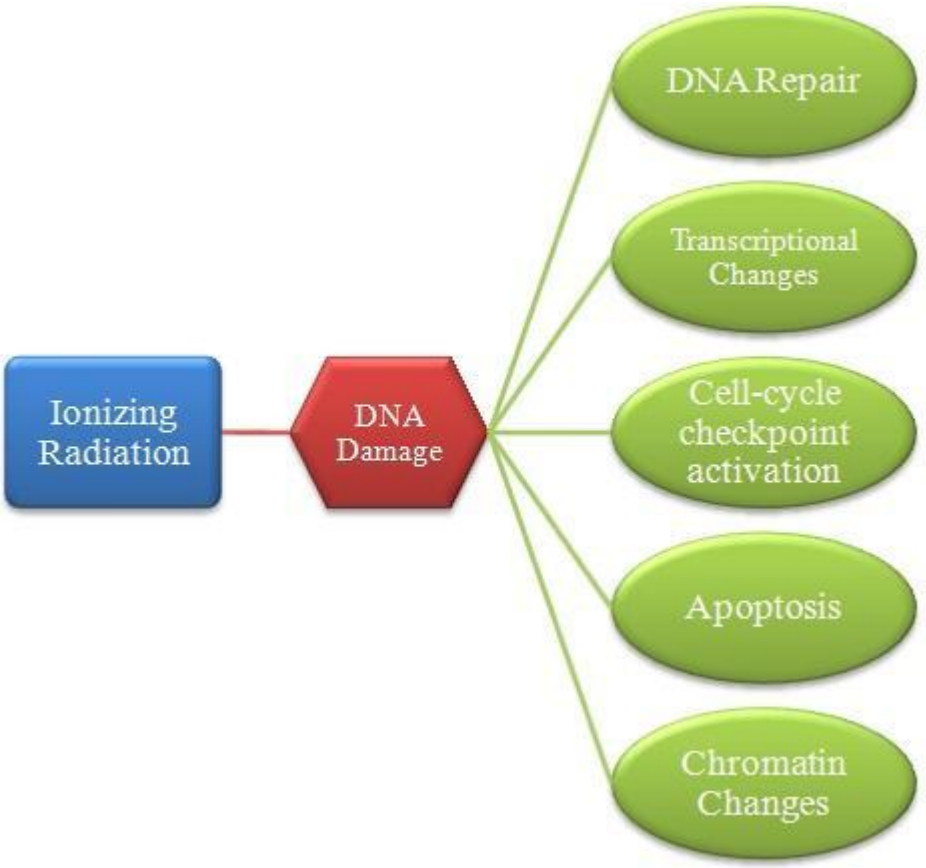

Figure 1.4: Schematic representation of different cellular responses in response to IR induced DNA damage in human cells.

One of the initial steps of DDR is the sensing and detection of DNA damage by signaling pathways that amplifies and transduce the signal to produce appropriate biological responses. The key DDR signaling components in human cells are PIKK (phosphophatidylinositol 3-kinase like kinase) family protein kinases, ATM (ataxia-telangiectasia) ATR (ATM and RAD3 related) and DNA-PK (DNA dependent protein kinase). These PIKKs are recruited to DNA damage site and gets activated through the interaction with different sensor molecules. ATM is recruited to DSBs by interacting with DSB sensor complex MRN, which consists of MRE11

(meiotic recombination 11 homologue), RAD50 and NBS1 (Nijmegan breakage syndrome 1). DNA-PK is recruited to DSBs through interaction with Ku proteins. The recruitment of ATR to damaged DNA depends on interaction with ssDNA binding protein replication protein A (RPA) adaptor protein known as ATR interacting protein (ATRIP). Activation of PIKKs leads to the phosphorylation of H2A.X residues at DSB site which serves as the docking site of several proteins involved in DNA repair, cell cycle checkpoints and chromatin remodeling. The ATM/ATR transduces the signal through mediator proteins like 53BP1, MDC1 and BRCA1 and activates protein kinases CHK1 and CHK2 which further mediates the activation of effector proteins like p53 transcription factor. Activated p53 up-regulates a number of target genes such as MDM2, GADD45A and CDKN1A/p21. The accumulation of these proteins activates cell cycle checkpoints and slows the cell cycle progression that allows the cells to repair the damaged DNA repair before it gets replicated. If the damage is beyond repair DDR signaling triggers cell death by apoptosis or cellular senescence to maintain the genomic stability. DDR enhances the repair of damage by activating and inducing DNA repair machinery transcriptionally or through post-translational modifications such as phosphorylation, acetylation, ubiquitination or sumoylation (*73-80*).

1.5 DNA repair pathways

In human cells, different DNA repair pathways have evolved to repair different kind of DNA lesions. Single strand breaks and base damages are repaired through base-excision repair pathway (BER) and nucleotide excision repair (NER), whereas DNA double strand breaks are repaired through homologous recombination (HR) or Non-homologous end joining (NHEJ) pathway (*59, 81-84*). Although cells can adapt to low levels of irreparable damage, as little as one DNA DSB can be sufficient to kill a cell if it inactivates an essential gene or triggers

apoptosis (*85-86*). In general, IR induces around 850 pyrimidine lesions, 450 purine lesions, 1000 single-strand breaks (SSB) and 20–40 double-strand breaks (DSB)/cell/Gy in mammalian cells with low linear energy transfer (LET) gamma-radiation (*66*).

Base excision repair (BER) is a multi-step process that corrects non-bulky damage such as bases damaged by oxidation, methylation and other small chemical modifications from DNA. These lesions are highly mutagenic and represent a significant threat to genome fidelity and stability. BER has two sub-pathways, both of which are initiated by the action of DNA glycosylase such as OGG1 (8-oxoguanine DNA glycosylase), MPG (3-methyl adenine DNA glycosylase) and NEIL1 (endonuclease VIII-like 1). These enzymes cleave the N-glycosidic bond between the damaged base and the sugar phosphate backbone of the DNA. This cleavage generates an apyrimidinic/apurinic (AP) or abasic site in the DNA. The AP site is subsequently processed by AP endonuclease (APE1, APEX, REF-1) During short patch BER, the remaining sugar backbone is removed by DNA polymerase beta (Pol β), which also inserts a new nucleotide. The strand nick is finally sealed by a DNA ligase3/XRCC1 complex, thus restoring the integrity of the DNA. The back-up pathway of BER, termed "long-patch" repair, is employed when a modified base resistant to the AP lyase activity of DNA Pol β is present in the DNA. Long-patch repair results in the replacement of approximately 2-10 nucleotides including the damaged base. The long-patch repair is a PCNA-dependent pathway where the DNA polymerases add several nucleotides to the repair gap, thus displacing damaged nucleotides as part of a "flap" oligonucleotide. The resulting oligonucleotide overhang is excised by the Flap endonuclease, FEN-1 prior to sealing of the nick by a DNA ligase (*82, 87-90*)

Nucleotide excision repair (NER) pathway repair bulky adducts and lesions such as pyrimidine dimers caused by the UV light. Other NER substrates include bulky chemical adducts and DNA

intra-strand crosslinks. The common features of lesions recognized by the NER pathway are that they cause both a helical distortion of the DNA duplex and a modification of the DNA chemistry (*91*). The NER process requires the action of more than 30 proteins in a stepwise manner that includes damage recognition, local opening of the DNA duplex around the lesion, dual incision of the damaged DNA strand, gap repair synthesis, and strand ligation (*92-93*). The two sub pathways of NER are: global genomic NER (GG-NER), which corrects damage in transcriptionally silent areas of the genome, and transcription coupled NER (TC-NER), which repairs lesions on the actively transcribed strand of the DNA. These two sub-pathways are fundamentally identical except in their mechanism of damage recognition (*94*). In GG-NER, the XPC/hRAD23B protein complex is responsible for the initial detection of damaged DNA. Conversely, damage recognition during TC-NER does not require XPC, but rather is thought to occur when the transcription machinery is stalled at the site of injury. The stalled RNA polymerase complex must then be displaced in order to allow the NER proteins access to the damaged DNA. This displacement is aided by the action of the CSA and CSB proteins, as well as other TC-NER-specific factors. XPA and the heterotrimeric replication protein A (RPA) then bind at the site of injury and further aid in damage recognition. Next, the XPB and XPD helicases, components of the multi-subunit transcription factor TFIIH, unwind the DNA duplex in the immediate vicinity of the lesion. The endonucleases XPG and ERCC1/XPF then cleave one strand of the DNA at positions 3' and 5' to the damage, respectively, generating an approximately 30 base oligonucleotide containing the lesion. The oligonucleotide is displaced, making way for gap repair synthesis. Finally, the DNA is re-synthesized by DNA pol δ/ε in co-ordination with PCNA and RPA and nick is sealed by a DNA ligase (*82, 89, 95*).

Mismatch Repair (MMR): The DNA mismatch repair (MMR) pathway plays an essential role in the correction of replication errors such as base-base mismatches and insertion/deletion loops (IDLs) that result from DNA polymerase mis-incorporation of nucleotides and template slippage, respectively. The overall process of MMR is similar to the other excision repair pathways such as long-patch BER and NER in that the DNA lesion is recognized, a patch containing the lesion is excised, and the strand is corrected by DNA repair synthesis and re-ligation.

The mammalian MMR pathway consists of at least seven proteins including MSH2 MSH3,MSH6, MLH1, MLH3, PMS1 and PMS2 (*96*). MMR proteins function as a heterodimeric complex. The MSH2 can form a heterodimer with either MSH6 (MutSα) or MSH3 (MutSβ). MutSα primarily recognizes base/base mismatches, whereas MutSβ primarily recognizes large insertion/deletion loops. Similarly MLH1 can form a heterodimer with PMS2 (MutLα), PMS1 (MutLβ), or MLH3. MutS initiates the process by recognition and binding to the misrepaired bases. Subsequently, MutL is recruited to the site and form a ternary complex with MutS heterodimer (*97*). This complex initiates the downstream signaling by recruitment of exonuclease (EXO1) that removes nucleotides between an adjacent SSB upto and beyond the mismatch on the daughter DNA strand. The resynthesis by DNA polymerase δ along with at two other proteins, proliferating cell nuclear antigen (PCNA) and replication protein A (RPA) and finally, the nick located in the daughter strand is sealed by a DNA ligase (*82, 98-102*).

Homologous Recombination (HR) : HR-directed repair corrects DSB defects in an error-free manner using a mechanism that retrieves genetic information from a homologous, undamaged DNA molecule. The majority of HR-based repair takes place in late S- and G2-phases of the cell cycle when an un-damaged sister chromatid is available for use as repair template. The RAD52 group of proteins, including RAD50, RAD51, RAD52, RAD54, and MRE11 mediate this process. The

RAD52 protein itself is thought to be the initial sensor of the broken DNA ends. Processing of the damaged ends ensues resulting in the production of 3' single-stranded DNA (ssDNA) overhangs. The newly generated ssDNA ends are bound by RAD51 to form a nucleoprotein filament. Other proteins including RPA, RAD52, RAD54, BRCA1, BRCA2, and several additional RAD51 related proteins serve as accessory factors in filament assembly and subsequent RAD51 activities. The RAD51 nucleoprotein filament then searches the undamaged DNA on the sister chromatid for a homologous repair template (*103*) . Once the homologous DNA has been identified, the damaged DNA strand invades the undamaged DNA duplex in a process referred to as DNA strand exchange. A DNA polymerase then extends the 3' end of the invading strand and subsequent ligation by DNA ligase I yields a hetero-duplexed DNA structure. This recombination intermediate is resolved and the precise, error-free correction of the DSB is complete (*104-106*).

Non Homologous End Joining (NHEJ): The NHEJ repair pathway functions by simply joining the DNA ends irrespective of their origin and does not require homology at the DNA ends. Thus, it does not have the potential of restoring the original sequence in the vicinity of the DSB (*107-108*). NHEJ is active in all phases of the cell-cycle and it repairs DSB with similar efficiency, however it is the predominant DSB repair in G_0/G_1 phase of cell cycle. NHEJ possesses only limited functionality for single ended DSB that arise during replication (*109*). The various steps involved in NHEJ repair pathway are as follows: (i) detection of the DSB and protection of the DNA ends, (ii) DNA end-processing to remove damaged or non ligatable groups, and (iii) DNA ligation. The major proteins required for NHEJ in human cells are the Ku heterodimer (composed of Ku70 and Ku80), the catalytic subunit of the DNA-dependent protein kinase (DNA-PKcs), Artemis, XRCC4, DNA Ligase IV and XLF (XRCC4-like factor) (*59, 82, 84, 110*).

1.6 Differential responses at low and high dose radiation exposures

Understanding the biological effects of acute and chronic low level radiation exposure in humans has been a challenging task. Several studies have shown that the cellular responses in terms of gene expression changes and DSB repair are quantitatively and qualitatively different at low and high doses of radiation exposure. It has been shown using transcriptome analysis approach where the expression of thousands of genes can be analysed simultaneously that genes expressed at low doses are different than the genes differentially expressed at high doses. Similarly, at acute doses it has been shown that repair of DSBs in terms of gamma H2AX foci is substantially compromised at doses less than 10 mGy as compared to higher doses (*15, 17, 67, 70, 111*). Hence, the experimental evidence at very low doses and the mechanistic studies at high doses vs. low doses might throw some insights for risk estimation.

1.7 DNA damage response and alteration in chromatin structure

Human genomic DNA is packaged into nucleosomes which are composed of a histone octamer consisting of four types of histone proteins (H2A, H2B, H3 and H4), wrapped by ~146 base pairs of double stranded DNA. Dynamic packaging of DNA results in different levels of chromatin compaction from 10 nm fiber to higher order structures (*112*) and plays a central role in DNA damage response. The packaging of human DNA is complex and the accessibility to damage sites for repair process to occur depends upon many factors including modifications and rearrangements in chromatin structure. It may thereby affect several cellular processes including transcription, replication and repair (*75, 78, 113-118*). Several studies have shown changes in the chromatin dynamics in response to radiation induced DNA double strand breaks (*75, 77, 116, 118-122*). DNA damage induces various post-translational modifications such as phosphorylation, acetylation etc. in histone proteins that alters chromatin structure (*75, 123*).

Exposure of cells to radiation is known to cause global changes in the chromatin architecture. Studies have shown that UV irradiation of cells appears to relax bulk chromatin structure within the entire nucleus (*112, 119, 124*). Similarly, local perturbations in nucleosomal structure may expose pre-existing methylated residues in core histones and also facilitates new histone modifications which serve as the docking sites for the DNA damage response proteins. In the recent years, the role of DNA damage responsive histone modifications like phosphorylation of core histone variant H2AX, acetylation of H3 and H4 in chromatin reorganization has been investigated substantially. However, the physical attributes/changes in the conformation of damaged chromatin have not been well characterized and thus poorly understood. Biophysical techniques such as Dynamic light scattering (DLS) or photon correlation spectroscopy may be used as a tool to investigate the global changes in the conformation of chromatin structure in response to radiation stress. It is a widely used technique in studying protein-protein interactions, protein dynamics like folding and aggregation as well as DNA- protein interactions. However, very few reports are available till date that employs scattering techniques as a tool in studying chromatin structure and DNA-histone interactions. DLS is a sensitive and non-invasive technique, which allows studying the internal dynamics of biological macromolecules in solution. It has an advantage over scanning techniques like Atomic Force Microscopy (AFM) and Scanning Electron Microscopy (SEM), where fixation of biomolecules is required (*125-129*). Light scattering techniques have been used in studying helical structures of chromatin in solution (*130*) finding linker/spacer regions in chromatin (*131-132*) and in understanding the higher order chromatin structure (*133-137*). Recently, DLS has also been used to study the effect of drug binding on chromatin structure (*138-139*). However, its application in

studying radiation induced changes in chromatin structure has not been explored yet and may be useful in studying chromatin conformational changes at low doses of radiation.

1.8 Gamma H2AX as biomarker for DNA double strand breaks

Exposure to IR induces plethora of DNA lesions, of which double strand breaks (DSBs) are considered to be highly deleterious. A single radiation track of low LET radiation can produce this kind of damage. One of the earliest events of cellular responses to DNA DSBs is the phosphorylation at Ser 139 residue of H2A variant H2A.X, which is referred to as gamma-H2AX. H2AX is a variant of the H2A protein family and constitutes around 10 % of nucleosomal H2A histone protein in human cells. Gamma H2AX foci formation occurs rapidly at the DSB sites and plays an important role in DNA damage response (DDR) signaling cascade (*17, 113, 140-148*). Phosphorylated H2AX triggers the accumulation of a various DNA damage signaling, chromatin modifying and DNA repair proteins at DSB site and form small discrete nuclear foci termed as IR-Induced Foci (IRIF) (*109, 144, 149-151*). Gamma H2AX is a very sensitive and specific biomarker to study double strand breaks in DNA. It is a very well established DSB marker and has been used to estimate DNA DSBs induction and repair in human cells exposed to very low doses (mGy levels) of IR (*15, 17, 152-155*). Gamma- H2AX has been used to estimate baseline frequency of DSBs in peripheral blood lymphocytes in human population. There are extensive efforts to use gamma H2AX in bio-dosimetry, population monitoring and radio-theraupeutic/medical exposures (*140, 142, 149, 156-158*) .

There are two technical approaches which can be used to study double strand breaks using gamma H2AX foci as biomarker. 1) Immunofluorescence assay where the number of gamma-H2AX foci are scored using fluorescence microscope. 2) Immunocytochemistry approach where the intensity of gamma H2AX fluorescence is measured in cells using flow

cytometry. The scoring of gamma H2AX foci is widely used for quantitative evaluation of DNA DSBs at low dose exposures. However, this approach is not ideal to quantitate DSBs at higher doses. At higher doses, it has been observed that gamma H2AX foci may get merged which may lead to incorrect estimation of DSBs. Flow cytometry based fluorescence measurements of gamma H2AX intensity is ideal approach to study DNA damage at higher doses. It is a high throughput approach where fluorescence intensity of thousand of cells at a single dose point can be measured accurately. This is comparatively a faster approach to quantify DSBs in exposed cells.

There are several assays to study DNA DSBs in individual cells including dicentrics and micronuclei, which are good indicators of radiation induced damage and are useful for biological dosimetry, radio-therapeutic, diagnostic and population monitoring studies. The dicentric assay is the current gold standard for radiation bio-dosimetry but its application in the particular situation of a mass casualty is limited due to time constraint. Indeed, in addition to the time required for the stimulation of cell division, the dicentric scoring is very time consuming. In addition, the sensitivity of this technique is upto 0.1 Gy only. There are efforts worldwide to establish new biomarkers for biological dosimetry, population monitoring and medical diagnostic tools. In the past decade, assays like comet assay, pulse field gel electrophoresis (PFGE) have become popular to study DNA damage. Both comet assay and PFGE reduces the time required to detect the damage but they lack in the sensitivity to detect damage at low and very low doses. Immunofluorescence based gamma-H2AX assay has several advantages over other assays as it is very rapid and is specific for DSBs. This method is around 100 times more sensitive to detect DNA damage as compared to comet assay and allows scoring of foci in single intact cells (*159*) and each focus represents one DSB in this assay (*17, 140, 143-144, 160*).

Gamma-H2AX is considered as a DSB specific marker and is widely used for quantitative evaluation of DSB formation and repair in human lymphocytes and cell lines exposed to IR (*156, 161-162*). Several studies have been conducted, where gamma H2AX foci was used to quantify the effect of partial or total body exposures during fractionated and mixed radio-therapeutic applications, CT/PET scans, X-rays, radio-iodine therapy etc (*145, 163-169*).

1.9 Gene expression changes as signature of radiation response

In human cells, DNA damage response may lead to the alteration of gene expression to orchestrate a variety of cellular events including growth arrest, apoptosis, and DNA repair (*170*). Alteration in transcriptome profile allows a cell to maintain its homeostasis following exposure to genotoxic agents like IR. In the past decade, several studies have shown the importance of gene expression profiling as a molecular biomarker or signature to radiation exposure. Importantly, studies have suggested the development of gene expression profiles in peripheral blood lymphocytes as an approach to radiation bio-dosimetry (*68-69, 171-181*). More recently, studies have shown that gene expression signatures can be used in estimating dose rate effects for human bio-dosimetry (*182-183*). However, there can be limitations as there are many genes which may not show altered expression depending upon the function or the biological networks they are involved in. Therefore, identifying dose responsive genes as radiation signatures is very important. Additionally, the qualitative difference of expression of the identified genes may be different at acute vs. chronic and low vs. high dose exposures. Hence, care must be taken while identifying the gene expression as radiation signature for population monitoring, biological dosimetry and medical/radio therapeutic applications.

Development of high throughput gene expression profiling has provided a much more rapid and non-invasive method to identify changes at molecular levels. Transcriptome analysis using

microarray chip provides information about global gene expression in response to any stress including IR (*67, 184-186*). Transcriptional profiling is a sensitive biomarker of radiation exposure and has been used to gain insight into the molecular mechanisms induced by low dose exposures in a variety of cell types such as cultures of human myeloid cells (*111, 174, 187*), human skin fibroblasts and keratinocytes (*67, 188-189*), peripheral blood mononuclear cells (*178, 182, 190-194*), umbilical vein endothelial cells (*195*), lymphoblastoid cells (*196-197*), tissue biopsy samples (*70*) and human embryonic cells (*198*). There are reports which have shown the induction of transcriptional changes after *ex vivo* acute exposure to doses as low as 1 cGy (*199*). Only a few studies investigated transcript profiles after *in vivo* low-dose exposures. A study carried out in brain tissue from irradiated mice identified several genes with modulated transcript levels after exposures of 10 cGy (*200*). There are few reports where *in vivo* studies have been carried out in humans (*190-192*). Fachin et al. (2009) and Morandi et al. (2009) studied gene expression profile in occupational radiation workers and medical workers respectively, Albanese et al. (2007) studied the expression of cytokine genes in chernobyl clean up workers. These studies demonstrated that doses as low as mGy levels of low-LET radiation are sufficient to modulate gene expression and has also demonstrated the potential of gene expression changes as important biomarkers of radiation exposure. However, till now studies are not available on gene expression patterns in human population exposed to low levels of chronic irradiation with a dose as low as mGy/y level. It will be interesting and informative to look for molecular signatures in the population chronically exposed to low dose and low dose rate radiation for generations in the Kerala coastal belt.

1.10 Radio-adaptive response, Radiation hormesis and Bystander effect

Radio-adaptive response (RAR) is a phenomenon in which cells exposed to small conditioning dose of IR (priming dose) reduces the biological effects of subsequent higher doses of radiation (challenging dose). It is widely accepted that IR at high doses is detrimental to the exposed organism. However, biological effects of low dose or low dose rate IR remain elusive. Radiation hormesis implies that radiation exposure comparable to and just above the natural background level of radiation is not harmful but beneficial while accepting that much higher levels of radiation are hazardous (*18-20, 201-202*). Low doses in the mGy range may cause a dual effect on cellular DNA. One is a relatively low probability of DNA damage per energy deposition event that increases in proportion to the dose. At background dose exposures the damage to DNA is much lower than that from endogenous sources, such as ROS. The other effect at comparable doses is adaptive response or protection against DNA damage mainly from endogenous sources, however, it depends on cell/tissue type, species and metabolism of the cells/tissues/organism. Protection by adaptive response leads to DNA damage prevention by activating repair mechanisms, immune system stimulation and activation of cell-cell communication (*20, 203*). It has been reported that RAR develops within few hours, may last for days to months, decreases steadily at doses above about 100 mGy to 200 mGy and seem to not been observed after acute exposures of more than about 500 mGy. Radiation-induced apoptosis and terminal cell differentiation also occur at higher doses and add to protection by reducing genomic instability and the number of mutated cells in tissues. It is assumed that at low doses reduction of damage from endogenous sources by adaptive response maybe equal to or outweigh radiation induced damage (*19*).

Radiation hormesis in humans has been reported in different radiation exposure groups ranging from atomic bomb survivors, nuclear workers, radiologists and radiation technicians, patients exposed to diagnostic radiation and/or radiotherapy, flight crews and astronauts, and residents living in a high background radiation environment (*18*). It has been reported that population residing in high level natural radiation areas in China and India have lower cancer mortality rate as compared to other areas (*11, 18, 25*). Nair et al. (2009) did not observe any excess cancer risk due to high level natural radiation exposure in Kerala population. Mine et al (1990) reported a significantly lower mortality from non-cancerous diseases in Atomic bomb survivors. A lower cancer death rate was reported in residents living in a high altitude compared to a low altitude environment (*22*). Importantly, among 10,000 Taiwanese population who were accidently exposed for a period of 9-20 years to an average radiation total dose of 0.4 Sv by contamination of cobalt-60 in building material of 1700 apartments, the incidence of cancer deaths was greatly reduced to about 3% of the incidence of spontaneous cancer death in the general Taiwan population. In addition, the incidence of congenital malformation was reduced as compared to general public (*29*). A study on nuclear workers and population exposed due to nuclear accidents concluded that incidence of solid cancers decreased in 21,500 radiation exposed workers at Mayak plant in Russia. The total cancer deaths in 8600 cleanup workers at Chernobyl (average dose received: 50mGy) was 12% lower than general Russian population. The leukemia death rate in 96000 nuclear workers exposed to over 400 mGy was only half than predicted (*18, 205*).

Several epidemiological and biological studies conducted in the population residing in HLNRA of Kerala coast did not show any effect of elevated background radiation at any of the biological end point studied. However, recently Kumar et al. (2015) observed reduced induction and efficient repair of DNA strand breaks in HLNRA individuals as compared to individuals from NLNRA. These results clearly indicated the existence of *in-vivo* radio adaptive response of long

term low dose IR (LDIR). Since, HLNRA individuals are chronically exposed to low levels of background radiation for several years, they are assumed to be primed with small background doses and peripheral blood mononuclear cells (PBMCs) from these individuals will provide an ideal source to carry out *in vivo* radio-adaptive studies. Therefore, molecular markers might help in identifying radiation signature of low dose and low dose rate radiation exposure to human population.

Although, there are evidences to support the hypothesis of radiation hormesis or radio-adaptive response occurring in human cells exposed to a low dose followed by a high challenging dose exposure, one of the important limitations is the inter-individual variation existing in population. The health effects of LDIR may significantly vary between individuals depending on age, sex, genetic susceptibility, health status, variability in complexity of exposure etc (*201, 206-207*).

Several studies carried out in cell lines and animal models have suggested the activation of immune response (*208-211*), DNA repair pathways (*15, 17, 212*), gap-junction mediated cell-cell communication (*203*) and involvement of signaling pathways like p53 and MAPK pathway (*213*) in radiation hormesis or radio-protective response but still the exact underlying mechanism behind this phenomenon is not known.

The radiation induced bystander effect/response is a phenomenon in which un-irradiated cells exhibits the effects of radiation as a result of signal received from nearby irradiated cells (*18*). This phenomenon was first observed by Parsons et al. (1954) where they observed changes in bone marrow following X-ray therapy to the human spleen in chronic granulocytic leukemia (*214*). Later, in cultured cells exposed to low fluence α particle, the sister chromatid exchange was observed in >30% of the total cells, whereas only 1% of the cell nuclei were traversed by particles (*215*). Radiation induced bystander effects have been studied in a variety of *in vitro* models using a range of endpoints including clonogenic survival, mutations, neoplastic transformation, apoptosis, micronucleus, chromosomal aberrations etc. (*216-218*). Bystander response have been reported to be

induced by different types of irradiation, including α-particle, X-ray, γ-ray etc.(*214, 216, 218-219*). Molecular processes like gap junction intercellular communication and ROS have been shown to be involved in the induction of biological effect (*220*). Signaling cascades such as MAPK, NF-kappaB, TNFα have been implicated in bystander response (*18, 221-223*). Bystander effects have also be reported in various *in vivo* studies done on Chinese hamster and rat models where increased chromosomal damage was observed in the cells which were not directly exposed to radiation (*216, 224-226*).

Biological end points such as chromosome aberrations, micronuclei, DNA strand breaks and gene expression have been used to study radio-adaptive and bystander effects in human lymphocy-tes and cell lines. It has been observed that there is a narrow window period of 4-6 h for radio-adaptive response to occur and the phenomena is transient. However, the long term effect of natural background radiation exposure to human population and radio-adaptation is something to be explored.

1.11 Human peripheral blood mononuclear cells (PBMCs)

One of the most important aspects of population study on human subjects is the accessibility and ease of collection of sample and sensitivity towards genotoxic agent including IR. In recent years, efforts have been made to develop biomarkers for radiation exposure by employing more sensitive and high through put approaches such as genomics and proteomics to understand cellular responses to IR. PBMCs are considered to be highly sensitive in response to IR exposure and suitable for studying *in vivo* effects as well as *ex vivo* studies. PBMCs are mainly consists of circulating lymphocytes and monocytes and are easily accessible and less invasive to collect from human subjects which make it as a material of choice for radiation studies. Moreover,

PBMCs can be used as surrogate cells that may mimic effects occurring in remote target tissues of exposure (*227-228*).

1.12 Aims and Objectives of the thesis

In the present thesis, an attempt has been made to understand cellular and molecular effect of low dose radiation, which might provide a better understanding of the underlying biological processes occurring in human cells exposed to chronic low dose radiation. DSBs are most deleterious form of DNA damage and even a single unrepaired DSB may be potentially carcinogenic. An attempt has been made to quantitate/ measure DNA DSBs in human population residing in HLNRA and NLNRA using a sensitive assay. The basal level frequency of DNA DSBs was measured. Also, induction and repair of DSBs was studied in resting human cells after giving challenging doses. Gene expression changes were studied at chronic as well as acute exposure in resting PBMCs.

The aim is to understand the molecular basis of the DNA damage response in human cells on exposure to low dose IR. The objectives are as follows:

1. To study DNA damage and repair using gamma-H2AX as a biomarker
2. Transcriptome analysis of human population residing in normal and high level natural radiation areas:
    - To find out the differentially expressed genes (up/down regulated), if any.
    - Bioinformatic analysis to understand the molecular networks of differentially expressed genes and their involvement in various pathways.
    - To carry out validation of selected differentially expressed genes using real time q-PCR.
3. Evaluation of the changes in chromatin structure/conformation on exposure to low dose radiation.

Chapter 2

Materials and Methods

2.1 Collection of human blood samples

2.1.1 Ethics Statement

Venous blood samples were collected from random and healthy volunteers with fully informed and written consent which was approved by Medical Ethics Committee, Bhabha Atomic Research Centre, Mumbai, India.

2.1.2 Study Subjects and sample collection

Chronic exposure studies: For studying the effect of chronic low dose exposure on humans, venous blood samples were collected from inhabitants of HLNR and NLNR areas of Kerala coast. Blood samples were collected by venipuncture in EDTA containing vaccutainers (BD vaccutainers systems, U.S.A). For all the studies, healthy male individuals within similar age group (18-59 y), having no chronic illness, having similar dietary habits and lifestyle, with no recent medical radiation exposure was included from HLNRA and NLNRA. A detailed questionnaire was used to obtain information on age, gender, tobacco smoking, occupation, previous radiation exposure and medical history. All the volunteers were taken to the nearby hospital for blood collection. After collection, blood samples were transported to the laboratory in refrigerated conditions and processed immediately.

All the studies i.e. spontaneous frequency of DNA double strand breaks (DSBs), induction and repair kinetics of DSBs using gamma H2AX as biomarker, transcriptome analysis using microarray technique and gene expression studies using real time quantitative PCR (RT q-PCR) were carried out on PBMCs isolated form venous blood samples collected from these individuals.

Acute exposure studies: For studying the effects of acute low dose IR, venous blood samples were collected from random volunteers from Mumbai. Studies on DNA damage using gamma

H2AX, gene expression profile and chromatin conformational changes was carried out on PBMCs isolated from these individuals. Blood samples were collected in EDTA containing vaccutainers. All the volunteers were taken to pathology lab, Modular lab dispensary, BARC for collection of blood and it was transported to laboratory in refrigerated condition and processed with PBMC isolation immediately.

2.2 Dosimetry to measure external levels of gamma radiation in HLNRA and NLNRA

Dosimetry was carried out to measure the external gamma radiation levels in each donor's house. It was done using a halogen quenched Geiger Muller (GM) tube-based survey meter consisting of a GM tube and a microprocessor-based digital display (Type ER-709, Nucleonix Systems, India). Both inside house as well as outside house measurements were done. Measurements were done at a height of 1 m inside (in the living room) and outside (near the entrance) of each house. The mean of three readings was taken for each measurement. The survey meter readings measured exposure in air (μR/ h) due to gamma rays and were converted to annual absorbed dose (mGy/ y) by multiplying with 24 h x 365 days x 0.876 x 10^{-5}, where 0.876 is the conversion factor from exposure to absorbed dose (*9, 30, 51, 229*) . The occupancy factor of 0.5 was used to calculate the contribution of inside and outside exposure to total absorbed dose received by an individual. The sex and age specific occupancy factors were estimated in a previous study conducted in this population (*230*).

2.3 Isolation of peripheral blood mononuclear cells (PBMCs) from whole blood

PBMCs were isolated by density gradient centrifugation using Histopaque 1077^{TM} (Sigma Aldrich, USA) solution. Histopaque solution was transferred carefully to 15 ml sterile polypropylene centrifuge tube and overlaid with equal volume of whole blood. Mixing was avoided since it affects the quality of PBMC separation. Centrifugation was done at 2000 rpm for

30 min at room temperature (RT). Supernatant containing plasma and platelets was carefully removed and the interface opaque layer containing PBMCs was carefully aspirated and transferred to fresh sterile centrifuge tube. Equal volume of chilled isotonic phosphate-buffered saline (PBS) solution was added to the tube and cells were washed gently. Centrifugation was done at 1400 rpm for 10 minutes. Washing with isotonic PBS buffer removes contaminants such as Histopaque solution, plasma or platelets and gives a transparent pellet containing lymphocytes and monocytes. The pellet was washed twice with isotonic PBS buffer before used for further experiments. Cells were stained with 0.4 % trypan blue and viable cell count was obtained by using hemocytometer.

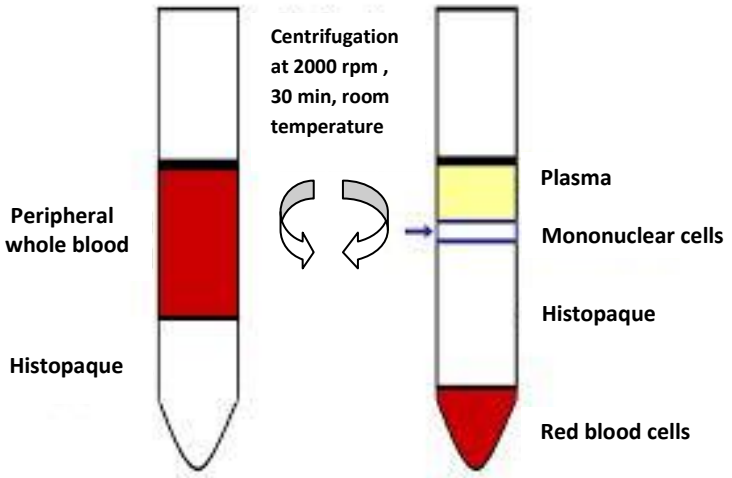

Figure 2.1: Schematic representation of separation of PBMCs from human blood by density gradient centrifugation.

2.4 Irradiation of PBMCs

PBMCs were separated and re-suspended in 1 ml RPMI medium containing 10% fetal bovine serum (FBS), 2mM L-glutamine and mixture of antibiotics (100µg/ml streptomycin and 100U/ml penicillin) and aliqoted into different tubes as per experiment and taken for irradiation.

2.4.1 Irradiation of PBMCs from HLNRA and NLNRA sample

For spontaneous or basal level frequency of DSBs and transcriptome analysis in HLNRA and NLNRA individuals, PBMCs were processed without giving any acute irradiation.

Induced DNA damage using gamma H2AX biomarker

Induced DNA DSBs were studied in 78 individuals (HLNRA, N=55 and NLNRA, N=23). PBMCs were separated and about 5-6 x 10^6 cells were obtained for each sample and aliqoted into four tubes (1-1.5 x 10^6 cells in each tube). Aliquots were irradiated with 0.25 Gy, 1.0 Gy and 2.0 Gy using a ^{60}Co gamma source (Low Dose irradiator-2000, BRIT, India) at a dose rate of 0.5 Gy/minute along with sham irradiated control (un-irradiated control). After irradiation, the tubes were immediately kept on ice and transferred to CO_2 incubator at 37ºC for 30 minutes.

DNA Repair kinetics using gamma H2AX biomarker

Repair kinetics of DSBs were studied in 30 individuals (HLNRA, N=22 and NLNRA, N=8) at 0.25 Gy and 2.0 Gy radiation doses at different time points between 0.5 to 24 h post irradiation. About 14-16 x 10^6 cells were obtained from each individual and was divided into 2 sets of 5 aliquots and a sham irradiated control aliquot, each aliquot had about 1-1.5 x 10^6 cells. For each sample, one set of aliquots was irradiated with 0.25Gy and another set of aliquots was irradiated with 2.0Gy. After irradiation, all the tubes were immediately kept on ice and transferred to CO_2 incubator at 37ºC. Aliquots were taken out and processed at different time intervals (0.5, 2.0, 4.0, 6.0 and 24 h) post-irradiation.

Transcriptional profile / Gene expression analysis after giving challenging dose

PBMCs were separated for each individual and divided into two aliquots (~1.5 to 2 x 10^6 per aliquot). One aliquot was used to study basal level of transcription profile in the individuals and another aliquot was irradiated with a challenging dose of 2.0 Gy and incubated for 4h at 37ºC

post irradiation. After incubation, cells were pelleted and re-suspended in 100µl RNA later solution (Sigma Aldrich, U.S.A) and stored at -20ºC till further processing.

2.4.2 Irradiation of PBMCs of Mumbai samples

DNA damage study: PBMCs were separated from 10 individuals and aliqoted into 5 tubes (about 1-1.5 x 10^6 cells per tube). PBMCs were irradiated with 0.25, 0.5, 1.0 and 2.0 Gy dose along with sham irradiated control. Irradiation was done using ^{60}Co gamma source (Bhabhatron II, Panacea Medical Technologies, Bangalore, India) at a dose rate of 1.0 Gy/minute at room temperature. PBMCs were incubated for 30 minute in CO_2 incubator and processed further.

***Gene expression studies*:** Study was carried out in 10 individuals. PBMCs were aliqoted into 2 sets and irradiated with 0.3, 0.6, 1.0 and 2.0 Gy doses with sham irradiated control. One set was processed immediately after irradiation (0 h) and the other set was processed after 4 h incubation at 37°C.

***Chromatin conformation studies*:** Study was carried out in 10 individuals. PBMCs were irradiated with 0.25, 1.0 and 2.0 Gy doses along with sham irradiated control. Irradiation was done using ^{60}Co gamma source (Bhabhatron II, Panacea Medical Technologies, Bangalore, India) at a dose rate of 1.0 Gy/minute at room temperature. PBMCs were incubated for 2 h in CO_2 incubator and processed further. ***Time kinetics experiment*:** PBMCs were isolated from 6 individuals. For each individual, cells were aliqoted in 5 tubes including sham irradiated control. PBMCs were irradiated with 1 Gy dose and incubated in CO_2 incubator for 15, 45, 90 and 120 minutes before proceeding with chromatin isolation.

2.5 DNA damage quantitation using gamma H2AX as biomarker

DNA damage in terms of DNA DSBs was studied in HLNRA and NLNRA populations using gamma H2AX as a sensitive and specific biomarker. Three different aspects were studied

1) Spontaneous frequency of gamma-H2AX foci (DSB) in HLNRA and NLNRA population 2) Induced DSBs after giving challenging doses 3) Repair kinetics of DSBs at different post irradiation timepoints. Fluorescence microscopy was employed to measure the spontaneous/basal level frequency of gamma-H2AX foci whereas for induced DSBs and repair kinetic studies, a high through-put approach of flow cytometry was employed.

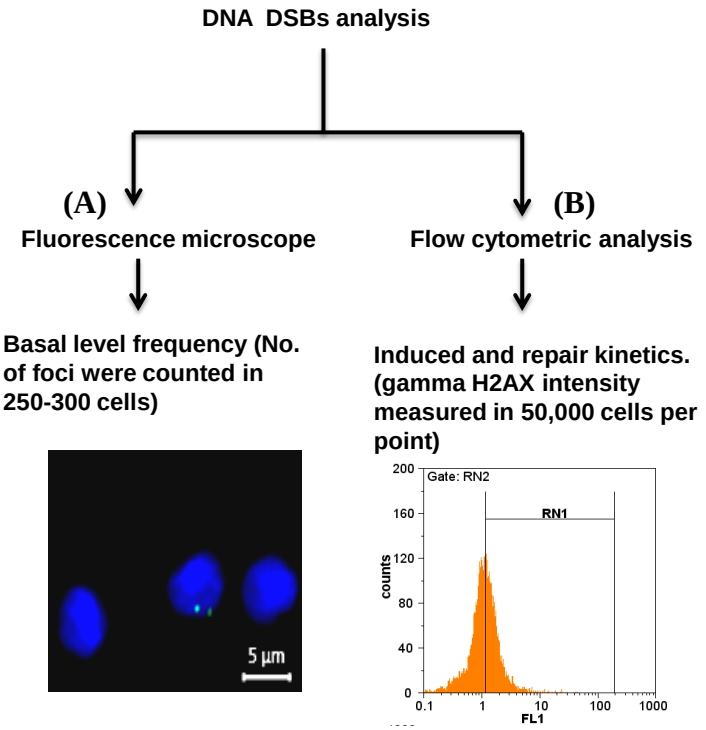

Figure 2.2: Schematic representation of DNA double strand break (DSB) analysis using gamma-H2AX biomarker. A) Gamma-H2AX foci analysis using fluorescence microscopy, B) Gamma-H2AX positive cells using flow cytometry.

2.5.1 Evaluation of basal level frequency of DNA double stand breaks (gamma-H2AX foci) using fluorescence microscopy.

The basal level/spontaneous frequency of gamma H2AX foci was measured in 91 individuals from NLNRA (N=30) and HLNRA (N=61) population. The HLNRA individuals were classified into Low Dose Group (LDG, 1.51-5.0 mGy/y) and High Dose Group (HDG, > 5.0 mGy/y).

Immunofluorescence staining*:* PBMCs were separated and re-suspended in 0.5 ml chilled PBS solution. Sample preparation for immunofluorescence assays was done as described elsewhere with few modifications (*231*). The cells were transferred in to a sterile 15 ml centrifuge tube containing freshly prepared chilled 1% formaldehyde solution (Sigma Aldrich). The suspension was mixed gently and kept for 15 min on ice for fixation. After fixation, tubes were centrifuged at 1500 rpm for 15 min at room temperature. Cells were washed with phosphate buffered saline (pH 7.5) and transferred to 1.5 ml sterile centrifuge tubes. PBMC were re-suspended in 70 % freshly prepared ethanol. The cells were stored at -20 °C till further processing and transported from our laboratory at Kollam, Kerala to BARC, Mumbai. In Mumbai, the tubes were centrifuged at 3000 rpm for 15 min and pellet was transferred to a fresh 1.5 ml tubes for further processing. PBMC were permeabilized with 0.2% Triton- X- 100 solution (Sigma) for 5 min at room temperature. Blocking was done with 1% bovine serum albumin (Sigma) and cells were incubated overnight at 4°C in 1:100 (0.1µg/ml) concentration of anti-phospho-histone H2AX (Ser139), antibody (Upstate-Millipore 05-636, CA, USA). After overnight incubation, cells were washed in 1% blocking solution and labeled with Alexafluor- 488 conjugated rabbit anti-mouse antibody (Molecular probes A-11059, Eugene, USA) for 1 hr at room temperature. After secondary antibody incubation cells were washed with PBS and diluted to a concentration of approximately 1 x 10^6 cells / ml. Around 100 µl of this cell suspension was layered onto poly-l-lysine coated coverslips (BD BioCoat™ 354085, USA). Coverslips were kept for 30 min at room temperature for adherence, washed with phosphate buffered saline and mounted onto glass slides using Prolong Gold Antifade DAPI (4',6-diamidino-2-phenylindole) reagent (Molecular Probes P 36931, USA).

Fluorescence microscopy : Imaging was carried out in dark at 40x magnification using fluorescence microscope (Carl Zeiss, Germany) equipped with DAPI and alexafluor filters. Two slides were prepared for each sample. Around 20-25 random images were captured from both the slides. About 250-300 independent cells were scored manually for gamma-H2AX foci for each individual. Scoring was carried out manually from the merged image obtained from DAPI and alexafluor filters. All the samples were blind coded and no information was known about the individual during the preparation and scoring of the slide. The number of gamma-H2AX foci seen in the cells was recorded. The information about multiple foci observed in the cells was also recorded. The results were analyzed as mean frequency of foci per cell. The mean frequency of foci was calculated by dividing the total number of foci observed by total number of cells scored for each sample. After completing the scoring the samples were classified according the background dose received by the individuals.

2.5.2 Measurement of induced DSBs and their repair kinetics using flow cytometry

Induced DSBs were measured in the PBMCs of 78 individuals (HLNRA, N=55 and NLNRA, N=23) after giving challenging doses of 0.25, 1.0 and 2.0 Gy. PBMCs were incubated at 37 ºC in CO_2 incubator (5%) for 30 minute. A subset of 30 individuals was taken to study repair kinetics of DSBs at different time points 0.5, 2, 4, 6 and 24 h post-irradiation after giving a challenging doses of 0.25 Gy and 2.0 Gy. After incubation was over, tubes were centrifuged at 3000 rpm for 10 minute and supernatant was removed. Cells were resuspended in 0.5 ml PBS and transferred to 1 % formaldehyde solution for fixation. PBMCs were processed and labeled with primary and secondary antibodies as described in previous section. After secondary antibody incubation was over, cells were washed and counterstained with DAPI (5µg/ml) stain for 30 minute at room temperature and taken for flow cytometric analysis.

Flow cytometry

Approximately 50000 cells were analyzed for each dose point or time point studied. Appropriate isotype controls were included during the measurements. Gating was done in order to include DAPI stained singlet cells in G_0/G_1 phase for analysis. The results were analyzed as percentage change in gamma H2AX positive cells at different experimental points as compared to control. The percentage of gamma-H2AX positive cells at different dose points and time points were normalized by subtracting the percentage of gamma-H2AX positive cells observed in sham-irradiated control. Analysis was carried out using FloMax software (Partec) and Cyflogic software (Version 1.2.1, www.cyflogic.com). In repair kinetics experiments, the percentage of repair was calculated at different time-points by using the formula (maximum DNA damage observed − damage at time 'T' after irradiation) / maximum DNA damage observed) × 100.

2.6 ***Global gene expression profiling (Transcriptome analysis) using high throughput microarray technique***

Global gene expression profiling was carried out using Human Genome U133 Plus 2.0 GeneChips (Affymetrix, U.S.A) in 36 individuals from HLNRA (N=27) and NLNRA (N=9). These probe arrays are high-density oligonucleotide microarrays which analyzes the expression level of up to 47,000 transcripts and variants representing almost 30,000 human genes. Each transcript is measured by 11 different 25mer oligonucleotide probes. Advantages of Affymetrix GeneChip arrays include highly standardized array fabrication, as well as standardized target preparation, hybridization, and processing protocols, resulting in low technical variability and good reproducibility between experiments. Venous blood samples were collected and PBMCs were separated. PBMCs were suspended in RNA later solution (Sigma) and stored at -20ºC till further processing. Multiple aliquots were prepared from each sample and used for microarray

experiment as well as validation of selected genes using real time q-PCR. A schematic representation is shown in figure 2.3.

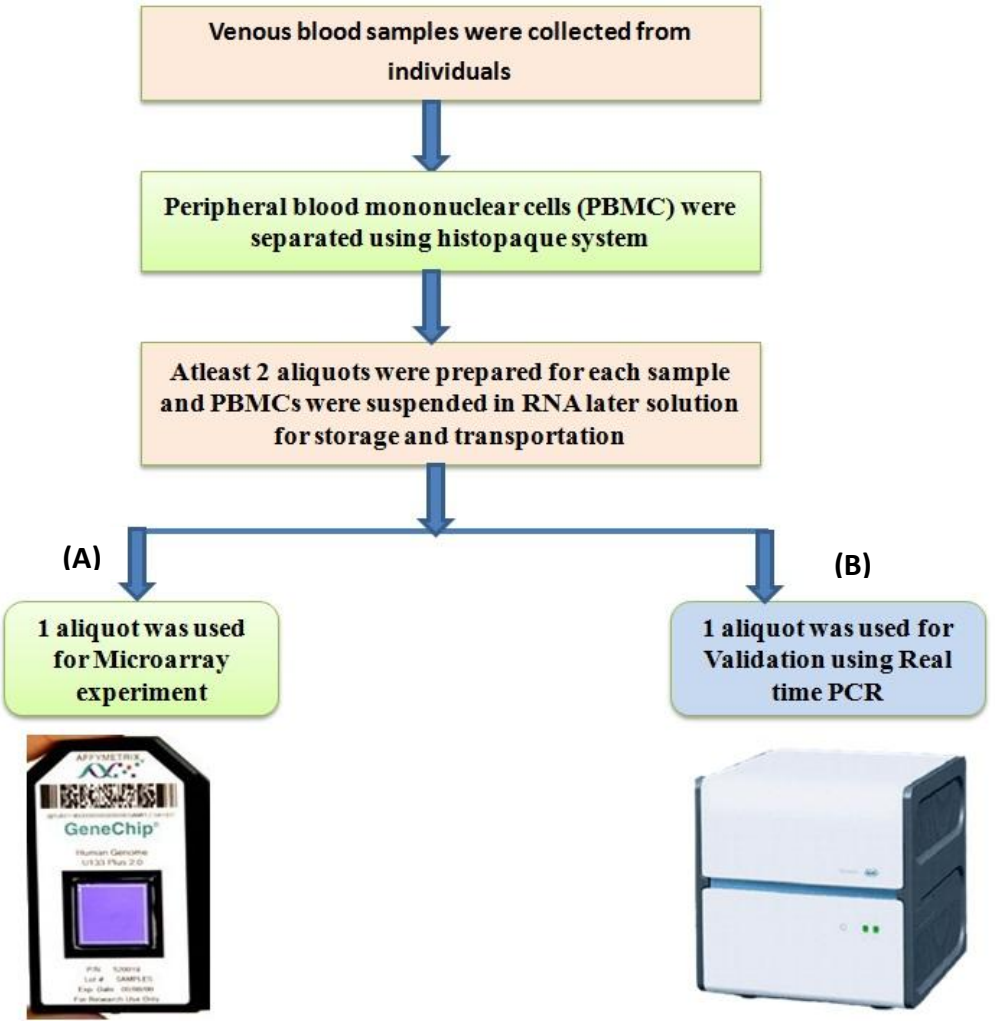

Figure 2.3: Schematic representation of gene expression analysis from human peripheral blood mononuclear cells (PBMCs). A) transcriptome analysis using affymetrix chip B) validation of gene expression using hydrolysis probe based real time q-PCR (LC480, Roche Diagnostics Pvt. Ltd.).

2.6.1 Isolation of total RNA

Total RNA was isolated from PBMCs using RNeasy Mini Kit (Qiagen, U.S.A) as per manufacturer's instructions. In brief, PBMCs stored in RNA later (Sigma Aldrich, U.S.A) were

centrifuged at 3000 rpm for 10 min. Supernatant was discarded and cells were washed with 1X PBS solution. After centrifugation, cell pellet was re-suspended in 350 µl lysis buffer (premixed with 10 µl of 14.5 M β- mercaptoethanol/ ml of lysis buffer) and mixed thoroughly. The cells were homogenized by vortexing for 1 min at 14000 rpm. The lysate was pipetted on to QIAshredder column and centrifuged for 2 min at 14000 rpm. This step removes insoluble debris and reduces the viscosity of the lysate. Further, 350 µl of 70 % ethanol was added to the lysate and mixed well by pipetting. Ethanol promotes selective binding of RNA to mini-spin column. All 700 µl of lysate was added onto RNeasy mini spin column and centrifuged for 15 sec. at 10,000 rpm. After binding, 700 µl of high salt pre-wash buffer was added and column was centrifuged for 15 sec at 10,000 rpm. Flow through was discarded and column were transferred into fresh 2 ml tubes and the membrane was washed twice with 500 µl of wash buffer containing absolute alcohol in 1: 4 proportion. The column was transferred to a fresh tube and centrifuged at 10,000 rpm for 2 min to remove any remnant of wash buffer and completely dry the membrane. It is essential to remove residual ethanol since it may interfere with elution of RNA. The column was transferred to fresh tube and 30 µl of elution buffer was added to it and centrifuged at 10,000 rpm for 1 min. The elute was stored at -80°C until further use. Repeated freeze and thaw of the sample was avoided which may cause denaturing of RNA.

2.6.2 RNA Purity and Integrity

RNA quality is of utmost importance for gene expression studies using microarray as well as RT q-PCR. RNA samples should be free from contaminating proteins, DNA, and other cellular material as well as ethanol and salts associated with RNA isolation procedures. Impurities can lower the efficiency of reverse transcription and subsequently reduce the level of amplification. The quality and quantity of isolated RNA was checked using NanoDrop® ND-1000

spectrophotometer (NanoDrop technologies). The RNA purity was assessed by measuring the ratio of absorbance readings at 260 and 280 nm. The ratio of A260 to A280 values was in the range of 1.8–2.1. The integrity of the RNA sample, or the proportion that is full length, is another important component of RNA quality. Reverse transcribing partially degraded mRNAs will generate complementary DNA (cDNA) that may lack portions of the transcripts that are interrogated by probes on the array. The integrity of isolated RNA was evaluated with microfluidic capillary electrophoresis using the Agilant 2100 Bioanalyzer with RNA LabChip® Kit (Agilent technologies). Primarily full-length RNA transcripts with ratio of 28S to 18S rRNA bands of 2:1 were used for the experiments. RIN (RNA integrity number) was calculated for all RNA samples and samples with RIN value of greater than 8.0 were taken for microarray experiments.

2.6.3 cDNA preparation, RNA amplification, labeling and hybridization

GeneChip®3′ IVT Express Kit (Affymetrix) was used for the preparation of biotin-labeled amplified RNA (aRNA). All the procedures were conducted according to manufacturer's instruction (Affymetrix). Briefly, 100 ng of total RNA was reverse transcribed to synthesize first strand cDNA using an oligo (dT) primer containing the T7 RNA polymerase promoter site provided with Labeling Kit. Second strand of cDNA was synthesized from single stranded cDNA using DNA polymerase and RNase H to simultaneously degrade the RNA and synthesize double stranded cDNA. In vitro transcription and amplification was carried out to synthesize multiple copies of biotin-labeled aRNA from double stranded cDNA templates. The aRNA was then purified to remove unincorporated nucleotide triphosphates, salts, enzymes, and inorganic phosphate. Prior to fragmentation and hybridization onto Human Genome U133 Plus 2.0 GeneChip expression arrays the aRNA concentration was measured using NanoDrop® ND-1000

spectrophotometer (NanoDrop technologies) and size of aRNA fragments were analysed using bioanalyzer and RNA 6000 nano kit (Agilent). The fragmentation of amplified RNA was carried out to produce a distribution of 35-200 nucleotide, aRNA fragments with a peak at approximately 100-200 nucleotide. The optimal fragmentation is necessary for optimal assay sensitivity. 12.5 µg of aRNA was hybridized onto Human Genome U133 Plus 2.0 GeneChip expression arrays using GeneChip hybridization, wash and stain kit (Affymetrix). Genome arrays were hybridized for 16 hours at 45°C following the affymetrix protocol. Following washing and staining, the GeneChips were scanned using the Affymetrix GeneChip Scanner 3000. The raw data file formats were generated using GeneChip operating software (GCOS). The schematic representation is shown in figure 2.4.

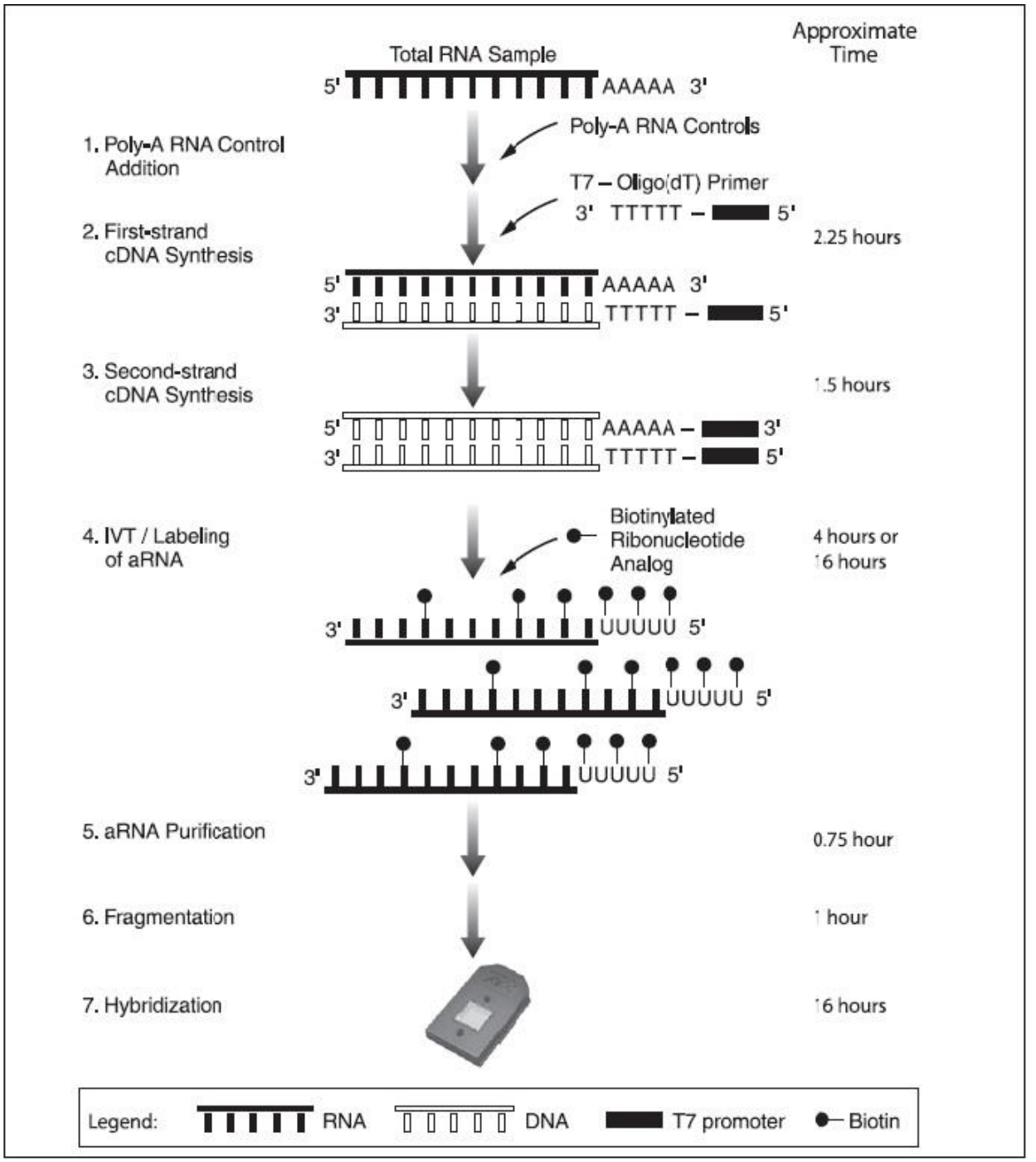

Figure 2.4: An overview of the steps involved in in-vitro amplification of RNA used in microarray experiment. Schematic representation of cDNA conversion from total RNA, in vitro transcription and labeling of amplified RNA, and hybridization to Gene Chip is shown (source: Affymetrix lab manual).

2.6.4: Data Analysis

The data analysis process involved sample processing (probe level background correction, normalization, probe-set summarization), quality check, differential expression analysis and gene enrichment analysis. Each analysis has been described in detail below:

2.6.4.1 Sample processing

.CEL (probe intensity) files obtained for each sample were processed through RMA (Robust multichip analysis) algorithm, which consists of probe level background correction, normalization and probe set summarization. In order to detect if the expression data for any sample has any abnormalities, the intensity distribution of samples is seen through Box plots in figure 2.5.

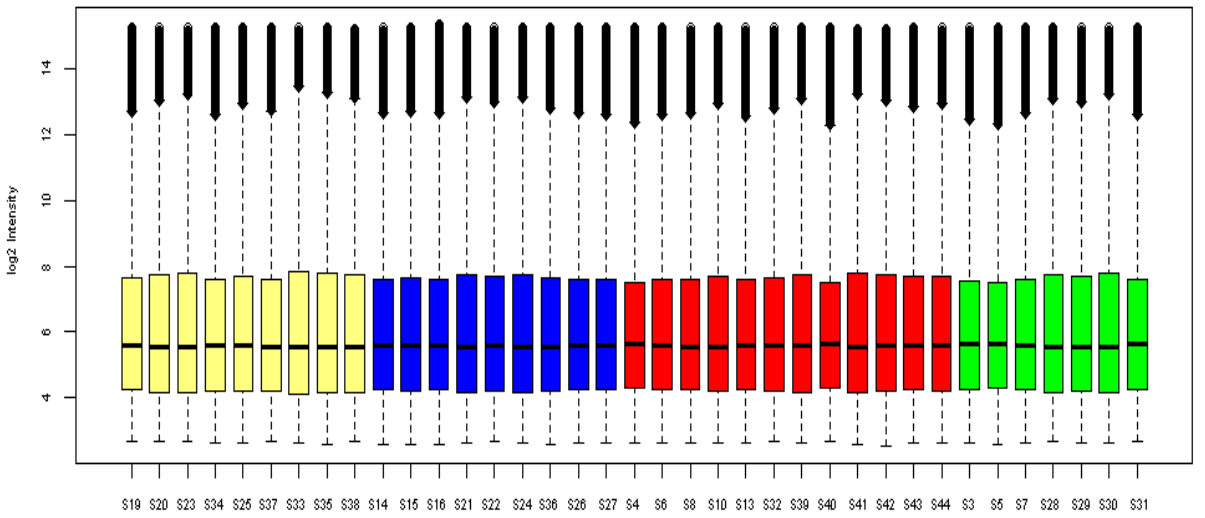

Figure 2.5: Box plot showing Robust multichip analysis (RMA) normalized intensity distribution obtained after background correction of the samples used for microarray analysis.

2.6.4.2 Quality Check (QC) and Controls

To assess the sample quality and to identify samples with unusual behavior, quality checks were performed at various levels. These include Chip parameter analysis, RNA degradation analysis, and sample correlation analysis. Details of each have been given below:

Chip Parameter Analysis: RPT file was generated for each chip, which consists of various chip parameters that could be used to assess the quality of chip. Values for these parameters were computed from MAS 5.0 algorithm. These parameters include:

Raw Q: Pixel-to-pixel variation among the probe cells used to calculate background. Acceptable value: < 3

***Average background*:** This was similar across all chips. If chips have significantly different average backgrounds this could be due to different amounts of aRNA were present in the hybridization cocktails, or because the hybridization was more efficient in one of the reactions, incorporating more label and producing a brighter chip.

% Present Calls: Present/Marginal/Absent calls were generated for each probe set, using MAS 5.0 algorithm recommended by affymetrix. % Present calls studied for each sample and observed to be more than 40% for all the samples. The samples qualified for the downstream analysis as per affymetrix recommendations.

***Scale factors*:** MAS 5.0 algorithm scales the intensity for every sample so that each array has the same mean. The amount of scaling applied is represented by the 'scale factor', which provides a measure of the overall expression level for an array and a reflection of how much labeled RNA is hybridized to the chip. Large variations in scale factors occur if there have been significant issues with RNA extraction, labeling, scanning or array manufacture. As recommended by affymetrix, all our samples had scale factors within 3-fold of one another.

***3':5' ratios*:** Most cell types ubiquitously express β-actin and GAPDH. These are relatively long genes, and the majority of Affymetrix chips contain separate probe sets targeting the 5', mid and 3' regions of their transcripts. By comparing the amount of signal from the 3' probe set to either the mid or 5' probe sets, it is possible to obtain a measure of the quality of the RNA hybridized to the chip. If the ratios are high then this indicates the presence of truncated transcripts. Hence, the ratio of the 3' and 5' signal gives a measure of RNA quality. GAPDH is the smaller of the two genes and the 3':5' ratio or 3': mid ratio should always be at or around 1. Affymetrix suggests that a β-actin 3':5' ratio of less than 3 is acceptable. All our samples had ratio within the permissible limits.

Spike-in controls (hybridization controls): In order to verify the efficiency of the hybridization step, some additional labeled aRNAs are added during the latter stages of the sample preparation protocol. These transcripts (BioB, BioC, BioD and CreX) are derived from *Bacillus subtiliis*. Ideally, BioB should be called present on every array: an acceptable level is for it to be called present on 70% of the chips in an experiment.

These chip parameters have been graphically represented in figure 2.6. The dotted vertical lines indicate scale ranging from -3 to 3. Each row shows the %present, average background, scale factors and GAPDH / beta-actin ratios for a chip.

● *GAPDH* 3': 5' (or 3': mid) values are plotted as circles. According to Affymetrix, they should be about 1. *GAPDH* values that are considered potential outlier (ratio > 1.25) are colored red, otherwise they are blue.

● *beta-actin* 3' : 5' (or 3': mid) ratios are plotted as triangles. Since the gene is longer, the recommendation is that the 3' : 5' (or 3': mid) ratio should be below 3. The values below 3 are colored as blue and those above as red.

● The blue strip in the image represents the range where scale factors are within 3-fold of the mean for all chips. Scale factors are plotted as a line from the middle line of the image. A line to the left corresponds to down-scaling and to the right corresponds to up-scaling. If any scale factors fall outside this ´3-fold region', they are all colored as red, otherwise they are blue.

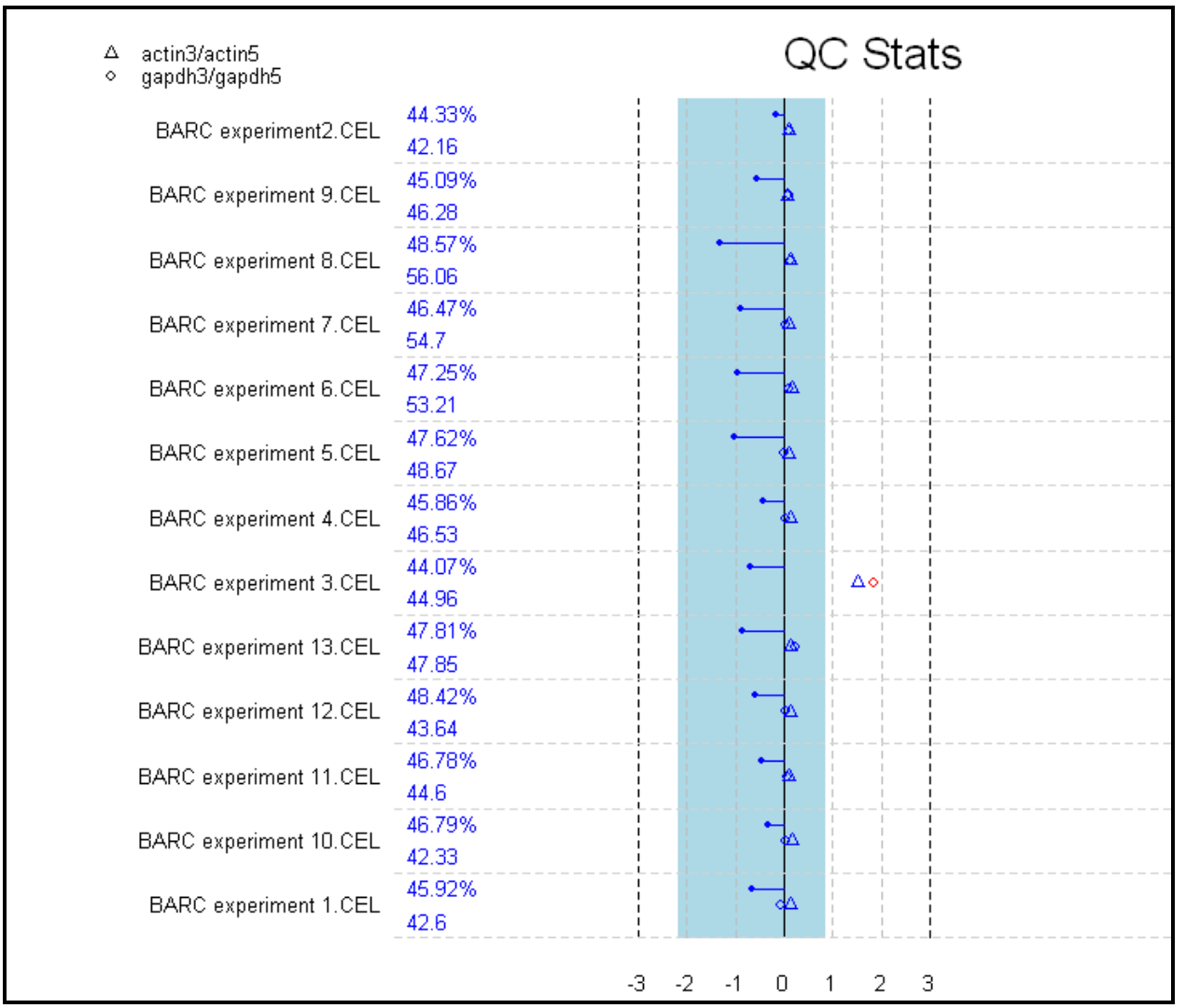

Figure 2.6: Graphical representation of chip parameters of the representative samples used in microarray experiment. The dotted vertical lines indicate scale ranging from -3 to 3. Each row shows the % present, average background, scale factors and *GAPDH / beta-actin* ratios for a chip. Circle represents *GAPDH* values and triangle represents beta-actin. The value in red circle shows the outlier.

RNA Degradation plot

RNA degradation plot assesses the differences in the quality of the RNA used in each array. It is known that degradation usually starts at the 5' end of the RNA molecule and finishes in the 3'. Therefore, for each transcribed gene in our samples, we would expect to find less chunks of RNA coming from near the 5' end than from the 3' end. After labeling and hybridization, within each probe set we find that the probes matching close to the 5' end have lower intensity measures than the probes matching closer to the 3' end. RNA degradation plots show expression as a function of 5'-3' position of probes. For each array and within each probe set, probes are arranged by their proximity to the 5' end of the gene. The plot shows the average intensity of the probes classified by this order. Each line corresponds to an array and the slope of its trend indicates potential degradation of the RNA hybridized to the array. In general, larger the slope, the more could be the degradation of the sample. Nevertheless, the purpose of this plot is to highlight differences in the laboratory treatments of the arrays. Plots showing lines with different trends (not parallel) correspond to groups of arrays having different degradation patterns and indicate possible differences in the laboratory procedures (Figure 2.7).

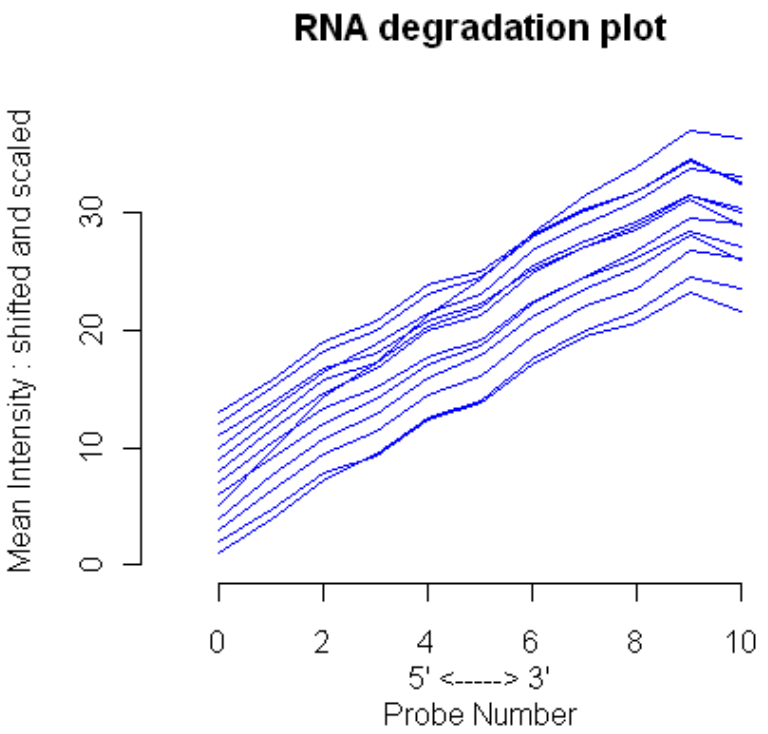

Figure 2.7: Representative image of RNA degradation plot of some of the representative samples used in microarray experiment. The plot shows the average intensity of the probes from 5' to 3' end. Each line corresponds to an array and the slope of its trend indicates potential degradation of the RNA hybridized to the array. X-axis represent probe number, Y-Axis represents mean intensity

Sample Correlation Analysis

Pair-wise correlations between the samples were studied through Pearson's correlation coefficient. A coefficient value close to 1.0 indicates linear relation between the two arrays. The plot depicting the correlations is shown in Figure 2.8. The minimum correlation between the sample was 0.95, which was above the acceptable criterion of 0.8.

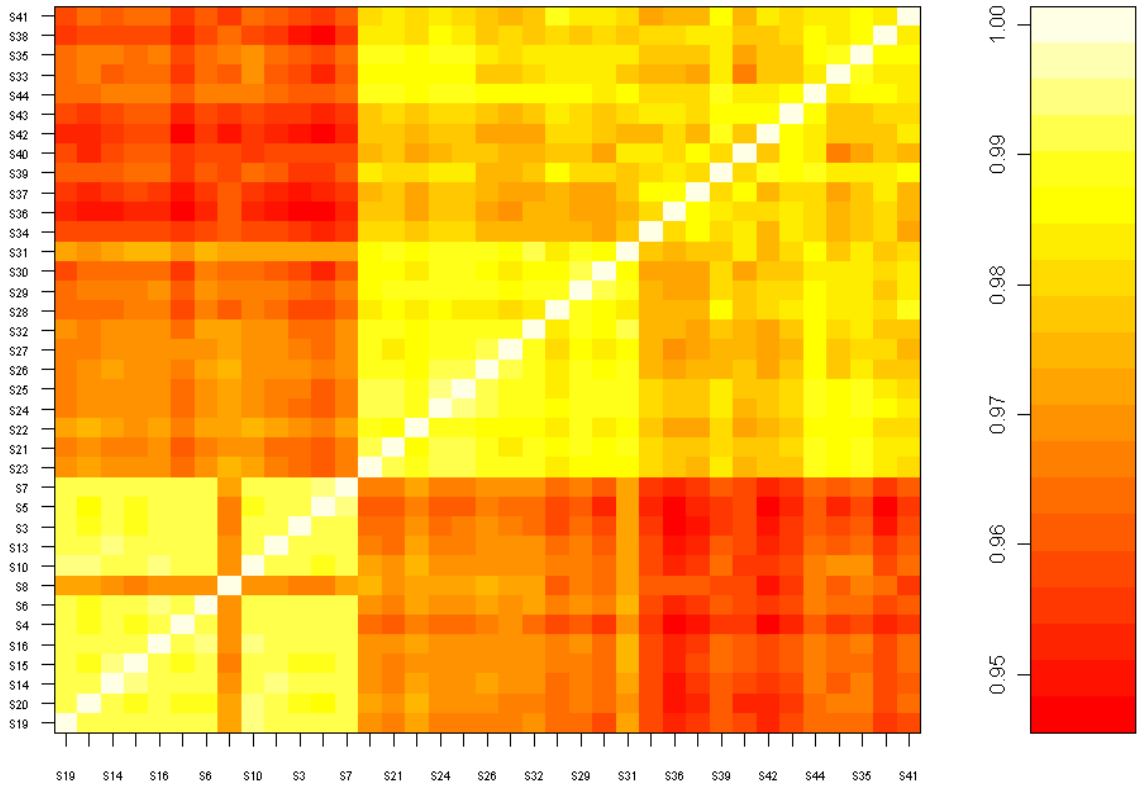

Figure 2.8: Sample correlation plot showing pair-wise correlation between the samples used in microarray experiment. Color panel represents the range of correlation coefficient obtained in the samples used in microarray experiment. Red to yellow represents increasing coefficient.

2.6.4.3 Differentially expressed genes

All samples (chips) were normalized, filtered and analysed with R software. Robust Multichip Analysis (RMA) normalization method was used for background correction, normalization and calculation of expression values. Baseline was set to median for all samples, where median of the log-transformed value of each probe from all samples was calculated and this value was subtracted from all samples. Multiple testing correction was performed using Benjamini and Hochberg False Discovery Rate (FDR). Identification of differentially expressed genes was performed with the Limma package available on Bioconductor. For each gene in the set of all arrays a linear model was fitted. The statistics used for significance analysis is the moderated t-

statistic, which is computed for each probe and for each contrast. To reduce the risk of false-positive, p-values were adjusted for multiple testing issues using Benjamini and Hochberg's method to control the false discovery rate (FDR). A gene was considered differentially expressed when the corresponding adjusted p-value ≤ 0.05 and the fold change greater than 1.3.

2.6.4.4 Gene Ontology and pathway analysis:

To determine the biological significance of the differentially expressed genes, functional classification was performed using Gene Ontology (GO) analysis. This classifies the genes into relevant ontology terms dealing with biological processes, molecular function and cellular component. The overabundance of a particular term could be decided based on the number of significant genes in the analysis, the number of significant genes relevant to the term. Fisher's exact test was used to determine the significance of the GO term. The threshold significance was set at $p \leq 0.05$. Similarly pathways analysis was carried out. Bioinformatic analysis was carried out using Genowiz and Explain 3.0 (Biobase database) software's. In the present study, for GO analysis, the data from Gene Ontology consortium was used, while for pathways, human KEGG pathways were referred.

2.7 Gene expression study at chronic and acute doses using real time q-PCR

Validation of selected differentially expressed genes from microarray data, Radio-adaptive response at transcriptional level in HLNRA and NLNRA individuals and gene expression changes at acute radiation exposure was carried out using sensitive and specific hydrolysis probe based approach in real time RT q-PCR. For validation, a total of 30 genes were selected from microarray data and their expression levels were validated in 54 individuals. The validation was carried out in two sets of individuals: the first set of 30 individuals was from microarray experiment and the second set of 24 random individuals was collected separately. PBMCs were

separated, re-suspended in RNA later solution and stored at -20ºC till further use. For radio-adaptive study, the background radiation doses received by HLNRA individuals were considered as priming dose and PBMCs from 20 individuals (HLNRA, N=10 and NLNRA, N=10) were separated and divided into 2 aliquots. mRNA expression at basal level and after giving a challenging dose with 2.0 Gy was studied. Gene expression of selected genes from microarray data was carried out at different acute doses (0.3 – 2.0 Gy). PBMCs were irradiated in two sets. One set was processed immediately after irradiation (0 h) and the other set was processed after 4 h incubation at 37°C.

2.7.1 Isolation of total RNA from human PBMCs

Total RNA was extracted from PBMCs using HiPurA™ Total RNA Miniprep Purification Kit (Hi-Media Laboratory Pvt. Ltd., India) as per manufacturer's protocol. In brief, about 350 µl of RNA lysis solution was added to PBMCs and mixed thoroughly. The cells were homogenized for 1 min by vortexing. This solution assists in cell disruption and denaturation. The lysate was added to 2.0 ml collection tube containing HiShredder and centrifuged for 2 min at 14,000 rpm. Further, about 350 µl of ethanol (70%) was added to the homogenized lysate and mixed thoroughly by pipetting. The lysate was added to HiElute Miniprep Spin Column and centrifuged for 30 sec at 14,000 rpm. After the binding step, prewash solution (700 µl) was added to the HiElute Miniprep Spin Column and centrifuged at 14,000 rpm for 30 sec. The flow through was discarded. Further, 500µl of wash solution was added to the HiElute Miniprep Spin column and centrifuged for 2 min at 14,000 rpm to dry the membrane. This short washing step was used to remove impurities like proteins, polysaccharides, low molecular weight metabolites and salts from the membrane. The HiElute Miniprep Spin column was transferred to a new 1.5 ml collection tube. Approximately 30 µl Elution Solution (RNase-Free Water) was directly added to

the HiElute Miniprep Spin 42 column and centrifuged for 1 min at 14,000 rpm. The elute was stored at -80°C. Repeated freeze and thaw of the sample was avoided which may cause denaturing of RNA.

2.7.2 RNA integrity and cDNA synthesis

RNA was quantified using Picodrop Microlitre Spectrophotometer (picodrop limited, UK) and the purity was checked by taking the ratio at 260 and 280 nm. RNA bands were visualised on agarose gel, which was stained with ethidium bromide. RNA samples with clear-cut 28S and 18S bands in 2:1 ratio were used for cDNA synthesis (Figure 2.9). Total RNA (250 ng) was reverse transcribed to cDNA using transcriptor high fidelity cDNA Synthesis kit (Roche Diagnostics Pvt Ltd. GmbH, Germany). The mixture containing total RNA (template) and 60 μM random primer was denatured by heating the tube at 65°C in a thermocycler with a heated lid (to minimize evaporation). This step ensures denaturation of RNA secondary structure. The tube was immediately cooled on ice. The mixture containing 1X buffer, 20 U RNase inhibitor, 5 mM DTT, dNTPs (1 mM each) and reverse transcriptase (10 U) was added to template-primer mixture. The tubes were heated at 50°C for 30 min followed by 85°C for 5 min. cDNA was stored at -20°C until further use.

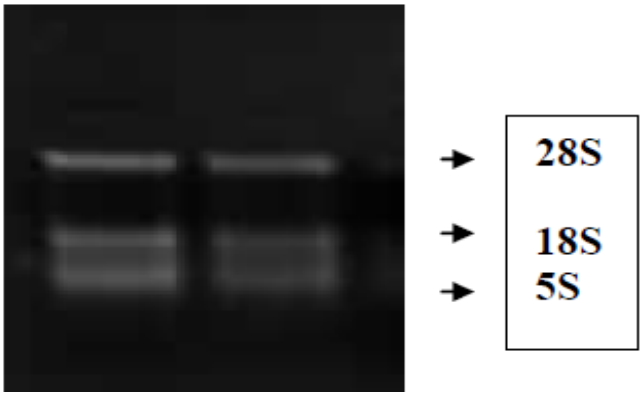

Figure 2.9 Ethidium bromide stained agarose gel (1%) showing different bands for total RNA (28S, 18S and 5S) [where S stands for Svedberg constant which is related to sedimentation rate]

2.7.3 Quantitation of relative gene expression using hydrolysis probe based real time q-PCR

Intron spanning PCR primers were designed using Probe finder software version 1.1 (www.universalprobelibrary.co) and specific hydrolysis probes from universal probe library (UPL) set for Humans (Roche Diagnostics Pvt. Ltd. GmbH, Germany) were used. All the primer sets were procured from Sigma Aldrich, USA. Primer sequences used in the study are given in table 2.1. PCR conditions were standardized for all the primer sets to obtain a clean and smooth amplification curves as well as single and desired amplicon (Figure 2.10 and 2.11).

Table: 2.1 Details of primer sequences, product size and UPL probe numbers of the genes studied using Real time q-PCR.

S No.	Gene Symbol	Primer Sequence (5’ - 3’)	Base pair (bp)	Product Size (bp)	Probe number
1	*SNRPA1*	PR1 5’ TCC GCA AGT CAG AGT ACT GG 3’ PR2 5’ CCG TTT GCC CTT GAA CAT T 3’	20 19	82	38
2	*METTL13*	PR1 5’ GCT GAG CTG TCG GCT AGA GT 3’ PR2 5’ ACA GAC AGA AAG GGG ACC TG 3’	20 20	77	33
3	*ATXN1*	PR1 5’ GAG CCT GTG GGA AGTCTC C 3’ PR2 5’ CAA CAG CAG CTC TGG ATG AA 3’	19 20	95	30
4	*NAMPT*	PR1 5’ GCC AGC AGG GAA TTT TGT TA 3’ PR2 5’ GCC ATT CTT GAA GAC AGT ATG GA 3’	20 23	91	65
5	*KIR3DS1*	PR1 5’ GGT CAA AAT CCC TTT CAC CA 3’ PR2 5’ TGG TCC ATT ACA GCA GCA TT 3’	20 20	85	35
6	*DHFRL1*	PR1 5’ TGA TGC CTT AAA ACT TAC TGA ACG 3’ PR2 5’ ATG GCC TAG GTG ATT CAT GG 3’	24 20	109	87
7	*PDK4*	PR1 5’ CAG TGC AAT TGG TTA AAA GCT G 3’ PR2 5’ TGG TCA TCT GGG CTT TTC TC 3’	22 20	79	31

S No.	Gene Symbol	Primer Sequence (5’ - 3’)	Base pair (bp)	Product Size (bp)	Probe number
8	*GADD45B*	PR1 5’ CAT TGT CTC CTG GTC ACG AA 3’ PR2 5’ TAG GGG ACC CAC TGG TTG T 3’	20 19	110	10
`9	*CDKN1A*	PR1 5’ CGA AGT CAG TTC CTT GTG GAG 3’ PR2 5’ CAT GGG TTC TGA CGG ACA T 3’	21 19	111	82
10	*PLK3*	PR1 5’ GAA GGT GGG GGA TTT TGG 3’ PR2 5’ GGG TGC CAC AGA TGG TCT 3’	18 18	74	6
11	*DDIT3*	PR1 5’ CAG AGC TGG AAC CTG AGG AG 3’ PR2 5’ TGG ATC AGT CTG GAA AAG CA 3’	20 20	95	9
12	*JUND*	PR1 5’ CAG CGA GGA GCA GGA GTT 3’ PR2 5’ GAG CTG GTT CTG CTT GTG TAA AT 3’	18 23	70	81
13	*KLF6*	PR1 5’ CTT CTC AAC TGT GGG GTT GC 3’ PR2 5’ TTC CCA TGA GCA TCT GTA AGG 3’	20 21	107	2
14	*EIF1*	PR1 5’CCA GAA CCT CCA CTC TTT CG 3’ PR2 5’GCC GTT TCT CTG TTG AAT TCT T 3’	20 22	109	04
15	*ZNF167*	PR1 5’ TGG AAA AGT CTC ACA CTC AGT CA 3’ PR2 5’ CCC TTC ATC ATG TTC TCA CCT 3’	23 21	101	86

S No.	Gene Symbol	Primer Sequence (5’ - 3’)	Base pair (bp)	Product Size (bp)	Probe number
16	BTG1	PR1 5’TGC AGA CCT TCA GCC AGA G 3’ PR2 5’ATC CCT TGC ATG GCT TTT C 3’	19 19	84	17
17	THAP2	PR1 5’TTG ACC TAA CAG GAC AAA CTC G 3’ PR2 5’AAA AGA TTC CTT GAC TTG AGT TTC A 3’	22 25	106	89
18	KDM6B	PR1 5’CAC CCA CTG TGG TCT GTT GT 3’ PR2 5’TGT CTC CGC CTC AGT AAC AG 3’	20 20	96	3
19	PAPD4	PR1 5’TGG AAA TGT CAG TCC AAT ACA GA 3’ PR2 5’ACC GTC AAG AGG AAG GTT TTT 3’	23 21	91	60
20	PMAIP1	PR1 5’GGA GAT GCC TGG GAA GAA G 3’ PR2 5’CCT GAG TTG AGT AGC ACA CTC G 3’	19 22	94	67
21	*TSC22D2*	PR1 5’TGA ACA GTC TGG CCA CCT C 3’ PR2 5’ACG CTT GGT AGA AAG CAG TTG 3’	19 21	90	9
22	DUSP10	PR1 5’TGA ATG TGC GAG TCC ATA GC 3’ PR2 5’TGG CAA TTC AAG AAG AAC TCA A3’	20 22	92	22
23	*GIMAP8*	PR1 5’ACG GAG GAC CCT ATC ATG TG 3’ PR2 5’TGC AGC TTC ATT CAC ACA ATC 3’	20 21	71	8
24	JUN	PR1 5’CCA AAG GAT AGT GCG ATG TTT3’ PR2 5’CTG TCC CTC TCC ACT GCA AC3’	21 20	62	19

S No.	Gene Symbol	Primer Sequence (5’ - 3’)	Base pair (bp)	Product size (bp)	Probe number
25	*DUSP1*	PR1 5’TTC AAC GAG GCC ATT GAC TT 3’ PR2 5’CCT GGC AGT GGA CAA ACA C 3’	20 19	70	65
26	*CSRNP1*	PR1 5’CCT GCC TGA CCG TGA CTT 3’ PR2 5’AGC CCG CTT CAG GAT AGA C 3’	18 19	64	57
27	*PPIF*	PR1 5’ GAA GGG CTT CGG CTA CAA A 3’ PR2 5’ CAT TGT GGT TGG TGA AGT CG 3’	19 20	86	39
28	*CCR2*	PR1 5’ TGA GAC AAG CCA CAA GCT GA 3’ PR2 5’ TTC TGA TAA ACC GAG AAC GAG AT 3’	20 23	104	56
29	*BBS10*	PR1 5’ TTC TCA GCC GGA ATG GAG 3’ PR2 5’ GAT GAC TGG AAA CAC AGT CCA C 3’	18 22	90	79
30	*SETDB2*	PR1 5’GGC ATT CTT CAC CAA CAG GT 3’ PR2 5’CCC ACA TTG GCA GAA GAT TT 3’	20 20	106	33
31	*HIST1H2B*	PR1 5’ AGC CAG CCA AGT CTG CTC 3’ PR2 5’ TCT TTC TTC TGC GCT TTG GT 3’	18 20	70	8
32	*XRCC4*	PR1 5’CTT GGG ACA GAA CCT AAA ATG G 3’ PR2 5’GAC GTC TCA GGT AGT GAA GAA TCA 3’	22 24	132	15
33	*LIG4*	PR1 5’AGT CCA CCA TCG CTC TGC 3’ PR2 5’GAT GCA ACA GTT TGT GAA GTT TG 3’	18 23	93	46

S No.	Gene Symbol	Primer Sequence (5’ - 3’)	Base pair (bp)	Product size (bp)	Probe number
34	*DCLRE1C*	PR1 5’GAG CTA GAA CAG TTC ACC GAG AC 3’ PR2 5’TGG CAG AGG ATC ATC AAA GAG 3’	23 21	65	69
35	*KU70*	PR1 5’GGA TTT GAT GGA GCC AGA AC 3’ PR2 5’CCA AGG AGC CCA GAC TTC TA 3’	20 20	70	86
36	*KU80*	PR1 5’ CCC AAA TCC TCC GAT TTC AGA 3’ PR25’ CCC GGG GAT GTA AAG CTC 3’	21 18	62	84
37	*PRKDC*	PR1 5’ AGA AGG CGG CTT ACC TGA GT 3’ PR2 5’ GAC ATT TTT GTC AGC CAA TCT TT 3’	20 23	70	37
38	*β -ACTIN*	PR1 5’CCA ACC GCG AGA AGA TGA 3’ PR2 5’CCA GAG GCG TAC AGG GAT AG 3’	18 22	97	64

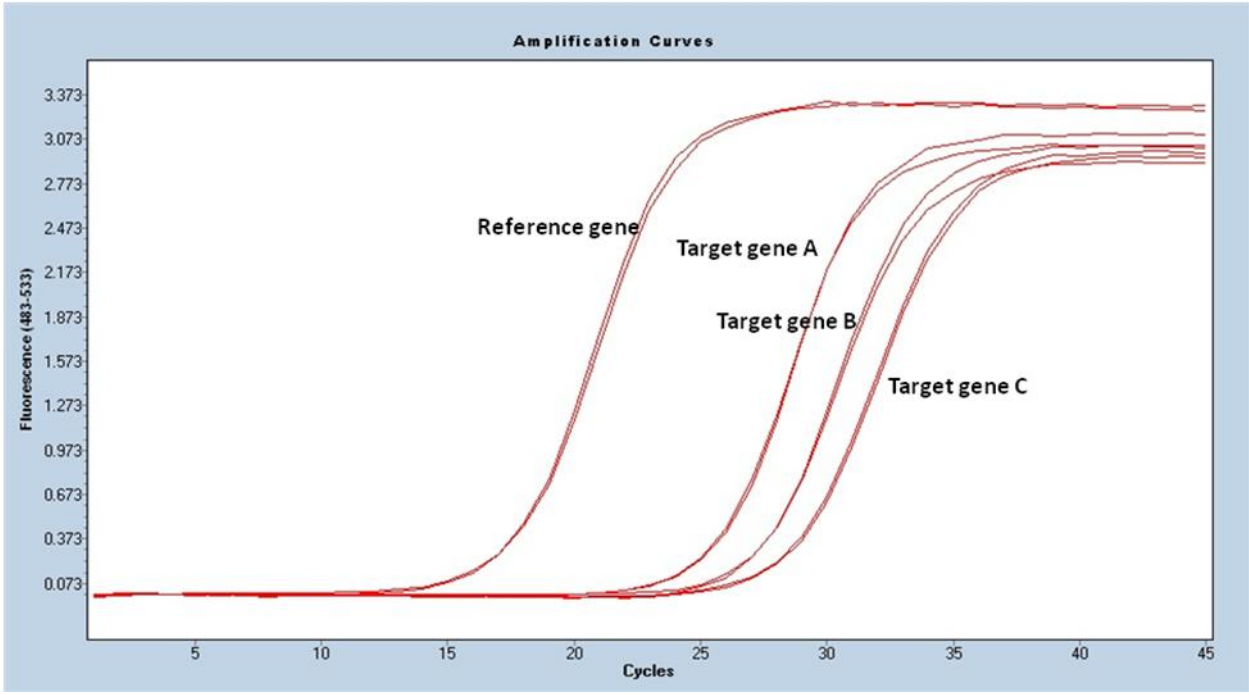

Figure 2.10: Representative amplification curves showing different Cp values (crossing point cycle) for reference and target genes. Cp value depends on the abundance of mRNA transcript in sample.

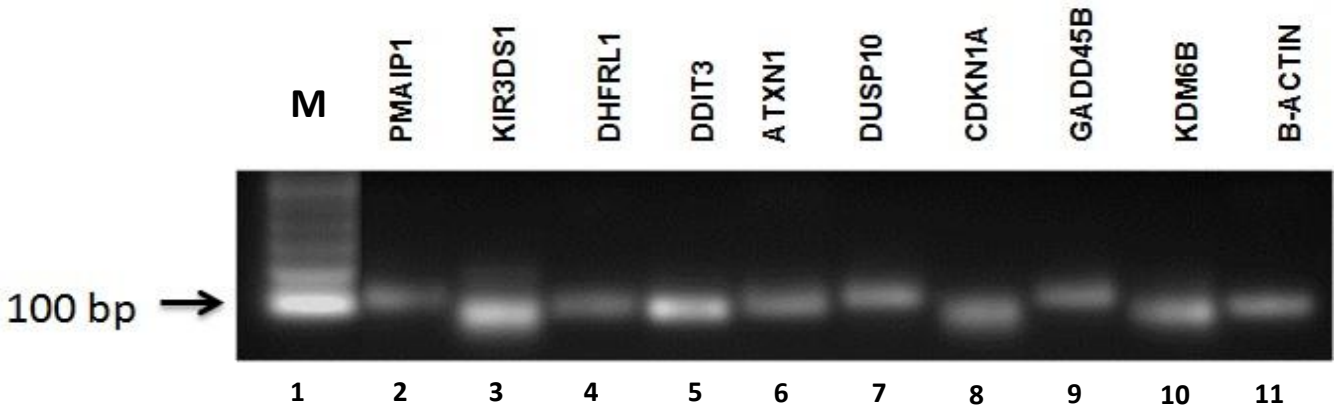

Figure 2.11: A representative ethidium bromide stained agarose gel (2%) showing specific amplification of single amplicon (PCR product) for the genes studied. Lane 1 : M: 100 base pair ladder. Lane 2-10: genes of interest, Lane 11: house- keeping gene (beta actin).

RT-qPCR reactions were performed in 96 multiwell plates using LC480 Real-time PCR Instrument (Roche Diagnostics). All the reactions were carried out in triplicates and relative quantification was calculated by normalizing the data with β-actin reference gene. Relative quantification was performed by using the LC480 software version 1.1. The results are expressed in normalized ratio as described by Pfaffl (2001).

$$\text{Normalized Ratio/expression} = \frac{(\text{Concentration of Target/Concentration of reference})_{\text{sample}}}{(\text{Concentration of Target/Concentration of reference})_{\text{calibrator}}}$$

Further, relative expression was calculated as,

$$\text{Relative expression} = \frac{(\text{Normalized ratio})_{\text{Irradiated sample}}}{(\text{Normalized ratio})_{\text{control sample}}}$$

2.8 Radiation induced chromatin conformational changes using dynamic light scattering

Conformational changes in terms of hydrodynamic diameter were measured in PBMCs exposed to different acute doses of gamma radiation (0.25, 0.5, 1.0 Gy) in 10 individuals using dynamic light scattering. Time kinetics experiments were carried out in PBMCs exposed to 1 Gy at different post-irradiation time points.

2.8.1 Chromatin Isolation from PBMCs

Isolation of native chromatin from irradiated PBMCs was carried out using the protocol described elsewhere (*126, 232*) with a few modifications. The protocol in brief is as follows: PBMCs were incubated in hypotonic buffer [0.25 M Sucrose, 10 mM Tris-HCl, pH 7.4, 10 mM KCl, 1.5 mM MgCl2, 0.1 mM Phenylmethylsulfonyl fluoride (PMSF), Sigma] and were kept on ice for 30 min. Cell lysate was centrifuged at 4000 rpm for 10 min to obtain nuclear pellet which was re-suspended in MNase *(Micrococcal nuclease)* digestion buffer (50 mM Tris-HCl, 1 mM CaCl2, 25 mM NaCl, 3 mM MgCl2, 0.2 mM PMSF) and partial digestion of nuclei was done

with 0.00125 U/O.D_{260} of MNase enzyme (Sigma) for 1 min at room temperature to obtain long and intact chromatin fibers. The digestion of nuclei was stopped with 10 mM EDTA and the tubes were kept on ice for 30 min to obtain chromatin fragments in solution. Nuclear debris was removed by centrifugation at 10,000 rpm for 10 min and chromatin fragments were dialyzed against 10 mM Tris-HCl (pH 7.4) buffer.

2.8.2 Dynamic Light Scattering analysis

Dynamic light scattering experiments were performed using a Malvern 4800 autosizer (Malvern Instruments Ltd, Malvern, Worcestershire, UK) employing 7132 digital correlator. Dialyzed chromatin at a concentration of 4 µg/ml (O.D_{260}) was taken for DLS measurements. The light source was an Ar-ion laser operated at 514.5 nm with maximum power output of 2 W. DLS measures time dependent fluctuations in the scattering intensity and uses this to determine the diffusion coefficient 'D' of the sample by means of its inbuilt auto-correlator. Size of the particle (Hydrodynamic diameter) is calculated using Stokes-Einstein equation,

$$D_h = \frac{kT}{f} = \frac{kT}{3\pi\eta D}$$

where D_h is the hydrodynamic diameter, k is the Bolzmann constant, f is particle frictional coefficient, η is solvent viscosity (here, we have taken the viscosity of water as the solvent viscosity), T is the absolute temperature and D is the diffusion coefficient. The distribution in diffusion coefficient was obtained by an Inverse Laplace Transformation algorithm 'CONTIN' supplied by instrument manufacturer. Multiple readings were taken for each sample and mean and standard deviation was calculated and used for further analysis.

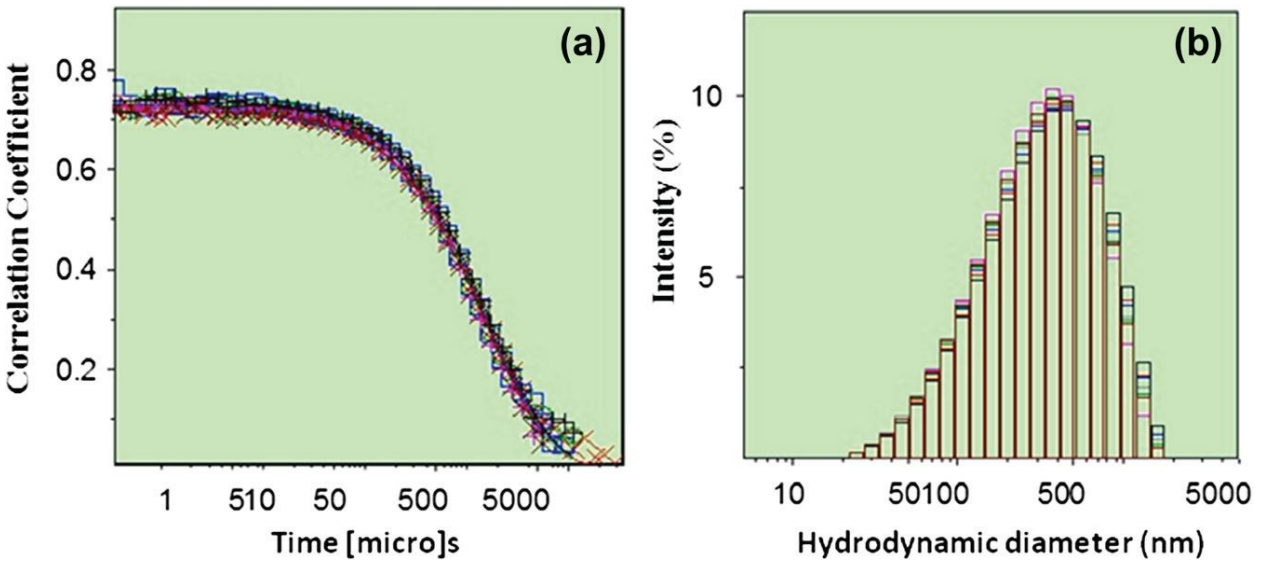

Figure 2.12: Representative images showing (a) autocorrelation of scattered light intensity with time. The autocorrelation function is used to obtain hydrodynamic diameter of chromatin fibers from human PBMCs. (b) Intensity weighted hydrodynamic diameter distribution of chromatin fibers. Each color represents different DLS readings obtained for each data point.

2.8.3 Analysis of damage in the chromatin fiber using Atomic Force Microscopy (AFM)

The level of fragmentation of chromatin fibers was studied using AFM. For that purpose, native chromatin was isolated from irradiated PBMCs at 5.0 Gy along with sham irradiated control (~2 x 10^6 cells each). The freshly prepared chromatin fragments were fixed with 0.1% glutaraldehyde solution and incubated overnight at 4°C. After fixation, the samples were spread onto a freshly cleaved mica substrate and kept at room temperature for 15 min. AFM imaging was carried out on mica sheet and the measurements were taken in contact mode using a scanning probe microscope (SPM-Solver P47, NT-MDT, Moscow, Russia). Rectangular cantilevers of silicon nitride having force constant of 3 N/m were employed for measurement.

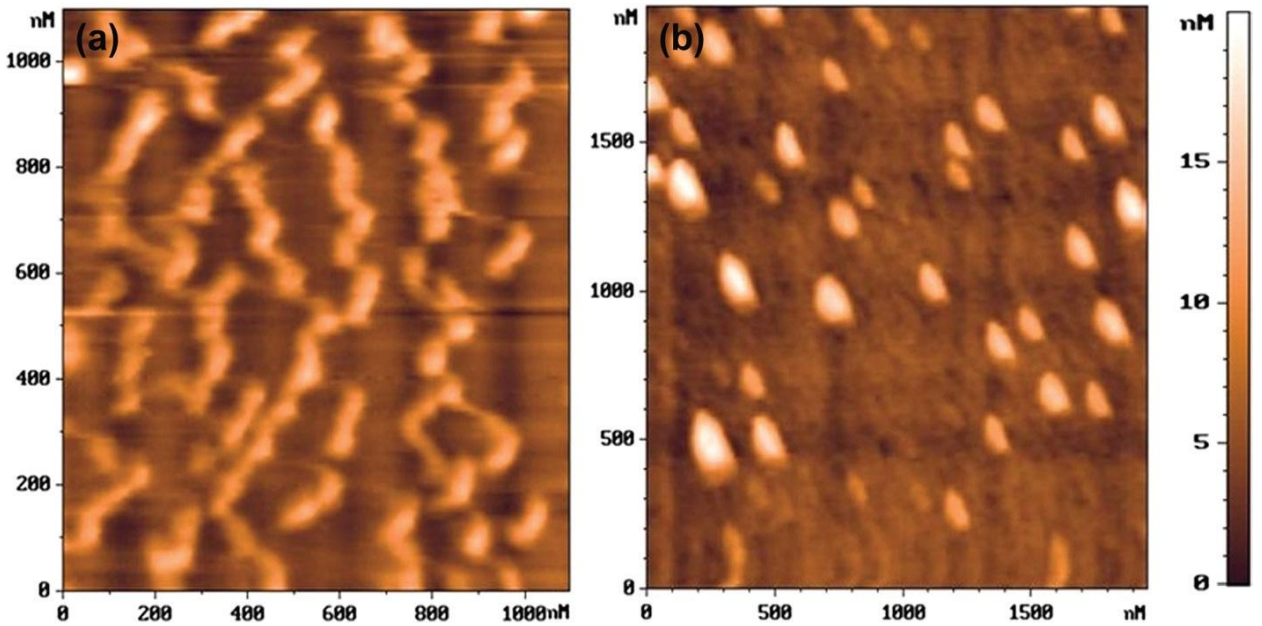

Figure 2.14: Atomic force Microscopy (AFM) image showing chromatin structure in human PBMCs. (a) Intact chromatin fragments in un-irradiated PBMCs (b) fragmented and diffused chromatin fragments after 5.0 Gy radiation dose. Depth indicator reflects the thickness/height of chromatin fibers (in nm) present on the surface scanned by AFM. Dark to light shade indicates increase in size (nm) of chromatin fiber.

2.9 Statistical Analysis

Statistical analysis was performed using SPSS software (version 17.0). The threshold for statistical significance was kept at $p \leq 0.05$ for all the analysis. The results are reported as Mean ± S.E.M for all the experiments. Analysis of variance was performed to compare the means of basal level frequencies of DSBs between NLNRA, LDG and HDG. Regression analysis was performed to study the interaction between DSB frequency, age of the individuals and background radiation dose received by them. Independent t test was performed to compare the means of gamma H2AX positive cells/intensity (DSBs) between NLNRA, LDG and HDG. Paired t test was performed to find out the difference between irradiated and un-irradiated samples for DNA damage at acute doses. Linear regression was performed to study dose

response at DNA damage level. For radio-adaptive study, independent‘t’ test was carried out to find out the significant difference at gene expression level between NLNRA and HLNRA. The statistical significance of difference between basal level expression and expression after challenging dose was assessed by paired ‘t’ test. Paired ‘t’ test was performed to find out the difference between irradiated and un-irradiated samples for mRNA expression at acute dose studies. For chromatin conformation study, paired t test was performed to study the difference in hydrodynamic diameter between irradiated and un-irradiated samples.

Chapter 3

Results

3.1 DNA damage and repair kinetics study using gamma-H2AX biomarker

In the present study, an attempt has been made to quantitate DNA double strand breaks (DSBs) in the PBMCs of individuals from NLNRA and HLNRA of Kerala coast. The spontaneous or basal level frequency of DSBs was measured in individuals from HLNRA and adjacent control areas. We have studied the radio-adaptive response if any, in terms of induced DSBs on in-vitro exposure of PBMCs from NLNRA and HLNRA individuals to challenging doses (0.25 - 2.0 Gy) of IR. Repair kinetics of DSBs was studied in PBMCs exposed to low (0.25 Gy) and high (2.0 Gy) challenging doses of gamma radiation at different post-irradiation time points (0.5, 2.0, 4.0, 6.0 and 24 h). Spontaneous frequency was measured by scoring gamma-H2AX foci in PBMCs of individuals using fluorescence microscope whereas induced DSBs and repair kinetics were studied by measuring gamma H2AX positive cells (fluorescence intensity) using flow cytometry.

3.1.1 Evaluation of basal level frequency of DNA DSBs in NLNRA and HLNRA individual.

The spontaneous frequency of DSBs was estimated using gamma-H2AX marker among 91 random male donors {NLNRA, N=30, and HLNRA, N=61 (LDG, N=20 and HDG, N=41)} from Kerala coast. The PBMCs of all the individuals were scored for gamma-H2AX foci using fluorescence microscope. Around 20-25 random images with ~8 to 10 well spreaded cells were captured from slides prepared for each sample. The scoring of gamma-H2AX foci was carried out in approximately 250 to 300 cells for each individual. The number of gamma-H2AX foci observed in each cell was recorded. The information about the multiple foci (2 or more foci) observed in the cells was also recorded. The mean frequency of gamma-H2AX foci per cell was calculated by dividing the total number of foci observed with the total number of cells scored for each individual. Analysis was also done in terms of percentage of cells having gamma-H2AX foci (positive cells) and the distribution of foci (number of foci per cell) was recorded for all the

individuals. For all the experiments, PBMCs irradiated with 1.0 Gy were used as positive control and cells without primary antibody labelling were used as negative control. Figure 3.1 is the representative fluorescence microscopy image showing gamma-H2AX foci in PBMCs counterstained with DAPI.

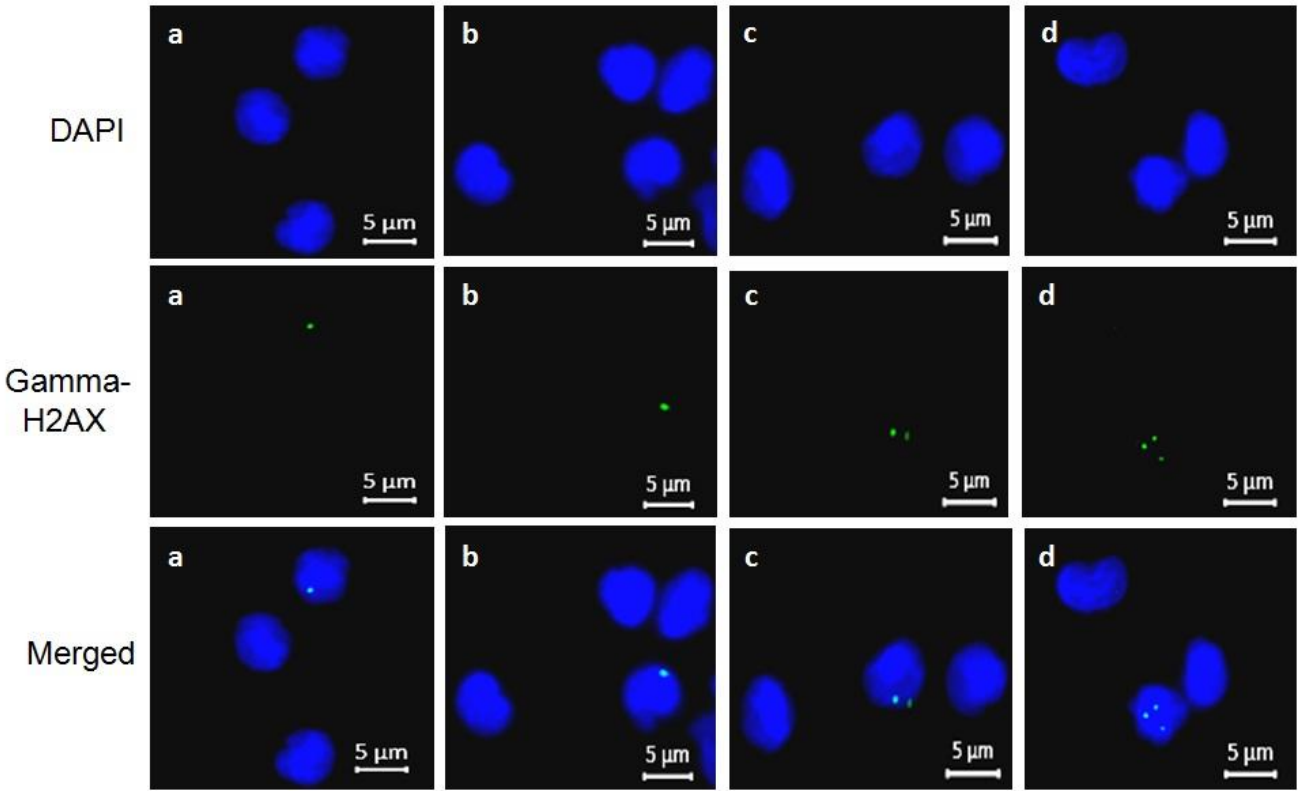

Figure 3.1: Representative fluorescence microscopy images showing gamma-H2AX foci in PBMCs counterstained with DAPI. Panel 1 shows DAPI staining, Panel 2 shows gamma-H2AX antibody staining and Panel 3 shows merged images. a) and b) single foci per cell c) 2 foci/cell d) 3 foci/cell.

Table 3.1: Mean frequency of gamma-H2AX foci per cell among individuals belonging to different background dose groups, NLNRA and HLNRA (LDG and HDG). Mean age in years and mean dose of individuals from different groups in mGy/y. HLNRA: High Level Natural Radiation Area, NLNRA: Normal Level Natural Radiation Area. LDG: Low Dose Group, HDG: High Dose Group, S.D: Standard deviation, S.E.M: Standard error of mean.

Area	**Background dose group (mGy/y)**	**Number of individuals (N)**	**Mean Age ±S.D. (years)**	**Mean background dose ± S.D. (dose range in mGy/y)**	**Frequency of gamma-H2AX foci/cell ± S.E.M (range)**
NLNRA	≤ 1.5	30	35.5± 6.3	1.3 ± 0.1 (1.1 - 1.5)	0.095 ± 0.009 (0.01 - 0.28)
HLNRA	LDG (1.51- 5.0)	20	34.2 ± 5.7	2.6 ± 0.8 (1.6 - 4.6)	0.096 ± 0.008 (0.05 - 0.17)
	HDG (> 5.0)	41	37.0 ± 8.0	11.0 ± 3.6 (5.5 - 21.6)	0.078 ± 0.004 (0.02 - 0.14)
	HLNRA (> 1.5)	61	36.1 ± 7.4	8.3 ± 5.0 (1.6 - 21.6)	0.084 ± 0.004 (0.02 - 0.17)

As shown in table 3.1, the mean background dose of the NLNRA individuals was 1.3 ± 0.1 (range 1.1- 1.5 mGy/y), whereas background dose level ranged from 1.6 to 21.6 mGy/y (Mean dose 8.3 ± 5.0 mGy/y) among HLNRA individuals studied. The mean age of NLNRA and HLNRA individuals were 35.5 ± 6.3 y and 36.1 ± 7.4 y respectively, and the mean age of all 91 individuals was 35.9 ± 7.9 y. The mean age of NLNRA and HLNRA individuals was statistically comparable (P=0.3). The mean frequency of gamma-H2AX foci among NLNRA individuals was 0.095 ± 0.009 per cell with a range between 0.01 to 0.28 foci per cell. The frequency of gamma-H2AX foci among HLNRA individuals was 0.084 ± 0.004 per cell with a range between 0.02-0.17 foci per cell. The frequencies of gamma-H2AX foci were not significantly (P=0.2) different between NLNRA and HLNRA individuals (figure 3.2).

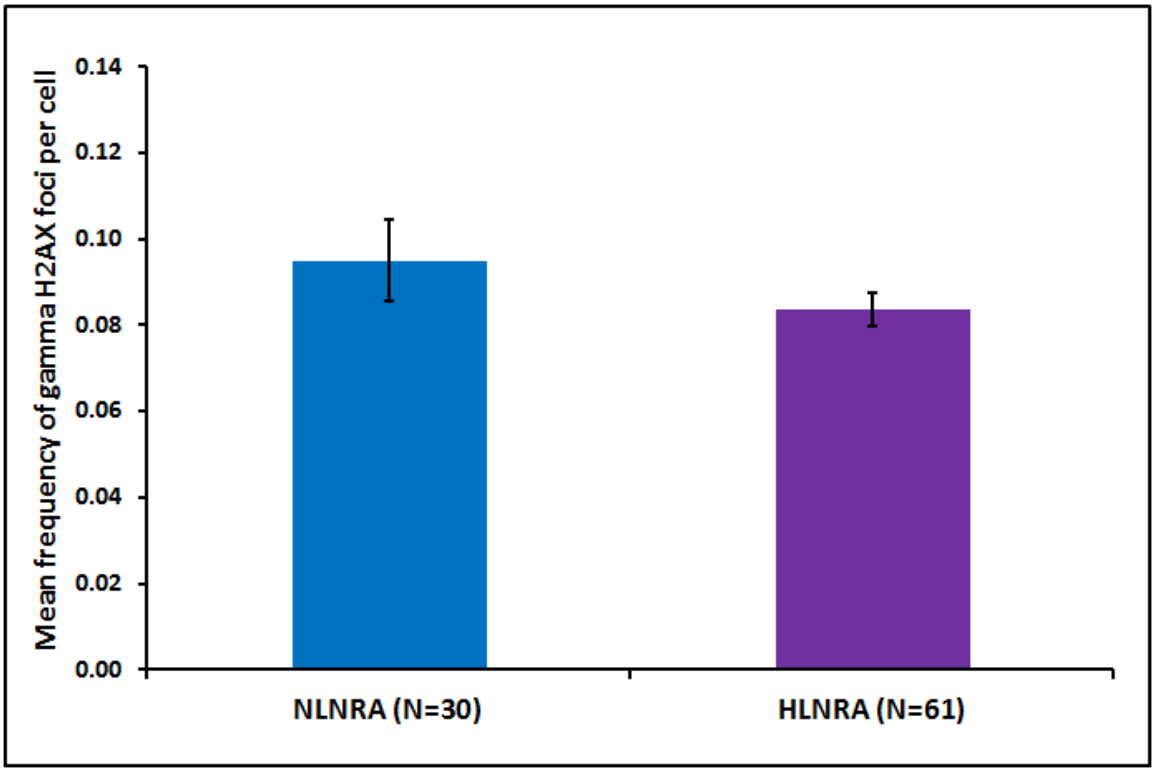

Figure 3.2: The mean frequency of gamma-H2AX foci in NLNRA (≤ 1.5 mGy/y) and HLNRA individuals (> 1.5 mGy/y). N: Number of individuals, HLNRA: High Level Natural Radiation Area, NLNRA: Normal Level Natural Radiation Area. Error bar represents S.E.M. (Standard error of mean).

The HLNRA individuals were further categorized into two different dose groups on the basis of annual background dose received by the individuals. These groups were Low Dose Group (LDG, 1.51-5.0 mGy/y, N=20, mean dose: 2.6 ± 0.8 mGy/y) and High Dose Group (HDG, > 5.0 mGy/y, N=41, mean dose: 11.0 ± 3.6 mGy/y). The mean age among NLNRA, LDG and HDG individuals were 35.5 ± 6.3, 34.2 ± 5.7 and 37.0 ± 8.0 y respectively. The frequency of gamma-H2AX foci in NLNRA, LDG and HDG was observed to be 0.095 ± 0.009, 0.096 ± 0.008 and 0.078 ± 0.004 per cell respectively (as shown in table 3.1 and figure 3.3). Analysis of variance (ANOVA) was carried out in order to compare the mean gamma-H2AX foci frequency between the groups (NLNRA, LDG and HDG). The analysis did not reveal any significant difference in gamma-H2AX foci frequency among NLNRA, LDG and HDG individuals ($F_{(2, 88)}$

= 2.22, P = 0.12). However, a marginal reduction in mean frequency was observed in HDG individuals as compared to LDG and NLNRA individuals (figure 3.3).

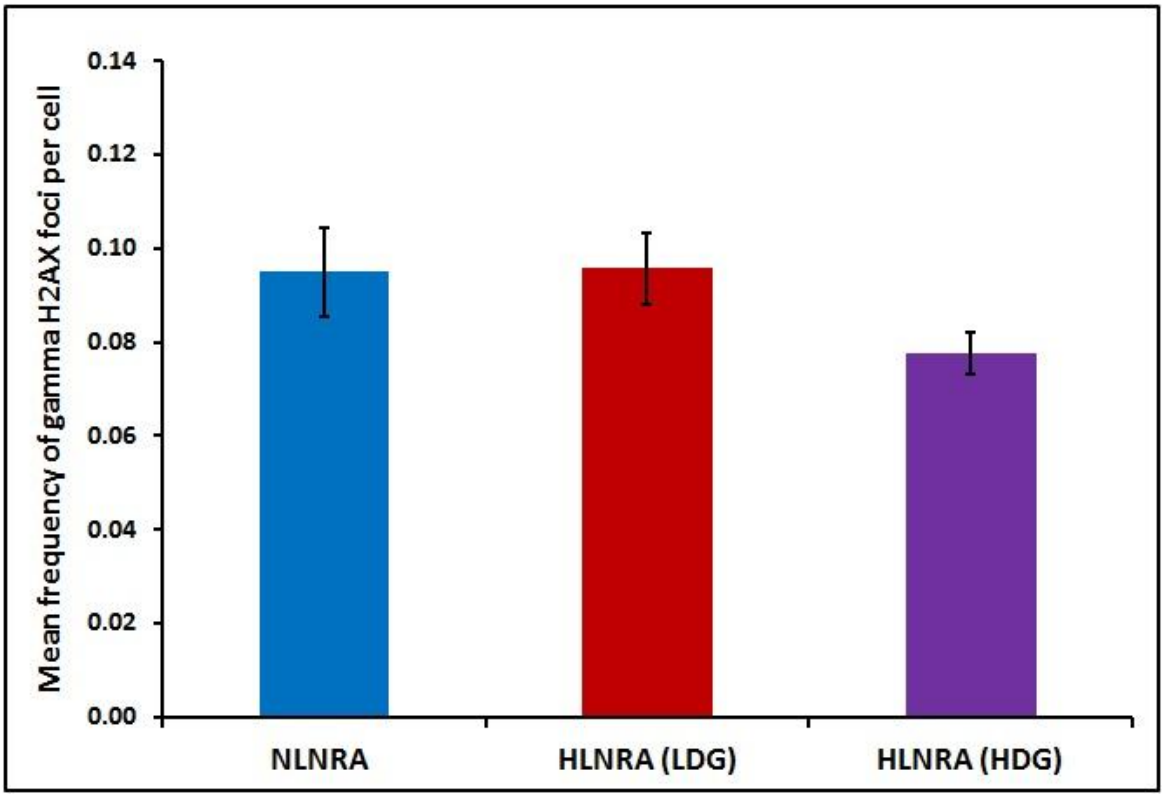

Figure 3.3: The mean frequency of gamma-H2AX foci per NLNRA, LDG and HDG individuals. HLNRA: High Level Natural Radiation Area, NLNRA: Normal Level Natural Radiation Area, LDG: Low Dose Group, HDG: High Dose Group. Error bar represents S.E.M. (Standard error of mean).

Table 3.2: The percentages of cells having gamma-H2AX foci among NLNRA and HLNRA individuals (LDG and HDG). Percentage of cells with multiple foci (2, 3 and 4 foci/cell) is also shown. Numbers shown in brackets represents the percentage of positive cells having multiple foci (2, 3 or 4 foci) with respect to total number of cells scored. HLNRA: High Level Natural Radiation Area, NLNRA: Normal Level Natural Radiation Area, LDG: Low Dose Group, HDG: High Dose Group

Area	**Dose Groups (mGy/y)**	**No. of cells scored**	**Distribution of gamma-H2AX foci/ cell**				
			Number of cells positive for gamma-H2AX foci (%)	**1 foci (%)**	**2 foci (%)**	**3 foci (%)**	**4 foci (%)**
NLNRA	≤ 1.5	7935	702 (8.8)	670 (8.4)	25 (0.3)	6 (0.1)	1 (0.01%)
HLNRA	LDG (1.51- 5.0)	5145	434 (8.4)	390 (7.6)	38 (0.7)	5 (0.1)	1 (0.02%)
	HDG (> 5.0 - 21.6)	10752	776 (7.2)	723 (6.7)	41 (0.4)	11 (0.1)	1 (0.01%)
	HLNRA (1.51 - 21.6)	15897	1210 (7.6)	1113 (7.0)	79 (0.5)	16 (0.1)	2 (0.01%)

As shown in table 3.2, the distribution of gamma-H2AX foci per cell was also analysed among 91 individuals. The percentage of cells having gamma-H2AX foci (positive cells) in NLNRA and HLNRA individuals were 8.8 and 7.6 respectively. The percentage of positive cells in LDG and HDG of HLNRA were 8.4 and 7.2 respectively.

In terms of percentages of positive cells with 1, 2, 3 and 4 foci, it was observed that around 90% of the cells with gamma-H2AX foci (positive cells) had only single foci in all the three dose groups (NLNRA=95.4%, LDG= 89.9%, HDG= 93.2%). However, percentage of positive cells in NLNRA, LDG and HDG individuals having two foci per cell were 3.6, 8.8 and 5.3 respectively. Approximately, only 2% of positive cells had more than 2 foci. (Percentages

were calculated by dividing the cells with 1, 2, 3 or 4 foci with total number of gamma-H2AX positive cells).

The distribution of gamma-H2AX foci with respect to background dose levels is shown in figure 3.4. The regression analysis did not reveal any significant correlation with respect to background dose levels (R=0.15, P=0.16). No dose response was observed in terms of frequency of gamma-H2AX foci /cell with respect to background dose.

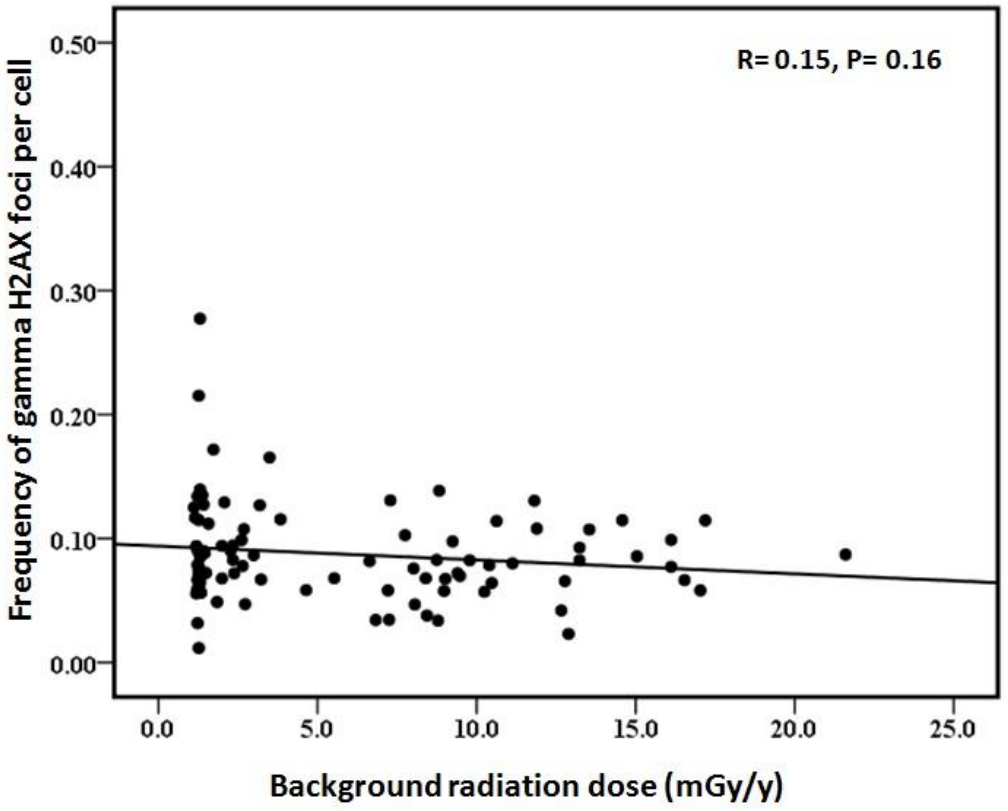

Figure 3.4: Distribution of gamma-H2AX foci with respect to background radiation dose (mGy/y). Each dot represents the frequency of gamma H2AX foci/cell for single individual.

The distribution of gamma-H2AX foci with respect to age of the individuals is shown in figure 3.5. The regression analysis has shown a marginal positive correlation of gamma-H2AX foci with increasing age of the individuals (R = 0.2, P=0.06). Further, regression analysis was also carried out for NLNRA and HLNRA individuals separately. Analysis revealed a significant influence of age on the frequency of foci in NLNRA individuals (R=0.37, P=0.04). However, no significant influence of age was observed among HLNRA individuals (R=0.11, P=0.39).

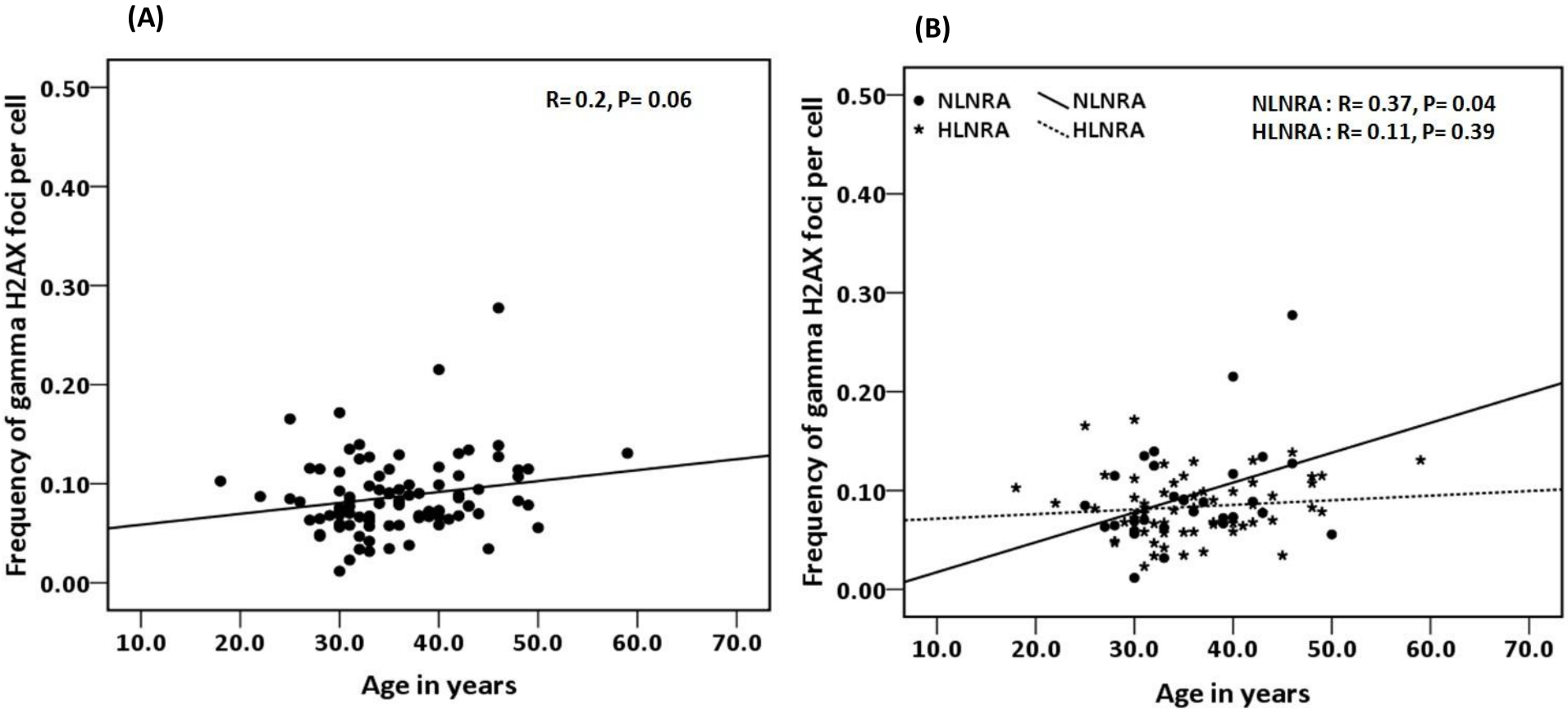

Figure 3.5: Distribution of the frequency of gamma-H2AX foci/cell in individuals from NLNRA (≤1.5mGy/y) and HLNRA (>1.5mGy/y) with respect to age. A: Regression analysis showing the influence of age in all the 91 individuals. Each dot represents the frequency of gamma-H2AX foci/cell for each individual studied. B: Regression analysis was carried out in HLNRA and NLNRA individuals separately. Each dot and star represents the frequency of gamma-H2AX foci/cell for each individual in NLNRA and HLNRA respectively.

3.1.2 Dose response study using gamma-H2AX and phospho-ATM markers in PBMCs exposed to acute radiation using flow cytometry

Dose response study was carried out in 10 random and healthy male donors from Mumbai. PBMCs were separated from whole blood and irradiated with different doses of gamma radiation between 0.25 Gy to 2.0 Gy. A representative image showing dose dependent increase in gamma-H2AX positive cells is shown in figure 3.6.

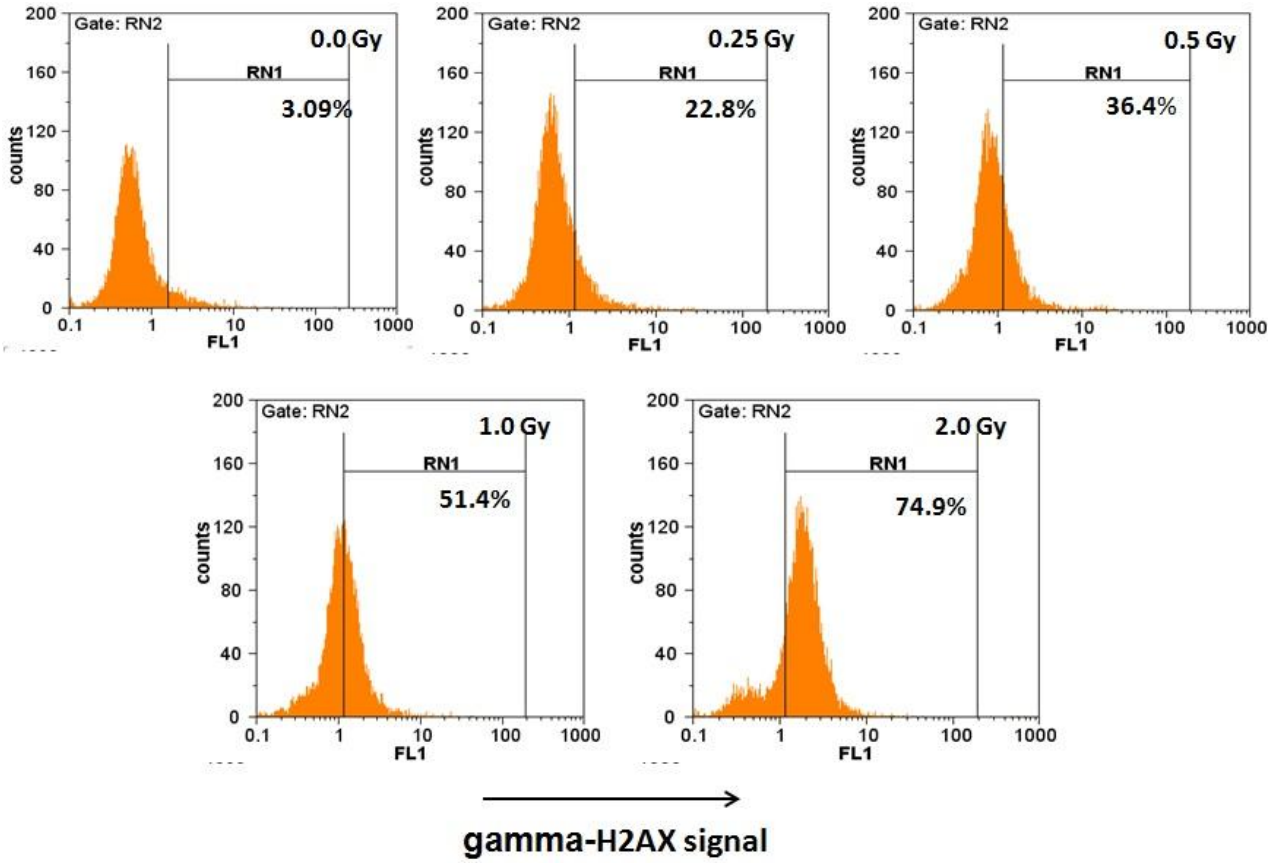

Figure 3.6: Representative image of flow cytometry analysis showing dose dependent increase in gamma-H2AX positive cells in human PBMCs. PBMCs were counterstained with DAPI and gating was done to include only DAPI positive singlet cells (Gate RN2) for the analysis. Gate RN1 represents percentage increase in gamma H2AX positive cells at different doses.

Our results revealed a dose dependent increase in gamma-H2AX positive cells at different doses studied. Also, a linear relationship (R^2 = 0.96) was observed between mean gamma-H2AX positive cells and different doses of gamma radiation (0.0, 0.25, 0.5, 1.0 and 2.0 Gy) given to PBMCs from 10 individuals (figure 3.7).

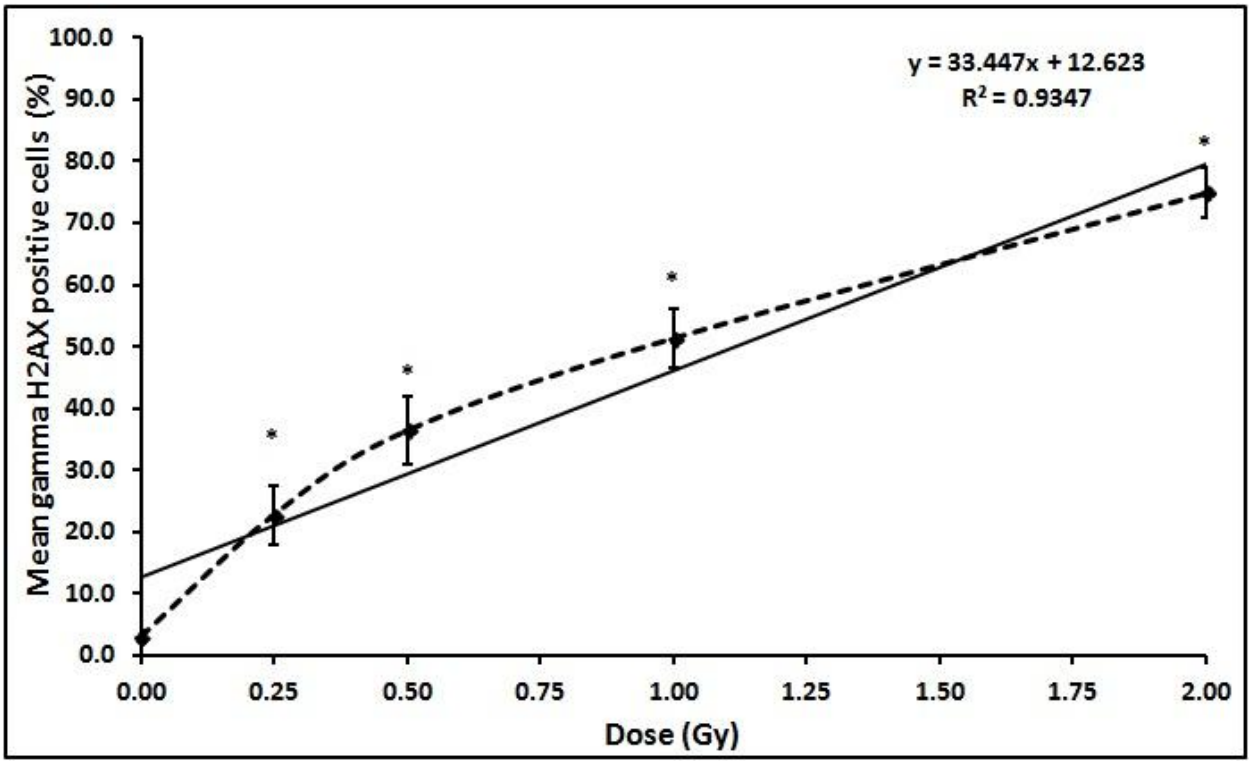

Figure 3.7: A linear dose dependent increase in mean gamma-H2AX positive cells in PBMCs of individuals (N=10) at different doses of gamma radiation (0.25, 0.50, 1.0 and 2.0 Gy). N= Number of individuals. (* $p \leq 0.05$), Error bar represents S.E.M (Standard Error of Mean)

Further, dose response observed in terms of gamma-H2AX positive cells was confirmed using another DNA DSB specific marker, phospho-ATM. Dose response study was simultaneously carried out for phospho ATM and gamma H2AX to compare the dose dependent increase in DNA damage in PBMCs exposed to acute doses of gamma radiation. Both gamma-H2AX (R^2 = 0.9) and phospho ATM (R^2 = 0.9) showed linear increase in DNA DSBs with respect to the radiation doses studied (figure: 3.8). It confirmed that the dose response shown by gamma-H2AX is consistent with the response shown by other DSB specific marker such as phospho-ATM.

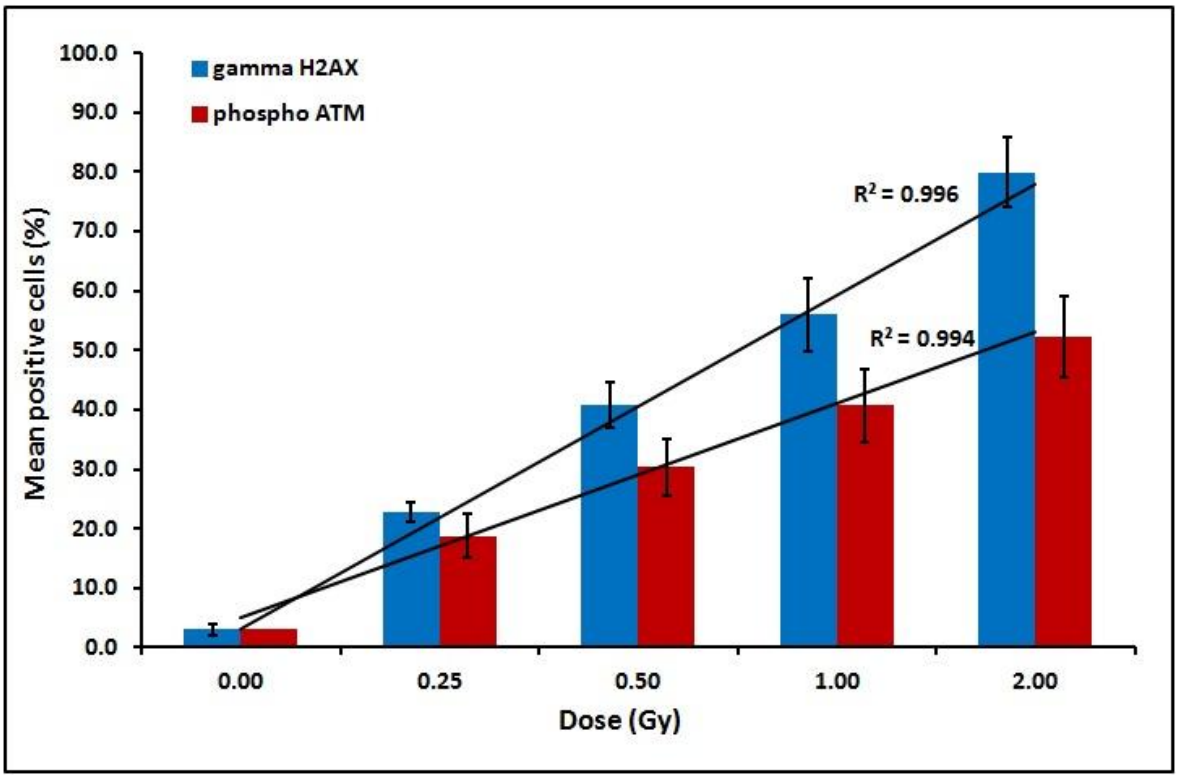

Figure 3.8: A linear dose dependent increase in mean gamma-H2AX positive cells and phospho-ATM positive cells at different doses of gamma radiation (0.25-2.0Gy) in the PBMCs of individuals studied.

3.1.3 Measurement of induced DSBs using gamma-H2AX marker in NLNRA and HLNRA individuals using flow cytometry

Induction of DNA DSBs was studied in PBMCs of 78 individuals (NLNRA, N=23 and HLNRA, N=55) exposed to three different doses of gamma radiation. The mean age of NLNRA and HLNRA individuals were 38.8 ± 6.7 and 38.2 ± 7.4 y respectively. The mean background dose received by NLNRA and HLNRA individuals were 1.3 ± 0.1 and 6.8 ± 3.8 mGy/y respectively. Since, HLNRA individuals are continuously exposed to low levels of chronic radiation, the background dose received by them was considered as priming/adapting dose in this study.

Radio-adaptive study was carried out at challenging doses of 0.25, 1.0 and 2.0 Gy. The PBMCs were separated from all the individuals and irradiated with challenging doses along with sham irradiated control (un-irradiated control). The PBMCs were incubated for 30 minutes post-irradiation and gamma-H2AX fluorescence intensity was measured at all the dose points along with sham-irradiated control for all the individuals. As shown in table 3.3 and figure 3.9, the mean gamma-H2AX positive cells observed at 0.25, 1.0 and 2.0 Gy for NLNRA individuals were 18.6%, 59.5% and 77.2% respectively. However, in HLNRA individuals the mean gamma-H2AX positive cells were observed to be 13.0%, 54.9% and 73.3 % at 0.25, 1.0 and 2.0 Gy respectively. A marginal decrease in gamma-H2AX positive cells was observed in HLNRA individuals at all the three doses studied. However, a significant reduction (P=0.03) in gamma-H2AX positive cells (induced DSBs) was observed at 0.25 Gy challenging dose.

Table 3.3: Percentages of mean gamma-H2AX positive cells in PBMCs of NLNRA, LDG and HDG individuals exposed to different doses (0.25, 1.0, 2.0 Gy) of gamma radiation. Mean positive cells were calculated after normalizing with sham-irradiated control in each dose group {NLNRA, HLNRA (LDG and HDG)}. NLNRA: Normal Level Natural Radiation Area, HLNRA: High Level Natural Radiation Area, LDG: Low Dose Group, HDG: High Dose Group, N: Number of individuals, S.D: Standard Deviation, S.E.M: Standard error of mean.

Area	Background Dose (mGy/y)	Number of individual studied (N)	Mean age (years) ± S.D	Mean dose (mGy/y) ± S.D (range)	Mean gamma-H2AX positive cells (%) ± S.E.M		
					0.25 Gy	1.0 Gy	2.0 Gy
NLNRA	NLNRA (≤ 1.5)	23	38.8 ± 6.7	1.3 ± 0.1 (1.2 - 1.5)	18.6 ± 2.5	59.5 ± 4.2	75.6 ± 2.6
HLNRA	LDG (1.51-5.0)	21	39.6 ± 7.6	2.7 ± 0.9 (1.6 - 4.5)	14.8 ± 2.3	58.1 ± 4.6	72.1 ± 3.4
	HDG (>5.0)	34	37.4 ± 7.1	9.4 ± 2.3 (5.5 - 15.0)	12.6 ± 1.1	53.0 ± 5.7	68.6 ± 3.5
	HLNRA (> 1.5)	55	38.2 ± 7.4	6.8 ± 3.8 (1.6 - 15.0)	13.0 ± 1.2	54.9 ± 4.2	69.8 ± 2.7

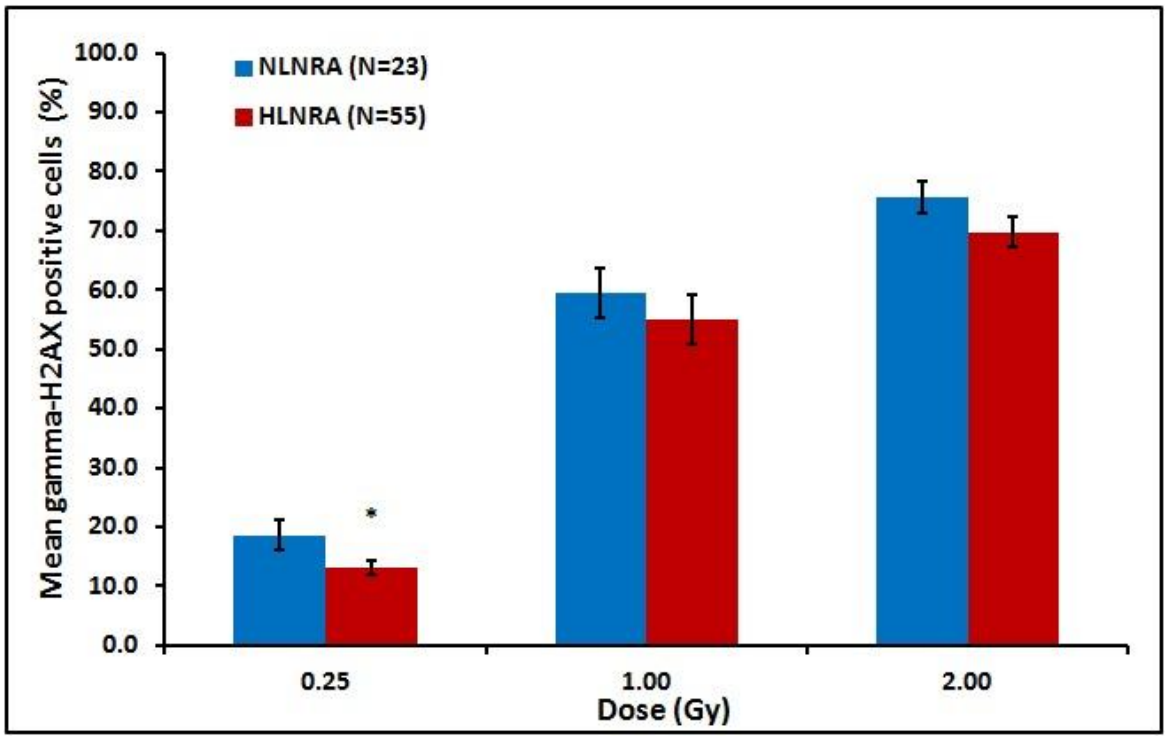

Figure 3.9: Induction of DNA DSBs in terms of mean gamma-H2AX positive cells (%) in PBMCs of NLNRA and HLNRA individuals exposed to different doses (0.25, 1.0 and 2.0 Gy) of gamma radiation. (*represents significant reduction in HLNRA as compared to NLNRA with p ≤0.05). Mean positive cells were calculated after normalizing with sham-irradiated control in each dose group. N: Number of individuals, NLNRA: Normal Level Natural Radiation Area, HLNRA: High Level Natural Radiation Area, Error bar represents S.E.M.(Standard Error of the Mean)

Further analysis was carried out in three groups: NLNRA and two HLNRA groups: Low Dose Group (LDG, 1.51 - 5.0 mGy/y, mean dose: 2.7 ± 0.9 mGy/y) and High Dose Group (HDG, > 5.0 mGy/y, mean dose: 9.4 ± 2.3 mGy/y). The mean age among NLNRA, LDG and HDG individuals were 38.8 ± 6.7, 39.6 ± 7.5 and 37.4 ± 7.1 y respectively. As shown in figure 3.10, a decreasing trend of induced damage was observed in HDG, LDG and NLNRA individuals at all challenging doses. However, statistically significant reduction in induced damage was only observed in HDG individuals at 0.25 Gy (P=0.03) as compared to NLNRA

individuals whereas no significant difference was observed between LDG and NLNRA individuals.

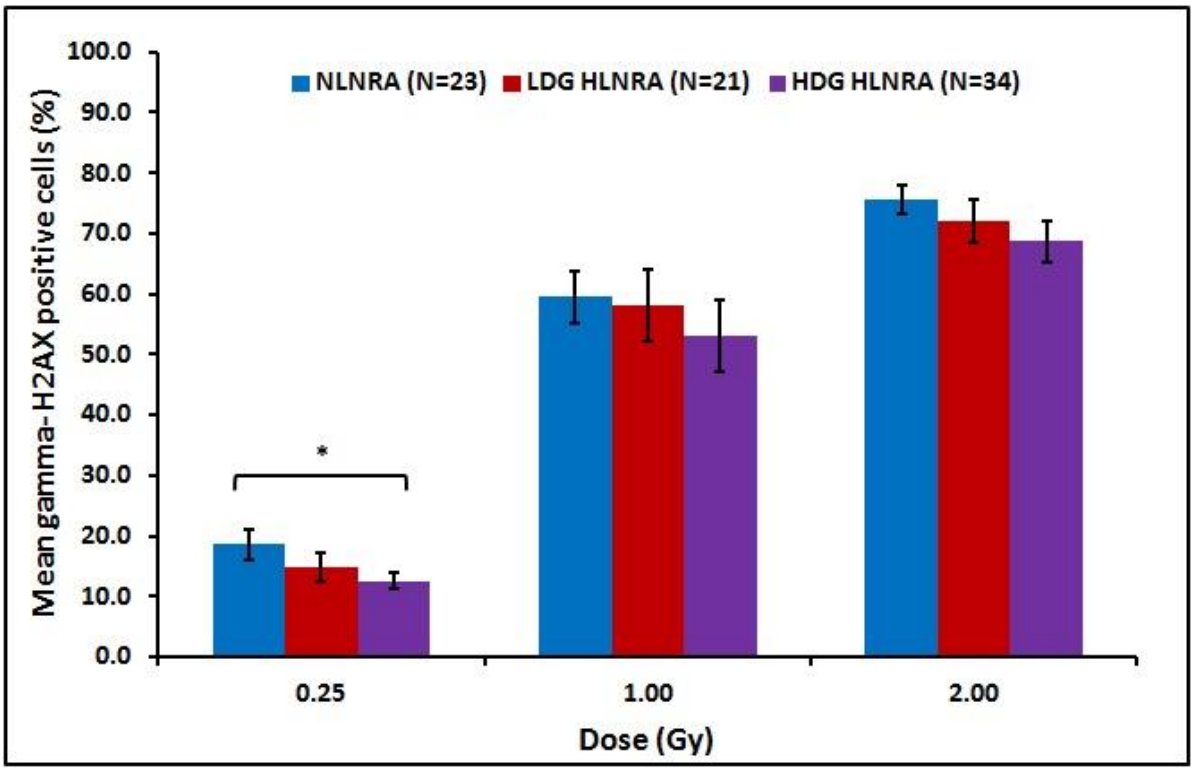

Figure 3.10: Induction of DNA DSBs in terms of mean gamma-H2AX positive cells (%) in PBMCs of NLNRA, LDG and HDG individuals exposed to different doses (0.25, 1.0 Gy and 2.0 Gy) of gamma radiation. Mean positive cells were calculated after normalizing with sham-irradiated control in each dose group. (* represents significant reduction in HLNRA as compared to NLNRA with $p \leq 0.05$). N: Number of individuals, NLNRA: Normal Level Natural Radiation Area, HLNRA: High Level Natural Radiation Area, LDG: Low Dose Group, HDG: High Dose Group, Error bar represents S.E.M. (Standard error of mean)

3.1.4 Repair Kinetics of DSBs in NLNRA and HLNRA individuals

In the present study, post-irradiation repair kinetics of DNA DSBs in terms of decrease in gamma-H2AX positive cells was carried out in PBMCs of 30 individuals from NLNRA (N=8) and HLNRA (N=22). The repair kinetics was carried out at high (2.0 Gy) and low (0.25 Gy) challenging doses. The gamma-H2AX fluorescence/positive cells (DNA DSBs) were measured at 0.5, 2.0, 4.0, 6.0 and 24.0 h post-irradiation in 30 individuals (NLNRA, N=8 and HLNRA, N=22) at 2.0 Gy and 26 individuals at 0.25 Gy (NLNRA, N=8, HLNRA, N=18) along with sham irradiated control. The results were analysed in terms of change in the percentage of gamma-H2AX positive cells at different time points as compared to sham irradiated control. The result was also analysed as percentage of DNA DSBs repaired at 4, 6 and 24 h post-irradiation. A representative figure showing percentages of gamma-H2AX positive cells at different post-irradiation time points with respect to sham irradiated control in PBMCs of an individual is shown in figure 3.11.

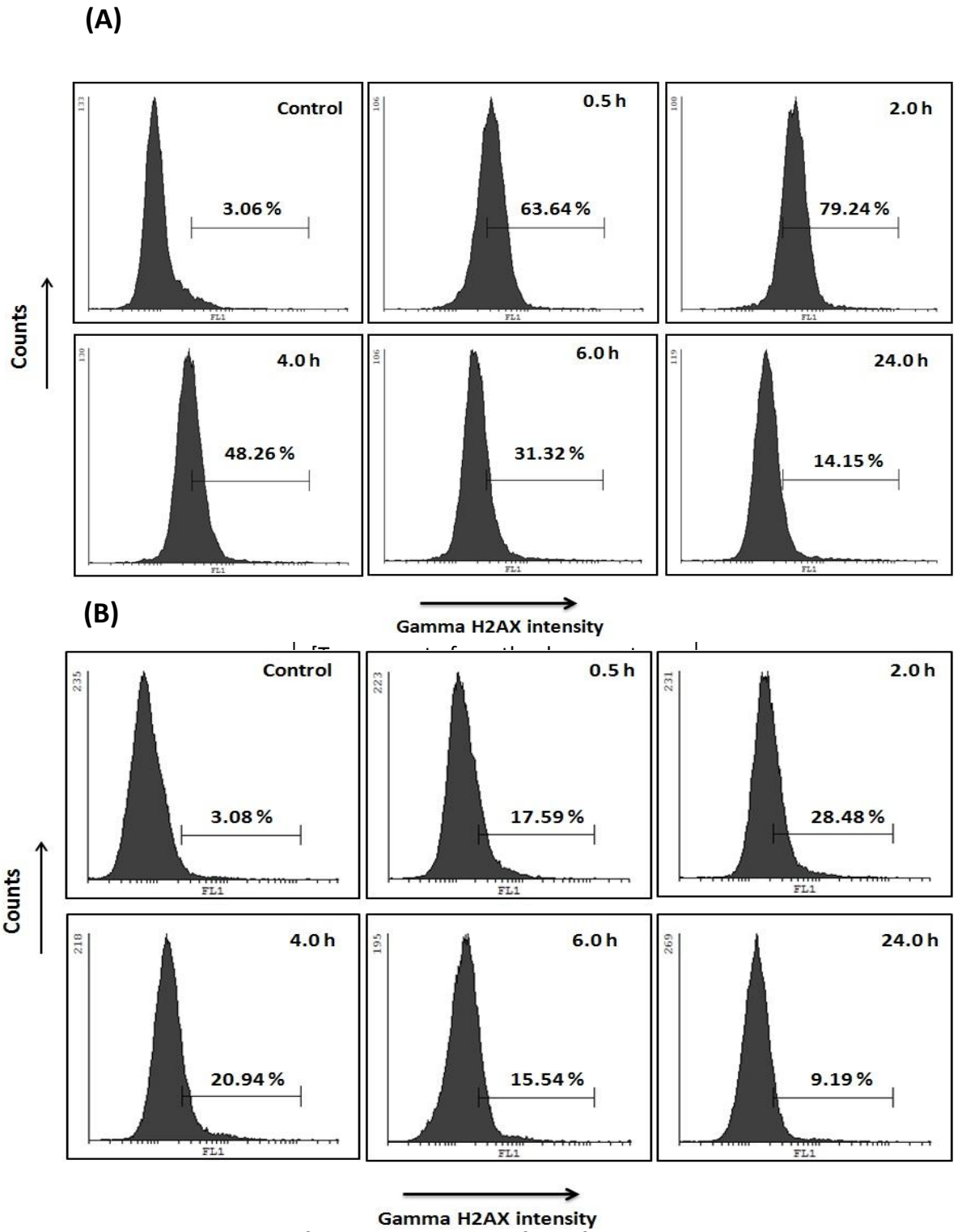

Figure 3.11: Representative flow cytometric profile of an individual showing percentage of gamma-H2AX positive cells in PBMCs exposed to high and low doses at different time points post-irradiation. (A) Flow cytometric profile at 2.0 Gy (B) Flow cytometric peak at 0.25 Gy.

***Repair kinetics at 2.0 Gy*:** As shown in figure 3.12 and table 3.4, the mean percentages of gamma-H2AX positive cells at 0.5, 2.0, 4.0, 6.0 and 24.0 h in NLNRA individuals were 69.7, 77.4, 65.4, 42.6 and 14.7 respectively after 2.0 Gy challenging dose. In HLNRA individuals, percent positive cells were observed to be 62.8, 76.3, 44.8, 29.1 and 11.9 at 0.5, 1.0, 2.0, 4.0, 6.0, 24.0 h respectively. The maximum damage was observed at 2.0 h time point which was similar in both NLNRA and HLNRA individuals. However, a significant reduction ($p \leq 0.05$) in DNA DSBs (gamma-H2AX positive cells) was observed at 4.0 h and 6.0 h time points in HLNRA individuals as compared to NLNRA.

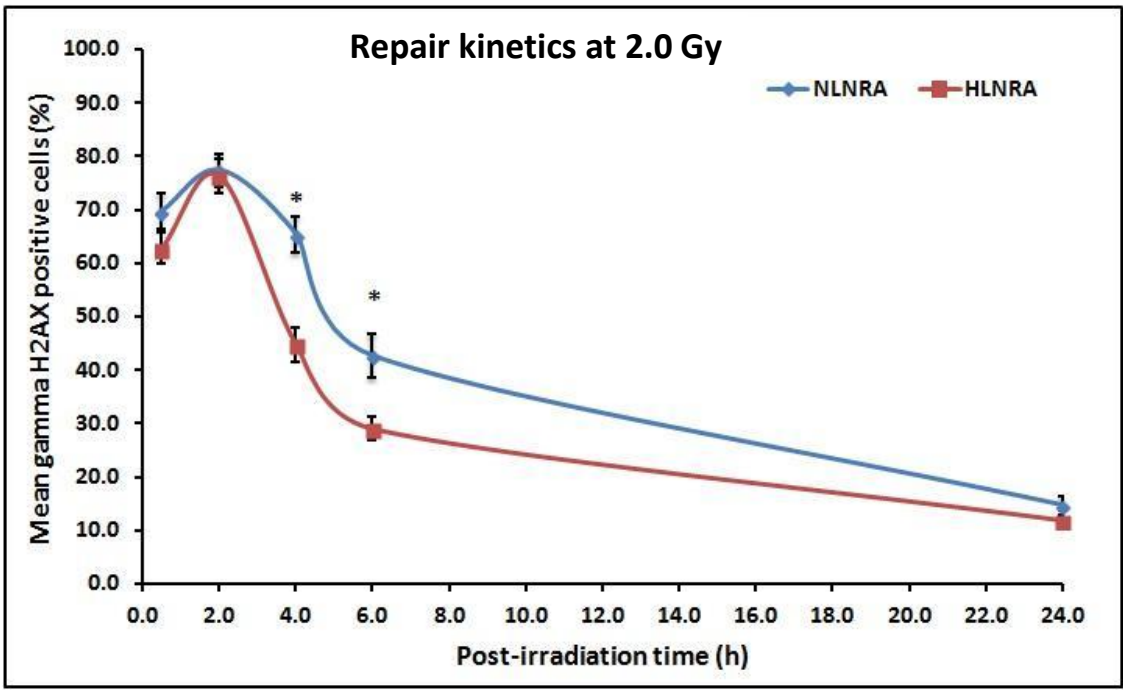

Figure 3.12: The mean percentages of gamma-H2AX positive cells in PBMCs of NLNRA and HLNRA individuals at different post-irradiation timepoints (0.5, 2.0, 4.0, 6.0 and 24.0 h) after 2.0 Gy challenging dose. (*represents significant difference ($p \leq 0.05$) between NLNRA and HLNRA). Mean positive cells at each time point were calculated after normalizing with sham-irradiated control. NLNRA: Normal Level Natural Radiation Area, HLNRA: High Level Natural Radiation Area. Error bars represents S.E.M (Standard Error of Mean)

Table 3.4: The mean percentages of gamma-H2AX positive cells with respect to different background dose groups at different time points (0.5, 2.0, 4.0, 6.0 and 24.0 h) post-irradiation with a challenging dose of 2.0 Gy. Mean positive cells at each time point were calculated after normalizing with sham-irradiated control in each dose group {NLNRA, HLNRA (LDG and HDG)}. NLNRA: Normal Level Natural Radiation Area, HLNRA: High Level Natural Radiation Area, LDG: Low Dose Group, HDG: High Dose Group, N: Number of individuals, S.D: Standard deviation, S.E.M: Standard error of mean.

Area	Background Dose (mGy/y)	Number of individual Studied (N)	Mean Age (years) ± S.D	Mean dose (mGy/y) ± S.D (range)	Mean gamma-H2AX positive cells (%) ± S.E.M at 2.0 Gy				
					0.5 h	2.0 h	4.0 h	6.0 h	24.0 h
NLNRA	≤ 1.5	8	34.9 ± 4.8	1.4 ± 0.1 (1.3 - 1.5)	69.7 ± 3.3	77.4 ± 3.2	65.4 ± 3.1	42.6 ±3.0	14.7 ±1.5
HLNRA	LDG (1.51-5.0)	7	42.6 ± 6.0	3.6 ± 0.5 (3.2- 4.5)	63.0 ± 5.2	76.4 ± 4.8	49.5 ± 3.7	31.2 ± 1.6	13.9 ± 1.5
	HDG (> 5.0)	15	38.8 ± 6.8	9.1 ± 1.8 (6.8 - 12.9)	60.6 ± 4.1	76.2 ± 4.2	45.2 ± 4.4	28.3 ± 3.0	11.1 ± 2.6
	HLNRA (> 1.5)	22	40.0 ± 6.5	7.3 ± 3.0 (3.2 - 12.9)	62.8 ± 2.9	76.3 ± 3.2	44.8 ±3.2	29.1 ± 2.1	11.9 ± 1.8

The percentage of DNA DSBs repaired with respect to maximum damage observed at 2.0 h was calculated. As shown in table 3.5, the percentages of DSBs (gamma-H2AX positive cells) repaired at 4.0 h, 6.0 h and 24.0 h were 41.3, 61.9 and 84.3 in HLNRA individuals. However, the percentages of repair in NLNRA individuals were 15.5, 44.9 and 81.0 after 4.0 h, 6.0 h and 24.0 h respectively. A significantly ($p \leq 0.05$) faster reduction was observed in gamma-H2AX positive cells (DNA DSBs) at 4.0 h and 6.0 h time point in HLNRA individuals. However, around 15 % and 19 % residual damage was still present after 24.0 h post-irradiation in HLNRA and NLNRA individuals respectively. A bi-exponential pattern of DSB repair in terms of decrease in gamma H2AX positive cells was observed in both NLNRA and HLNRA individuals. A faster repair of DSBs was observed upto 6.0 h time point where more than 50% of maximum damage observed was repaired whereas, after 6.0 h slow repair takes place.

Table 3.5: Mean percentage of DNA DSBs repaired calculated in terms of percent decrease in gamma-H2AX positive cells with respect to maximum positive cells observed in the PBMCs exposed to 2.0 Gy post-irradiation at different time intervals (4.0, 6.0 and 24.0 h). Percentages of residual DSBs are also shown. NLNRA: Normal Level Natural Radiation Area, HLNRA: High Level Natural Radiation Area, LDG: Low Dose Group, HDG: High Dose Group.

Area	Background Dose (mGy/y)	Percentage of DSBs (gamma- H2AX positive cells) repaired at 2.0 Gy			Percentage of residual DSBs (gamma-H2AX positive cells) at 2.0 Gy		
		4.0 h	6.0 h	24.0 h	4.0 h	6.0 h	24.0 h
NLNRA	≤ 1.5	15.5	44.9	81.0	84.5	55.1	19.0
HLNRA	LDG (1.51-5.0)	35.3	59.2	81.8	64.7	40.8	18.2
	HDG (> 5.0)	40.7	62.9	85.4	59.3	37.1	14.6
	HLNRA (> 1.5)	41.3	61.9	84.3	58.7	38.1	15.7

Further analysis was carried out in three groups NLNRA, LDG and HDG. The number of individuals in each group were NLNRA (N=8, mean dose: 1.4 ± 0.1 mGy/y), LDG (N=7, mean dose: 3.6 ± 0.5 mGy/y) and HDG (N=15, mean dose: 9.1 ± 1.8 mGy/y). The percentage of gamma-H2AX positive cells at different time points (0.5 - 24 h) was between 14.7 to 77.4 in NLNRA, 13.9 to 76.4 in LDG and 11.1 to 76.2 was in HDG (table: 3.4). A significant reduction ($p \leq 0.05$) was observed at 4.0 h and 6.0 h in both LDG and HDG individuals as compared to NLNRA individuals. All the three group of individuals showed similar trend of repair, however, marginally better repair was observed HDG individuals as compared to LDG individuals (figure 3.13). In terms of percentage of repair in three groups, highest repair was observed in HDG followed by LDG and NLNRA individuals. Around 40.7% damage was repaired in HDG at 4.0 h as compared to 35.3% and 15.5% in LDG and NLNRA individuals respectively. At 6.0 h, 62.9% damage was repaired in HDG whereas 59.2% and 44.9 % repair took place in LDG and NLNRA individuals respectively.

However, when compared with maximum damage at 2.0 h, HLNRA individuals showed fastest repair at 4.0 h wherein 41.3% of DSBs were repaired as compared to only 20.6 % repair observed between 4.0 h and 6.0 h. A slower repair was observed in NLNRA individuals where only 15.5 % damage was repaired at 4.0 h whereas 29.4 % DSBs were repaired between 4.0 h and 6.0 h. Further, HDG individuals showed highest repair among HLNRA individuals as compared to LDG individuals. Around 15%, 18 % and 19% of residual DSBs were observed in HDG, LDG and NLNRA respectively at 24.0 h post irradiation.

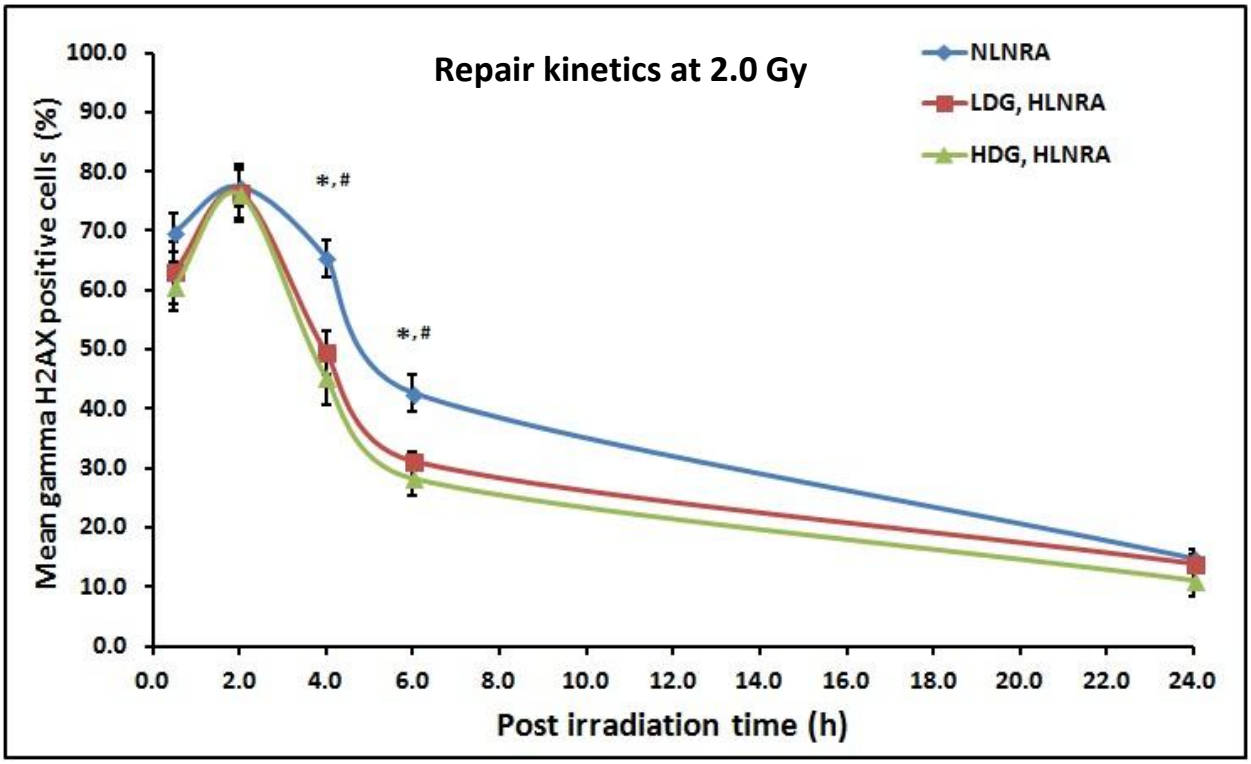

Figure 3.13: The percentage of gamma-H2AX positive cells in PBMCs of NLNRA, LDG and HDG individuals at different post-irradiation timepoints (0.5, 2.0, 4.0, 6.0 and 24.0 h) after 2.0 Gy challenging dose. Mean positive cells at each time point were calculated after normalizing with sham-irradiated control in each dose group. * represents significant difference ($p \leq 0.05$) between NLNRA and LDG whereas, # shows significant difference ($p \leq 0.05$) between NLNRA and HDG. NLNRA: Normal Level Natural Radiation Area, HLNRA: High Level Natural Radiation Area, LDG: low Dose Group, HDG: High Dose Group. Error bars represents S.E.M (Standard Error of Mean)

Repair kinetics at 0.25 Gy: As shown in table 3.6 and figure 3.14, the percentage of mean gamma-H2AX positive cells at different post-irradiation time points (0.5, 2.0, 4.0, 6.0 and 24.0 h) in NLNRA individuals were 19.6, 34.8, 26.6, 16.9 and 8.6 respectively. However, the percentages of gamma-H2AX positive cells were 14.3, 24.8, 17.0, 10.9, 5.2 in HLNRA individuals. A significantly reduced ($p \leq 0.05$) induction of DSBs was observed at 0.25 Gy challenging dose in PBMCs of HLNRA individuals as compared to NLNRA individuals. Interestingly, similar trend of DSB repair was observed both NLNRA and HLNRA individuals.

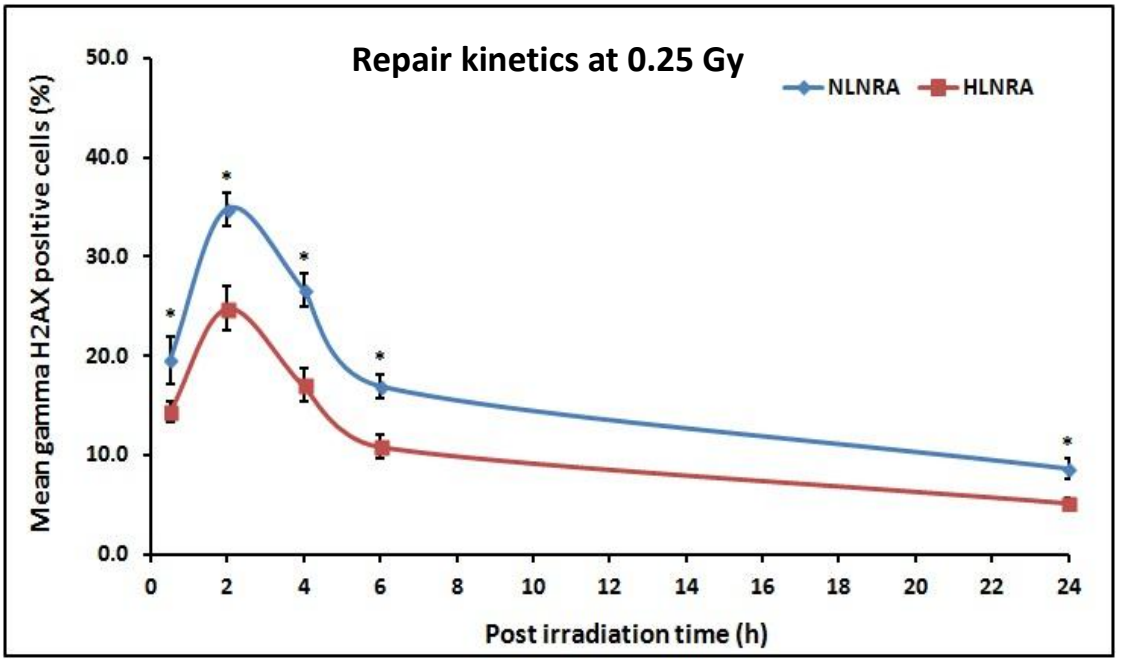

Figure 3.14: The mean percentages of gamma-H2AX positive cells in PBMCs of NLNRA and HLNRA individuals at different post-irradiation timepoints (0.5, 2.0, 4.0, 6.0 and 24.0 h) after 0.25 Gy challenging dose. Mean positive cells at each time point were calculated after normalizing with sham-irradiated control in each dose group * Significant difference ($p \leq 0.05$) between NLNRA and HLNRA. NLNRA: Normal Level Natural Radiation Area, HLNRA: High Level Natural Radiation Area. Error bars represents S.E.M (Standard Error of the Mean)

Table 3.6: The mean percentage of gamma-H2AX positive cells with respect to different background dose groups at different time points (0.5, 2.0, 4.0, 6.0 and 24.0 h) post-irradiation with a challenging dose of 0.25 Gy. Mean positive cells were calculated after normalizing with sham-irradiated control in each dose group {NLNRA, HLNRA (LDG and HDG)}. NLNRA: Normal Level Natural Radiation Area, HLNRA: High Level Natural Radiation Area, LDG: Low Dose Group, HDG: High Dose Group, N: Number of individuals, S.D, Standard Deviation, S.E.M: Standard error of mean.

Area	Background Dose (mGy/y)	Number of individual Studied (N)	Mean Age (year) ± S.D	Mean dose (mGy/y) ± S.D (range)	Mean gamma-H2AX positive cells (%) ± S.E.M at 0.25 Gy				
					0.5 h	2.0 h	4.0 h	6.0 h	24.0 h
NLNRA	≤ 1.5	8	34.9 ± 4.8	1.4 ± 0.1 (1.3 - 1.5)	19.6 ± 2.4	34.8 ± 2.4	26.6 ± 1.6	16.9 ± 1.2	8.6 ± 0.9
HLNRA	LDG (1.51-5.0)	7	42.6 ± 6.02	3.6 ± 0.5 (3.2 - 4.5)	14.5 ± 1.8	25.4 ± 3.9	17.9 ± 2.2	12.5 ± 1.9	6.1 ± 1.5
	HDG (> 5.0)	11	38.5 ± 6.4	9.6 ± 1.8 (7.7 - 12.9)	13.5 ± 1.4	24.4 ± 2.6	16.3 ± 2.4	10.0 ± 1.5	4.5 ± 1.0
	HLNRA (> 1.5)	18	40.11 ± 6.40	7.2 ± 3.3 (3.2 - 12.9)	14.3 ± 1.0	24.8 ± 2.2	17.0 ± 1.7	10.9 ± 1.2	5.2 ± 0.6

As shown in table 3.7, the percentage of DSB repair at 4.0 h, 6.0 h and 24.0 h was observed to be 31.4, 56.3 and 79.9 in HLNRA individuals as compared to 23.4, 51.3 and 75.2 respectively in NLNRA. However residual damage after 24.0 h was observed to be around 20-24 % in HLNRA and NLNRA individuals.

Table 3.7: Mean percentage of DNA DSBs repaired calculated in terms of percent decrease in gamma-H2AX positive cells with respect to maximum positive cells observed in the PBMCs exposed to 0.25 Gy post-irradiation at different time intervals (4.0, 6.0 and 24.0 h). Percentages of residual DSBs are also shown. NLNRA, Normal level natural radiation area, HLNRA, High level natural radiation area, LDG, low dose group, HDG, high dose group.

Area	Background Dose (mGy/y)	Percentage of DSBs (gamma-H2AX positive cells) repaired at 0.25 Gy			Percentage of residual DSBs (gamma-H2AX positive cells) at 0.25 Gy		
		4.0 h	6.0 h	24.0 h	4.0 h	6.0 h	24.0 h
NLNRA	≤ 1.5	23.5	51.3	75.2	76.5	48.7	24.8
HLNRA	LDG (1.51-5.0)	29.7	50.9	75.9	70.3	49.1	24.1
	HDG (> 5.0)	33.2	59.1	81.5	66.8	40.9	18.5
	HLNRA (> 1.5)	31.4	56.3	79.2	68.6	43.7	20.8

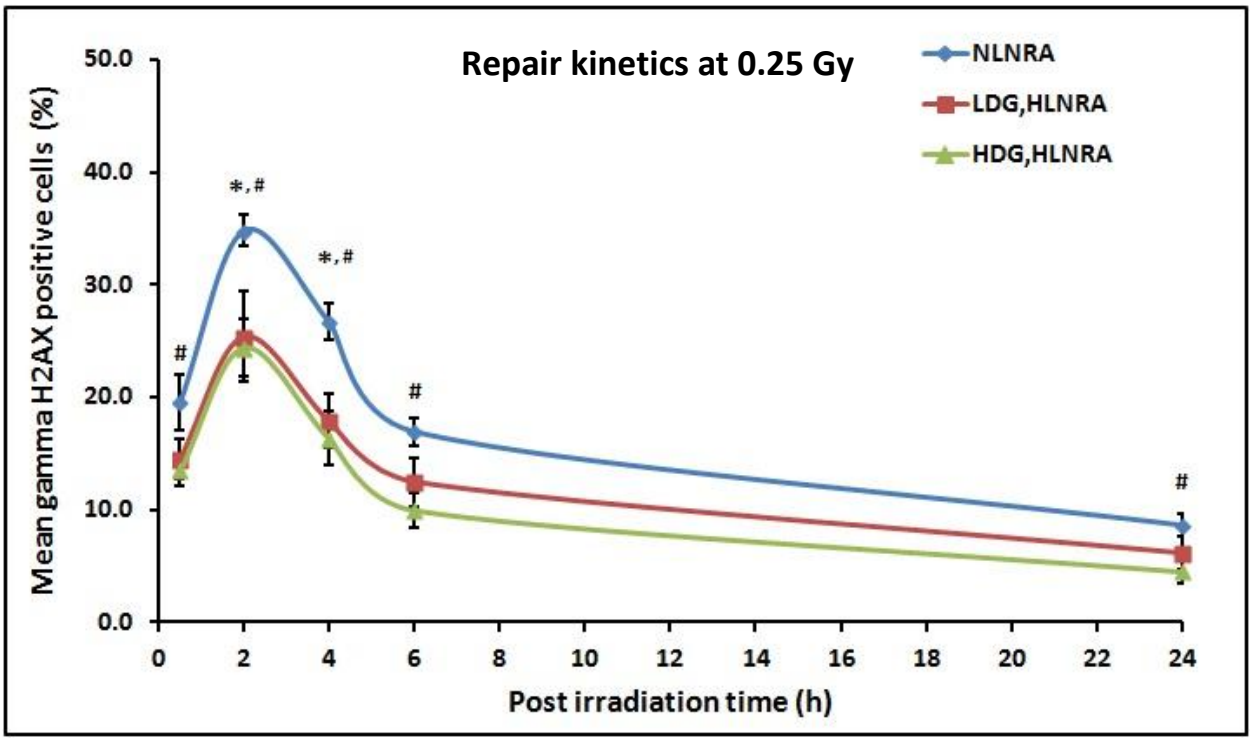

Figure 3.15: The percentage gamma H2AX positive cells in NLNRA and HLNRA (LDG and HDG) individuals at different time points post-irradiation with 0.25 Gy challenging dose.* Significant difference ($p \leq 0.05$) between NLNRA and LDG whereas # shows significant difference ($p \leq 0.05$) between NLNRA and HDG. Mean positive cells at each time point were calculated after normalizing with sham-irradiated control in each dose group. NLNRA: Normal Level Natural Radiation Area, HLNRA: High Level Natural Radiation Area, LDG: low Dose Group, HDG: High Dose Group. Error bars represents S.E.M (Standard Error of Mean)

Further analysis was carried out in three groups, NLNRA, LDG and HDG. The percentages of gamma-H2AX positive cells at different time points (0.5- 24.0 h) were observed to be between 8.6 to 34.8, between 6.1 to 25.4 and 4.5 to 24.4, 16.3, 10.0, 4.5 in NLNRA, LDG and HDG individuals respectively (table 3.6, figure 3.15). In terms of percentage of repair in three groups, highest repair was observed in HDG followed by LDG and NLNRA individuals. Around 33.2% damage was repaired in HDG at 4.0 h as compared to 29.7% and 23.4% in LDG and NLNRA individuals respectively. At 6.0 h, 59.1% damage was repaired in HDG whereas 50.9 % and 51.5% repair observed in LDG and NLNRA individuals respectively. The residual

damage observed at 24.0 hr in NLNRA, LDG and HDG group was 24.8 %, 24.1% and 18.5% respectively (table 3.7).

In summary, at both low and high challenging doses studied, a bi-exponential pattern of repair was observed with a fast repair kinetics phase where approximately 50% DSBs were repaired within 6.0 h post-irradiation. A slow repair kinetics observed beyond 6.0 h where approximately 10-20 % of initial damage was still present at 24.0 h post-irradiation with 0.25 and 2.0 Gy. The residual damage was observed to be more in NLNRA and LDG individuals as compared with HDG individuals at both the challenging doses.

3.2 Gene expression study at acute and chronic exposure

To investigate the effects of chronic low dose IR at cellular and molecular level, gene expression analysis was carried out in individuals from NLNRA and HLNRA areas. In the present study, transcriptome profile analysis was carried out in PBMCs of individuals from high background and normal level areas. In this study we have employed high throughput microarray technique to find out all the statistically significant differentially expressed genes in different HLNRA dose groups with respect to NLNRA group using Human HG-133 plus 2.0 gene chip (Affymetrix). This array can detect the expression level of 47,000 transcripts from more than 38,000 well characterized human genes simultaneously for a single sample. In addition, validation of selected genes was carried out using specific hydrolysis probe based real time q PCR (RT q-PCR). Radio-adaptive response was studied in non homologous end joining (NHEJ) DNA repair pathway genes at a challenging dose of 2.0 Gy. Gene expression of selected genes was also carried out in the PBMCs irradiated with different acute doses of gamma radiation (0.3 to 2.0 Gy) at different post-irradiation time points.

3.2.1 Global gene expression profile (transcriptome analysis) in NLNRA and HLNRA individuals using microarray

Transcriptome analysis was carried out in 36 individuals from NLNRA (N=9) and HLNRA (N=27). Venous blood samples were collected from all the individuals with informed and written consent. A detailed questionnaire containing information on all confounding factors such as age, smoking habit, chewing habit, occupation, ethnicity, lifestyle, medical history, diagnostic exposure to radiation etc. were collected. Individual dosimetry was carried out for all the individuals as discussed in materials and methods section. Venous blood samples were collected and kept in refrigerated condition and processed within 30 minutes of collection.

The individuals were classified into four groups (NLNRA and 3 HLNRA) on the basis of annual background radiation dose received by each of them. The HDG individuals (> 5.0 mGy/y) were further divided into two groups. The four dose groups were Group I (NLNRA) ≤ 1.5 mGy/y, N=9, Group II (LDG, HLNRA) 1.51 - 5.0 mGy/y, N=9, Group III (HDG, HLNRA) > 5.01 – 15.0 mGy/y, N=11, Group IV (HDG, HLNRA) > 15 mGy/y, N=7 as shown in table 3.8. The mean age of individuals was 39.7 ± 4.7 y (NLNRA, Group I), 41.9 ± 6.8 y (HLNRA, Group II), 40.5 ± 6.9 y (HLNRA, Group III) and 39.3 ± 4.3 y (HLNRA, Group IV).

Table 3.8: Distribution of individuals with different background dose groups studied for transcriptome analysis. The HLNRA individuals were stratified in three dose groups {Group II (LDG), Group III (HDG) and Group IV (HDG)}. NLNRA: Normal Level Natural Radiation Area, HLNRA: High Level Natural Radiation Area, LDG: Low Dose Group, HDG: High Dose Group, N: Number of individuals, S.D: Standard deviation.

Background dose groups	Dose rate (mGy/y)	Mean Dose ± S.D.	Individuals per group (N)
Group 1 (NLNRA)	≤ 1.5	1.4 ± 0.1	9
Group II (LDG, HLNRA)	> 1.51 - 5.0	2.1 ± 0.7	9
Group III (HDG, HLNRA)	> 5.01 – 15.0	11.1 ± 1.1	11
Group IV (HDG, HLNRA)	> 15.0 - 28.0	16.7 ± 2.1	7

3.2.1.1 Differentially expressed genes in HLNRA individuals as compared to NLNRA

Analysis was carried out to find out the differentially expressed genes (up-regulated and down-regulated) between each HLNRA dose groups (Group II, Group III and Group IV) as compared to NLNRA (Group I) as shown in table 3.8. To obtain differentially expressed genes, moderated t-statistic was implemented. Since each analysis involved large number of genes, the multiple testing corrections was performed using Benjamin & Hochberg (BH) correction adjusting for the false discovery rate (FDR). A threshold adjusted p-value was set to 0.05 and the fold-change threshold was set to 1.3. These settings were retained throughout the analysis to select gene list across different comparisons.

Table 3.9: Differentially expressed genes (up and downregulated) at fold change of 1.3, 1.5 and 2.0 in different dose groups of HLNRA (Group II, Group III and Group IV) as compared to NLNRA (Group I).

Dose groups	1.3 fold		1.5 fold		2.0 fold	
	Up	Down	Up	Down	Up	Down
Group 1 vs II	39	99	10	17	3	3
Group1 vs III	611	750	167	165	15	9
Group 1 vs IV	889	1538	347	422	72	25

The numbers of differentially expressed genes were obtained between following group comparisons. 1) Group I (NLNRA) and Group II (HLNRA), 2) Group I (NLNRA) and Group III (HLNRA), 3) Group I (NLNRA) and Group IV (HLNRA). As shown in table 3.9, a total of 138 (39 up and 99 down), 1361 (611 up and 750 down), 2427 (889 up and 1538 down) genes were found to be differentially expressed between Group I vs. Group II, Group I vs. Group III and Group I vs. Group IV respectively. Overall, a total of 1539 and 2387 genes were found to be significantly up and down regulated in HLNRA individuals as compared to NLNRA.

Similar analysis was carried out to find out differentially expressed genes at fold change threshold of 1.5 and 2.0. As shown in table 3.9, a total of 27 (10 up and 17 down), 332 (167 up and 165 down) and 769 (347 up and 422 down) genes were differentially expressed at 1.5 fold difference whereas at 2.0 fold difference, 6 genes (3 up and 3 down), 24 (15 up & 9 down), 97 (72 up and 25 down) were differentially expressed in Group I vs. II, Group I vs. III and Group I vs. IV respectively (figure 3.16).

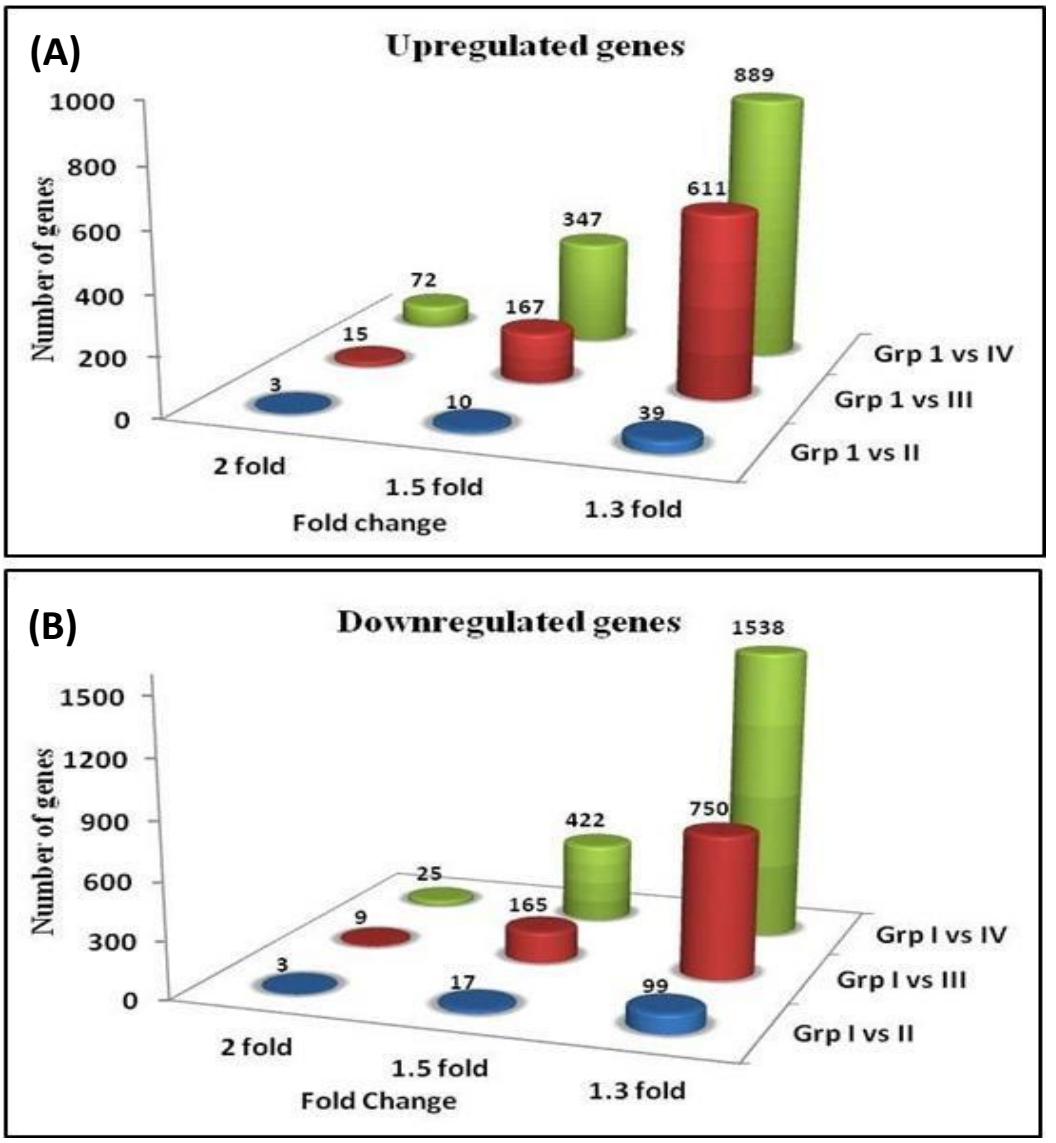

Figure 3.16: Graphical representation of (A) up-regulated and (B) down-regulated genes in different dose groups of HLNRA (Group II, Group III and Group IV) as compared to NLNRA (Group I).

Our analysis showed a large number of genes were differentially expressed in HLNRA groups as compared to NLNRA. Interestingly, a background dose related increase in the number of differentially expressed genes was observed in HLNRA individuals as compared to NLNRA.

The scatter plot representation of differentially expressed genes (up and down-regulated) is shown as volcano plots (figure 3.17). The horizontal line at 1.301 corresponds to adjusted p-value of 0.05, while the two vertical lines correspond to the lower and the upper fold change thresholds of 1.3. The spots in the blue and red are significantly up and down-regulated genes. The black spots show insignificant genes. Figure 3.17 showing volcano plots for Group I vs Group II, Group I vs Group III and Group I vs Group IV comparisons.

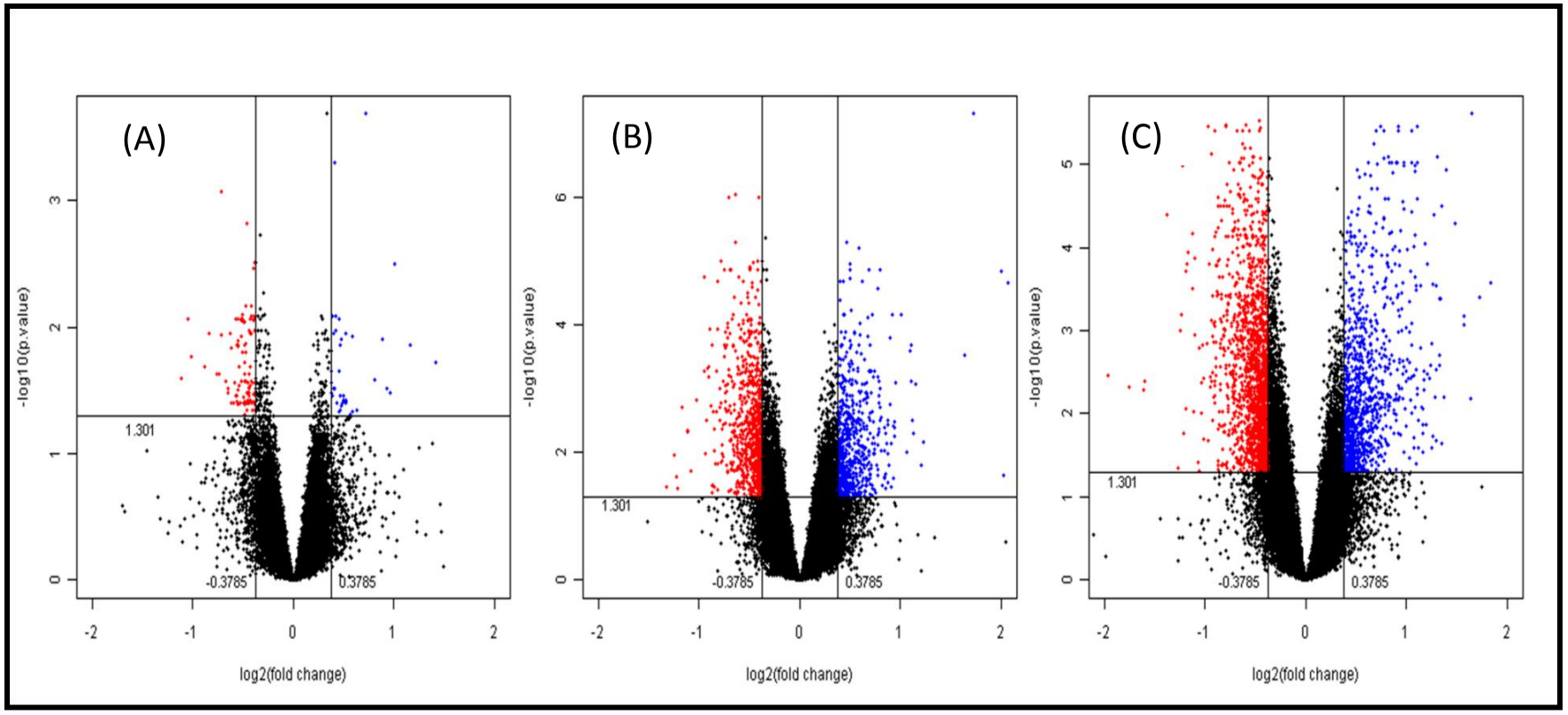

Figure 3.17: Volcano plots representing the differentially expressed genes (up and down-regulated) at 1.3 fold in different HLNRA groups (Group II, III and IV) as compared to NLNRA (Group I). A) Group I vs. II, B) Group I vs. III, C) Group I vs. IV. Blue dots represent significant ($p \leq 0.05$) up-regulated genes and red dots represent significant down- regulated genes.

Cluster analysis of the differentially expressed genes with $p \leq 0.05$ was carried out. Difference in the level of expression of all statistically significant genes across all the samples in a particular group comparison was plotted as heat maps. The heat map is a graphical representation of data where the individual expression values are represented as a range of colors indicating varying intensity levels. It allows comparing expression levels of multiple genes in multiple comparable samples. Cluster analysis was carried out using average linkage hierarchical clustering approach with Euclidean distance measure from R statistical package to obtain relatedness of samples as well as differentially expressed genes. The samples and genes which show similar expression patterns are clustered together and represented in the form of dendrograms. As shown in figure 3.18 and 3.19, the individuals from Group I, Group II, Group III and Group IV have observed to be clustering within the group. It shows that the expression pattern among individuals belonging to the same group is consistent and comparable.

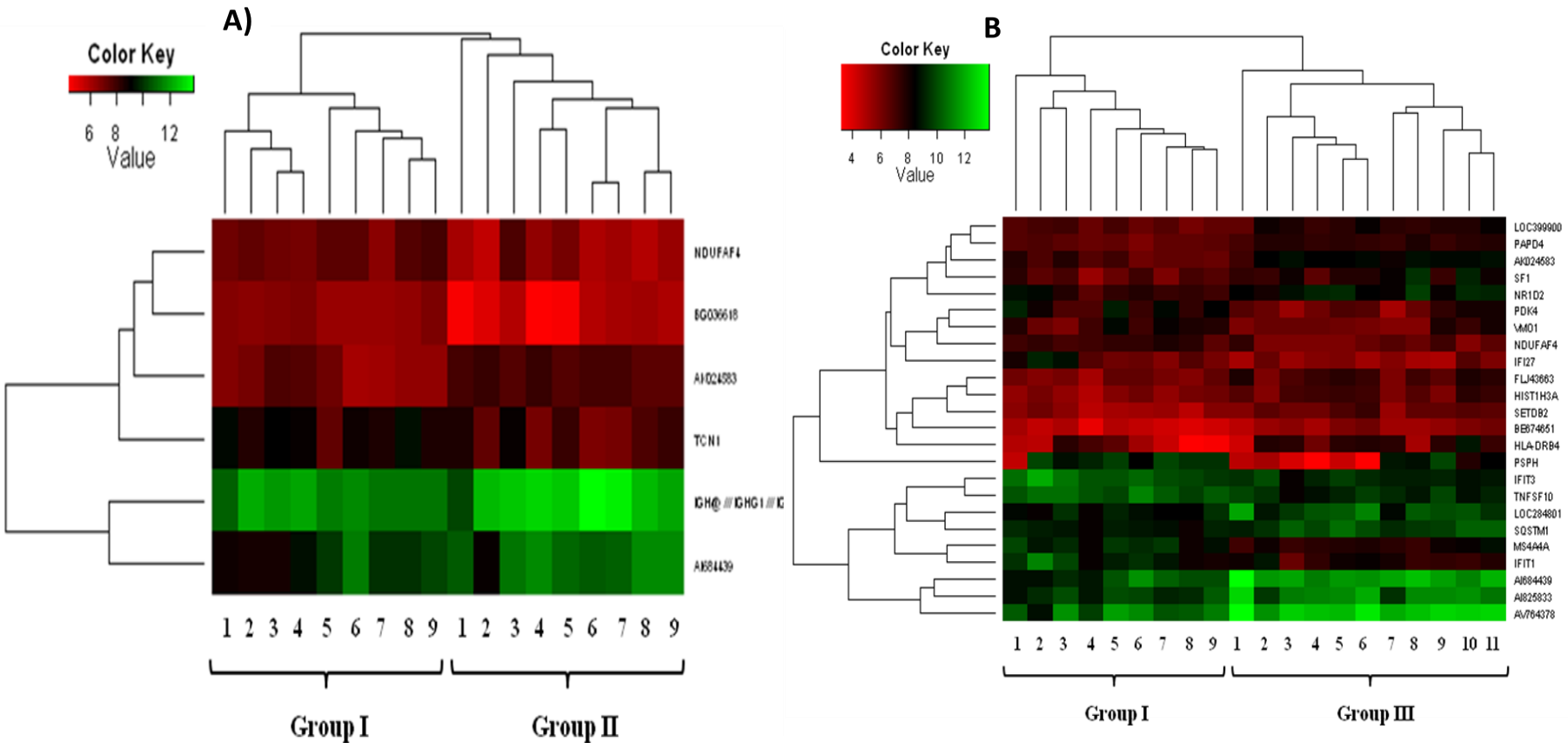

Figure 3.18: Representative heat maps showing clustering of samples and genes among NLNRA and HLNRA groups. A) Heat map of differentially expressed genes at 2.0 fold in group I vs. group II (B) Heat map of differentially expressed genes at 2.0 fold in Group I vs. Group III.

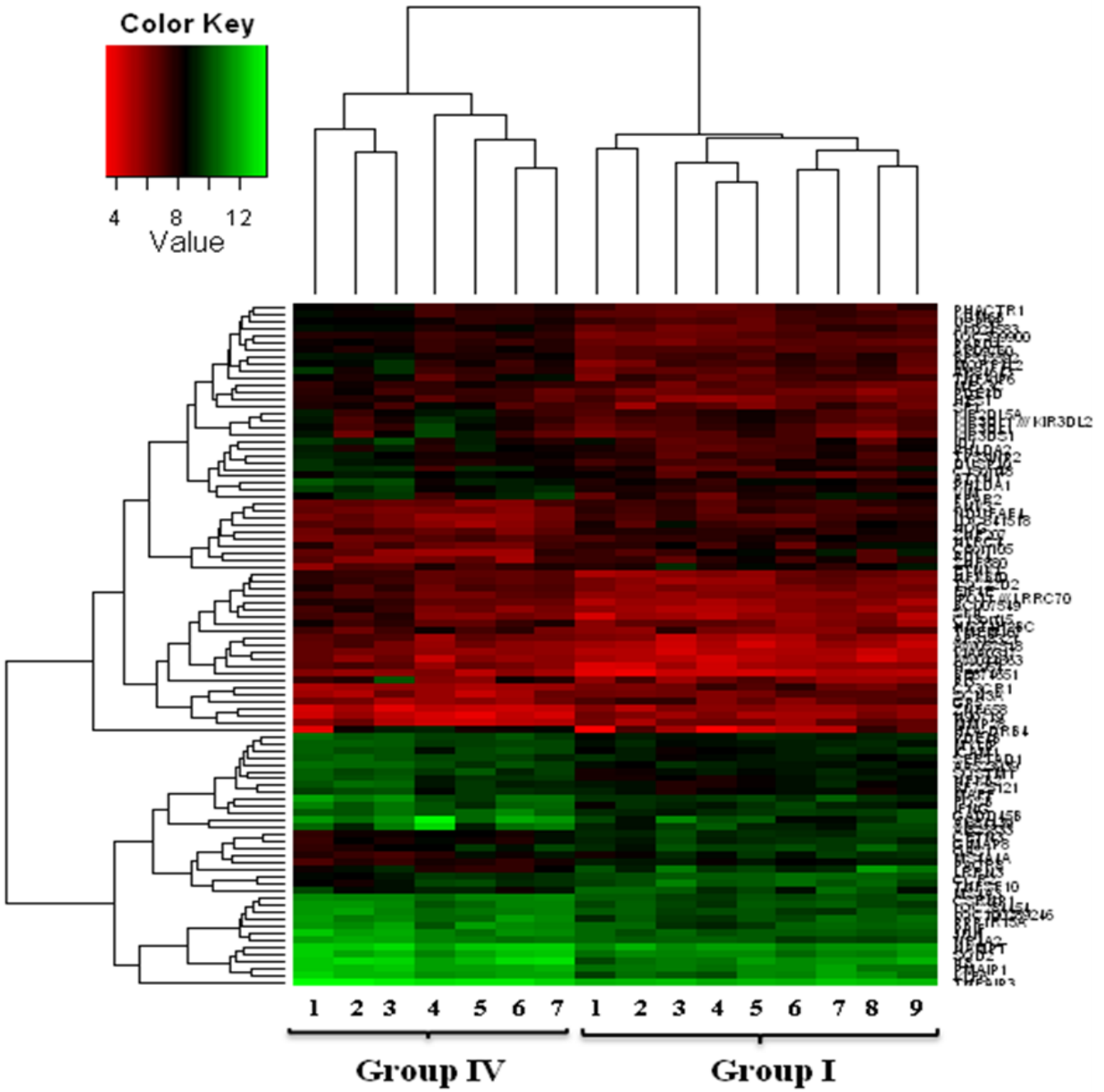

Figure: 3.19: Representative heat maps showing clustering of samples and genes among NLNRA and HLNRA groups. Heat map of differentially expressed genes at 2.0 fold in Group I vs. Group IV is shown.

3.2.1.2 Identification of common genes among different background radiation dose groups.

As shown in figure 3.16, a large number of genes were differentially expressed in different HLNRA dose groups (Group II, III and IV) with respect to NLNRA (Group I). Further analysis was done to find out the number of common genes and unique genes between the dose groups which is represented in the form of venn diagrams.

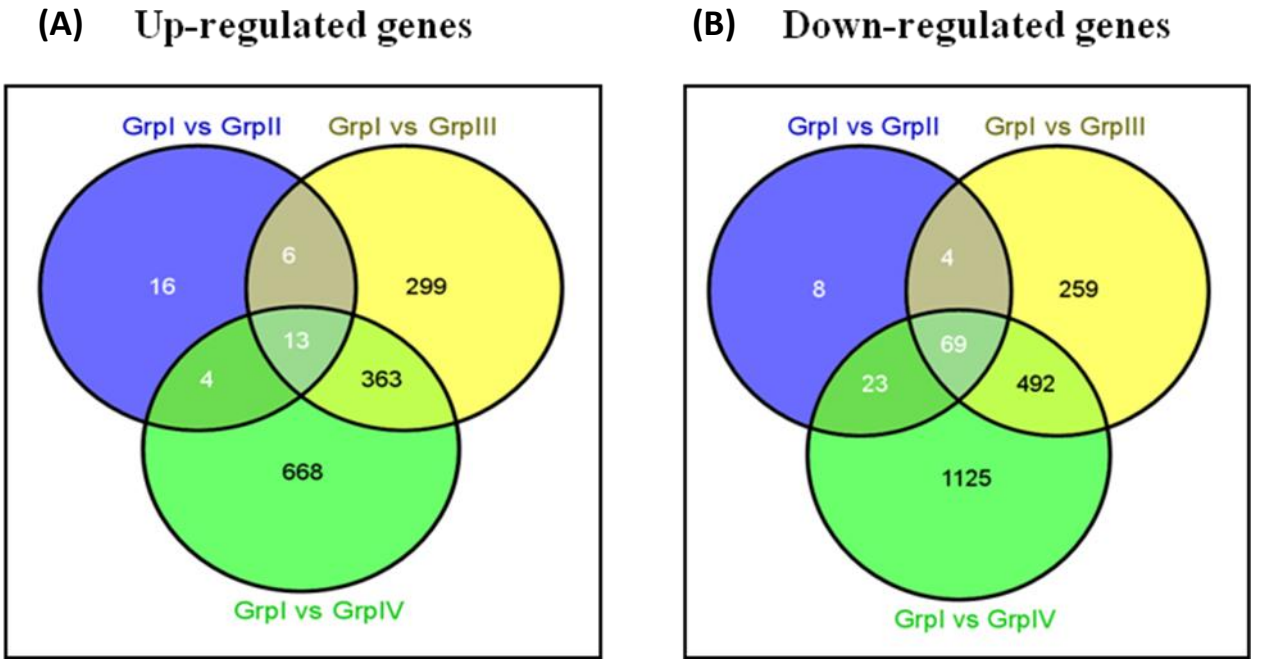

Figure 3.20: Venn diagram showing (A) up-regulated and (B) and down- regulated common and unique genes expressed in different dose groups. Genes showing ≥ 1.3 fold change was considered for analysis. NLNRA (Group I) and HLNRA (Group II, III and IV).

A criteria of ≥ 1.3 fold change and 5 % cut off on corrected p values were used to identify common genes. As shown in venn diagram (Figure 3.20), a total of 82 genes (13 up-regulated and 69 down- regulated) were found to be differentially expressed in all the 3 groups. Details and characteristics of the common genes are given as table 3.10 (A and B). We also analyzed the common genes between Group II and Group III, Group II and Group IV, Group III and Group IV. Our analysis showed a total of 92 (19 up and 73 down), 109 (17 up and 92 down)

and 937 (376 and 561) genes were common between Group II and III, Group II and IV and Group III and IV respectively. Similarly, unique genes expressed in each group were also analyzed. A total of 24 (16 up and 8 down), 558 (299 up and 259 down) and 1793 (668 up and 1125 down) genes were found to be uniquely expressed in Group II, Group III and Group IV respectively.

Table 3.10A : Set of common genes showing up-regulation at > 1.3 fold change in all 3 HLNRA dose groups (Group II, Group III, Group IV) with respect to NLNRA (Group I) with p- value ≤ 0.05.

Gene Symbol	**Accession number**	**Fold change (Group II)**	**Fold change (Group III)**	**Fold change (Group IV)**	**Function**
ZBTB24	BC036731	1.38	1.39	1.45	Transcription regulation
EIF4G3	BC030578	1.55	1.59	1.87	Translation initiation
PDE4B	L20966	1.85	1.66	2.04	Signal transduction
EIF1	AL516854	1.50	1.72	1.87	Translation initiation
HNRNPM	AK024911	1.42	1.39	1.41	mRNA processing
AF070620	AF070620	1.64	1.61	1.63	-
USP36	NM_025090	1.75	1.54	2.27	Protein degradation
RPL10	AW057781	1.39	1.38	1.41	Ribosome synthesis
USP15	AK023703	1.44	1.32	1.52	Protein degradation
AK024583	AK024583	2.01	3.30	3.14	-
AI684439	AI684439	2.67	4.19	3.56	-
AW009425	AW009425	1.39	1.44	1.37	-
SNRPA1	AA872471	1.47	1.67	1.41	RNA splicing

Table 3.10 B : Set of common genes showing down-regulation of > 1.3 fold change in all HLNRA dose groups (Grp II, Grp III, Grp IV) with respect to NLNRA (Grp I) with p- value ≤ 0.05

Gene Symbol	**Accession number**	**Fold change Group II**	**Fold change Group III**	**Fold change Group IV**	**Function**
NT5E	BC015940	-1.69	-1.60	-1.81	Nucleotide metabolism
LOC100287896	BC019340	-1.64	-1.69	-1.97	-
BET1	BC000899	-1.50	-1.60	-1.61	Protein transport
NUPL2	NM_007342	-1.35	-1.38	-1.43	mRNA transport
ZBTB1	NM_014950	-1.48	-1.63	-1.67	Transcription regulation
GTF2E1	NM_005513	-1.44	-1.66	-1.82	Transcription initiation
ZNF167	NM_018651	-1.49	-1.68	-1.81	Transcription regulation
JRKL	NM_003772	-1.31	-1.43	-1.73	-
GRB10	D86962	-1.35	-1.31	-1.60	Insulin receptor binding.
IL16	M90391	-1.54	-1.67	-1.56	Cytokine activity
SLC4A7	AF047033	-1.39	-1.48	-1.75	Ion transport
HGF	X16323	-1.48	-1.32	-1.55	Cell growth
FEM1B	AI799061	-1.33	-1.58	-1.66	Apoptosis
METTL13	AK001172	-1.41	-1.42	-1.62	Methyltransferase activity
MED20	AK023092	-1.31	-1.42	-1.35	Transcription regulation
KLHL9	AW138594	-1.40	-1.39	-1.42	Cell cycle regulation
TTC9	AW235608	-1.43	-1.31	-1.54	Cell growth
ISOC1	NM_016048	-1.36	-1.42	-1.33	-

Contd…

Gene Symbol	Accession number	Fold change Group II	Fold change Group III	Fold change Group IV	Function
SAR1B	NM_016103	-1.32	-1.44	-1.34	Protein transport
MANEA	NM_024641	-1.46	-1.43	-1.34	Protein transport
ETNK1	NM_018638	-1.31	-1.39	-1.32	Cell metabolism
TMEM184C	NM_018241	-1.31	-1.41	-1.44	Cell growth
BOLA1	NM_016074	-1.43	-1.46	-1.69	Not known
BBS10	NM_024685	-1.45	-1.65	-1.76	Protein folding
TRIM36	NM_018700	-1.40	-1.39	-1.35	Cell cycle regulation
L1TD1	NM_019079	-1.36	-1.50	-1.43	Not known
CALHM2	BC000039	-1.49	-1.37	-1.38	Ion transport
CCDC28B	AL049795	-1.36	-1.50	-1.35	cilia development
PPIL1	BC003048	-1.42	-1.77	-1.63	Protein folding
TRNT1	BE552215	-1.54	-1.60	-1.59	Nucleotide metabolism
ARRB1	BC003636	-1.35	-1.45	-1.34	Signal transduction
GBP3	AL136680	-1.48	-1.42	-1.56	GTPase activity
EXOSC3	AF281132	-1.33	-1.47	-1.52	RNA processing
THAP2	AL136607	-1.66	-1.66	-1.90	Apoptosis
ANUBL1	AF311324	-1.36	-1.39	-1.39	Cell cycle regulation
YIPF5	AW001618	-1.64	-1.65	-1.86	Protein transport
SLC35F5	AA044835	-1.37	-1.39	-1.38	Ion transport

Contd…

Gene Symbol	Accession number	Fold change Group II	Fold change Group III	Fold change Group IV	Function
NAPEPLD	BF382393	-1.78	-1.52	-1.79	Cell metabolism
APH1B	AW237258	-1.38	-1.39	-1.44	cleavage of integral proteins
KDM5A	AI672662	-1.39	-1.44	-1.65	Histone demethylation
TMTC3	AA428286	-1.35	-1.35	-1.50	Transmembrane protein
MED11	AL531790	-1.32	-1.55	-1.52	Transcription regulation
NDUFAF4	AL521129	-2.02	-2.03	-2.16	Mitochondrial respiratory chain.
ZNF322A	AW511258	-1.47	-1.31	-1.47	Transcription regulation
CCDC126	AK026684	-1.40	-1.57	-1.59	Cell metabolism
MFSD8	AW611550	-1.40	-1.38	-1.65	Ion transport
ZEB2	AI912571	-1.55	-1.66	-1.70	Transcription regulation
PPM1N	BE732320	-1.38	-1.37	-1.39	Cell cycle regulation
ZNF823	AI417785	-1.46	-1.47	-1.57	Transcription regulation
ZNF585A	BE550717	-1.42	-1.59	-1.48	Transcription regulation
KCTD21	AI391633	-1.37	-1.60	-1.74	Ion transport
LPAR5	AW183080	-1.47	-1.64	-1.66	Signal transduction
AI673025	AI673025	-1.41	-1.35	-1.35	-
TUBD1	AK022771	-1.43	-1.62	-1.70	Microtubule formation
BPNT1	AI439695	-1.35	-1.45	-1.73	Nucleotide metabolism

Contd…

Gene Symbol	Accession number	Fold change Group II	Fold change Group III	Fold change Group IV	Function
ARL6	AL138043	-1.37	-1.33	-1.65	membrane protein trafficking
DHFRL1	AW104373	-1.51	-1.65	-1.82	Cell metabolism
AI823600	AI823600	-1.59	-1.49	-1.76	-
AI738675	AI738675	-1.40	-1.58	-1.47	-
ZNF738	AI758317	-1.57	-1.49	-1.48	Transcription regulation
AW770320	AW770320	-1.31	-1.36	-1.59	-
R63578	R63578	-1.38	-1.48	-1.72	-
ZNF234	BE909177	-1.33	-1.34	-1.49	Transcription regulation
SOAT1	AA946876	-1.33	-1.56	-1.52	Cell metabolism
ABHD6	AA209239	-1.39	-1.61	-1.34	Cell metabolism
PIGV	AA203365	-1.38	-1.64	-1.47	Signal transduction

The expression intensity of differentially expressed (up and down-regulated) common genes in different individuals of the group is shown as heat map in Figure 3.21 and 3.22. Also, mean intensities of differentially expressed genes in different dose groups is plotted and shown in figure 3.20 and 3.21. The function of these genes are shown in Table 3.10 A and B

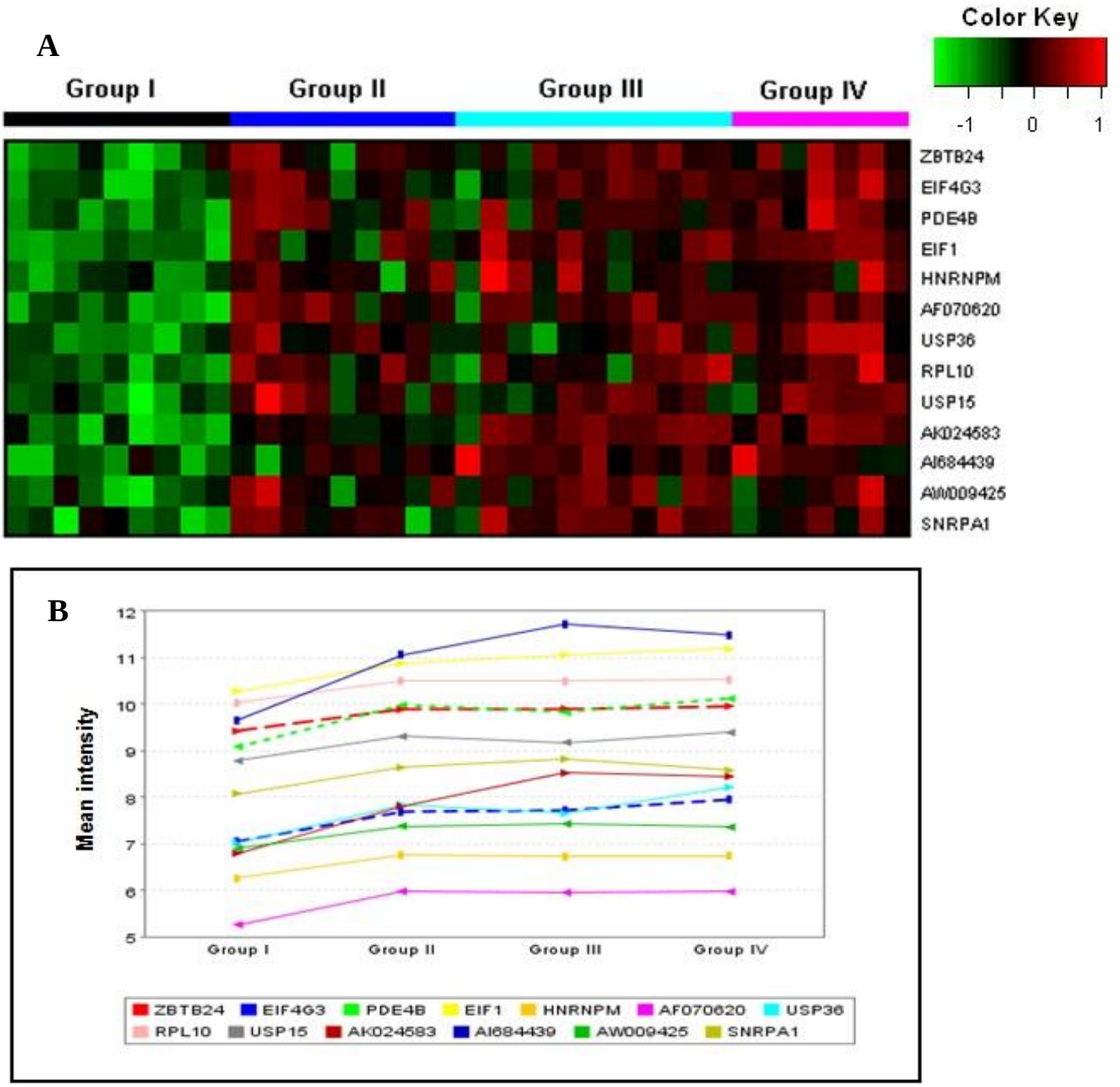

Figure 3.21: A) Heat map showing expression intensity of up-regulated common genes in NLNRA (group I) and three HLNRA (group II, group III and group IV). B) Mean intensity of up-regulated genes in different dose groups are shown. Color key represents increase in expression intensity from green to red color.

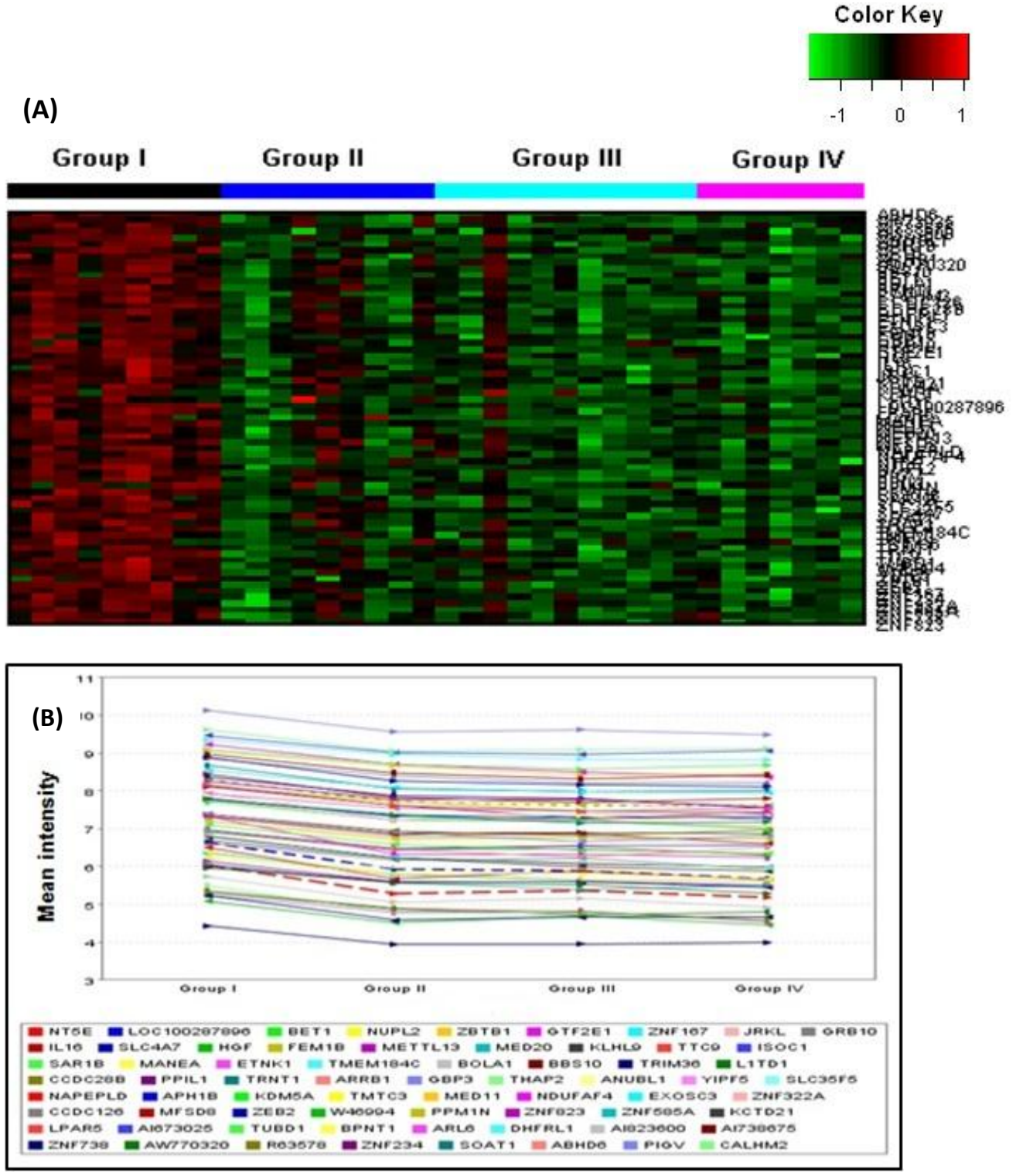

Figure 3.22: A) Heat map showing expression intensity of down-regulated common genes in NLNRA (group I) and three HLNRA (group II, group III and group IV). B) Mean intensity of down-regulated genes in different dose groups are shown. Color key represents increase in expression intensity from green to red color.

3.2.2 Bioinformatic analysis of differentially expressed genes in HLNRA individuals

Gene Ontology (GO) and pathway analysis was done to find out the biological significance of the differentially expressed genes. The differentially expressed genes obtained in three HLNRA groups (Group II, Group III and Group IV) as compared to NLNRA (Group I) were analyzed for their overabundance in different GO terms as well as biological and molecular pathways. Analysis was done to find overrepresented biological processes, cellular components, molecular functions and important pathway in differentially expressed genes with the statistical significance of $P \leq 0.05$. Bioinformatic analysis was done using EXPLAIN® Version 3.1 (Biobase Biological Database, Germany), Genowiz^{TM,} TRANSPATH® and KEGG pathway databases.

3.2.2.1 Gene ontology analysis of differentially expressed genes in HLNRA individuals

Detailed analysis was carried out to find over-represented gene ontology terms in differentially expressed genes in Group I vs. Group II, Group I vs. Group III and Group I vs. Group IV. Our analysis revealed that in Group II (≤ 5.0 mGy/y), up-regulated genes were involved in biological processes such as regulation of translation initiation *(EIF1, EIF4G3)*, regulation of transcription (*ZBTB24, SOX5*) cell proliferation (*BCAT1, MXD1*), RNA splicing (*HNRNPM, SNRPA1*), immune response (*IGHG1, IL1A*), transmembrane transport (*SCN1A, SLC2A3*) etc whereas down regulated genes were involved in regulation of transcription (*ZBTB1, GTF2E1, ARRB1*) protein transport (*YIPF5, BET1*), cellular membrane organization (*ARRB1, SAR1B*), metabolic process (*NT5E, METTL13*) etc (as shown in table 3.11). However, it is interesting to note here that very few genes were represented in each biological process.

Gene enrichment analysis of higher dose groups (Group I vs. III and Group I vs. IV) revealed that the majority of upregulated genes were involved in transcriptional regulation,

mRNA processing, apoptosis, response to oxidative stress, cell proliferation, protein ubiquitination, response to DNA damage, cell cycle arrest, signal transduction, DNA repair and chromatin modification. Whereas over-represented biological process in down-regulated genes were protein transport, immune response, metabolic process, chromatin modification, protein folding, inflammatory response, transmembrane transport, cell adhesion, DNA repair etc . Some of the important genes such as *RAD21, LIG4, DCLRE, XRCC4* (DNA repair), *CDKN1A, DDIT3, GADD45B* (DNA damage response), *HLA-DRB4, IL8, KIR3DS1* (Immune response), *HIST1H1E, H3F3B, HIST1H2BC, HP1BP3, KDM6B, ING3, SETDB2* (chromatin modification), *HIPK1, PMAIP1, APAF1, PPP1R15A* (apoptosis) were found to be differentially expressed in HLNRA population. Details of the biological processes and their representative genes are given in table 3.11.

Table 3.11 List of significantly over-represented biological processes in differentially expressed genes of HLNRA groups (Group II, Group III and Group IV) as compared to NLNRA (Group I)

Group II	GO term (Biological Processes)	No. of genes /database count	P Value	Representative Genes
Up-regulated genes	regulation of translational initiation	(2 / 24)	0.0001	*EIF1, EIF4G3*
	nuclear mRNA splicing, via spliceosome	(2 / 44)	0.0003	*HNRNPM, SNRPA1*
	cell proliferation	(3 / 295)	0.0005	*IL1A, BCAT1, MXD1*
	ubiquitin-dependent protein catabolic process	(2 / 151)	0.003	*USP36, USP15*
	RNA splicing	(2 / 267)	0.008	*HNRNPM, SNRPA1*
	regulation of transcription	(3 / 989)	0.01	*MXD1, SOX5, ZBTB24*
	immune response	(2 / 362)	0.01	*IGHG1, IL1A*
	transmembrane transport	(2 / 508)	0.03	*SCN1A, SLC2A3*
Down-regulated genes	regulation of transcription	(8 / 989)	0.0002	*GTF2E1, ZBTB1, ZNF322A*
	ER to Golgi vesicle-mediated transport	(2 / 42)	0.002	*BET1, SAR1B*
	protein transport	(4 / 408)	0.004	*NUPL2, BET1, YIPF*
	cellular membrane organization	(2 / 58)	0.004	*ARRB1, SAR1B*
	apoptosis	(4 / 461)	0.006	*WDR92, C16orf5, APH1B*
	protein folding	(2 / 151)	0.03	*TTC9, PPIL1*
	metabolic process	(3 / 485)	0.04	*METTL13, NT5E, PNPLA4*

Contd…

Group III	GO term (Biological Processes)	No. of genes /database count	P Value	Representative Genes
Up-regulated genes	regulation of transcription	(56 / 989)	5.84E-028	*KLF6, FOXO3, JUN*
	RNA splicing	(22 / 267)	9.82E-015	*SRRM1, SF1, RBM8A*
	protein ubiquitination	(12 / 88)	6.04E-011	*UBE2B, RBBP6, SMURF1*
	mRNA processing	(16 / 246)	1.13E-009	*PAPD4, PTBP1, SFRS2*
	protein transport	(18 / 408)	3.35E-008	*TMED2, SEC31A, PSEN1*
	apoptosis	(19 / 461)	3.91E-008	*SIAH1, PMAIP1, CASP2*
	cell cycle	(19 / 470)	5.22E-008	*DUSP1, CDC14A, CCNK*
	cell cycle arrest	(10 / 108)	7.15E-008	*CDKN1A, DDIT3, RB1*
	response to oxidative stress	(6 / 104)	0.0003	*DUSP1, BTG1, PRNP*
	response to DNA damage stimulus	(5 / 84)	0.0009	*GADD45B, CDKN1A, DDIT3*
	signal transduction	(29 / 1959)	0.005	*CSNK1A, NFKB2, STK4*
	chromatin modification	(6 / 206)	0.009	*KDM6B, MYST4, SETDB2*
	DNA repair	(5 / 192)	0.026	*RAD23B, RAD21, DCLRE1A*
Down-regulated genes	regulation of transcription	(47 / 989)	1.14E-014	*ZBTB1, GTF2E1, POLR3K*
	protein transport	(26 / 408)	2.98E-011	*NUPL1, BET1, SNX5*
	immune response	(19 / 362)	2.40E-007	*CCR2, IL16, IL27RA*

Contd…

Group III	GO term (Biological Processes)	No. of genes /database count	P Value	Representative Genes
	metabolic process	(21 / 485)	1.14E-006	*TMEM68, METTL13, ATP7A*
	protein ubiquitination	(9 / 88)	2.67E-006	*DCAF7, UBE2H, RNF14*
	signal transduction	(49 / 1959)	3.07E-006	*AKT3, MAP3K8, MAPK1*
	mRNA processing	(13 / 246)	1.75E-005	*HNRNPA0, PAPOLG, RBM8A*
	cell cycle	(18 / 470)	3.13E-005	*CDKN2B, CETN3, CCNT2*
	RNA splicing	(12 / 267)	0.0001	*SNRNP48, PPP4R2, CRNKL1*
	inflammatory response	(11 / 230)	0.0001	*CCR5, CXCL11, TNFRSF1A*
	response to DNA damage stimulus	(6 / 84)	0.0007	*XIAP, UBR5, OBFC2A*
	apoptosis	(14 / 461)	0.002	*APAF1, TRIM69, APH1B*
	cell proliferation	(10 / 295)	0.004	*CLKF, IFI16, TRIM27*
	DNA repair	(6 / 192)	0.032	*LIG4, RAD51C, RAD18*

Contd…

Group IV	GO term (Biological Processes)	No. of genes /database count	P Value	Representative genes
Up-regulated genes	regulation of transcription	(70 / 989)	2.48E-029	*NR4A2, TP53BP1, STAT3*
	apoptosis	(38 / 461)	1.90E-018	*SIAH1, PPP1R15A, JMJD6*
	signal transduction	(74 / 1959)	6.99E-016	*MAPK6, AKAP8, NAMPT*
	response to DNA damage stimulus	(11 / 84)	3.69E-008	*CDKN1A, DDIT3, GADD45B*
	RNA splicing	(17 / 267)	1.75E-007	*SRRM1, STRAP, HNRNPM*
	cell cycle	(22 / 470)	4.69E-007	*SIK1, DBF4,CCNL1*
	actin cytoskeleton organization	(11 / 119)	9.22E-007	*SH2B2, NRAS, CKAP2*
	ubiquitin-dependent protein catabolic process	(12 / 151)	1.32E-006	*USP12, USP36, UBE2B*
	mRNA processing	(15 / 246)	1.52E-006	*RBM4, RBM8A, PAPD4*
	cell differentiation	(21 / 485)	2.75E-006	*JMJD6, GNA13, SLC2A14*
	inflammatory response	(14 / 230)	3.45E-006	*IL1RN, TNFRSF4, CXCR1*
	protein ubiquitination	(9 / 88)	4.21E-006	*DCAF1, RBBP6, UBE2B*
	protein transport	(18 / 408)	1.10E-005	*COL1A1, NUPL1, SEC31A*
	cell cycle arrest	(9 / 108)	1.94E-005	*CDKN1A, PPP1R15A, DDIT3*
	response to oxidative stress	(8 / 104)	9.49E-005	*SOD2, DUSP1, PRNP*
		(18 / 537)	0.0003	*HES1, ICAM1, NEDD9*

Contd…

Group IV	GO term (Biological Processes)	No. of genes /database count	P Value	Representative genes
	immune response	(14 / 362)	0.0003	*IL8, KIR3DS1, IL1RAP*
	DNA repair	(8 / 192)	0.004	*PMS1, POLB, UBE2B*
	chromatin modification	(8 / 206)	0.006	*KDM6B, SETDB2, HIST1H2B*
	metabolic process	(13 / 485)	0.013	*ATP13A4, NAMPT, AMPD2*
	transmembrane transport	(13 / 508)	0.026	*NUPL1, SLC2A14, MFSD2A*
Down-regulated genes	protein transport	(50 / 408)	4.59E-019	*BET1, AP4S1, SEC63*
	regulation of transcription	(78 / 989)	2.99E-018	*SFRS13A, RUVBL1, ZNF32*
	metabolic process	(43 / 485)	3.60E-012	*TMEM68, PEC1, METTL13*
	ubiquitin-dependent protein catabolic process	(23 / 151)	3.25E-011	*UBR1, SMURF2, USP37*
	cell cycle	(40 / 470)	6.33E-011	*CDKN2B, CETN3, CDC23*
	mRNA processing	(25 / 246)	9.81E-009	*HNRNPR, SF3B3, RBM4B*
	protein folding	(19 / 151)	2.70E-008	*DNAJC10, PP1L1, PFDN6*
	RNA splicing	(25 / 267)	4.30E-008	*HNRNPA0, POLR2B, SFRS12*
	apoptosis	(34 / 461)	4.52E-008	*BIRC6, TRIM69, STK17A*
	response to DNA damage stimulus	(14 / 84)	8.35E-008	*TP53TG1, ATM, ATMIN*
	signal transduction	(85 / 1959)	7.83E-007	*MAP3K7, PDK4, AKT3*
	DNA repair	(19 / 192)	8.12E-007	*ERCC4, RAD54B, APEX2*

Contd…

Group IV	GO term (Biological Processes)	No. of genes /database count	P Value	Representative genes
	translation	(18 / 211)	1.05E-005	*EIF5B, RPS27L, HBS1L*
	transmembrane transport	(29 / 508)	4.58E-005	*NUPL2, TMEM48, MFSD8*
	chromatin modification	(15 / 206)	0.0002	*BRD8, ARRB8, HDAC8*
	inflammatory response	(14 / 230)	0.002	*CCR2, TNFRSF1A, TLR5*
	cell differentiation	(23 / 485)	0.003	*TUBD1, PAQR8, FAM65B*
	response to oxidative stress	(8 / 104)	0.005	*OXR1, PRDX2, PCEF1*
	cell adhesion	(21 / 537)	0.03	*RAB13, SIRPG, ITGA2B*

Analysis was also done in terms of important molecular functions and cellular component of differentially expressed genes. Most of the differentially expressed genes in Group II were involved in DNA binding, protein binding, cytokine activity, transferase activity, hydrolase activity etc. However, in Group III and Group IV, some of the highly over-represented molecular functions performed by differentially expressed genes were transcription regulator activity, DNA, RNA and protein binding, Molecular transducer activity, ubiquitin-protein ligase activity, transferase activity, ligase activity, protein kinase activity, histone binding activity, metal ion binding, helicase activity, transporter activity, methyltransferases activity, endonuclease activity etc. (figure 3.23 A-C).

In terms of cellular location, differentially expressed genes of Group II, III and IV showed similar percentages. Around 23-29 % genes coded for nuclear proteins, 19-22 % coded for cytoplasmic proteins, 4-8 % was mitochondrial genes, 15 to 17 % were involved in membrane bound activities and around 3 to 7 % were involved in extracellular activities (figure 3.24 A-C).

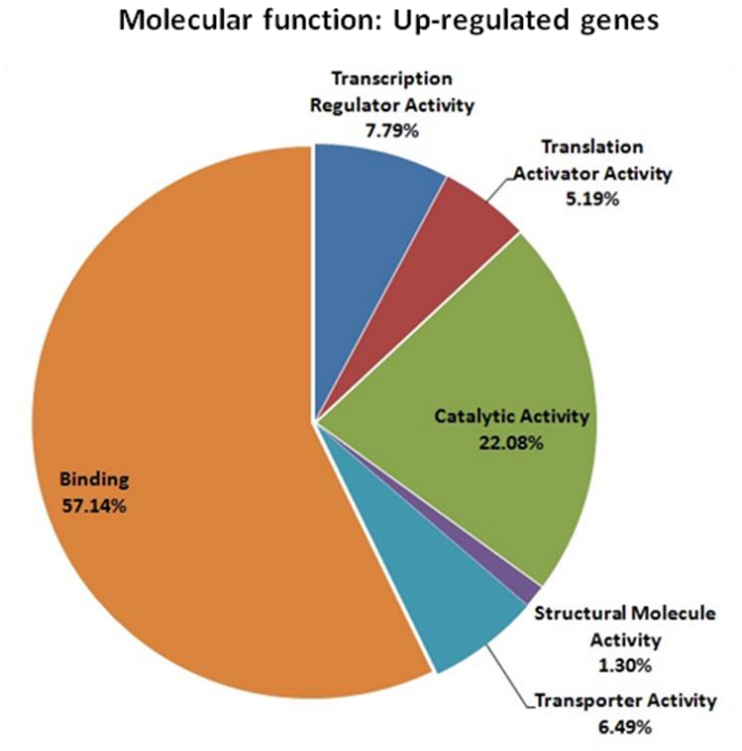

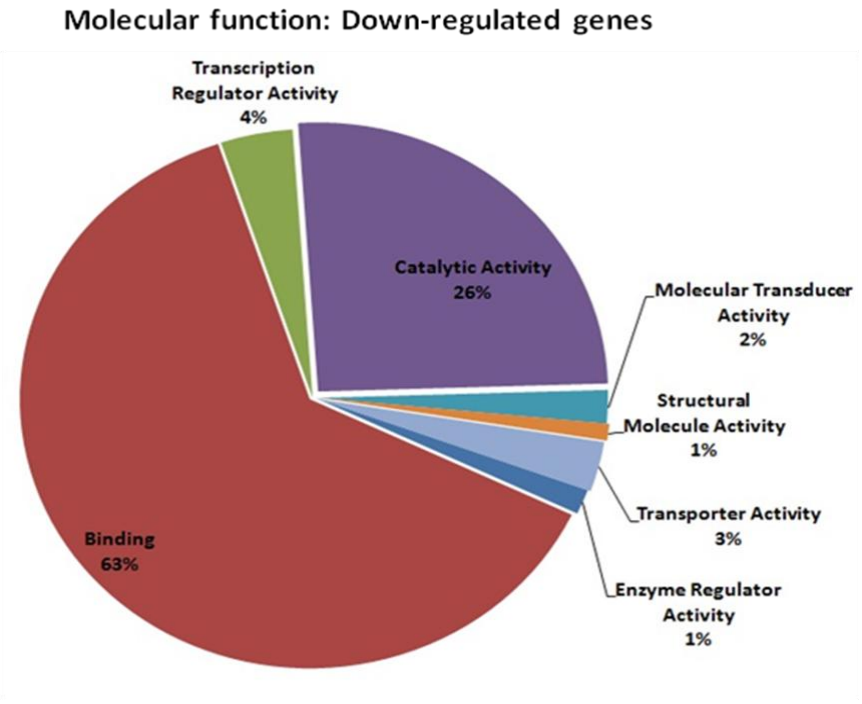

Figure 3.23 A: Representative molecular function terms (GO analysis) over-represented in up and down-regulated genes of Group II (Low Dose Group, HLNRA) as compared to Group I (NLNRA).

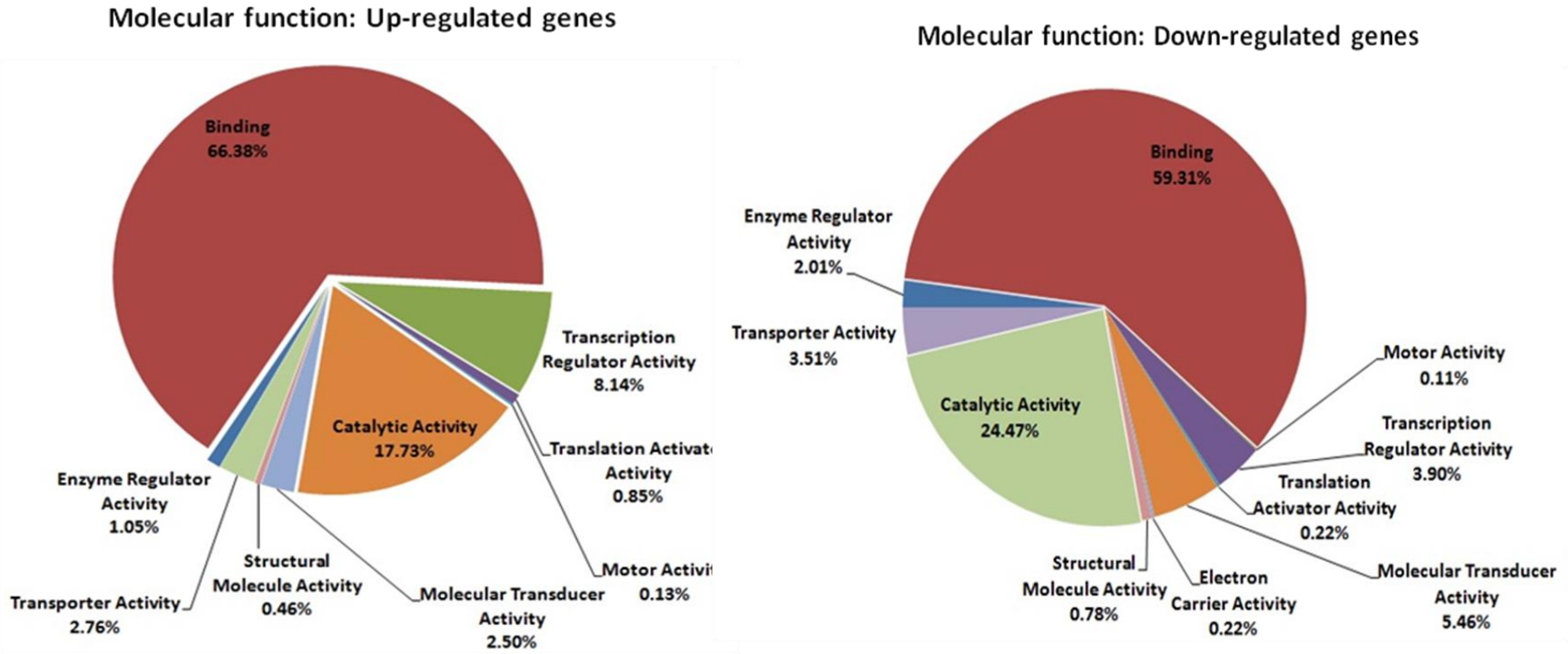

Figure 3.23 B: Representative molecular function terms (GO analysis) over-represented in up and down-regulated genes of Group III (High Dose Group, HLNRA) as compared to Group I (NLNRA).

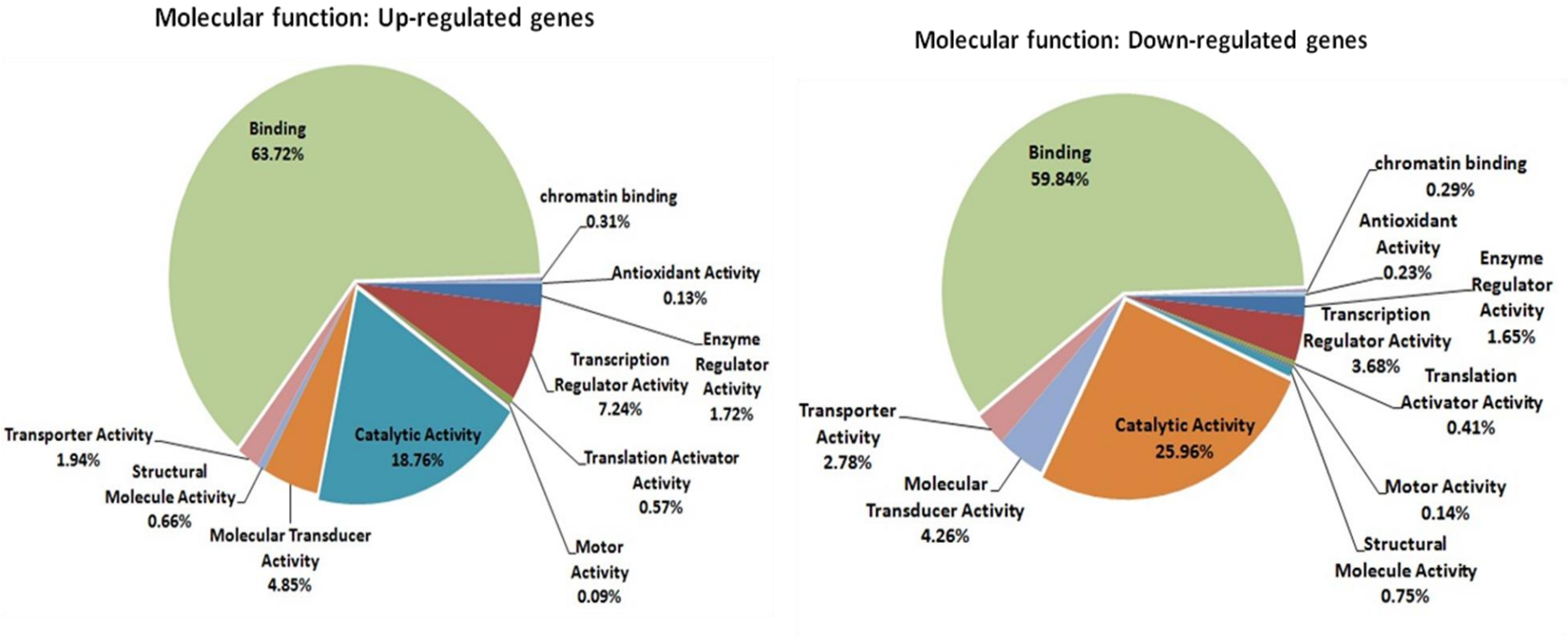

Figure 3.23 C: Representative molecular function terms (GO analysis) over-represented in up and down-regulated genes of Group IV (High Dose Group, HLNRA) as compared to Group I (NLNRA).

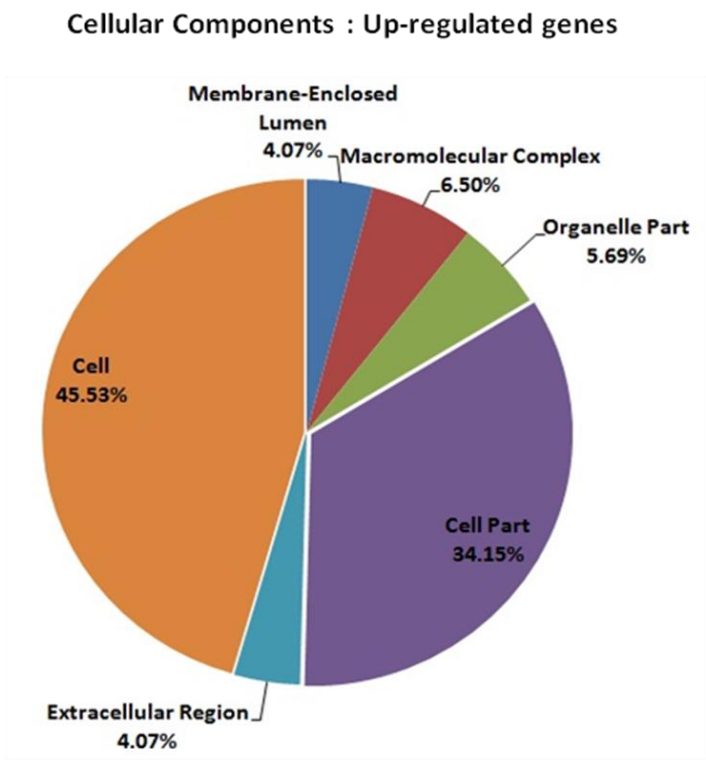

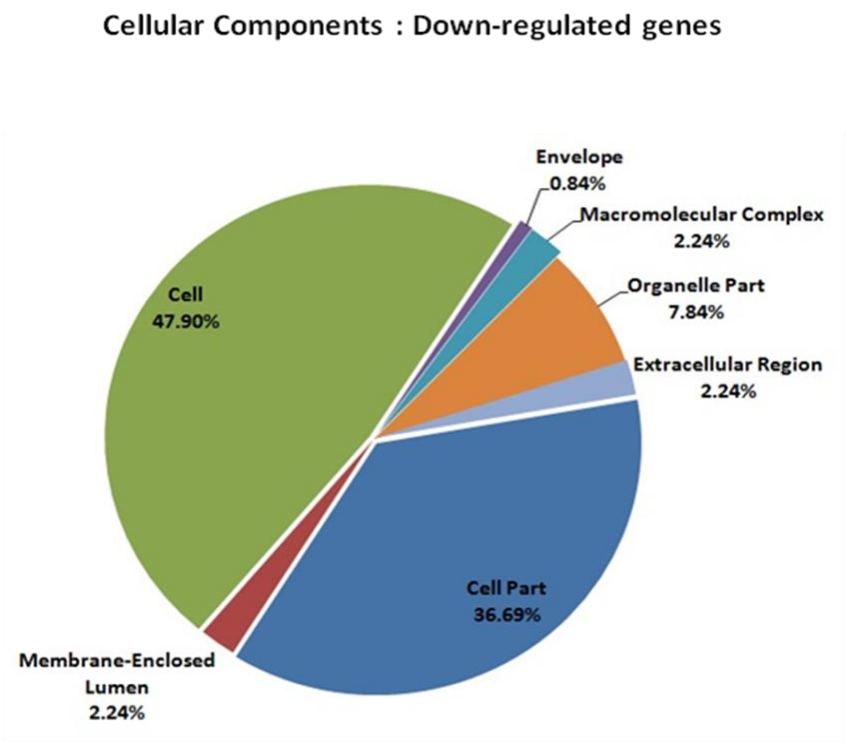

Figure 3.24 A: Representative cellular component terms (GO analysis) over-represented in up and down-regulated genes of Group II (Low Dose Group, HLNRA) as compared to Group I (NLNRA).

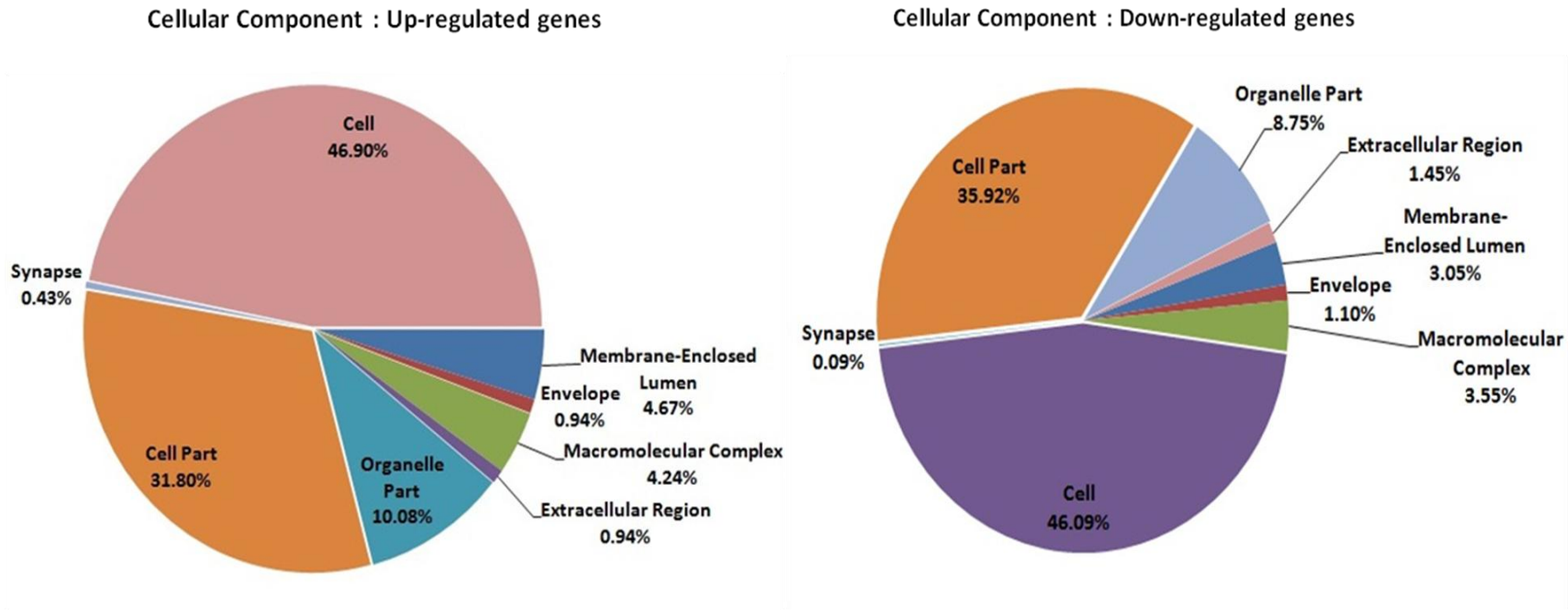

Figure 3.24 B: Representative cellular component terms (GO analysis) over-represented in up and down-regulated genes of Group III (High Dose Group, HLNRA) as compared to Group I (NLNRA).

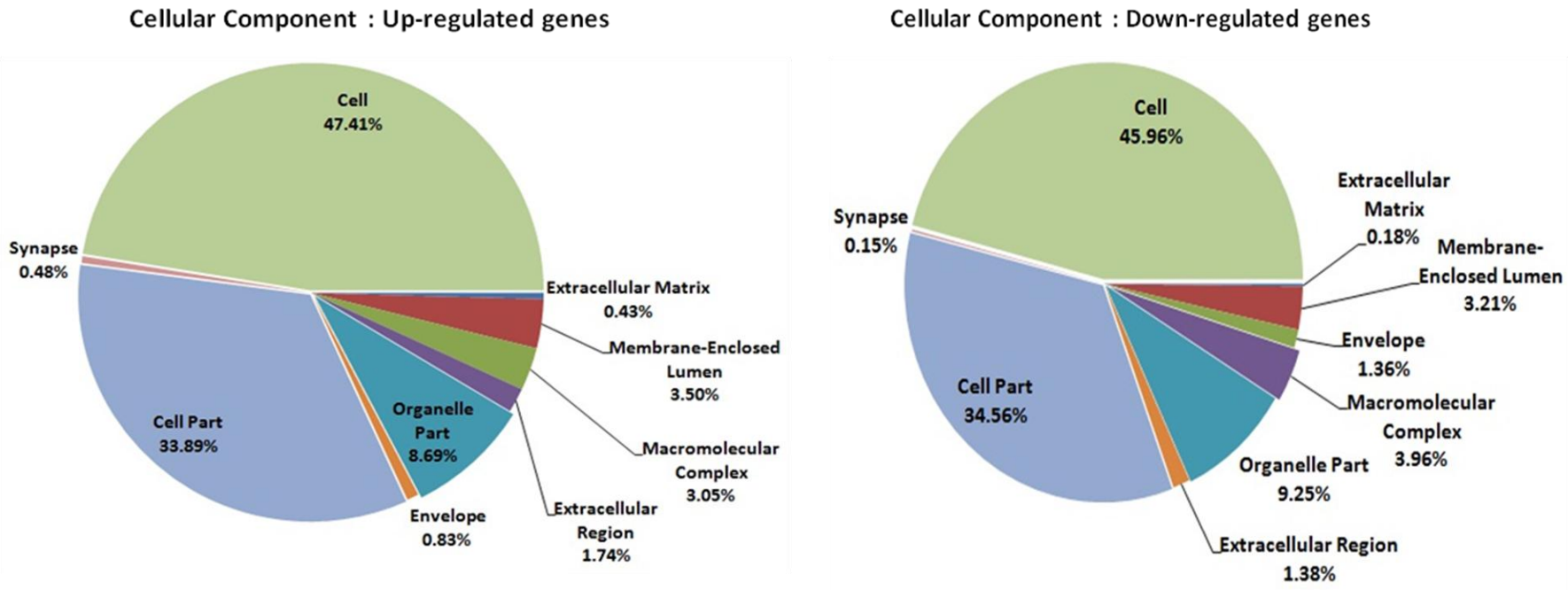

Figure 3.24 C: Representative cellular component terms (GO analysis) over-represented in up and down-regulated genes of Group IV (High Dose Group, HLNRA) as compared to Group I (NLNRA).

3.2.2.2 Pathway Analysis of differentially expressed genes in HLNRA groups as compared to NLNRA

Pathway analysis was done to find out important biological and molecular pathways activated in HLNRA individuals. Analysis was done in differentially expressed genes observed in HLNRA groups (Group II, Group III and Group IV). Our analysis revealed that in LDG individuals (Group II), very few pathways were overrepresented and numbers of genes in each overrepresented pathway were very few. However, in HDG individuals (Group III and Group IV), various important pathways were observed to be overrepresented. Some of the pathways found to be active were MAPK signaling pathway, Jak-STAT signaling pathway, p53 signaling pathway, T cell receptor signaling pathway , B cell receptor signaling pathway, Insulin signaling pathway, Purine metabolism, Apoptosis, Cell Cycle, DNA Repair, Ubiquitin mediated proteolysis, focal adhesion, Gap junction etc. Some of the important genes from each pathway is given in table 3.12. Representative heat maps of various pathways activated in Group IV (HLNRA) as compared to Group I (NLNRA) is shown in Figure3.25 and 3.26.

Table 3.12 List of over-represented pathways in HLNRA groups (Group II,Group III and Group IV) as compared to NLNRA (Group I).

Group II	Pathway name	No. of genes/database count	P value	Representative genes
Up-regulated genes	Valine, leucine and isoleucine biosynthesis	(1 / 11)	0.01	*BCAT1*
	Pantothenate and CoA biosynthesis	(1 / 15)	0.01	*BCAT1*
	MAPK signaling pathway	(2 / 272)	0.01	*PTPN7, IL1A*
	Porphyrin and chlorophyll metabolism	(1 / 41)	0.02	*UROD*
	Graft-versus-host disease	(1 / 42)	0.02	*IL1A*
	Type I diabetes mellitus	(1 / 44)	0.02	*IL1A*
	Hematopoietic cell lineage	(1 / 87)	0.04	*IL1A*
	Apoptosis	(1 / 89)	0.05	*IL1A*
Down-regulated genes	Sulfur metabolism	(1 / 13)	0.02	*BPNT1*
	Glycosylphosphatidylinositol(GPI)-anchor biosynthesis	(1 / 23)	0.04	*PIGV*
	Nicotinate and nicotinamide metabolism	(1 / 24)	0.04	*NT5E*
	Bile acid biosynthesis	(1 / 31)	0.05	*SOAT1*
	Regulation of autophagy	(1 / 35)	0.05	*ATG12*

Group III	Pathway name	No. of genes/database count	P value	Representative genes
Up-regulated genes	Cell cycle	(10 / 119)	1.66E-007	*CDKN1A, RB1, CCND2*
	p53 signaling pathway	(8 / 69)	3.05E-007	*PMAIP1, GADD45B, SIAH1*
	MAPK signaling pathway	(13 / 272)	1.16E-006	*JUN, DUSP10, ATF2*

Contd…

Group III	Pathway name	No. of genes/database count	P value	Representative genes
	Ubiquitin mediated proteolysis	(8 / 139)	3.86E-005	*UBE2B, SMURF1, UBE2Z*
	mTOR signaling pathway	(5 / 52)	0.0001	*AKT2, PRKAA1, CAB39*
	B cell receptor signaling pathway	(5 / 65)	0.0003	*INPP5D, NRAS, JUN*
	Insulin signaling pathway	(6 / 138)	0.001	*INPP5D, PRKAA1, NRAS*
	Wnt signaling pathway	(6 / 152)	0.002	*CCND2, CSNK1A1, PSEN1*
	T cell receptor signaling pathway	(5 / 108)	0.002	*JUN, AKT2, LCP2*
	TGF-beta signaling pathway	(4 / 87)	0.007	*BMPR2, SMURF1, TFDP1*
	Apoptosis	(4 / 89)	0.008	*TNFRSF10B, CAPN1, AKT2*
	Purine metabolism	(5 / 149)	0.01	*PDE4B, AK3L1, PRIM2*
Downregulated genes	MAPK signaling pathway	(15 / 272)	2.47E-006	*MAP3K8, MAPK1, AKT3*
	Apoptosis	(8 / 89)	2.28E-005	*APAF1, XIAP, TNFSF10*
	Cytokine-cytokine receptor interaction	(13 / 263)	3.39E-005	*IL7, IL6R, CCR2*
	Jak-STAT signaling pathway	(8 / 155)	0.0008	*STAM2, SOS1, AKT3*
	Natural killer cell mediated cytotoxicity	(7 / 135)	0.001	*TNFSF10, ICAM2, FASLG*
	Toll-like receptor signaling pathway	(6 / 102)	0.001	*TLR5, CXCL11, IFNAR1*
	Ubiquitin mediated proteolysis	(7 / 139)	0.001	*UBR5, UBE2H, KLHL9*
	T cell receptor signaling pathway	(6 / 108)	0.002	*SOS1, MAPK1, FYN*
	Wnt signaling pathway	(7 / 152)	0.003	*PSEN1, CTBP2, PRKACB*
	Focal adhesion	(7 / 203)	0.01	*HGF, ITGAV, SOS1*
	Purine metabolism	(5 / 149)	0.03	*NT5E, PNP, POLR1B*

Contd…

Group IV	Pathway	No. of genes/database count	P value	Representative genes
Upregulated genes	MAPK signaling pathway	(24 / 272)	9.87E-013	*AKT2, MAP3K3, FOS*
	T cell receptor signaling pathway	(14 / 108)	5.81E-010	*NFKB1A,BCL10, IFNG*
	Natural killer cell mediated cytotoxicity	(15 / 135)	9.96E-010	*TNFRSF10B, KIR3DL1, ICAM1*
	B cell receptor signaling pathway	(9 / 65)	4.21E-007	*BCL10, CHP, NRAS*
	Ubiquitin mediated proteolysis	(12 / 139)	5.83E-007	*UBE2B, UBE3C, PIAS2*
	Cytokine-cytokine receptor interaction	(14 / 263)	1.46E-005	*IL2RB, IL8, IL1RAP*
	Jak-STAT signaling pathway	(10 / 155)	5.34E-005	*JAK1, STAT3, AKT2*
	Wnt signaling pathway	(9 / 152)	0.0002	*SIAH1, WNT10A, CSNK1E*
	Gap junction	(7 / 96)	0.0003	*TUBB3, GNAS, TUBB2C*
	p53 signaling pathway	(6 / 69)	0.0003	*CDKN1A, GADD45B, PMAIP1*
	Focal adhesion	(10 / 203)	0.0004	*VEGFA, PDGFD, COL1A1*
	Toll-like receptor signaling pathway	(6 / 102)	0.002	*ARAF, NRAS, AKT2*
	Insulin signaling pathway	(7 / 138)	0.002	*NRAS, SH2B2, ARAF*
	Cell cycle	(6 / 119)	0.005	*CDKN1A, GADD45B, TWHAZ*
	Apoptosis	(5 / 89)	0.006	*AKT2, TNFRSF10B, NFKB1A*
	Tight junction	(6 / 135)	0.009	*EXOC4, RRAS2, SPTAN1*
	Purine metabolism	(5 / 149)	0.04	*PDE4B, AMPD2, PRIM2*
Downregulated genes	Ubiquitin mediated proteolysis	(17 / 139)	2.08E-007	*UBR5, UBE2I, UBE2Q1*
	Apoptosis	(11 / 89)	2.60E-005	BIRC3, FADD, IRAK3
	Purine metabolism	(14 / 149)	3.73E-005	*NT5E, FHIT, PDE3B*

Contd…

Group IV	Pathway	No. of genes/database count	P value	Representative genes
	Insulin signaling pathway	(13 / 138)	6.82E-005	*IRS1, CALM1, GSK3B*
	Fatty acid metabolism	(7 / 45)	0.0002	*ACAT1, ACOX3, CPT2*
	Toll-like receptor signaling pathway	(10 / 102)	0.0003	*TRAF3,TLR5, TLR4*
	Non-homologous end-joining	(4 / 14)	0.0007	*LIG4, XRCC4, DCLRE1C*
	Focal adhesion	(14 / 203)	0.0007	*BCL2, ITGA2B, PDGFC*
	Wnt signaling pathway	(11 / 152)	0.001	*PSEN1, RUVBL1, SFRP5*
	Tight junction	(10 / 135)	0.002	*AKT3, RAB13, PARD68*
	Nucleotide excision repair	(5 / 44)	0.005	*ERCC4, GTF2H5, GTF2H1*
	T cell receptor signaling pathway	(8 / 108)	0.006	*SOS1, CD8B, GSK3B*
	Homologous recombination	(4 / 28)	0.006	*RAD51C, RAD54B, RAD51L1*
	Cell cycle	(8 / 119)	0.01	*CDKN2B, CDKN2C, CDC23*
	Gap junction	(7 / 96)	0.01	*LPAR1, NPR2, PRKACB*
	Cytokine-cytokine receptor interaction	(12 / 263)	0.04	*CCR7, IL6R, IL5RA*
	MAPK signaling pathway	(12 / 272)	0.04	*MAP3K7, DUSP7, AKT3*

Up-regulated pathways in Group IV (HLNRA)

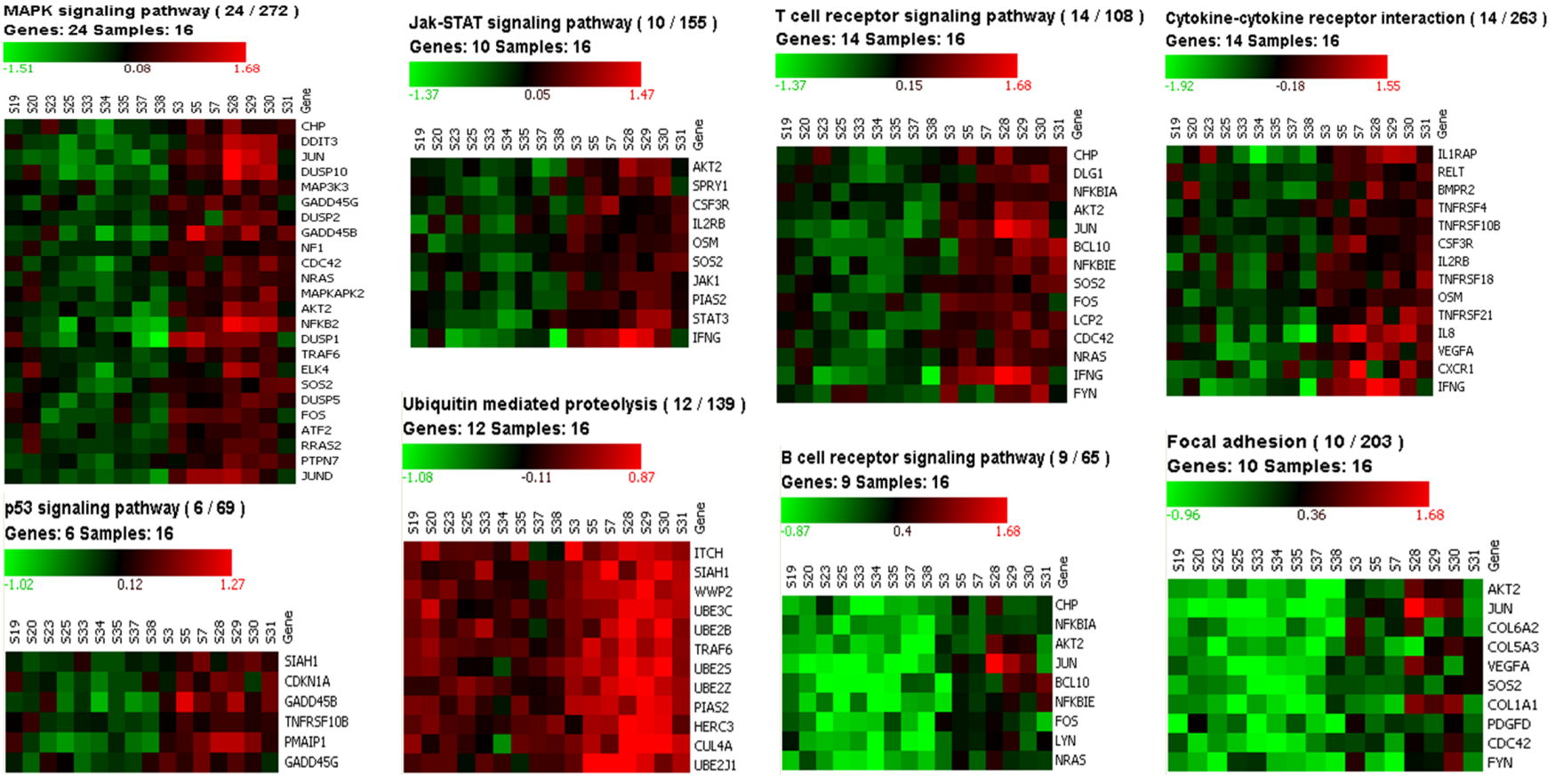

Figure 3.25: Representative heat maps for the respective pathways of up-regulated genes in Group IV (high dose group, HLNRA) as compared to NLNRA (Group I). Color diagram shows expression intensity levels of genes involved in each pathway.

Down-regulated pathways in Group IV (HLNRA)

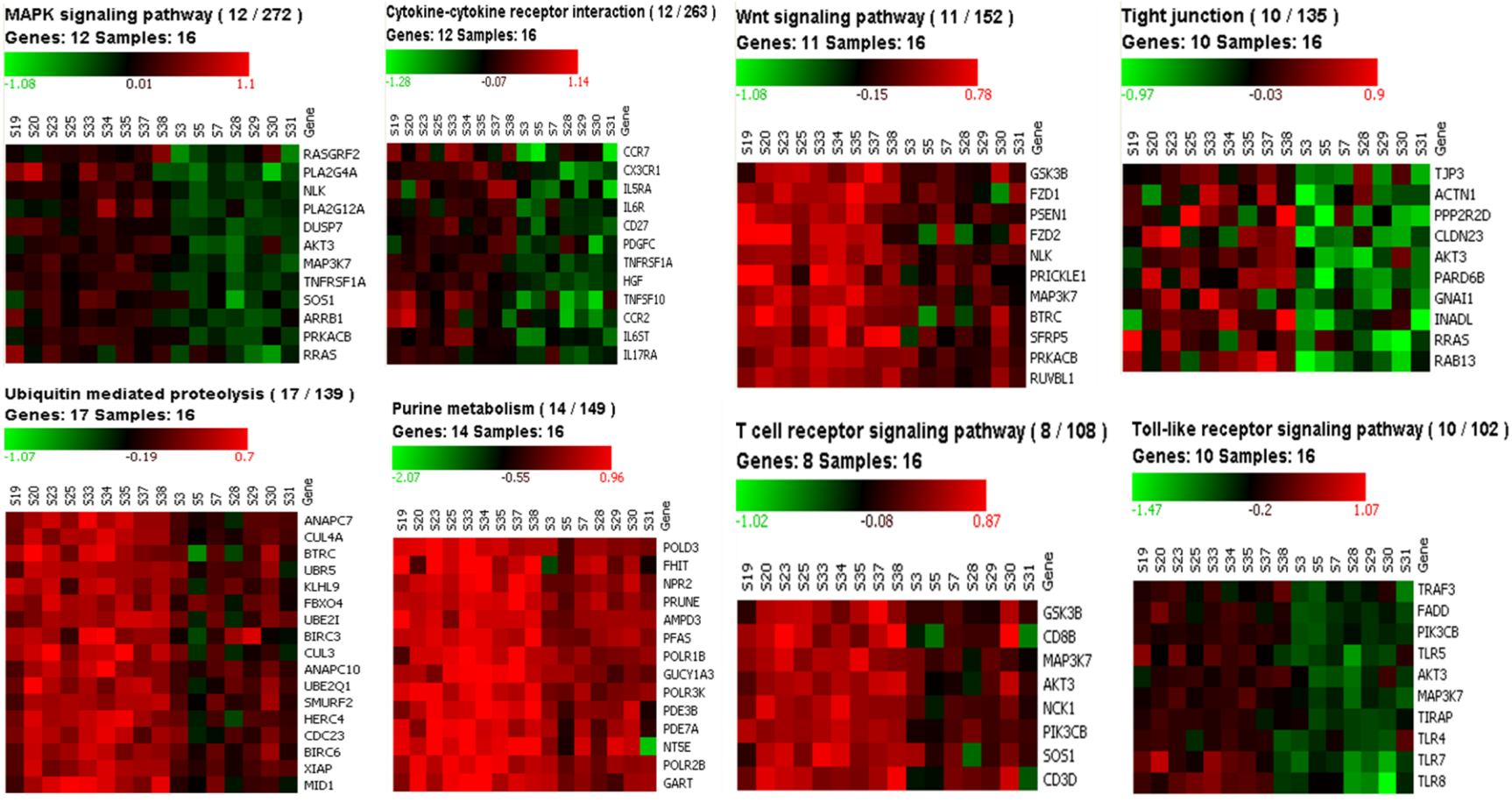

Figure 3.26: Representative heat maps for the respective pathways of pathways of down-regulated genes in Group IV (high dose group, HLNRA) as compared to NLNRA. Color panel shows expression intensity levels of genes involved in each pathway.

3.2.2.3 Representation of DNA damage response and repair genes in HLNRA individuals.

Data was analyzed to find out differentially expressed genes which are involved in different DNA damage response processes such as DNA repair, cell cycle regulation, apoptosis, immune reponse, chromatin modification etc. Our main focus was to identify chronic low dose induced genes which are involved in DNA damage response processes and hence might be playing some important role in adaptation to chronic dose exposure in HLNRA population. Our analysis revealed that the gene set differentially expressed in Group II (LDG, < 5.0 mGy/y) have important genes involved in processes like immune response (IL1A, IGHG1), apoptosis (WDR92, APH1B), RNA splicing (SNRPA1, HNRNPM) and translational initiation (EIF1, EIF4G3) etc. However, group III and group IV (HDG, HLNRA) have higher representation of genes involved in DNA damage response, DNA repair, cell cycle regulation, apoptosis, chromatin modification and other stress responsive genes.

Several important genes involved in different repair pathways were present in our data. Genes involved in non-homologous end joining (NHEJ) repair *(XRCC4, LIG4, DCLRE1C, DCLRE1B, DCLRE1A),* base excision repair *(APEX2, UNG, POLB),* nucleotide excision repair (*RAD23B, GTF2H1*, *GTF2H3, GTF2H5, ERCC4*), homologous Recombination (*RAD54B, RAD51B*), mismatch Repair (*PMS1)* other repair pathways (*RAD21, RAD 18, RMI1*, *POLH, UBE2B, UBE2T, FANCE, FANCF, PALB2, REV3L, HLTF*) were found to be overrepresented in HLNRA population. Important pathways known to be regulated in DDR in human cells MAPK signaling pathway, p53 signaling pathway, JAK-STAT signaling pathways were activated in higher dose groups. We observed a network of genes which regulates/regulated through these pathways to be differentially expressed in Group III and IV. Although, in our microarray data we did not observe any change in the expression levels of p53 gene. However, detailed analysis

revealed that p53 regulated genes to be present in our data set. Few of them were *CDKN1A, TRAF4, ATF3, TNFRSF10B, APAF1, DUSP1, PMAIP1, GADD45B, BCL6, PLK3* etc. Some of the important genes involved in MAPK pathway were *DUSP1, DUSP10, AKT2, ATF2, BCL10, CD38, CDC42, CSNK1A1, DDIT3, DUSP5, GFRAL, GNAS, HIPK3, IL8* etc. Several important transcription factor and signaling molecules such as *cJUN, cFOS, JUND, CREBZF, FOXO3, ATF family, HEY1* etc which are involved in regulating DNA damage response and repair were found to be activated in higher dose groups. Interestingly, we observed the expression levels of DDR genes was not same in group III and Group IV, few genes were present both the groups where as there were few genes unique to each group. A representative list of important genes involved in DDR processes is given in table 3.13. Representative heat maps showing overrepresented DDR and repair gene in higher dose group is shown in figure 3.27.

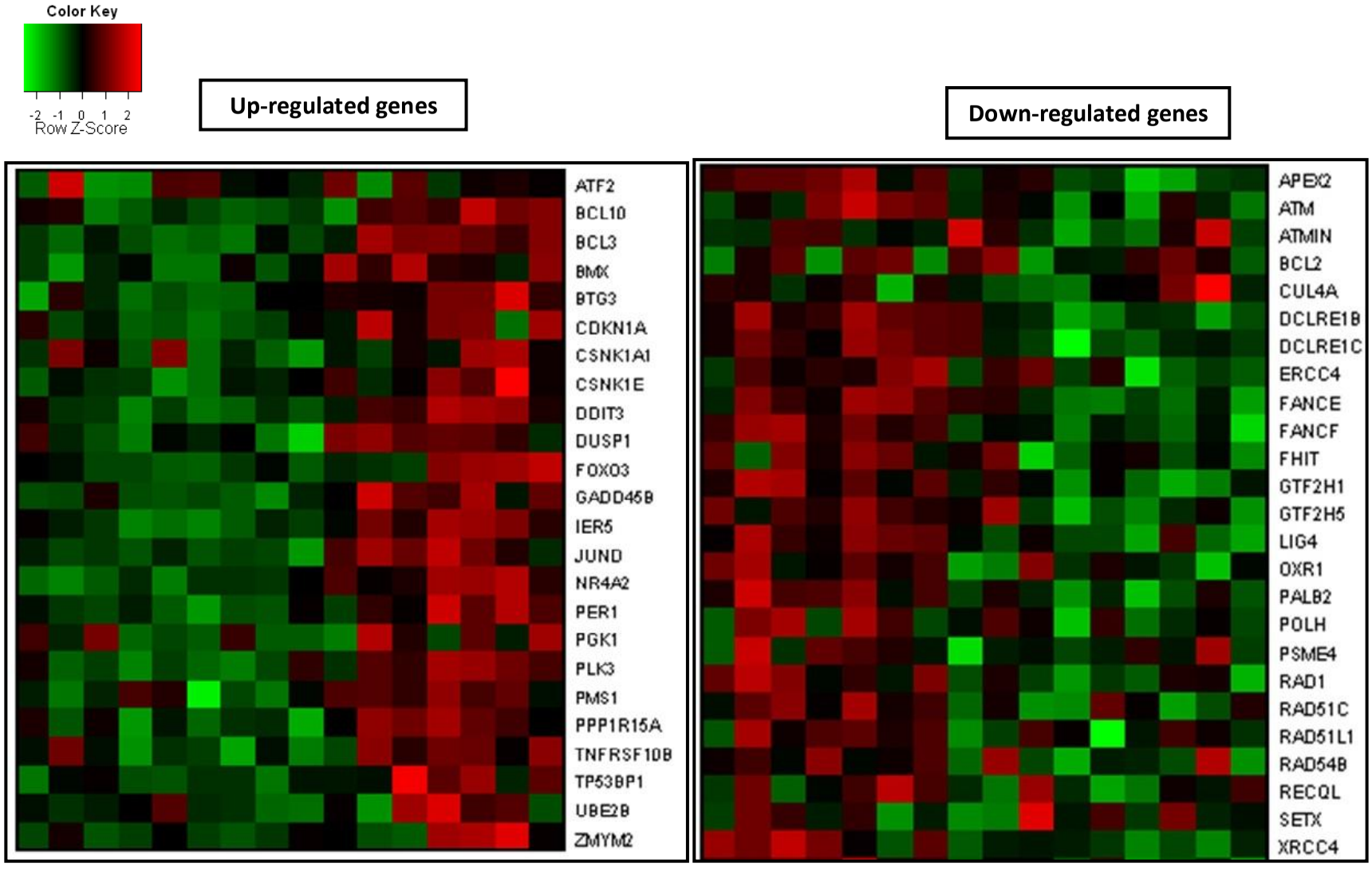

Figure 3.27: Representative heat maps showing intensity values of up and down regulated DNA damage response and repair genes in high dose group (Group III and Group IV) of HLNRA

Table 3.13: List of important genes involved in various processes of DNA damage response and repair in our data set. Fold change values in different groups is also given.

Gene name	Accession no.	Chromosomal location	Group II	Group III	Group IV
DNA repair genes					
APEX2	NM_014481	chr Xp11.21	-	-	-1.30
UNG	NM_080911	chr 12q24.11	-	-	-1.32
XRCC4	NM_003401	chr 5q14.2	-	-	-1.35
LIG4	NM_002312	chr 13q33.3	-	-1.32	-1.45
DCLRE1C	NM_022487	chr10 p13	-	-	-1.44
DCLRE1B	NM_022836	chr10p13.2	-	-	-1.35
DCLRE1A	NM_014881	chr10q25.1	-	1.41	-
RAD51L1	NM_002877	chr14q23	-	-	-1.32
RAD54B	NM_012415	chr8q21.3	-	-	-1.44
RAD51C	NM_002876	Chr17q22	-	-1.32	-1.36
RAD21	NM_006265	chr9q31.2	-	1.64	-
RAD23B	NM_002874	chr9q31.2	-	1.34	-

Cntd…

Gene name	Accession no.	Chromosomal location	Fold change Group II	Fold change Group III	Fold change Group IV
RAD18	NM_020165	chr3p25-p24	-	-1.31	-
GTF2H1	NM_001142307	chr11p15.1	-	-1.42	-1.45
GTF2H5	NM_207118	chr6q25.3	-	-	-1.31
GTF2H3	NM_001516	chr12q24.31	-	-	-1.46
ERCC4 (XPF)	NM_005236	chr16p13.12	-	-	-1.58
PMS1	NM_000534	chr2q31	-	-	1.57
RMI1	NM_024945	chr9q21.32	-	-1.50	-1.72
POLB	NM_002690	chr8p11.2	-	1.56	1.58
POLH	NM_006502	chr6p21.1	-	-1.33	-1.42
UBE2B	NM_003337	chr5q23-q31	-	1.34	1.36
UBE2T	NM_014176	chr1q32.1	-	-1.39	-1.47
FANCE	NM_021922	chr6p21.31	-	-	-1.31
FANCF	NM_022725	chr11p14.3	-	-	-1.72
PALB2	NM_024675	chr16p12.1	-	-	-1.32

Cntd…

Gene name	Accession no.	Chromosomal location	Fold change Group II	Fold change Group III	Fold change Group IV
REV3L	NM_002912	chr6q21	-	1.41	-
HLTF	NM_003071	chr3q25.1	-	-	-1.37
PER1	NM_002616	chr17p13.1	-	-	1.77
Cell Cycle & Apoptosis					
GADD45B	NM_015675	chr19p13.3	-	1.79	2.04
DDIT3	NM_004083	chr12q13.1	-	1.55	1.96
BTG3	NM_001130914	chr21q21.1	-	-	1.73
PLK3	NM_004073	chr1p34.1	-	-	1.79
CDKN1A	NM_000389	chr6p21.2	-	1.34	1.48
BANP	NM_001173539	chr16q24.2	-	1.31	1.49
MDM4	NM_002393	chr1q32	-	1.59	-
MDM2	NM_001145336	chr12q14.3	-	-1.48	-
CCNG2	NM_004354	chr4q21.1	-	-1.68	-1.69
TP53BP1	NM_001141979	chr15q15-q21	-	-	1.36
ATM	NM_000051	chr11q22-q23	-	-	-1.33
ATMIN	NM_015251	chr16q23.2	-	-	-1.30

Cntd…

Gene name	Accession no.	Chromosomal location	Fold change Group II	Fold change Group III	Fold change Group IV
RIF1	NM_001177663	chr2q23.3	-	-1.33	-1.41
BCL2	NM_000633	chr18q21.33	-	-	-1.48
WAC	NM_018604	chr10p12.1	-	1.56	1.54
DUSP10	NM_007207	chr1q41	-	1.67	2.01
DUSP1	NM_004417	chr5q34	-	1.79	1.99
CKAP2	NM_001098525	chr13q14	-	-	1.58
GADD45G	NM_006705	chr9q22.1	-	-	1.39
PPP2R5C	NM_001161725	chr14q32	-	-	1.47
PMAIP1	NM_021127	chr18q21.32	-	1.52	2.12
TNFRSF10B	NM_003842	chr8p22-p21	-	1.33	1.33
BTG1	NM_001731	chr12q22	-	1.57	1.96
TSC22D2	NM_014779	chr3q25.1	-	1.72	2.14
Immune response					
KIR3DL1	NM_006737	chr19q13.4	-	-	2.17

Cntd…

Gene name	Accession no.	Chromosomal location	Fold change Group II	Fold change Group III	Fold change Group IV
IL1RAP	NM_001167928	chr3q28	-	-	1.97
IFNG	NM_000619	chr12q14	-	-	2.46
KIR3DS1	NM_001083539	chr19q13.4	-	-	3.10
KIR2DL5A	NM_020535	chr19p13.3	-	-	2.05
IL8	NM_000584	chr4q13-q21	-	-	2.50
IL1RN	NM_000577	chr2q14.2	-	-	1.50
BCL6	NM_001130845	chr3q27	-	-	1.68
Chromatin modification					
ACTR8	NM_022899	chr3p21.1	-	-	-1.36
ALKBH2	NM_001001655	chr12q24.11	-	-	-1.35
ASF1A	NM_014034	chr6q22.31	-	-	-1.36
UBE2B	NM_003337	chr5q23-q31	-	1.34	1.36
C16orf53	NM_024516	chr16p11.2	-	-	-1.39
RUVBL1	NM_003707	chr3q21	-	-	-1.31
ING5	NM_032329	chr2q37.3	-	-	-1.49

Cntd…

Gene name	Accession no.	Chromosomal location	Fold change Group II	Fold change Group III	Fold change Group IV
SETDB2	NM_001160308	chr13q14	-	2.13	1.60
MYST4 *(KAT6B)*	NM_012330	chr10q22.2	-	1.40	-
NCOA3	NM_001174087	chr20q12	-	1.45	1.46
JMJD6	NM_001081461	chr17q25	-	-	1.75
HIST1H2BC	NM_003526	chr6p21.3	-	-	2.37
HIST1H1E	NM_005321	chr6p21.3	-	1.85	-
HIST1H3A	NM_003529	chr6p21.3	-	2.09	-
KDM6B	NM_001080424	chr17p13.1	-	1.33	2.00
SIRT2	NM_012237	chr19q13	-	-	1.90
HDAC8	NM_00116641	chrXq13	-	-	-1.31
SUV420H1	NM_016028	chr11q13.2	-	-1.61	-1.31
Other important genes and transcription factors					
IER5	NM_016545	chr1q25.3	-	-	1.55
SOD2	NM_000636	chr6q25.3	-	-	2.08
JUN	NM_002228	chr1p32-p31	-	1.93	2.30
JUND	NM_005354	chr19p13.2	-	1.7	1.93

Cntd…

Gene name	Accession no.	Chromosomal location	Fold change Group II	Fold change Group III	Fold change Group IV
CREBZF	NM_001039618	chr11q14	-	1.52	1.40
ATF2	NM_001880	chr2q32	-	1.38	1.39
HEY1	NM_001040708	chr8q21	-	-	1.53
NR4A2	NM_006186	chr2q22-q23	-	-	2.44
FOS	NM_005252	chr14q24.3	-	-	1.48
FOXO3	NM_001455	chr6q21	-	1.33	1.42

3.2.2.4 Identification of differentially expressed genes showing dose related changes in HLNRA population

Further analysis was carried out to find out the genes showing a background radiation dose related increase or decrease in their expression profile. To determine clear cut dose response observed in expression pattern, highly expressed genes showing a fold change ≥ 2.0 fold in Group IV and a fold change of atleast 1.5 fold in Group III were filtered. We observed that around 64 genes (36 up-regulated and 28 down-regulated) satisfied above cut-off. Further, the genes were divided in to three groups for representation. Figure 3.28 and 3.29 represents the fold changes in the expression of these genes in different background dose groups. Few genes showed linear increase or decrease (A). Few genes showed sharp change in group III (B) Few genes showed sharp change in group IV.

Gene ontology analysis of above genes have shown that most of these genes are involved in Cell cycle regulation *(GADD45B, BTG1, GNAS, , GIMAP8, GIMAP4),* immune system (*NFKB2, CXCR1, TNFSF10, CCR2*), stimulus to DNA damage *(DDIT3, DUSP1, JUN, GADD45B, JUND, BTG1),* apoptosis *(PMAIP1, PPIF, TSC22D2, SIK3, NLRC4),* mRNA processing *(CRNKL1, SFRS3, SFRS5, FUSIP1, PHAX),* transcriptional regulation *(JUN, JUND, KLF6, ATXN1, MED13, MED26, ZNF302, NFKB2 ZNF207, ZNF658)* and signal transduction *(DUSP1, DUSP10, LPXN, MYLIP, LGALS3, PAQR8),* Ubiquitin dependent proteolysis *(SQSTM1, UBQLN2)* etc. These genes may be used as the signatures of low dose IR exposure.

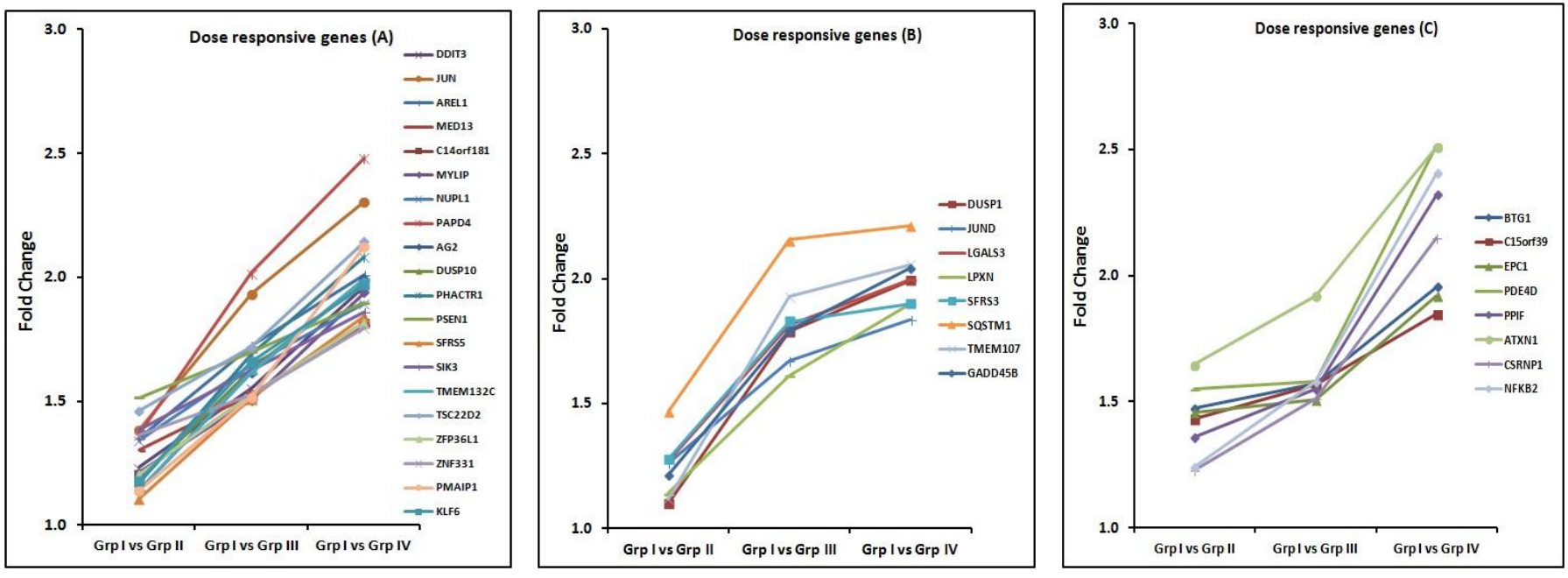

Figure 3.28: Dose responsive genes showing background dose dependent increase in expression among different dose groups. Genes were divided in to three groups A, B and C on the basis of dose response trend shown by them. NLNRA (Group I), HLNRA (Group II, Group III and Group IV).

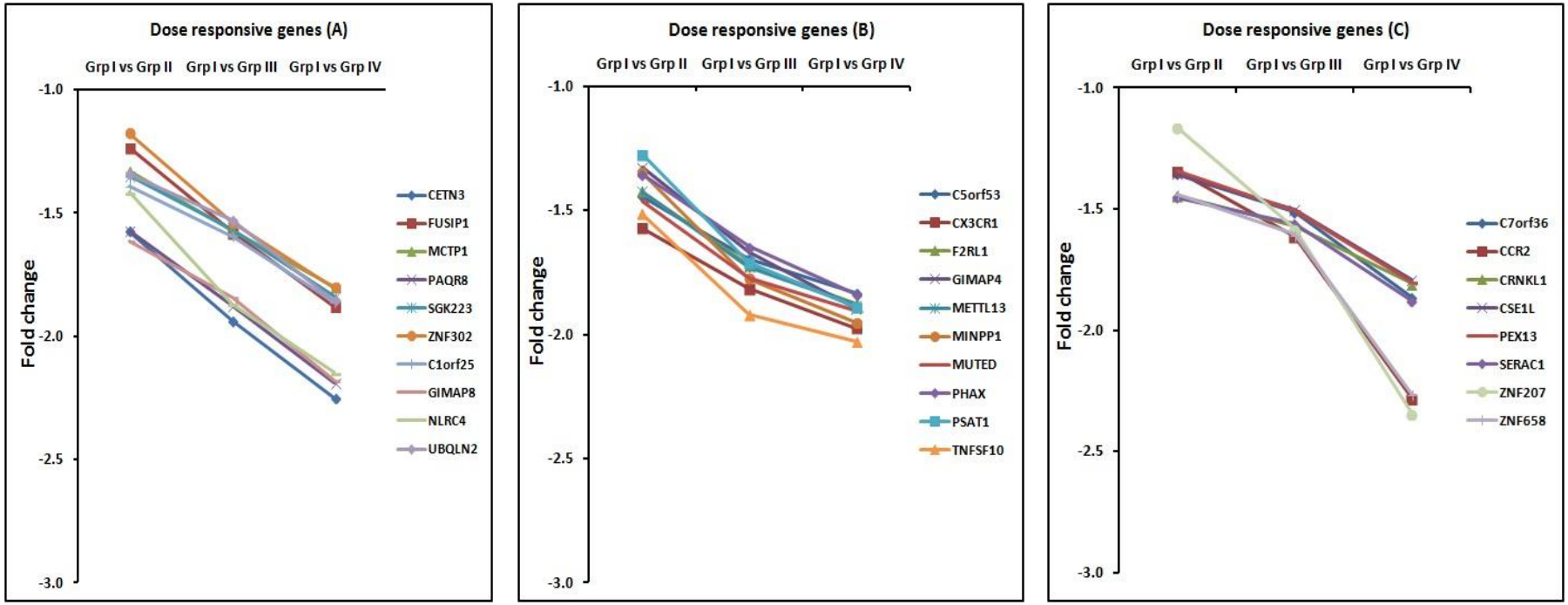

Figure 3.29: Dose responsive genes showing background dose dependent decrease in expression among different dose groups. Genes were divided in to three groups A, B and C on the basis of dose response trend shown by them. NLNRA (Group I), HLNRA (Group II, Group III and Group IV).

3.2.3 Validation of selected differentially expressed genes from microarray data using Real time q-PCR.

Validation of differentially expressed genes (up and down-regulated) of microarray data was carried out using specific approach of hydrolysis probe based assays using Universal Probe Library in Light Cycler 480 real time q-PCR. Hydrolysis Probes are sequence specific 8-10 basepair long fragments which bind selectively to a specific target in mRNA and give an accurate measure of transcript copy number of a gene in a particular sample.

For validation, 30 differentially expressed genes (22 up-regulated and 8 down-regulated) were selected on the basis of their representation in different group comparisons, involved in various biological processes, having different expression levels etc. so as to get a good representation from our microarray data. Details of the genes are as follows: Common genes in Group II, III and IV included *SNRPA1, METTL13, EIF1, ZNF167, DHFRL1, BBS10, THAP2*, Common in HDG (Group III and IV): *CCR2, KLF6, ATXN1, KDM6B, SETDB2, PDK4, NAMPT, KIR3DS1*, Dose responsive genes: *TSC22D2, CSRNP1, PAPD4, GIMAP8, PPIF, BTG1, DNA* damage response genes: *GADD45B, CDKN1A, JUN, JUND, PMAIP1, DDIT3, , DUSP10, DUSP1, PLK3.*

Level of gene expression was analyzed in 30 genes among 54 individuals (NLNRA, N=19 and HLNRA, N=35) using RT q- PCR. These 54 individuals belonged to two different set of individuals. The first set consisted of 30 individuals which were included in microarray experiments. One aliquot of PBMCs was used for microarray experiment and the other aliquot for validation experiment using probe based real time q-PCR.

Validation of above genes was also carried out in another set of 24 random individuals which were collected separately. The purpose of this experiment was to determine, whether the results obtained in microarray analysis are consistent in randomly selected HLNRA individuals.

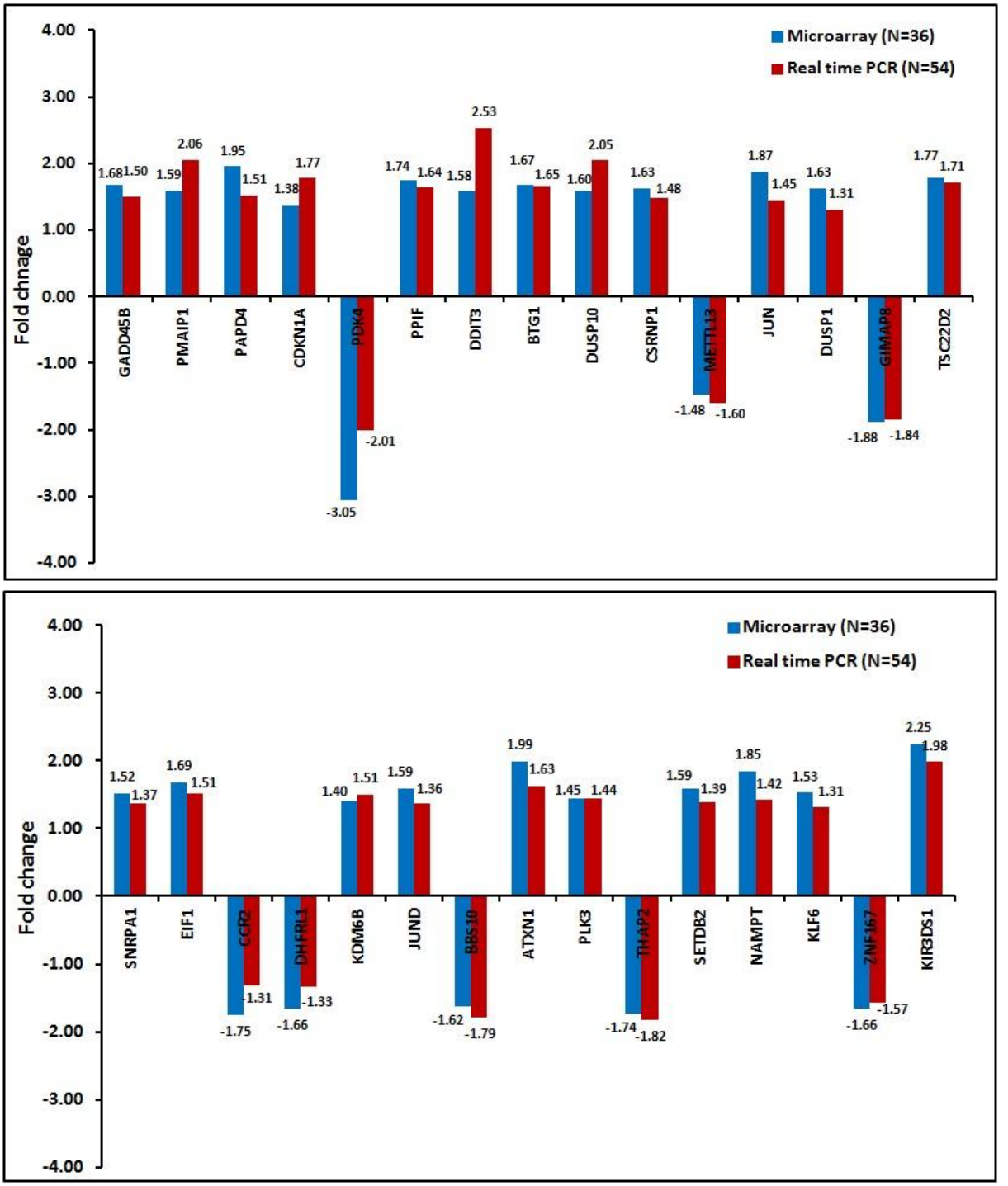

Figure 3.30: A comparison of average fold change values obtained from microarray experiment and hydrolysis probe based real time q-PCR. Blue bars represent microarray fold change values. Red bar represents RT q-PCR fold change values. N=Number of individuals. Fold change values are shown above each bar for all the genes.

As shown in figure 3.30, the average fold change values of these 30 genes obtained from microarray experiments (N=36) and fold change values obtained from q-RT PCR. Data showed similar trend and good correlation between fold change values obtained from microarray analysis and RT q-PCR.

Further, RT q-PCR results obtained from two different set of individuals were analyzed separately and comparison was done between fold change values obtained in microarray experiment (N=36) with fold change values obtained in RT q-PCR from 30 individuals (Microarray samples) and 24 individuals (new set of individuals). As shown in figure 3.31 and 3.32, comparison between the groups showed a similar trend and comparable fold change values. Our results showed consistent gene expression profile of the genes in microarray experiment as well as RT q-PCR experiments. We also observed similar expression values of the genes in new random set of individuals suggesting the results obtained are consistent in HLNRA individuals.

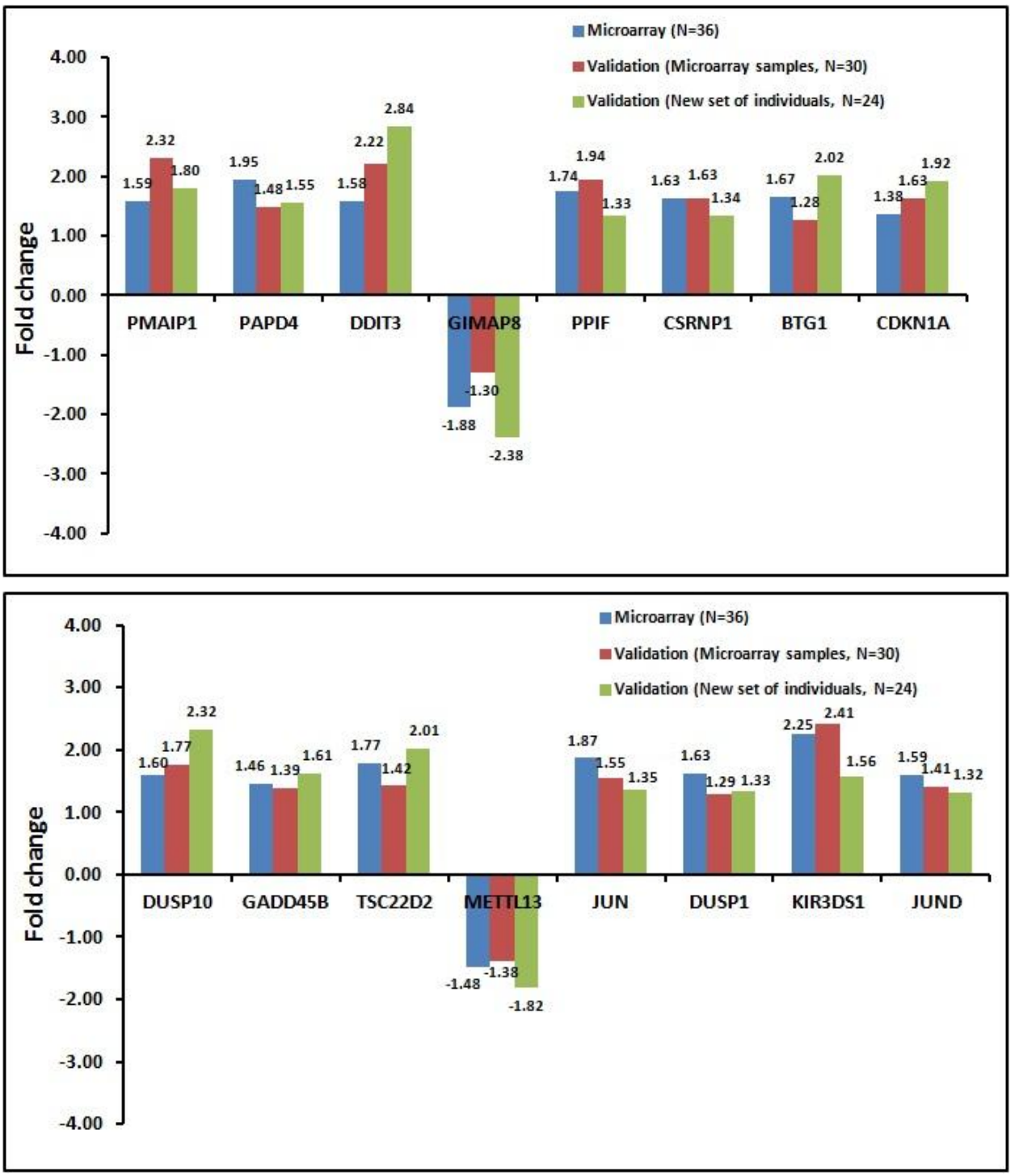

Figure 3.31: A comparison of average fold change values obtained from RT q- PCR experiment in two different sets of individuals with microarray results. Blue bar represents microarray results, Red bar shows RT q-PCR results of microarray samples, Green bar shows RT q-PCR results of new set of samples. Fold change values are shown above each bar in all the genes.

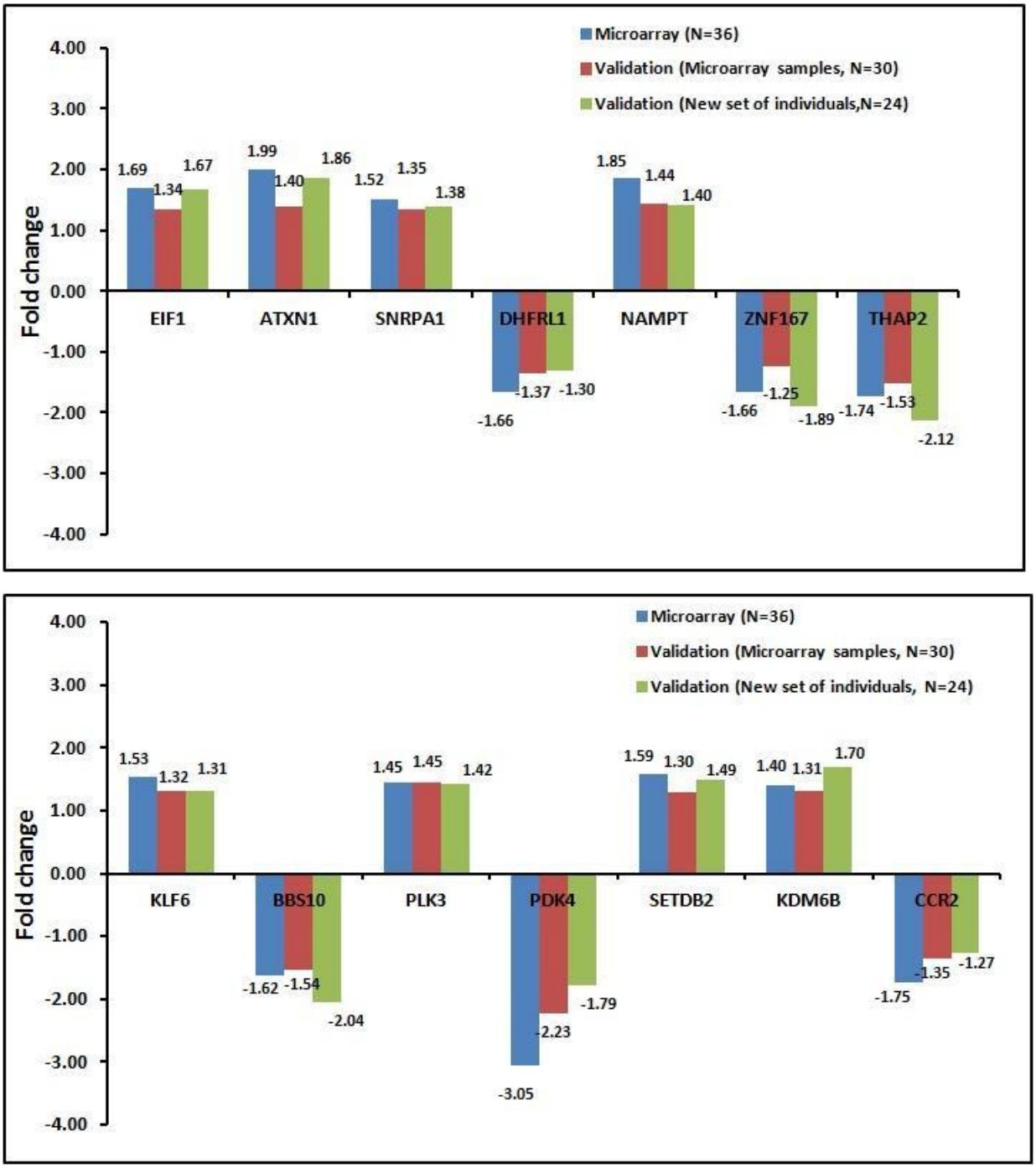

Figure 3.32: A comparison of average fold change values obtained from RT q- PCR experiment in two different sets of individuals with microarray results. Blue bar represents microarray results, Red bar shows RT q-PCR results of microarray samples, Green bar shows RT q-PCR results of new set of samples. Fold change values are shown above each bar in all the genes.

We further analyzed the results obtained from q-RT PCR for the dose responsive genes to determine whether similar background dose dependent increase is observed in q RT PCR results. Gene expression changes of 12 *(GADD45B, PMAIP1, DUSP10, PPIF, BTG1, CSRNP1, JUN, DDIT3, KIR3DS1, PAPD4, TSC22D2, DUSP1)* dose responsive genes were compared between microarray experiment and RT q-PCR. The number of individuals studied using microarray and q-RT PCR were stratified into 4 dose groups on the basis of background radiation dose received by them (table: 3.14).

Table 3.14: The number of individuals studied in microarray experiment and real time q-PCR validation in each dose group are shown. HLNRA: high level natural radiation area, NLNRA: Normal level natural radiation area. N: Number of individuals.

Dose groups	Dose rate (mGy/y)	Microarray No. of Individuals	Real time PCR No. of individuals
Group 1 (NLNRA)	≤ 1.5	N=9	N=19
Group II (HLNRA)	> 1.51 - 5.0	N=9	N=6
Group III (HLNRA)	> 5.01 – 15.0	N=11	N=16
Group IV (HLNRA)	> 15.0	N=7	N=13

Figure 3.33 shows the fold change value of these genes obtained in microarray analysis and q-RT PCR respectively. In the results, all the genes showed similar trend and good correlation between microarray analysis and q-RT PCR. We observed that except TSC22D2 and PAPD4 all other 10 genes also showed dose related changes similar to microarray analysis in RT q- PCR. Scatter plots showing expression values of these genes in all the individuals in RT q-PCR and microarray is given in figure 3.34 and 3.35 respectively.

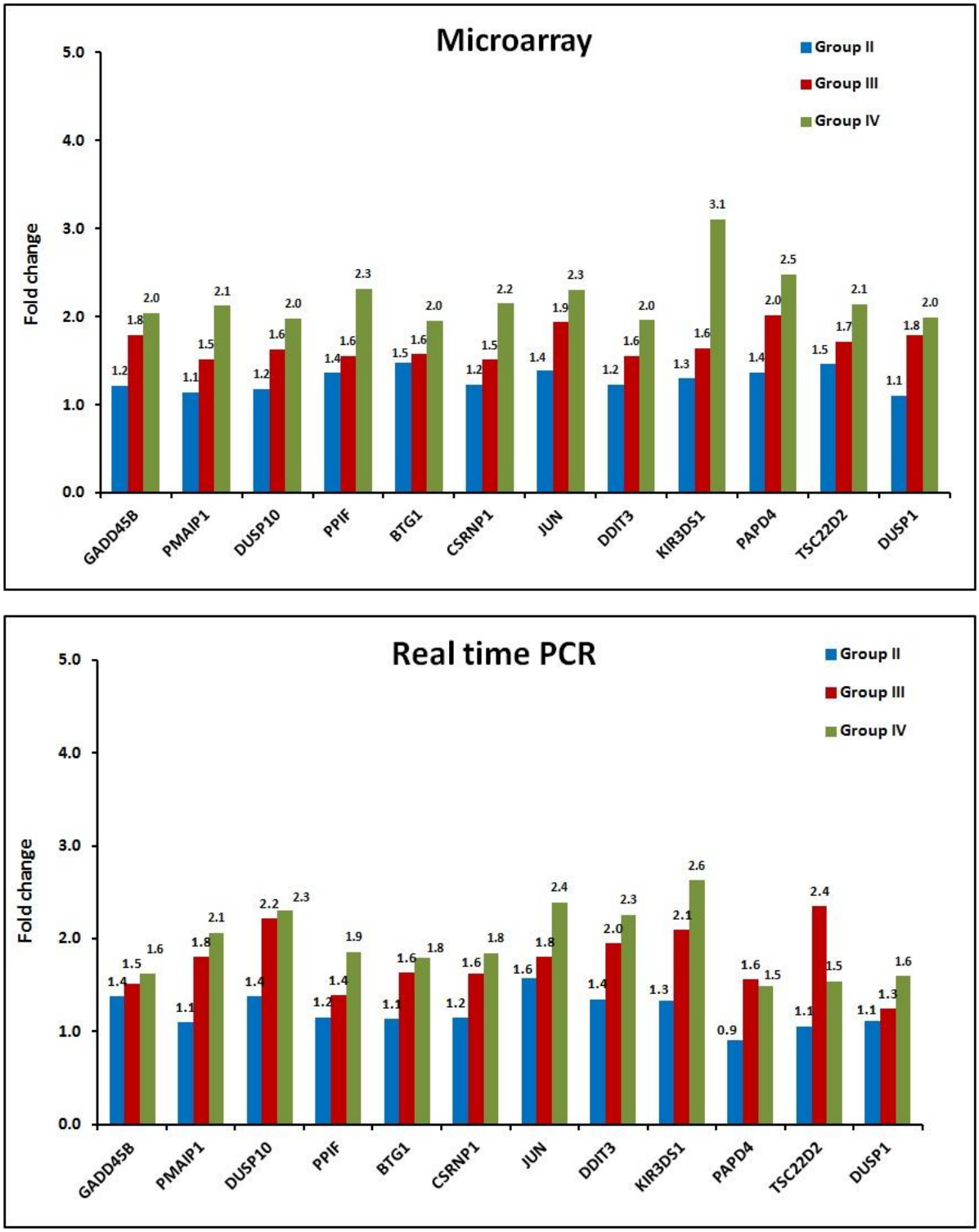

Figure 3.33: Stratification of average fold change values obtained in microarray (N=36) and RT q- PCR (N=54) into different background dose groups. Blue bar represents Group II (HLNRA, >5.0 mGy/y), Red bar represents Group III (HLNRA, 5.1 -15.0 mGy/y), Green bar represents Group IV (HLNRA, > 15.0 mGy/y).

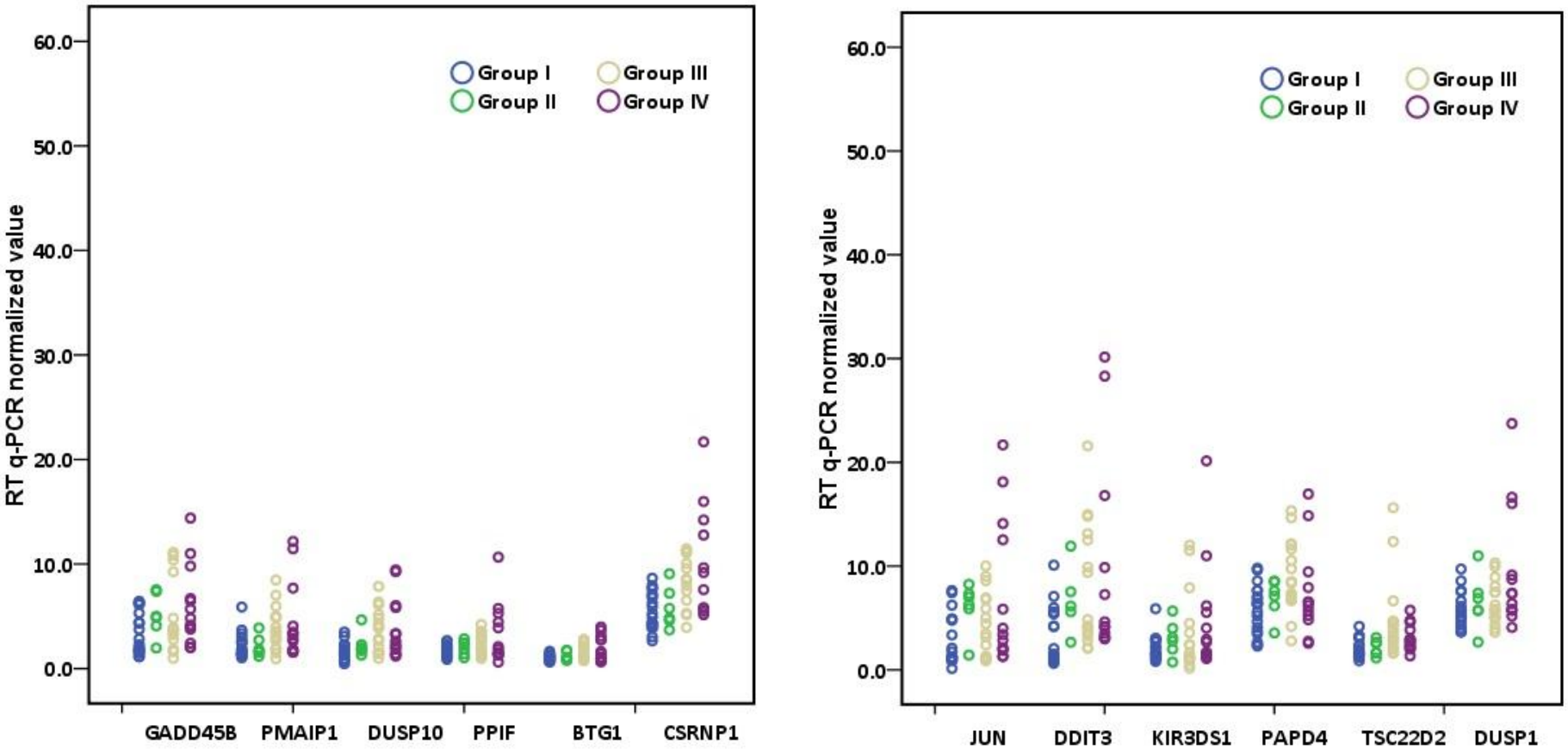

Figure 3.34: Scatter plot showing the expression level of different genes in the individuals belonging to different background dose groups (NLNRA, Group I and HLNRA. Group II, III and IV) using probe based RT q-PCR. Each dot represents normalized value in one individual. Different colored dots represent individuals belonging to different dose groups.

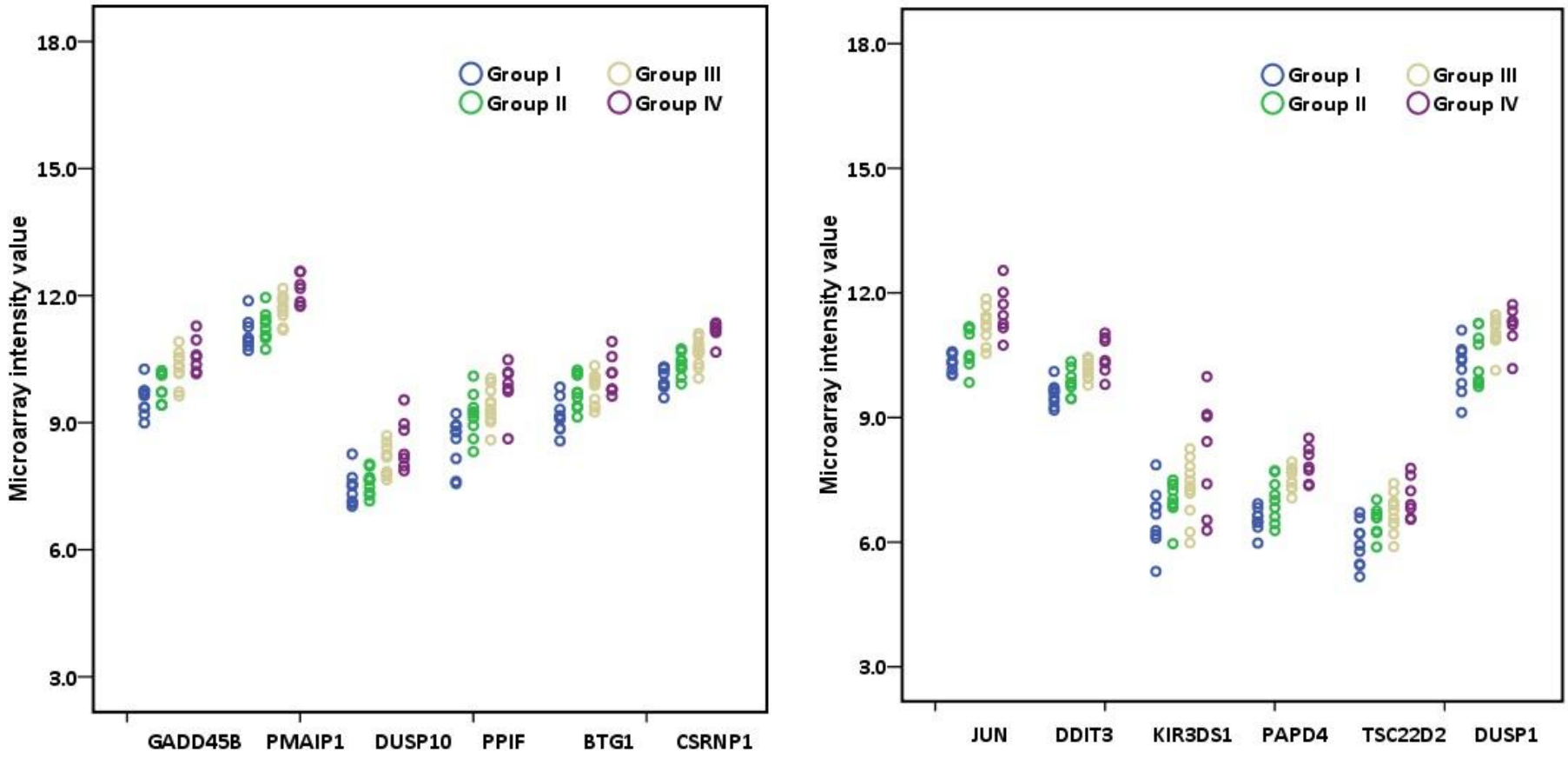

Figure 3.35: Scatter plot showing the expression level of different genes in the individuals belonging to different background dose groups (NLNRA, Group I and HLNRA. Group II, III and IV) in transcriptome analysis using microarray. Each dot represents normalized value in one individual. Different colored dots represent individuals belonging to different dose groups.

In summary, the dose response observed in *GADD45B, PMAIP1, DUSP10, PPIF*, *BTG1, CSRNP1, JUN, DDIT3, KIR3DS1, DUSP1* genes in microarray analysis was confirmed using RT q- PCR which suggests that these genes may be used as possible novel signatures of chronic low dose exposure in human PBMCs.

3.2.4 Expression profile of genes involved in DNA repair pathway after a challenging dose in NLNRA and HLNRA individuals

We have observed a fast and efficient repair of DSBs in PBMCs of HLNRA individuals. The transcriptome study showed over representation of DNA repair and damage response genes in HLNRA individuals indicating their possible role in efficient repair of DSBs in HLNRA. In DNA repair kinetics study, we observed that at 4.0 hr post-irradiation with 2.0 Gy challenging dose, the repair of DSBs was maximum suggesting the optimal induction of repair pathways at that time point. Keeping above observations in mind, we studied radio-adaptive response in genes involved in non-homologous end joining repair pathway (NHEJ). NHEJ is the prominent repair pathway which repairs DNA DSBs in human PBMCs which are resting stage cells.

Radio-adaptive response of six NHEJ genes {*KU70 (XRCC6), KU80 (XRCC5), DCLRE1C, XRCC4, PRKDC* and *LIG4*} involved in DSB repair was studied at 4 h after giving the challenging dose of 2.0 Gy in 20 individuals (HLNRA, N=10 and NLNRA, N=10). In the study, natural background radiation received by HLNRA and NLNRA individuals was considered as adapting/priming dose and a challenging dose of 2.0 Gy was used to observe transcriptional changes in NLNRA and HLNRA individuals. For each individual two experimental points were studied a) baseline expression without challenging dose b) expression after 2 Gy challenging dose and 4.0 h incubation.

As shown in figure 3.36, the baseline expression *KU70 (XRCC6), KU80 (XRCC5)* showed significant ($p \leq 0.05$) up regulation in HLNRA as compared to NLNRA where as *XRCC4, DCLRE1C* and *LIGASE IV (LIG IV)* showed slight down-regulation however it was not significant. At challenging dose of 2.0 Gy after 4.0 h post irradiation, a significant up-regulation was observed in the expression profile of *KU70(XRCC6), KU80(XRCC5) , XRCC4, PRKDC* in NLNRA individuals whereas except LIG4 all other genes showed significant up-regulation in HLNRA individuals.

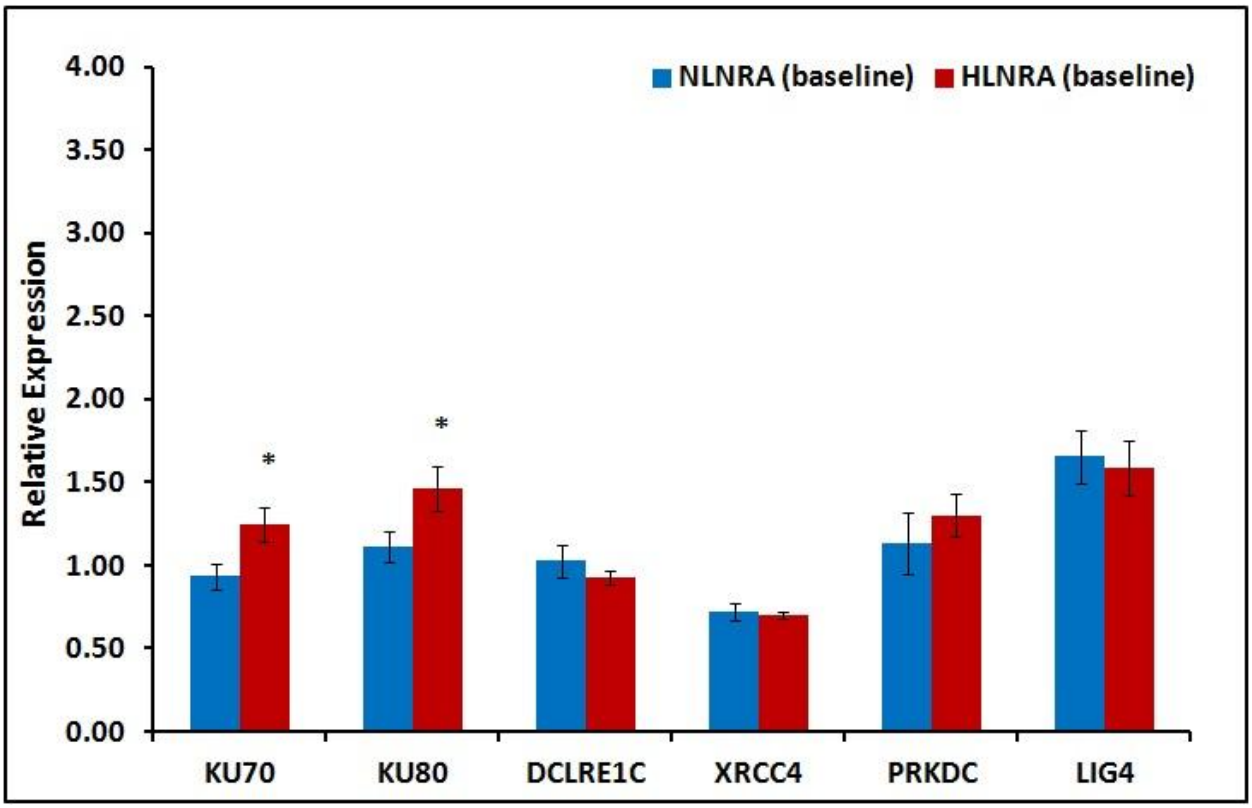

Figure 3.36: The baseline expression levels of NHEJ pathway genes in HLNRA and NLNRA individuals are shown. Relative expression values shown are normalized with β-actin. Significantly (* $p \leq 0.05$) increased expression observed for *KU70 and KU80* genes. Error bars represents S.E.M.(Standard error of mean)

When expression was compared between HLNRA and NLNRA individuals after giving 2.0 challenging dose, a significant up-regulation was observed in KU80, XRCC4 and DCLRE1C genes in HLNRA individuals (figure 3.37).

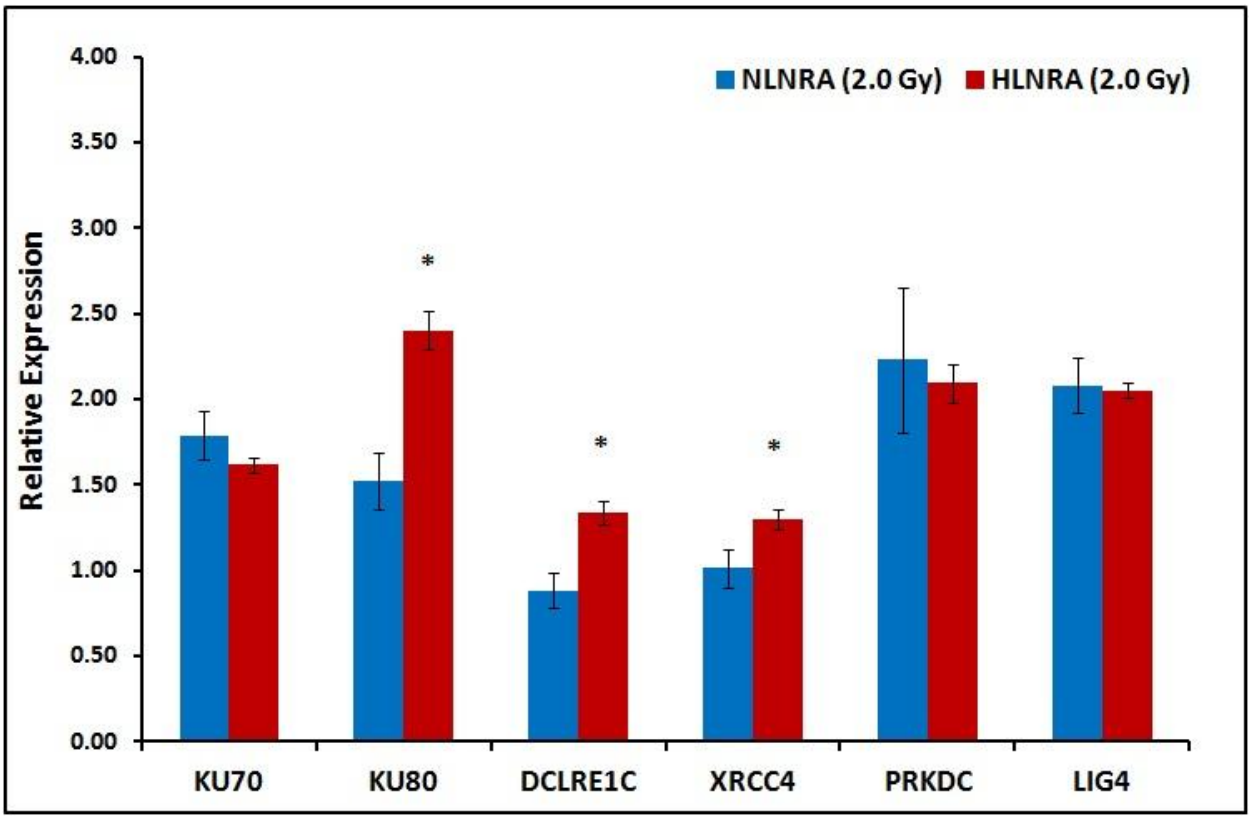

Figure 3.37: The expression levels of NHEJ genes in PBMCs of NLNRA and HLNRA individuals exposed to challenging dose of 2.0 Gy are shown. Relative expression values shown are normalized with β-actin. Significantly (* $p \leq 0.05$) increased expression observed for *KU80, DCLRE1C, XRCC4* genes. Error bars represents S.E.M.

A comparative analysis of fold changes in gene expression at baseline and after a challenging dose of 2.0 Gy is given in table 3.15.

Table 3.15: Fold changes in the expression of genes involved in Non-Homologous End Joining (NHEJ) repair pathway obtained at the level of baseline and after a challenging dose of 2.0 Gy in NLNRA and HLNRA individuals. w.r.t : with respect to.

Gene Name	HLNRA (baseline) w.r.t NLNRA (baseline)	NLNRA (2.0 Gy) w.r.t NLNRA (baseline)	HLNRA (2.0 Gy) w.r.t HLNRA (baseline)	HLNRA (2.0 Gy) w.r.t NLNRA (2.0 Gy)
KU70 (XRCC6)	**1.34***	**1.92***	**1.30***	**0.90**
KU80 (XRCC5)	**1.32***	**1.37***	**1.64***	**1.58***
DCLRE1C	**0.91**	**0.86**	**1.44***	**1.52***
XRCC4	**0.97**	**1.40***	**1.86***	**1.29***
PRKDC	**1.15**	**1.96***	**1.61***	**0.94**
LIG4	**0.96**	**1.26**	**1.29**	**0.98**

Interestingly, *KU80, XRCC4, DCLRE1C* genes showed significantly increased fold change of expression in HLNRA after a challenging dose of 2.0 Gy as compared to NLNRA. Since, *KU80, DCLRE1C and XRCC4* genes play crucial role in DSB recognition, end processing and ligation, our results are indicative of the active involvement of NHEJ repair pathway in adaptation to chronic low dose radiation in individuals residing in HLNRA areas.

3.2.5 Gene expression profile of selected genes after exposure to acute doses of ionizing radiation

There are several reports which have shown that the pattern of gene expression profile is different at low doses as compared to high doses. Also, there are reports showing different cellular response in cells exposed to protracted and fragmented doses as compared to single dose exposure. However, very few studies are available where gene expression changes have been studied at chronic doses as well as acute doses. Here, we have selected few of the highly expressed genes of microarray data and attempted to study their transcription profile at acute low dose exposure.

Dose response was studied at mRNA level for *PMAIP1, DDIT3, PLK3, HISTH2B, DUSP10, JUN, PAPD4 and BTG1* genes after exposing PBMCs with 0.3, 0.6, 1.0 and 2.0 of acute radiation at immediate time point 0.0 h and 4.0 h post-irradiation time point in 10 individuals.

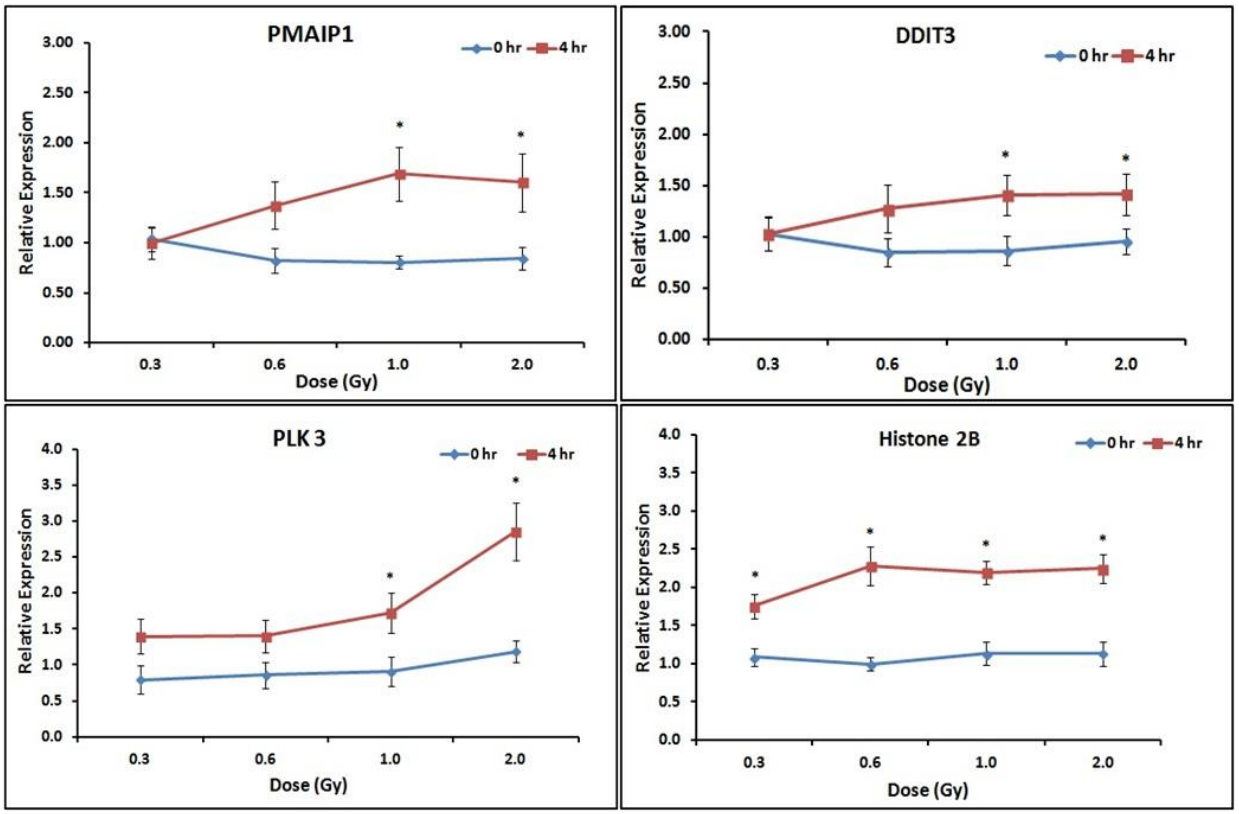

Figure 3.38: Average gene expression of *PMAIP1, DDIT3, PLK3* and *Histone 2B* at different doses (0.3, 0.6, 1.0 and 2.0 Gy) at 0 h and 4 h post irradiation. Error bars represents S.E.M. (standard error of mean). (*) represents significant increase ($p \leq 0.05$) in the level of relative mRNA expression at 4 h as compared to 0 h.

Dose response of *PMAIP1, DDIT3, PLK3* and *Histone H2B* is shown in figure 3.38. The average relative expression of PMAIP1 and DDIT3 genes was observed to be significantly up-regulated at 1.0 and 2.0 Gy. A dose response was observed up to 1.0 Gy whereas at 2.0 Gy similar levels were observed as seen at 1.0 Gy for both the genes. For PLK3, a significant increase was observed at 1.0 and 2.0 Gy, however maximum increase was observed at 2.0 Gy. For *Histone H2B*, significant increase was observed at all the doses studied. However similar response was observed at higher doses 0.6, 1.0 and 2.0 Gy.

Dose response of *DUSP10, JUN, PAPD4 and BTG1* is shown in figure 3.39. The average relative expression of *DUSP10 and JUN* genes was observed to be significantly up-regulated only at 2.0 Gy.

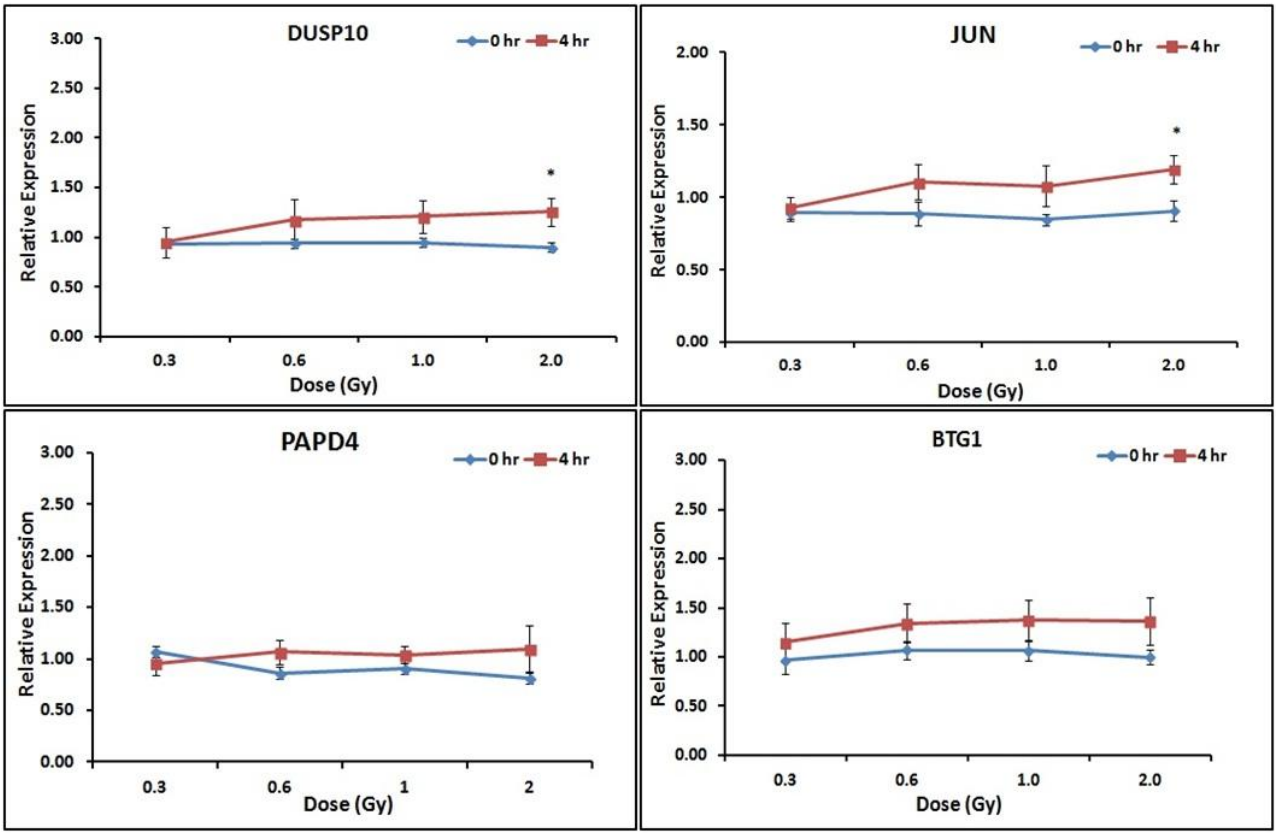

Figure 3.39: Average gene expression of *DUSP10, JUN, PAPD4* and *BTG1* at different doses (0.3, 0.6, 1.0 and 2.0 Gy) at 0 h and 4 h post irradiation. Error bars represents S.E.M. (standard error of mean). (*) represents significant increase ($p \leq 0.05$) in the level of relative mRNA expression at 4 h as compared to 0 h.

A dose response was observed for *DUSP10 and JUN*, however significant increase was only observed at 2.0 Gy. However, for *PAPD4 and BTG1* genes, no significant increase in expression level was observed at any of the doses studied at 4 h as compared to 0 h.

In summary *PMAIP1, DDIT3, PLK3, Histone H2B, DUSP10* and *JUN* showed significant up regulation at chronic as well as acute doses of IR. Hence they may be important signature genes in response to acute as well as chronic low dose radiation.

3.3 Radiation induced chromatin conformational changes at acute doses of ionizing radiation

Radiation induced conformational changes in chromatin fibers were studied in human PBMCs of 10 individuals using Dynamic Light Scattering (DLS) where hydrodynamic diameter of chromatin fibers was measured. Hydrodynamic diameter measured in DLS is the size of the sphere that has the same translational diffusion coefficient as the particle being measured. The translational diffusion coefficient depends on the size, shape and the surface charge of the particle in solution and hence provides information about the conformational changes taking place in chromatin structure following DNA damage.

Dose response study was carried out to measure changes in hydrodynamic diameter (nm) of chromatin fiber isolated from PBMCs irradiated with 0.25, 0.5 and 1.0 of acute radiation doses. Chromatin isolation was carried out at 2 h post-irradiation and multiple DLS measurements were taken at each dose point for 10 independent individuals.

Initial analysis was carried out where average of hydrodynamic diameter (nm) was calculated for each dose point in 10 individuals. We did not observe any significant change in the average values of hydrodynamic diameter (nm) of chromatin fibers of 10 individuals after exposure of their PBMCs to 0.25 Gy, 0.5 Gy and 1.0 Gy as compared to sham-irradiated control (un-irradiated). The average hydrodynamic diameter for chromatin fibers from 10 individuals was observed to be 193.2 ± 22.4 nm, 196.7 ± 29.4 nm, 195.9 ± 32.1 nm and 194.2 ± 24.2 nm at 0.0 Gy (un-irradiated control), 0.25 Gy, 0.50 Gy, and 1.0 Gy respectively. Inter-individual variation in the hydrodynamic size was clearly observed. Among the 10 individuals studied, significant changes were observed in the chromatin fibers among nine individuals at 0.25 Gy. Only one individual did not show any significant difference as compared to control.

As shown in table 3.16 chromatin fibers of six individuals showed changes both at 0.25 Gy and 0.50 Gy and only two individuals showed changes at 1.0 Gy. Further, we observed two different patterns of change in hydrodynamic diameter (increase or decrease in size) at 0.25 Gy among nine individuals (Figure 3.40).

Table 3.16: Hydrodynamic diameter (nm) of the chromatin fibers in PBMCs of 10 individuals at different doses of gamma radiation. Mean ± S.D is given for each donor**.** S.D: Standard deviation.

Dose (Gy)	Donor 1 (Mean ± S.D)	Donor 2 (Mean ± S.D)	Donor 3 (Mean ± S.D)	Donor 4 (Mean ± S.D)	Donor 5 (Mean ± S.D)	Donor 6 (Mean ± S.D)	Donor 7 (Mean ± S.D)	Donor 8 (Mean ± S.D)	Donor 9 (Mean ± S.D)	Donor 10 (Mean ± S.D)
0.0	184.2 ± 5.5	208.3 ±5.9	203.0 ± 7.7	195.9 ± 9.7	244.4 ± 7.7	159.4 ± 7.5	186.2 ± 6.8	183.3 ± 6.9	182.2 ± 6.2	185 ± 4.4
0.25	213.6 ±7.3*	231 ± 7.0*	235.1 ± 6.1*	173.9 ± 2.8*	212.5 ± 8.9*	142.6 ± 5.0*	188.0 ± 6.3	166.8 ± 6.4*	193.6 ± 5.4*	210 ± 8.9*
0.5	205.7 ±6.9*	224.3 ± 5.2*	252.4 ± 7.6*	209.2 ± 7.1	211.1 ± 8.7*	135.9 ± 3.2*	184.0 ± 4.3	188.1 ± 7.2	179.1 ± 9.3	169.2 ± 2.2*
1.0	187.2 ± 7.5	211.5 ± 7.5	226.4 +/- 8.1*	205.2 ± 6.6	220.9 ± 8.6*	148.7 ± 6.6	205.5 ± 4.6	176.1 ± 7.1	187.8 ± 8.5	172.6± 6.3

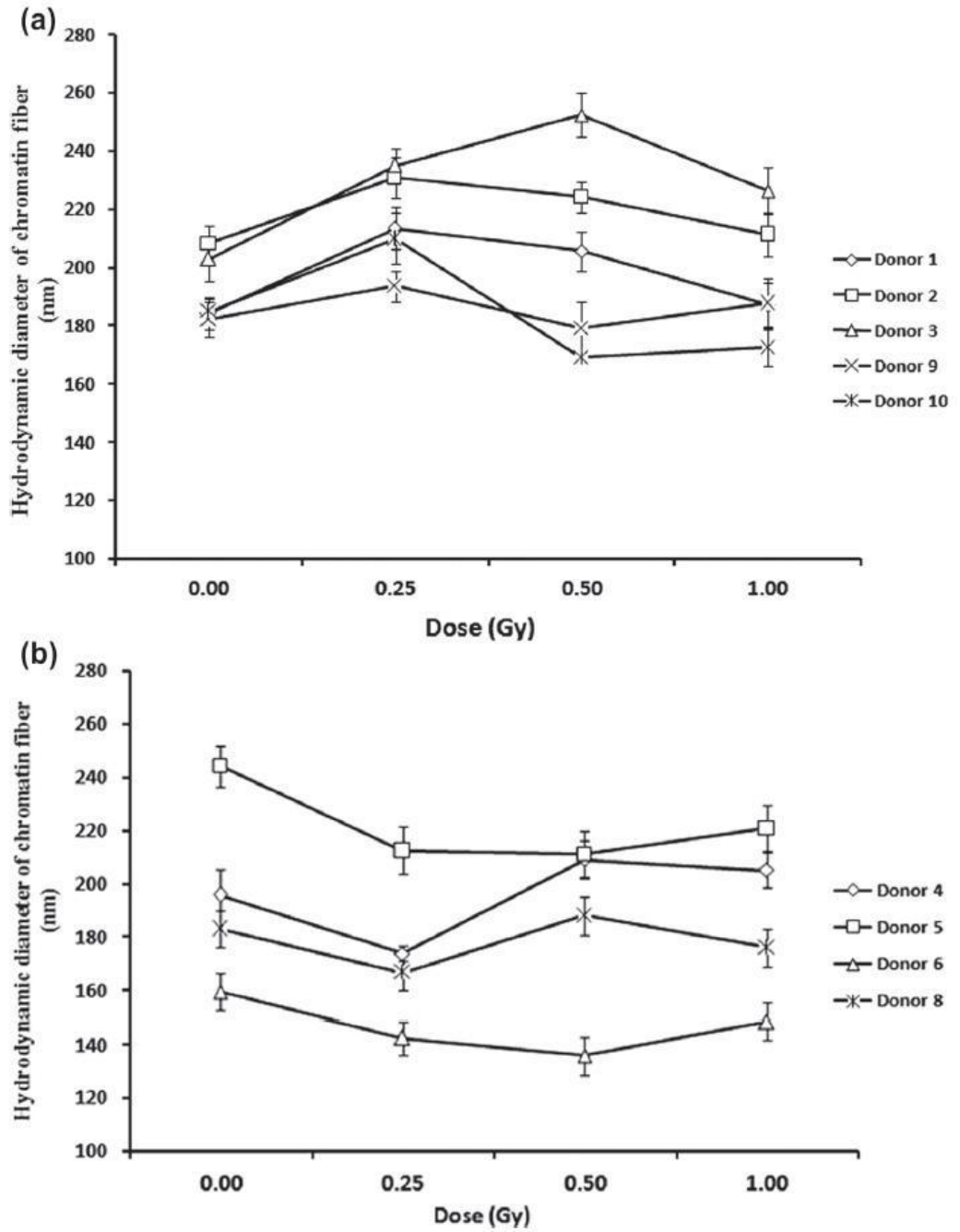

Figure 3.40: Dose-dependence of hydrodynamic diameter (D_h) of chromatin fiber in irradiated PBMCs of nine donors. (a) Significant increase ($p \leq 0.05$) in hydrodynamic diameter of chromatin fibers of five donors after exposure to 0.25 Gy (b) Significant decrease ($p \leq 0.05$) in hydrodynamic diameter of chromatin fiber of four donors after exposure to 0.25 Gy. Error bars represent standard deviation which is calculated from 10 DLS measurements obtained at each dose point from each donor.

Chromatin fibers from five individuals showed significant increase (P= 0.002) in the average hydrodynamic diameter of the chromatin fibers at 0.25 Gy (Trend A) whereas significant decrease (P= 0.009) was observed in the chromatin from four individuals (Trend B) (Figure 3.41). The average hydrodynamic diameter in trend A and trend B at 0.25 Gy was observed to be 216.7 ±16.8 nm and 173.95 ± 28.98 nm respectively. In summary, significant changes at the chromatin level were observed at lower dose points (0.25 Gy and 0.50 Gy) which recovered to its unirradiated state at higher dose points (1.0 Gy).

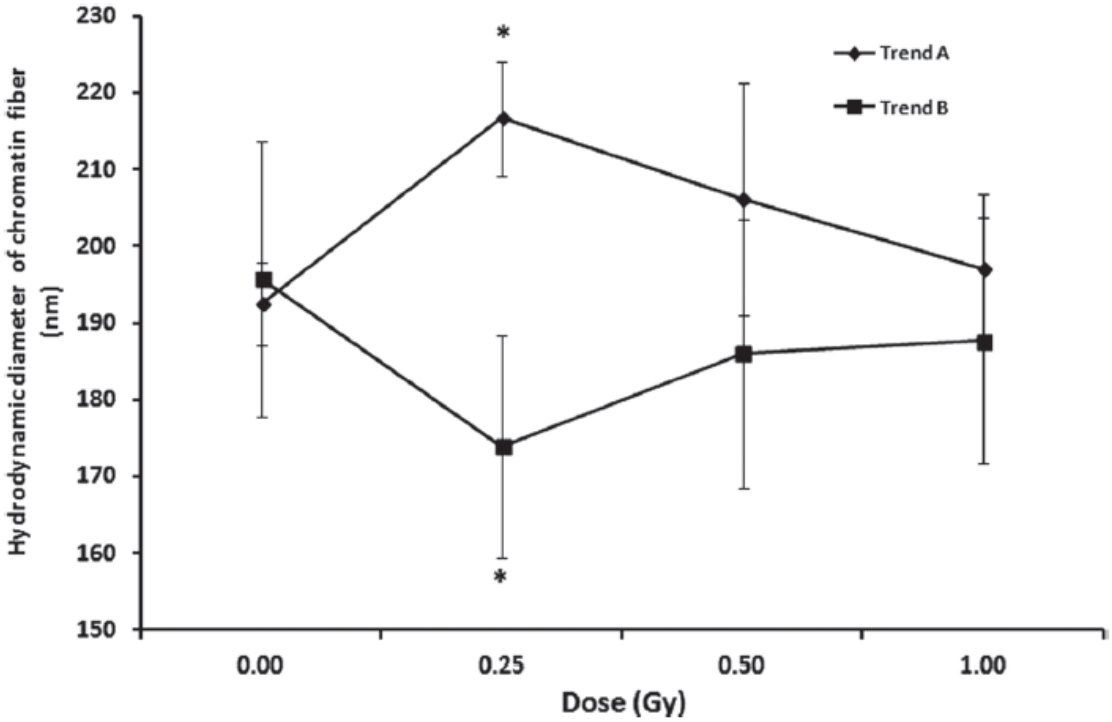

Figure 3.41: Average hydrodynamic diameter of chromatin fiber from PBMCs of nine donors after exposure to different doses of radiation. (a) Trend A: Average hydrodynamic diameter of five donors showing significant increase (*P= 0.002) at 0.25 Gy. (b) Trend B: Average hydrodynamic diameter of four donors showing significant decrease (*P= 0.009) at 0.25 Gy. The standard error of the mean is calculated from the average values obtained from the donors in each group.

Since, chromatin from majority of individuals did not show significant difference in hydrodynamic diameter at 1.0 Gy, we carried out time kinetics experiments at 15, 45, 90 and 120 min at 1 Gy post-irradiation in chromatin from six individuals (three individuals from trend A and three from trend B).Interestingly, we observed significant changes in average hydrodynamic diameter at 45 min and 90 min ($p \leq 0.05$) time intervals, but at 120 min we have observed recovery of the size of the chromatin fiber, which was comparable with that of un-irradiated control cells (Figure 3.42).

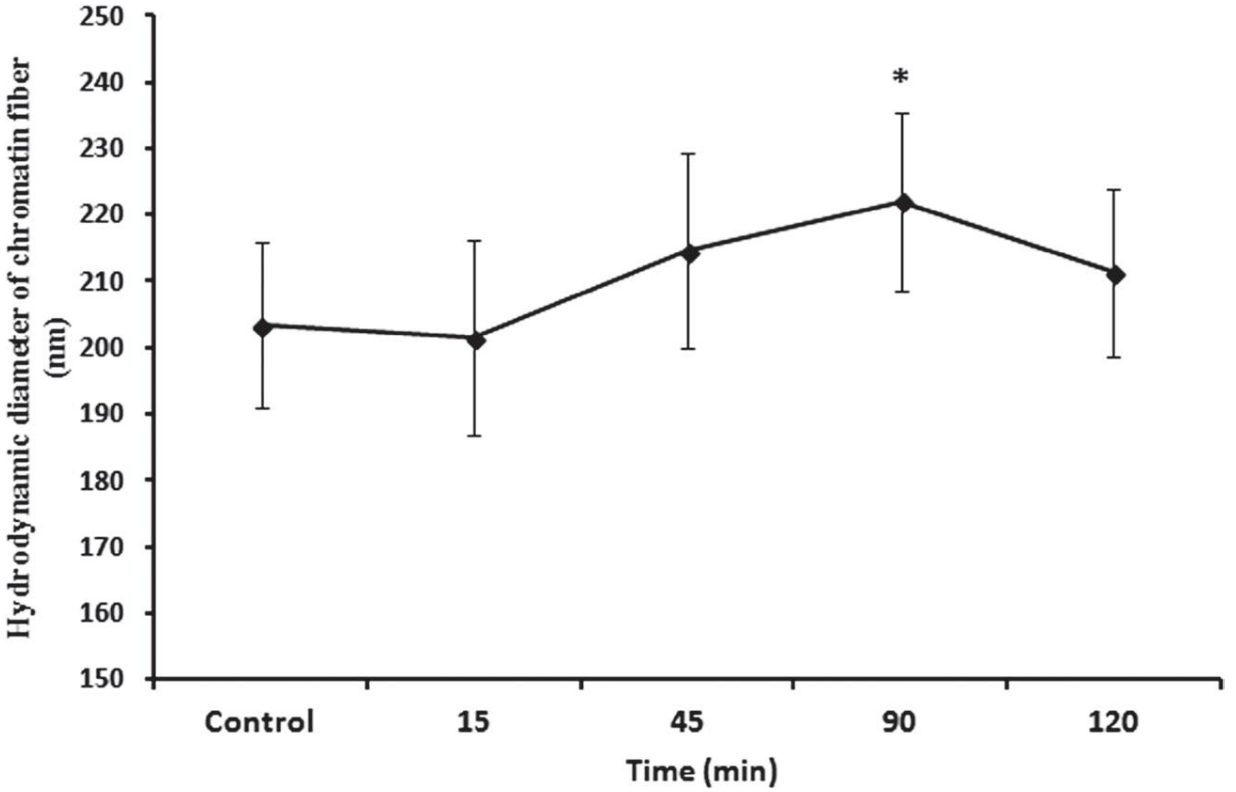

Figure 3.42: Time point changes in the average hydrodynamic diameter of chromatin fibers in PBMC of six donors exposed to 1.0 Gy of radiation. The error bar represents the standard error of the mean which is calculated from average values of six donors. * denotes $p \leq 0.05$.

In the present thesis, spontaneous or basal level frequency of DSBs was measured in the population living in HLNRA and NLNRA of Kerala coast using a sensitive biomarker gamma H2AX. We observed a marginal reduction at higher dose groups of HLNRA (> 5.0 mGy/y) as compared to NLNRA individuals. A significant reduction in induced DSBs was observed in HLNRA individuals at challenging dose of 0.25 Gy. A fast and efficient repair of DNA DSBs was observed in HLNRA individuals as compared to NLNRA individuals suggesting active DNA damage response and repair processes in HLNRA. Transcriptome analysis revealed dose related increase in number of differentially expressed genes involved in DNA damage response and signaling suggested increased induction cellular response with increase in background dose. Further, active role of NHEJ repair pathway in faster repair of DSBs in HLNRA individuals was observed. Our results yields a set of chronic low dose responsive signature genes which may be involved *in vivo* adaptation observed in HLNRA individuals. Radiation induced physical changes in chromatin conformation were studied using Dynamic light scattering at acute doses of gamma radiation.

Chapter 4

Discussion

The discussion section of the present thesis begins with a brief outline on the effect of natural chronic low dose and low dose rate IR in human population residing in normal and high level natural radiation areas of Kerala coast. Further it is focused on basal level frequency, induction and repair kinetics of DNA DSBs using DSB specific gamma-H2AX as a marker in NLNRA and HLNRA population. The induction of DNA DSBs with low and high challenging doses and the pattern of DNA repair kinetics are discussed. Also, the involvement of NHEJ genes during repair process has been discussed. In addition, cellular responses of IR in terms of global gene expression changes and its importance in terms of low dose *in vivo* exposure have been highlighted. In addition acute low dose IR induced chromatin conformational changes in human PBMCs have been discussed.

The annual per capita exposure of the human population in HLNRA of Kerala coast is approximately 4.0 mGy/y. However, the background radiation level in this area varies from <1.0 mGy/y to 45.0 mGy/y. In some places, it has been reported as high as 70 mGy/y (*10*). Therefore, it is interesting to study the cellular and molecular responses of long term low dose IR exposure in population residing in this area. Because of the lack of conclusive scientific evidence at low dose exposure, public concern regarding the potential risk of low doses to health is pertinent. There is an increasing concern about the potential risks of low doses of radiation to public health through various sources such as medical exposures (diagnostic and therapeutic), frequent air travel, cosmic and cosmogenic radiation and elevated level of natural background radiation. Even the existing exposure situations after the nuclear accidents like Chernobyl and Fukushima Daiichi etc. pose further concern among the public as a large number of population gets exposed to the levels of radiation, which are higher than permissible limits.

Biological effects of high doses of IR in humans are well documented. However, there is uncertainty regarding the effect at low dose and dose rate exposures in humans. Risk estimation at low doses of radiation has been extrapolated from epidemiological data obtained at high doses of radiation mainly from life span cohort study done in atomic bomb survivors. Additionally, due to low statistical power, epidemiological data becomes inconsistent and inconclusive. Although there are mixed reports regarding the induction of cancer incidences at lower doses, in recent years, non-cancer diseases such as cardiovascular and other chronic diseases (*233-234*) have shown few concerns. At the same time, biological mechanisms especially non-targeted effects such as adaptive response and bystander effects are gaining importance at low dose exposures. Hence, the direct linear extrapolation from effects at high doses may not be appropriate for low-dose exposures.

Accumulating evidences suggest that the biological responses to low and high doses of radiation are qualitatively and quantitatively different (*15, 17, 67, 111*). However, these studies are mainly carried out *in-vitro* conditions i.e., either in cell lines or in animal models. So far, very few studies have been carried out to understand the *in vivo* effects of low level radiation exposure in humans (*190-191*). This necessitates the direct study on low dose responses to understand potential risks to human health. In view of all the above facts, human population exposed to elevated level of background radiation, either from high level natural radiation areas or from the human population exposed to chronic low dose external radiation exposure after Chernobyl and Fukushima Daiichi disasters (existing exposure situation) provide ideal source to study the effect of low dose radiation.

Population residing in HLNRAs of Kerala coast provides an unique opportunity to study the *in vivo* effects of chronic exposure to low levels of IR. Most importantly, due to non-uniform

distribution of background radiation levels, it is also possible to study *in vivo* dose response if any, at various biological end points. Till date, several epidemiological and radio-biological studies have been conducted in this population and none of the studies have revealed any adverse or deleterious health effects of chronic low level radiation exposure. So far, no significant change in the incidence of any of the cancers, congenital malformations, micronuclei frequency, chromosomal aberrations, attrition of telomere length and DNA damages in terms of strand breaks has been observed in individuals from high level areas as compared to nearby normal level natural radiation areas (*6-10, 30, 32, 46-48, 51*). It is interesting to observe that individuals exposed to more than 8-10 times higher background radiation levels as compared to control areas do not exhibit any adverse effects at phenotypic, cytogenetic or DNA damage level. These observations indicate possible occurrence of adaptation to low dose radiation in HLNRA individuals. However, it is essential to carry out studies at cellular and molecular levels in order to understand the possible mechanisms activated due to the chronic exposure with elevated levels of background radiation in the human population residing in this area. Hence, high-throughput techniques should be employed to delineate the minute changes if any due to low doses of IR at genomic, transcriptomic and epigenomic level.

Non-targeted effects of IR at low doses are complex and have not been fully explored. Radio-adaptive response (RAR) is a phenomenon in which cells exposed to a small conditioning or priming dose of IR reduces the biological effects of subsequent higher doses of radiation (challenging dose). RAR is a transient phenomenon which occurs within 4-6 h and may last for days to months (*19*). There are several reports, which showed reduced cytogenetic damage (*235*), low mutation rate (*236*), reduced tumor growth (*237*) after pre-exposure of cell lines or mice to low priming doses. RAR is reported in different population groups exposed to ionizing radiation (*18*). Adaptive

response and bystander effects in human cells or tissues in response to radiation stress signal further complicate biological responses at low dose range. Carcinogenesis at low doses has not been proven. At the same time, when few cells are hit due to single track of radiation at low doses, biological responses such as apoptosis and intercellular communication may occur to eliminate the affected cells and protect the unexposed cells.

Understanding the biological effects of chronic low level radiation exposure in humans has been a challenging task for decades. A recent study on DNA damage and repair using single cell gel electrophoresis (alkaline comet assay) carried out in PBMCs of NLNRA and HLNRA individuals have revealed that high challenging doses (2.0 Gy or 4.0 Gy) given to both the population groups (NLNRA and HLNRA) showed significant reduction of DNA damage in terms of percentage of DNA in tail (%T) in HLNRA individuals (*30*). It also showed an enhanced rejoining of DNA strand breaks at early stages of repair in HLNRA individuals. However, it is to be pointed out here that single cell alkaline gel electrophoresis detects alkali labile sites, single strand breaks as well as double strand breaks. Further specific DSB markers are required to find out the frequency of the most deleterious lesion, if any, due to chronic low dose exposure. Hence, in the present study, sensitive and high-through put methods were employed to detect minute changes at cellular and molecular level in human cells in HLNRA population.

DNA damage and repair

Exposure to ionizing radiation induces a plethora of DNA lesions, of which double strand breaks (DSBs) are most lethal and may result into deleterious effects such as mutations and cancer. A single radiation track of low LET radiation can produce this kind of damage. One of the important challenges in low dose radiation biology has been the sensitivity of assays which can detect DNA damage at very low dose and dose rates exposures. In the present study, gamma-H2AX assay was employed to quantitate DNA DSBs in NLNRA and HLNRA individuals. Gamma-H2AX is a sensitive and specific biomarker to study induction and repair of DNA DSBs. It has been widely used by several investigators to estimate induction of DNA DSBs and their repair kinetics in human PBMCs exposed to very low doses (mGy levels) of ionizing radiation (*152, 154, 158*). Gamma-H2AX foci formation gives direct correlation with DSBs in 1:1 ratio (*113, 143-144*) and disappearance of gamma-H2AX foci reflects DSB rejoining (*15, 17, 140*). It has been shown that radiation induced foci gets merged at high dose exposures (*118, 151*). Hence, depending upon the radiation dose exposures different methodology (either fluorescence microscopy or flow cytometry) to detect gamma-H2AX foci/positive cells can be employed. In this study, we employed fluorescence microscopy based scoring of gamma-H2AX foci to find out basal level frequency of DSBs in NLNRA and HLNRA individuals. However, for induction and repair of DSBs where PBMCs were exposed to high acute challenging doses, flow cytometry based gamma-H2AX assay was employed. It was more appropriate as it avoids the possibility of merging of the foci at high doses.

In the present study, basal level frequency of DSBs in terms of gamma-H2AX foci was measured in PBMCs of individuals exposed to chronic low level ionizing radiation in HLNRA of Kerala coast and the adjacent NLNRA. The number of gamma-H2AX foci per cell was counted

in the PBMCs of 91 individuals. Assuming that HLNRA individuals have already received low dose exposure in their life time, we have assessed radio-adaptive response if any, in terms of induced DSBs on *in-vitro* exposure of PBMCs from NLNRA and HLNRA individuals to challenging doses of (0.25, 1.0 and 2.0 Gy) of IR. Considering the quantitative difference in the induction of DSBs, we have also studied the repair kinetics of DSBs after exposing PBMCs to low (0.25 Gy) and high (2.0 Gy) doses of IR at different post-irradiation time points (0.5, 2.0, 4.0, 6.0 and 24.0 h). The dose response or dose rate effect if any, in HLNRA individuals was studied by stratifying them into two dose groups: Low dose group (LDG) : 1.51-5.0 mGy/y and high dose group (HDG) : > 5.0 mGy/y.

Interestingly, our results did not show any significant difference in the basal level frequency of gamma-H2AX foci between the NLNRA and two HLNRA groups (LDG and HDG). However, a marginal reduction (P=0.1) in the frequency of gamma-H2AX foci was observed in HDG (HLNRA) individuals as compared LDG (HLNRA) and NLNRA individuals. The mean frequency of gamma-H2AX foci in NLNRA, LDG and HDG was observed to be 0.095 ± 0.009, 0.096 ± 0.008 and 0.078 ± 0.004 per cell respectively, which is comparable with studies conducted in human PBMCs by other researchers (*152, 154, 238*). Our results suggest that the individuals from HDG (HLNRA) may have lower basal levels of DSBs as compared to LDG and NLNRA individuals. It is noteworthy that, we did not observe any dose dependent increase on basal frequency of DSBs in these individuals. Even, interestingly, the levels of DSBs were not increased in HDG individuals, which were exposed to a mean background dose of ~ 11.0 ± 3.57 mGy/y as compared to NLNRA (mean dose: 1.3 ± 0.09 mGy/y), that is almost 8-10 times higher than the control individuals. Moreover, DSB frequency in HDG was observed to be marginally reduced (P=0.1). There could be following plausible explanations for observations of

the present investigation. Firstly, it is possible that DNA damage signaling is induced in HDG individuals, which may have led to the activation of DNA repair machinery and enhanced repair of DSBs in PBMCs of HDG individuals. Secondly, it may be because of the elimination of cells having un-repaired DSBs by apoptosis. It has been reported earlier using gamma-H2AX marker that at low doses (< 10 mGy), the DSB repair process is substantially slow as compared to higher doses (*15, 17*). It is a fact that a certain threshold level of damage is essential to elicit cellular response to DNA damage (*15*). It has also been reported that at doses < 5.0 mGy, the cell signaling and DNA repair processes are not activated (*21, 152*). These might be the possible reasons, why similar frequency of gamma-H2AX foci was observed in LDG (mean dose: 2.63 ± 0.8) and NLNRA individuals (mean dose: 1.3 ± 0.09 mGy/y).

The baseline frequency of gamma-H2AX foci observed in our study is comparable to the gamma-H2AX frequencies reported by others. For instance, Lefevre et al. (2010) reported 0.09 ± 0.05 foci/ per cell among 21 individuals from French population and 0.07 ± 0.05 foci/cell in 6 cuban individuals. Rothkamm et al. (2007) reported the base line value of 0.06 ± 0.02 foci/cell, whereas, Djuzenova et al. (2013) reported 0.12 ± 0.10 foci /cell among 12 individuals. In the present study, a comparatively larger number of samples (91 individuals) were analyzed and the overall baseline frequency of gamma-H2AX foci was observed to be 0.087 ± 0.039, which is comparable to the above published reports. Importantly, till date, no data is available on basal level frequencies of DSBs in population of HLNR areas around the world.

Our results have shown significant (P=0.04) association between age and DSB frequency in the individuals from normal level natural radiation areas. A positive correlation (P=0.04, R=0.37) was observed between DSB frequency in terms of gamma-H2AX foci and the age of the individuals from NLNRA. However, no positive correlation was observed between the frequency

of gamma-H2AX and the age of the individuals from HLNRA (P=0.39, R= 0.11). In an earlier published report, a significant negative correlation was observed between DNA damage with respect to age among HLNRA individuals, whereas among NLNRA individuals significant positive influence of age was observed using alkaline comet assay (*51*). There are also reports which have shown increased frequency of endogenous gamma-H2AX foci with age and also delayed processing of DSBs was shown with increase in age (*239*). Interestingly, in the present study, we did not observe increase in DSB frequency with respect to age in HLNRA, which suggests that elderly individuals residing in high level natural radiation areas seems to be having lesser DNA damage as compared to normal level individuals.

Induction and repair kinetics of DSBs was also studied using gamma-H2AX in HLNRA and NLNRA individuals. A significant reduction in DSBs was observed at 0.25 Gy in HDG individuals as compared to LDG and NLNRA individuals. At higher doses (1.0 and 2.0 Gy), a decreasing trend of DSBs was observed in HDG and LDG as compared to NLNRA suggesting that induction of damage at low and high doses have different response. Initial induction of DSBs was studied at 0.5 h post-irradiation, which is the optimum time-point to study gamma-H2AX signal. Further, repair kinetics of DSBs was studied at different post-irradiation time points with low (0.25 Gy) and high (2.0 Gy) challenging doses. Repair kinetics of DSBs using gamma-H2AX positive cells followed a biphasic curve with a rapid induction of gamma-H2AX signal up to 2.0 h followed by exponential decay phase. A rapid induction of gamma-H2AX intensity at 0.5 h post-irradiation followed by a peak at 2.0 h at both 0.25 and 2.0 Gy challenging doses was clearly seen indicating similar DNA damage response in terms of DSB processing or end joining. Interestingly, both NLNRA and HLNRA individuals showed similar trend of maximum induction peak at 2.0 h followed by bi-exponential decay kinetics up to 24.0 h.

Recently, Sharma et al. (2015) have also reported similar pattern of gamma H2AX repair kinetics.(*240*). The other interesting finding is that our results showed a significantly faster repair of DSBs at 4.0 h and 6.0 h times points in HLNRA (HDG and LDG) individuals as compared to NLNRA individuals. Further, at low challenging dose of 0.25 Gy, significantly lower induction of DSBs was observed at 0.5 h and 2.0 h in HLNRA and NLNRA individuals as compared to 2.0 Gy, where both HLNRA and NLNRA showed similar induction (peak) at 2.0 h. It may be due to following reasons: IR induced DSBs include both isolated and complex damages such as clustered DNA damages, which include DSBs along with non DSB clustered lesions (*53-54, 56*). Clustered DNA damages are two or more lesions formed within one or two helical turns of the DNA by passage of a single radiation track (*54, 241*). In human cells DSB repair starts within few minutes of sensing of DSBs and the rate of repair depends on the complexity and type of DNA lesions. It is known that the complexity of DNA damage increases with increasing radiation dose and about 20-40 % of initial damage is complex which requires proper processing of the damaged DNA (*57-58, 60*). Our results also showed difference in repair kinetics at low (0.25 Gy) and high (2.0 Gy) doses. It could be due to the fact that complexity of DNA damage may be much higher at 2.0 Gy as compared to 0.25 Gy. Hence, the cells would take more time to process the damage at 2.0 Gy, whereas, at 0.25 Gy, the repair of DSB would be much easier probably because the complexity of the lesions is less.

A biphasic pattern of repair kinetics of DSBs was prominent at low as well as high dose exposures to IR in NLNRA, LDG and HDG individuals. There were two different phases of repair with fast and slow phases/components. The fast phase of repair, where > 50% of maximum damage was repaired within 6.0 h and after which a slow repair phase began, where 15-20 % of residual DSBs was still persistent at the end of 24.0 h. Similar biphasic nature of

DSB repair have been reported by different investigators (*145, 163, 166, 242*). Some of important reasons attributable to this biphasic nature of DSB repair are : involvement of different repair pathways to repair fast component and slow component (*59, 106, 145*), the complexity at the site of DNA break/ends (*53, 56, 243*) or the surrounding chromatin structures (*244*).

Our results clearly demonstrated that HLNRA individuals (LDG and HDG) have shown efficient and faster repair of DSBs as compared to NLNRA individuals. It may be due to different efficiencies of DNA damage response and active DNA repair machinery in HLNRA individuals as compared to NLNRA. It may be perhaps due to different chromatin organization in terms of distribution of heterochromatin and euchromatin (*245-246*) and transcriptional status of DSB repair genes in HLNRA population. Efficient repair of DSBs is also indicative of *in vivo* radio-adaptive response of HLNRA individuals. In summary, our above findings are suggestive of radio-adaptive response occurring in HLNRA individuals due to chronic low level ionizing radiation exposure. This report is first of its kind as no such data is available in any of the HLNRAs of the world on DSB repair kinetics. This data also gives a clue that at low dose region of the dose response curve, repair component exists which may challenge the fact that very low dose exposure is as harmful as high dose exposure as suggested by LNT hypothesis.

We further explored the possibility of the role of non-homologous end joining (NHEJ) repair genes, as it is the predominant repair pathway for G_0/G_1 lymphocytes in efficient repair of DSBs observed in HLNRA individuals. NHEJ is the prevalent DSB repair pathway that operates throughout the cell cycle and is one of the major pathways for repair of radiation-induced DSBs in mammalian cells especially at G_0/G_1 phase of the cell cycle (*59, 82-83*). NHEJ repair pathway recruits Ku70-Ku80 heterodimer, DNA-PK catalytic subunit (DNA-PKcs), XRCC4, and DNA ligase IV (LIG4) to the repair sites. Role of NHEJ genes and proteins and their active

involvement has been reported in radio-adaptive response in human PBMCs exposed to acute doses of gamma radiation (*110*). In the present study, we have observed that DSB repair was maximum at 4.0 h post-irradiation time point. Considering the fact that radio-adaptive response is a transient response and usually occurs at 4.0 h in many of the in-vitro studies, we chose to study the transcriptional status of NHEJ genes at baseline level as well as 4 h post-irradiation after giving a challenging dose of 2.0 Gy. Our results showed that at basal level *KU70 (XRCC6)* and *KU80 (XRCC5)* had significantly ($p \leq 0.05$) higher expression level in HLNRA individuals. Interestingly, after 4h post-irradiation with challenging dose of 2.0 Gy, we observed that *KU80, XRCC4 and DCLRE1C* (Artemis) showed significantly higher expression in HLNRA individuals as compared to NLNRA. It is an interesting finding as Ku80 is an important protein which along with Ku70 forms a heterodimer and binds to DSB site and thereafter recruits *DNA-PKcs and DCLRE1C* (Artemis) to the damaged site. Artemis has an endonuclease activity and play crucial role in end processing of DSB sites, hence facilitates rejoining of DSBs by *XRCC4* and *LIGASE4* (*83-84*). Our results strongly suggest the role of NHEJ repair proteins/genes in efficient repair of DNA DSBs in HLNRA individuals.

Gene expression studies

Alteration in the gene expression profile is another important aspect of cellular response to genotoxic stress including IR. DNA damage elicits a complex and well orchestrated cellular response in human cells, which activates various biological processes to maintain the integrity of the genome. DNA damage response includes sensing and detection of DNA damage that leads to check point activation and cell cycle arrest, which allows the cells to repair the damage by activating various DNA repair pathways. If the cells are unable to repair the damage, or the damage is mis-repaired, it may undergo senescence or apoptosis to remove the damaged cell to

preserve the genomic integrity. Transcriptional alteration of many genes that are involved in cell cycle arrest, DNA repair, apoptosis, chromatin modification, immune response, cell signaling etc plays a crucial role in maintaining the genomic stability.

Several investigators have used gene expression profile as an indicator of cellular responses to low dose radiation (*172-173, 187-188*). More recently, high-through microarray techniques have been used to study the differential expression of genes at low dose exposures in cells both *in vitro* and *in vivo* (*67, 111, 185-186, 188, 247*). The signaling networks unravel the molecular mechanism of radiation response. In recent years, global gene expression profiling have greatly enhanced the knowledge on different signaling networks and help to unravel the molecular mechanisms of radiation response. Since *in vivo* data on global gene expression profile in response to low dose IR is not available, the present transcriptome data becomes highly relevant in terms of DNA damage response and cellular and molecular networks in human PBMCs. It has few important implications; firstly, it may unravel the genes which can be used as chronic low dose radiation signatures. Secondly, the qualitative data on gene expression profile at low dose exposure may be used for high acute dose exposures. Thirdly, the networks and pathways revealed by this study may give new insights to understand the underlying biological processes in HLNRA population.

Keeping all these points in mind, transcriptome analysis was carried out in order to understand the effects of chronic low dose and dose rate IR at basal level of gene expression in the PBMCs of individuals from NLNRA and HLNRA. High throughput microarray technique was employed to get a snapshot of complete transcriptome profile in PBMCs of individuals from different background dose groups of Kerala coast. Transcriptome analysis provides information on the expression profile of actively expressed genes (differentially expressed in terms of up and

down regulation) in a cell population at any given point of time or at any genotoxic stress. It is extremely useful and a powerful tool to identify and understand the molecular changes occurring in a cell population in response to certain external environmental conditions. For instance, in this study, human HG-133 plus 2.0 gene chip (Affymetrix) array was employed, which could detect the expression level of ~47,000 transcripts from more than 30,000 well characterized human genes simultaneously for a single sample. Hence, the results obtained from this entire gene expression analysis give a detailed understanding of the molecular and cellular network of genes involved in HLNRA population.

Transcriptome analysis was carried out on 36 male individuals from NLNRA (≤ 1.5 mGy/y, Group I) and three HLNRA groups {(1.51-5.0 mGy/y, Group II), (5.1-15 mGy/y, Group III) and (> 15.0 mGy/y, Group IV)}. Interestingly, our results revealed background dose dependent increase in the number of differentially expressed genes in HLNRA individuals as compared to NLNRA. This finding suggests, increased stimulation of cellular responses in PBMCs of individuals living in higher background radiation areas. Perhaps it may be due to the fact that individuals belonging to higher dose groups have a higher cumulative dose of radiation. Detailed gene ontology analysis revealed an over-representation of genes involved in DNA damage response and repair, cell cycle regulation, mRNA processing, protein transport, stress response, chromatin modification, apoptosis, transcription regulation, signal transduction, and immune response in individuals belonging to higher dose groups of HLNRA (> 5.0 mGy/y).

Some of the important genes identified from this data such as *RAD21, LIG4, DCLRE1C, XRCC4 (DNA repair), CDKN1A, DDIT3, GADD45B* (DNA damage response), *IL8, KIR3DS1* (Immune response), *HNRNPM, SNRPA1, PAPD4* (mRNA processing) *HIST1H1E, H3F3B, HIST1H2BC, HP1BP3, KDM6B, ING3, SETDB2* (chromatin modification/nucleosome

assembly), *HIPK1, PMAIP1, APAF1, PPP1R15A* (apoptosis) were significantly differentially expressed in HLNRA population.

Modulation of gene expression may play an important role in low dose and low dose rate induced radio-adaptive response, radio-resistance and bystander effect in human cells. Adaptive response leads to DNA damage prevention by activating repair mechanisms, immune system stimulation, activation of cell-cell communication (*20, 203*) etc. Elimination of damaged cells by apoptosis may play a crucial role in reducing genomic instability. Low dose induced apoptosis is assumed to operate through intercellular signaling from normal cells. The replacement of pre-damaged cells with healthy cells may be the major route of *in-vivo* removal of oncogenic transformed cells. Importantly, at low doses, reduction of damage from endogenous sources by adaptive protection may be equal to or outweigh induced damage (*19*).

IR induced transcriptional regulation of DNA repair genes and their role in adaptation has been reported (*90*). However, DNA repair pathways are highly complex and involve DNA damage response signals and a network of proteins to be working in well orchestrated manner. Interestingly, important DNA repair genes such as *UNG* and *APEX2* involved in base excision repair, *RAD23B* and *ERCC4* genes which play important role in nucleotide excision repair and *DCLRE1C* (Artemis*), XRCC4, LIG4* important genes involved in NHEJ pathway were differentially expressed in HLNRA individuals. Uracil-DNA glycosylases *(UNG*) plays a crucial role in preventing mutagenesis by eliminating uracil from DNA molecules by cleaving the N-glycosylic bond and initiating the BER process. RAD23B is involved in XPC complex which along with other factors like *XPA, RPA* and the *TFIIH* complex plays a role in DNA damage detection. *ERCC4* is an important structure-specific DNA repair endonuclease responsible for the 5-prime incision during NER. *DCLRE1C (Artemis*) has 5'-3' exonuclease activity and play a

crucial role in end processing of DSBs in NHEJ repair pathway. *XRCC4* and *LIG4* form a complex and carry out the important ligation step in NHEJ pathway. Involvement of all these genes from different repair pathways suggests that long term exposure of low dose and low dose rate radiation has activated almost all the DNA repair pathways in HLNRA thus leading to a better adaptation of the human population.

It has been reported that the induction of DNA repair resulting in adaptive response is only visible through a narrow window of dose and time. It may be because at low doses, the DNA damage levels may not be high enough to activate DDR and at high doses, transcriptional inhibition by DNA adducts nullifies the effect of gene activation. Therefore, a balanced expression of DNA repair genes is important for avoiding erroneous repair due to excessive base removal and DNA cleavages (*90*). It might be possible that the expression of differentially expressed genes in HLNRA individuals might be regulated through feedback mechanisms involving a set of transcription factors like c- JUN, ATF2, JUND, NF-kB, CREB etc which are up-regulated in HLNRA individuals.

The signal transduction pathways such as mitogen activated protein kinase (MAPK) pathway, Jun amino-terminal kinases (JNK) pathway and p53 pathway have been shown to play important role in low dose radiation induced adaptive response (*18, 248-249*). The transcriptome data showed involvement of MAPK pathway (DUSP1, DUSP10, AKT2, ATF2, DDIT3, DUSP5, GNAS, HIPK3, IL8 etc) and p53 pathway (CDKN1A, MDM2, TRAF4, TNFRSF10B, APAF1, PMAIP1, GADD45B etc) in higher dose groups of HLNRA. Interestingly, in our study the transcription of P53 gene was not observed to be altered, however, it is known that activity of P53 protein is regulated through various post-translational modifications. It an important pathway, which regulates various DNA damage response processes like cell cycle arrest, apoptosis,

transcriptional regulation and DNA repair. CDKN1A and GADD45B are important TP53 regulated genes, which are known radiation responsive genes and play an important role in cell cycle check point activation leading to cell cycle arrest. MDM2 is an important gene which interacts with p53 and facilitates its degradation thus playing role in regulating p53 associated activities in response to stress. In addition, gap junction mediated inter-cellular communication plays a role in radio-adaptive response at low doses (*250*), we have observed important genes involved in gap junction, tight junction and cell adhesion pathways which are important findings at low dose and low dose rates. Some of the important genes involved in modulation of immune response have been observed in HLNRA groups suggesting their role *in vivo* radio-adaptation. Considering the fact that low LET radiation hits a few number of cells in the single track of radiation can activate bystander effects and thereby inducing adaptive response in human cells. The role of the genes involved in gap junction, tight junction and cell adhesion pathways are very important in un-ravelling the non-targeted effect of low dose radiation. Most importantly, adaptive response and bystander effects in G_0/G_1 lymphocytes might give important information in low dose radiation biology. Further analysis on this line may be fruitful in unraveling the contribution of these two phenomena towards low dose region radio-biological data.

Another important finding of the present study is the transcriptional induction of important transcription factors (TFs) such as *c-JUN, JUND, FOS, ATF2, NR4A2, Sp1, FOXO3, CREBZF*, which are known to play important role in DNA damage response and repair. Genes such as *JUN, FOS, ATF2* and *CREBZF* belong to AP1 family of transcription factors (TFs). AP1 family TFs are stress responsive transcription activators and has been implicated in DNA repair by its ability to regulate a large set of genes functioning in DNA repair (*251*). Also in the recent past it has been shown that TFs such as ATF2, NR4A2 and Sp1 (*252*) not only regulates the

transcription of genes involved in DNA repair, but they also translocate to the site of DNA lesion and play a direct role in DNA repair. Bhoumik et al (2005) have shown that following DNA damage, ATF2 translocate to DNA DSBs and get phosphorylated by ATM at ser490, ser498 and presence of phospho-ATF2 at DNA damage induced DSB foci have also been reported. Induction of these important transcription factors in HLNRA individuals are suggestive of their active role in DNA damage response and repair in HLNRA individuals.

Another important class of transcription factors NR4A family of nuclear receptor (NR4A2 and NR4A3) is known to play a direct role in DNA repair. NR4As proteins are known to be rapidly induced by adaptive and stress induced physiological functions. Their direct role in DNA DSBs has been elucidated. It has been shown that upon DNA damage, NR4A2 rapidly gets translocated to DNA repair foci, where it gets phosphorylated by DNA-PKcs and co-localizes with other repair proteins such as gamma-H2AX, DDB2 and XPC and act directly to promote DNA end ligation (*253-254*). In our study, increased expression of NR4A2 and NR4A3 genes was observed suggesting their active involvement in DNA DSB repair at high dose groups of HLNRA individuals (> 5.0 mGy/y).

Gene expression responses to low dose ionizing radiation are not well known. A comparative study carried out at low and high doses in human fibroblasts cells revealed qualitative and quantitative differences in gene expression profile (*67*). This study also showed cell-cell signaling, signal transduction and DNA damage responses as main biological processes responding to low dose radiation (2 cGy) as compared to cell proliferation and apoptosis, which were active at high doses (4.0 Gy). Our results on signal transduction pathways, cell-cell signaling, DNA damage response and repair pathways are the new findings for chronic low dose radiation exposure to human population. Importantly, very few studies are available where *in-*

vivo gene expression changes have been studied in human population. Few studies have been carried out where transcriptional response in occupational workers exposed to very low dose ionizing radiation have been reported (*190-191*). Interestingly, over-representation of histone modification genes involved in DNA packaging, chromatin architecture and DNA metabolism genes was observed in the study of Morandi et al. (2009). In our study, we also observed large number of genes (*HIST1H1E, H3F3B, HIST1H2BC, HP1BP3, KDM6B, ING3,MYST4 SETDB2 etc)* involved in these processes to be represented in our data set. It indicates the alteration of chromatin structure in one of the important cellular response to chronic low dose exposure. Faschin et al. (2009) observed several biological processes such as ubiquitin cycle (*UHRF2 and PIAS1*), DNA repair (*LIG3, XPA, ERCC5, RAD52, DCLRE1C*), cell cycle regulation/proliferation (*RHOA, CABLES2, TGFB2, IL16*), and stress response (*GSTP1, PPP2R5A, DUSP22*) to be active chronic low level radiation exposures. Interestingly, such pathways are over-represented in our data suggesting their involvement in chronic low dose radiation exposure.

In summary, our findings clearly indicated that individuals exposed to background doses of > 5.0 mGy/y, have shown alteration of gene expression of many important functions or pathways. These included DNA damage response processes along with other important associated processes like RNA metabolism, histone modifications, DNA methylation to be highly active. These may be the primary reason of not getting any detectable change at phenotypic and DNA damage levels in HLNRA individuals exposed to higher background doses. DNA damage study using gamma-H2AX marker did not reveal any observable or significant increase in DSB frequency. The possible reason could be the activation of DNA damage responses including damage detection and signaling, activated DNA repair pathways and

apoptosis to remove highly damage cells if any. We also did not observe PBMCs with more than two foci in our analysis indicating that complex damages are very few in HLNRA individuals. Activation of several chromatin modifying genes may be responsible for opening up of chromatin architecture, which enhances the accessibility of DNA repair proteins to damage sites. This also facilitates the transcription of important genes required for damage correction. The presence of chromatin modifying genes in our data perhaps indicating that damage correction is occurring in HLNRA population thus excess damage is not seen in HLNRA groups.

Transcriptional response to IR has been studied by several investigators at various doses of acute radiation exposure, where it has reported as radiation signatures and can be used as a biomarker of radiation exposure (*68-69, 177*). Importantly, it has been reported that transcriptional response is not similar at all the doses. It has been observed that transcriptional response can be qualitatively and quantitatively different (*67, 111, 174, 255*). However, very limited studies have been carried out to understand the transcriptional response at very low and low dose rate exposures (*196*). In recent years, there are few reports available on exposure to low doses. For instance, gene expression analysis has been carried out in mouse liver tissue exposed to low doses of radiation (1-20 mGy/day)(*181*). *In vivo* transcriptional response has been studied in human skin after exposure to 10 cGy (*70*). Similarly, gene expression analysis is carried out in nuclear workers exposed to doses in the range of few milligrays (*190, 192*). However, there is no report on *in vivo* transcriptional response on humans exposed to chronic low level radiation throughout their life span. The present study revealed a set of low dose responsive genes, which may be important signatures of chronic level radiation exposure on humans. We selected 30 genes from our data set and their expression level was validated using hydrolysis probe based RT q-PCR. Expression level was validated in same individuals where

microarray experiment was carried out and also on a random set of individuals collected separately to check the reproducibility of our results in HLNRA population. We observed a good correlation in expression levels between the two groups of individuals confirming their use as radiation signatures.

There has been reports which have shown the usefulness of gene expression changes in radiation bio-dosimetry (*173, 178, 182-183, 256-261*). In our study we also identified important genes which showed dose related changes in their expression level in different background dose groups. Some of the highly expressed dose responsive genes observed were *DDIT3, GADD45B, JUN, PMAIP1, DUSP1, PAPD4, DUSP10, BTG1, PPIF, TSC22D2, TMEM132C, GIMAP8, METTL13, CSRNP1, KIR3DS1, TNFSF10* etc. We further selected 12 of the above genes and validated the dose response observed using RT q-PCR. We observed 10 of the above genes (*DDIT3, GADD45B, JUN, PMAIP1, DUSP1, DUSP10, BTG1, PPIF, CSRNP1, KIR3DS1*) showed similar dose rate related changes in RT q-PCR. These genes may be used as possible marker for low dose bio-dosimetry in humans.

Further, several researchers have reported that different set of genes are expressed at low dose exposures as compared to high dose exposures suggesting qualitative and quantitative difference in gene expression profile at low and high doses.(*70, 111, 177*). An attempt was made to compare the mRNA expression levels of selected highly expressed genes from our data with chronic exposures with their transcriptional response at acute exposures. The mRNA expression levels of *PMAIP1, PAPD4, DDIT3, BTG1, JUN, HISTH2B (Histone H2B), PLK3* and *DUSP10* genes was studied in PBMCs at different acute dose exposures (0.3 - 2.0 Gy). Our results showed radiation induced increase in mRNA expression levels of *PMAIP1* (apoptosis), *DDIT3* (DNA damage response), *JUN* (transcription regulation), *HISTH2B* (nucleosome assembly), *PLK3*

(Apoptosis), *DUSP10* (Cell proliferation) genes with maximum induction observed at 2.0 Gy dose. However, BTG1 and PAPD4 which showed significant up-regulation at chronic low level exposures in HLNRA individuals did not show any induction in mRNA levels at acute dose radiation.

Our results have supported the previous findings that gene expression changes are not linearly correlated from low dose to high dose radiation exposure. It further emphasize that the cellular responses are quantitatively as well as qualitatively different at low doses and biological effects of ionizing radiation at low doses especially at chronic exposure may not be always correlated with high acute dose exposure.

Radiation induced changes in chromatin structure

Alteration in chromatin structure is another important aspect of cellular response to DNA damage. Dynamic nature of chromatin structure plays a critical role in recognition of damage and initiation of DNA damage response in human cells. Radiation induced post-translational modifications in histone proteins have been reported in human cells. They play an important role in reorganization of chromatin structure. In the present thesis, attempt has been made to study the conformational changes occurring in chromatin structure in response to acute low dose exposures.

A biophysical technique such as Dynamic Light Scattering (DLS) was used to measure the conformational changes in terms of hydrodynamic diameter (nm) of the chromatin isolated from PBMCs exposed to acute doses gamma radiation between 0.25 to 1.0 Gy. We have observed maximum change in hydrodynamic diameter in PBMCs exposed to 0.25 Gy at 2.0 h post-irradiation, whereas no difference was observed at high dose (1.0 Gy). Inter-individual variation was clearly observed. We observed two different trends of response in the individuals

studied. The individuals could be divided into two groups: one group showed significant increase in hydrodynamic diameter at 0.25 Gy followed by dose related recovery up to 1.0 Gy where as another group showed significant decrease in hydrodynamic diameter followed by recovery at 1.0 Gy. The two trends observed at 0.25 Gy might be explained on the basis of the random distribution of DNA damage between different chromatin compartments, i.e., heterochromatin and euchromatin. Since, induction of DNA damage by radiation is a random phenomenon, thus the distribution of DNA damage between chromatin compartments might influence the overall dynamics of chromatin. It has also been reported (*246*) that DNA lesions are more complex in heterochromatin and their processing is slower in heterochromatin as compared to euchromatin compartment (*122, 262*).

Post irradiation time point kinetics at 1.0 Gy at different time intervals between 15min to 2.0 h post-irradiation was done in isolated chromatin from PBMCs. Interestingly, we observed that at high dose of 1.0 Gy maximum change was observed at 90 minutes post-irradiation and recovery was observed at 120 minutes (2 h) post-irradiation. Our findings show that cellular response in terms of changes in hydrodynamic diameter of irradiated chromatin are different at low dose and high doses of acute radiation exposure.

Human peripheral blood mononuclear cells are most radiosensitive and are ideal to study the radiation-induced changes at the level of chromatin *in vitro*. It will be ideal to employ new techniques to find out chronic low-dose radiation-induced changes if any, at the molecular level. The present study offers DLS as a novel technique to study radiation-induced changes of chromatin dynamics at such low-dose radiation exposures. It may be a useful tool in studying the physical conformational changes occurring in chromatin structure, however it does not give any information on mechanistic aspect of chromatin remodeling.

In summary, the present thesis has novel findings in terms of efficient repair capacity of DNA DSBs in HLNRA individuals exposed to chronic levels of low dose ionizing radiation. It also throws some important insights on the cellular and molecular responses active at chronic low level radiation exposure. The important finding of transcriptome analysis emphasized overabundance of DNA damage response and repair, apoptosis, chromatin/histone modification, immune response genes in HLNRA population. Further, active role of NHEJ repair pathway in faster repair of DSBs in HLNRA individuals was observed. Our results yields a set of chronic low dose responsive signature genes which may be involved *in vivo* adaptation observed in HLNRA individuals. All these above findings clearly suggest *in vivo* radio-adaptation of HLNRA population due to long tern chronic exposure. The cellular and molecular effects of low dose radiation in the present thesis throw new insights to low dose radiation biology. Employing new high-through techniques and unravelling many new facets of low dose radiation biology in terms of DNA damage, repair, gene expression and chromatin dynamics is novelty of the present work. The data on NLNRA and HLNRA population is unique and one of its kind which is not available elsewhere in the world. The active involvement of DNA damage response and repair processes in higher level background radiation groups is noteworthy.

Chapter 5

Summary and Conclusions

Understanding the biological and health effects low dose IR, especially below 100 mSv has important implications to human health and radiation protection science. High level natural radiation areas provide unique opportunity to study the effect of low dose/dose rate radiation directly on humans. The present thesis emphasized the importance of biological effects of acute and chronic IR and its implication in monitoring of human population. The quantitative and qualitative biological response of IR has been explored using high throughput techniques to detect changes at low dose exposures.

The cellular and molecular response to chronic low level radiation exposure was investigated in human population residing in normal and high level natural radiation areas of Kerala coast. The areas receiving an annual background dose of > 1.5 mGy/y were considered as HLNRA, whereas areas with a background dose of ≤ 1.5 mGy/y were considered as control areas. The quantitative study of DNA DSB induction and repair was done using gamma-H2AX as a marker. The basal levels of DNA DSBs were evaluated in individuals from NLNRA and HLNRA (LDG, 1.51 - 5.0 mGy/y and HDG, > 5.0 mGy/y). It was interesting that no significant increase in the basal levels of DSBs was observed in HLNRA individuals, in spite of the fact that they are exposed to at least 6-8 times higher background radiation doses as compared to NLNRA. In-vitro radio-adaptive response study in terms of induction of DSBs after giving challenging doses to the PBMCs of individuals belonging to NLNRA and HLNRA (LDG and HDG) showed decreasing trend of induction of DSBs in HLNRA individuals at all the doses, However, at low challenging dose of 0.25 Gy significantly reduced induction of DSBs was observed in HLNRA individuals.

The other important observation was the biphasic pattern of DNA repair kinetics observed at low and high doses, where a rapid induction was seen upto 2.0 h time point, followed

by bi-exponential repair. It is interesting because of the fact that processing of DSB takes some time before the end joining repair process starts. Importantly, a fast and efficient repair of DNA DSBs was observed in HLNRA individuals, which is suggestive of *in-vivo* adaptation occurring in HLNRA individuals due to chronic exposure to low dose IR. Assuming that HLNRA individuals have already received priming or adaptive dose due to chronic exposure, a radio-adaptive study at transcriptional level was carried out after giving a challenging dose of 2.0 Gy. Interestingly, transcription profile of non-homologous end joining genes (*KU80, DCLRE1C (artemis) and XRCC4)* showed significant upregulation in HLNRA individuals suggesting an active role of NHEJ repair pathway in *in vivo* adaptive response.

Further investigation on the effects of chronic low level radiation at molecular and cellular level was worth-pursuing to find out the changes, if any, due to low level radiation exposure to humans. Transcriptome analysis carried out in individuals belonging to different background dose groups revealed new insights on molecular or cellular responses to low dose IR. The transcriptome analysis gave an overall picture of cellular and molecular networks of the genes involved in HLNRA. The differential expression (up and down-regulation) of a larger number of genes with increasing background dose groups was an interesting finding, which may be important to understand the low dose IR response. Interestingly, the involvement of majority of differentially expressed genes in DDR, DNA repair, histone/chromatin modification, cell cycle, apoptosis and stress response in high dose groups of HLNRA (> 5.0 mGy/y) is one of the important highlights of our findings. It clearly indicates that there is some trigger due to chronic low dose IR in HLNRA.

Similarly, activation of some of the important pathways such as p53 pathway, MAPK pathways etc. in higher background dose group (>5.0mGy/y) indicated active DDR

signaling/processes in HLNRA. The DDR signaling might be involved in either lower induction or faster repair of damage in HLNRA population and thus leading to radio-adaptation. This could be the reason why reduced frequency of basal level of DSBs observed in HDG of HLNRA individuals that might have influenced faster and efficient repair of DSBs observed in HLNRA individuals.

Another, significant finding in transcriptome analysis was the presence of dose responsive genes with respect to background radiation doses which included *DDIT3, GADD45B, PMAIP1, DUSP1, JUN, DUSP10* etc. Validation of these genes by real time q-PCR in two separate groups of individuals confirmed these as low dose radiation signatures. Further, the usefulness of chronic low dose signature genes was tested in high acute dose exposures. Interestingly few of the genes *(PLK3, HISTH2B, DDIT3, PMAIP1, JUN,* and *DUSP10)* showed transcriptional changes both at acute and chronic exposures. However, few genes such as BTG1 and PAPD4 which showed significant up-regulation at chronic dose exposures did not show any changes in mRNA levels at high acute dose exposures. This important finding suggests that gene expression profile at acute and chronic exposures can be different.

DNA damage response may lead to changes in chromatin conformation. Radiation induced conformational changes in chromatin structure was studied in random and healthy individuals to find out changes at low and high acute dose exposures. Our findings clearly showed chromatin conformational changes can be detected at doses as low as 0.25 Gy. Our study also confirmed that Dynamic light scattering (DLS) as a novel tool to detect chromatin changes in human cells. In summary, the present study revealed novel aspects of low dose radiation induced DNA damage response at the level of transcription, repair and chromatin conformation.

Conclusions :

The present thesis entitled**, "Studies on cellular responses to DNA damage in human cells exposed to low dose ionizing radiation"** leads to the following important conclusions.

- ❖ No increase in the basal level frequency of DNA DSBs was observed in HLNRA individuals as compared to NLNRA individuals.
- ❖ No background dose related increase in DSB frequency was observed in HLNRA individuals. However, there was a marginal reduction in basal level frequency of DNA DSBs in individuals belonging to high dose groups of HLNRA (> 5.0 mGy/y) as compared to NLNRA. It perhaps indicates efficient removal of damaged cells or efficient repair of DSBs in HLNRA individuals.
- ❖ A significant ($p \leq 0.05$) association between age and DSB frequency was observed in NLNRA individuals. However, in HLNRA individuals no association between age and DSB frequency was observed.
- ❖ A significant ($p \leq 0.05$) reduction in induced DSBs was observed at 0.25 Gy in high dose group individuals of HLNRA (> 5.0 mGy/y). However, a marginal but insignificant decrease was observed at 1.0 and 2.0 Gy of challenging doses. A reducing trend in induced DSBs was observed from NLNRA to LDG and HDG individuals at all the doses.
- ❖ In repair kinetics study, a biphasic pattern of induction and repair of DNA DSBs was observed with a peak of maximum induction at 2.0 h post-irradiation followed by exponential repair of DSBs.
- ❖ Bi-exponential repair kinetics of DNA DSBs was observed in the PBMCs of HLNRA and NLNRA individuals. A fast phase of repair showed the maximum repair of almost 50% or

more within 6.0h followed by a slow phase of recovery up to 24 h. Almost 15-20 % of residual damage was observed after 24 h in HLNRA and NLNRA individuals.

- A significantly ($p \leq 0.05$) fast and efficient repair of DSBs was observed at 4.0 h and 6.0 h in HLNRA individuals as compared to NLNRA individuals at 0.25 and 2.0 Gy challenging doses. Above finding is important and suggests the activation of *in vivo* radio-adaptive response in HLNRA individuals exposed to chronic levels of low dose radiation.
- Radio-adaptive response : A significant up-regulation of *KU80, DCLRE1C* and *XRCC4* genes involved in NHEJ DSB repair pathway was observed in HLNRA individuals after giving challenging dose of 2.0 Gy. It is an important finding which indicates the active involvement of NHEJ repair pathway in *in vivo* adaptation in HLNRA population.
- Transcriptome analysis revealed a dose related increase in the number of differentially expressed genes in different background dose groups of HLNRA individuals as compared to NLNRA individuals. It indicates the induction of cellular processes in HLNRA individuals.
- An over-representation of DNA damage response and repair, cell cycle regulation, apoptosis, immune response, transcription regulation, RNA processing and chromatin/histone modification genes was observed in high dose group individuals of HLNRA (>5.0 mGy/y). It suggests the active of DNA damage response in HLNRA individuals.
- Important pathways such as MAPK signaling, p53 signaling, T cell activation, JAK-STAT signaling, protein ubiquitination etc were activated in HLNRA individuals as compared to NLNRA.
- We identified few dose responsive genes which showed background dose dependent changes in their mRNA expression levels. Some of important genes were *DDIT3, GADD45B, JUN,*

PMAIP1, DUSP1, PAPD4, DUSP10, BTG1. These genes may be used as signatures of chronic low dose exposure in PBMCs of human population.

- ❖ mRNA expression level of selected transcriptome analysis genes was studied at different acute doses (0.3 - 2.0 Gy). *PMAIP1, DDIT3, JUN, HISTH2B, PLK3* and *DUSP10* genes showed increased induction at acute as well as chronic exposure where as *BTG1* and *PAPD4* did not show any induction at acute doses. Above findings shows that gene expression changes are different at acute and chronic doses.
- ❖ Radiation induced chromatin conformational changes (physical changes) in terms of hydrodynamic diameter showed different response at low dose (0.25 Gy) as compared to high dose.
- ❖ Dynamic light scattering (DLS) is an useful tool in studying the radiation induced changes in chromatin structure at low dose exposures and can be explored further in high level natural radiation areas of Kerala coast.

References

1. UNSCEAR. (2000) Sources and Effects of Ionizing Radiation, *United Nations Scientific Committee on the Effects of Atomic Radiation (UNSCEAR) 2000. New York: United Nations.*
2. BEIR VII. (2006) Committee to Assess Health Risks from Exposure to Low Levels of Ionizing Radiation. Health Risks From Exposure to Low Levels of Ionizing Radiation: BEIR VII Phase 2. National Academy of Sciences,National Research Council. The National Academies Press, Washington, U.S.A
3. UNSCEAR. (2012) United Nations Scientific Committee on the Effects of Atomic Radiation ; BIOLOGICAL MECHANISMS OF RADIATION ACTIONS AT LOW DOSES; A white paper to guide the Scientific Committee's future programme of work, United Nations, NewYork.
4. Boice, J. D., Jr., Hendry, J. H., Nakamura, N., Niwa, O., Nakamura, S., and Yoshida, K. (2010) Low-dose-rate epidemiology of high background radiation areas, *Radiat Res 173*, 849-854.
5. Cardis, E., Vrijheid, M., Blettner, M., Gilbert, E., Hakama, M., Hill, C., Howe, G., Kaldor, J., Muirhead, C. R., Schubauer-Berigan, M., Yoshimura, T., Bermann, F., Cowper, G., Fix, J., Hacker, C., Heinmiller, B., Marshall, M., Thierry-Chef, I., Utterback, D., Ahn, Y. O., Amoros, E., Ashmore, P., Auvinen, A., Bae, J. M., Solano, J. B., Biau, A., Combalot, E., Deboodt, P., Diez Sacristan, A., Eklof, M., Engels, H., Engholm, G., Gulis, G., Habib, R., Holan, K., Hyvonen, H., Kerekes, A., Kurtinaitis, J., Malker, H., Martuzzi, M., Mastauskas, A., Monnet, A., Moser, M., Pearce, M. S., Richardson, D. B., Rodriguez-Artalejo, F., Rogel, A., Tardy, H., Telle-Lamberton, M., Turai, I., Usel, M., and Veress, K. (2005) Risk of cancer after low doses of ionising radiation: retrospective cohort study in 15 countries, *BMJ 331*, 77.
6. Das, B. (2010) Genetic studies on human population residing in High Level Natural Radiation Areas of Kerala coast., In *BARC News Letter*, pp 28-37.
7. Jaikrishan, G., Andrews, V. J., Thampi, M. V., Koya, P. K., Rajan, V. K., and Chauhan, P. S. (1999) Genetic monitoring of the human population from high-level natural radiation areas of Kerala on the southwest coast of India. I. Prevalence of congenital malformations in newborns, *Radiat Res 152*, S149-153.

8. Jaikrishan, G., Sudheer, K. R., Andrews, V. J., Koya, P. K., Madhusoodhanan, M., Jagadeesan, C. K., and Seshadri, M. (2013) Study of stillbirth and major congenital anomaly among newborns in the high-level natural radiation areas of Kerala, India, *J Community Genet 4*, 21-31.
9. Koya, P. K., Chougaonkar, M. P., Predeep, P., Jojo, P. J., Cheriyan, V. D., Mayya, Y. S., and Seshadri, M. (2012) Effect of low and chronic radiation exposure: a case-control study of mental retardation and cleft lip/palate in the monazite-bearing coastal areas of southern Kerala, *Radiat Res 177*, 109-116.
10. Nair, R. R., Rajan, B., Akiba, S., Jayalekshmi, P., Nair, M. K., Gangadharan, P., Koga, T., Morishima, H., Nakamura, S., and Sugahara, T. (2009) Background radiation and cancer incidence in Kerala, India-Karanagappally cohort study, *Health Phys 96*, 55-66.
11. Tao, Z., Zha, Y., Akiba, S., Sun, Q., Zou, J., Li, J., Liu, Y., Kato, H., Sugahara, T., and Wei, L. (2000) Cancer mortality in the high background radiation areas of Yangjiang, China during the period between 1979 and 1995, *J Radiat Res 41 Suppl*, 31-41.
12. Koya, P. K., Jaikrishan, G., Sudheer, K. R., Andrews, V. J., Madhusoodhanan, M., Jagadeesan, C. K., and Das, B. (2015) Sex ratio at birth: scenario from normal- and high-level natural radiation areas of Kerala coast in south-west India, *Radiat Environ Biophys 54*, 453-463.
13. Morgan, W. F., and Bair, W. J. (2013) Issues in low dose radiation biology: the controversy continues. A perspective, *Radiat Res 179*, 501-510.
14. Canadian Nuclear Safety Commission. (2013) Fact sheet : Linear-Non-Threshold Model, Canadian Nuclear Safety Commission, Canada, www.nuclearsafety.gc.ca
15. Grudzenski, S., Raths, A., Conrad, S., Rube, C. E., and Lobrich, M. (2010) Inducible response required for repair of low-dose radiation damage in human fibroblasts, *Proc Natl Acad Sci U S A 107*, 14205-14210.
16. Kesavan, P. C. (2014) Linear, no threshold response at low doses of ionizing radiation: ideology, prejudice and science., *Current Science 107*, 46-53.
17. Rothkamm, K., and Lobrich, M. (2003) Evidence for a lack of DNA double-strand break repair in human cells exposed to very low x-ray doses, *Proc Natl Acad Sci U S A 100*, 5057-5062.

18. Tang, F. R., and Loke, W. K. (2015) Molecular mechanisms of low dose ionizing radiation-induced hormesis, adaptive responses, radioresistance, bystander effects, and genomic instability, *Int J Radiat Biol 91*, 13-27.
19. Feinendegen, L. E. (2005) Evidence for beneficial low level radiation effects and radiation hormesis, *Br J Radiol 78*, 3-7.
20. Vaiserman, A. M. (2010) Radiation hormesis: historical perspective and implications for low-dose cancer risk assessment, *Dose Response 8*, 172-191.
21. Tubiana, M., Feinendegen, L. E., Yang, C., and Kaminski, J. M. (2009) The linear no-threshold relationship is inconsistent with radiation biologic and experimental data, *Radiology 251*, 13-22.
22. Amsel, J., Waterbor, J. W., Oler, J., Rosenwaike, I., and Marshall, K. (1982) Relationship of site-specific cancer mortality rates to altitude, *Carcinogenesis 3*, 461-465.
23. Olivieri, G. (1999) Adaptive response and its relationship to hormesis and low dose cancer risk estimation, *Hum Exp Toxicol 18*, 440-442.
24. Olivieri, G., Bodycote, J., and Wolff, S. (1984) Adaptive response of human lymphocytes to low concentrations of radioactive thymidine, *Science 223*, 594-597.
25. Nambi, K. S., and Soman, S. D. (1987) Environmental radiation and cancer in India, *Health Phys 52*, 653-657.
26. de Toledo, S. M., Asaad, N., Venkatachalam, P., Li, L., Howell, R. W., Spitz, D. R., and Azzam, E. I. (2006) Adaptive responses to low-dose/low-dose-rate gamma rays in normal human fibroblasts: the role of growth architecture and oxidative metabolism, *Radiat Res 166*, 849-857.
27. Azzam, E. I., de Toledo, S. M., Raaphorst, G. P., and Mitchel, R. E. (1996) Low-dose ionizing radiation decreases the frequency of neoplastic transformation to a level below the spontaneous rate in C3H 10T1/2 cells, *Radiat Res 146*, 369-373.
28. Azzam, E. I., de Toledo, S. M., Gooding, T., and Little, J. B. (1998) Intercellular communication is involved in the bystander regulation of gene expression in human cells exposed to very low fluences of alpha particles, *Radiat Res 150*, 497-504.
29. Chen, W. L., Luan, Y. C., Shieh, M. C., Chen, S. T., Kung, H. T., Soong, K. L., Yeh, Y. C., Chou, T. S., Mong, S. H., Wu, J. T., Sun, C. P., Deng, W. P., Wu, M. F., and Shen,

M. L. (2007) Effects of cobalt-60 exposure on health of Taiwan residents suggest new approach needed in radiation protection, *Dose Response 5*, 63-75.

30. Kumar, P. R., Seshadri, M., Jaikrishan, G., and Das, B. (2015) Effect of chronic low dose natural radiation in human peripheral blood mononuclear cells: Evaluation of DNA damage and repair using the alkaline comet assay, *Mutat Res 775*, 59-65.
31. George, K. P., Sundaram, K., Mistry, K. B., and Gopal-Ayengar, A. R. (1976) Investigations on human populations residing in high background radiation areas of Kerala and adjoining regions. Reprint from ‘‘Biological and environmental effects of low level radiation.”IAEA, Vienna, SM- 202/703, *2*, 325-329.
32. Cheriyan, V. D., Kurien, C. J., Das, B., Ramachandran, E. N., Karuppasamy, C. V., Thampi, M. V., George, K. P., Kesavan, P. C., Koya, P. K., and Chauhan, P. S. (1999) Genetic monitoring of the human population from high-level natural radiation areas of Kerala on the southwest coast of India. II. Incidence of numerical and structural chromosomal aberrations in the lymphocytes of newborns, *Radiat Res 152*, S154-158.
33. Bharatwal, D. S., and Vaze, G. H. (1958) Radiation dose measurements in the monazite areas of kerala state in India., *Proceedings of the 2nd UN International Conference on Peaceful uses of Atomic Energy. United Nations, NewYork. 23*, 156.
34. Sunta, C. M. (1993) A review of the studies of high background areas of the S-W coast of India., *Proceedings of the international conference on high levels of natural radiation. Atomic Energy Organization of Iran, Tehran*, 71.
35. Mistry, K. B., Bharathan, K. G., and Gopal-Ayengar, A. R. (1970) Radioactivity in the diet of population of the Kerala coast including monazite bearing high radiation areas, *Health Phys 19*, 535-542.
36. Gopal-Ayengar, A. R., Sundaram, K., Mistry, K. B., Suntha, C. M., Nambi, K. S. V., Kaithuria, S. P., Basu, A. S., and David, M. (1971) Evaluation of the long term effects of high background radiation on selected population groups of Kerala coast. In Proceedings of the IV International Conference on Peaceful uses of Atomic Energy, United Nations,New York., *2*, 31-61.

37. Gopal-Ayengar, A. R., Nayar, G. G., George, K. P., and Mistry, K. B. (1970) Biological effects of high background radioactivity: studies on plants growing on the monazite bearing areas of Kerala coast and adjoining regions., *Indian J. Exp. Biol. 8*, 313-318.
38. Nayar, G. G., George, K. P., and Gopal-Ayengar, A. R. (1970) On the biological effects of high background radioactivity: studies on Tradescancia grown in radioactive monazite sand., *Radiat. Bot. 10*, 287-292.
39. Gruneberg, H. (1964) Genetical research in an area of high natural radioactivity in South India., *Nature 204*, 222-224.
40. Gruneberg, H., Bains, G. S., Berry, R. J., Riles, L., Smith, C. A. B., and Weiss, R. A. (1966) A search for genetic effects of high natural radioactivity in South India., *Report SRS 307, Medical Research Council, Her Majesty's Stationary Office, London*.
41. Kochupillai, N., Verma, I. C., Grewal, M. S., and Ramalingaswamy, V. (1976) Down Syndrome and related abnormalities in an area of high background radiation in coastal Kerala . *Nature 262*, 60-61.
42. Sundaram, K. (1977) Down ' s syndrome in Kerala [letter], *Nature 267*, 728.
43. Forster, L., Forster, P., Lutz-Bonengel, S., Willkomm, H., and Brinkmann, B. (2002) Natural radioactivity and human mitochondrial DNA mutations, *Proc Natl Acad Sci U S A 99*, 13950-13954.
44. Premi, S., Srivastava, J., Chandy, S. P., and Ali, S. (2009) Unique signatures of natural background radiation on human Y chromosomes from Kerala, India, *PLoS One 4*, e4541.
45. Ramachandran, E. N., Karuppasamy, C. V., Cheriyan, V. D., Soren, D. C., Das, B., Anilkumar, V., Koya, P. K., and Seshadri, M. (2013) Cytogenetic studies on newborns from high and normal level natural radiation areas of Kerala in southwest coast of India, *Int J Radiat Biol 89*, 259-267.
46. Das, B., and Karuppasamy, C. V. (2009) Spontaneous frequency of micronuclei among the newborns from high level natural radiation areas of Kerala in the southwest coast of India, *Int J Radiat Biol 85*, 272-280.
47. Das, B., Saini, D., and Seshadri, M. (2009) Telomere length in human adults and high level natural background radiation, *PLoS One 4*, e8440.

48. Das, B., Saini, D., and Seshadri, M. (2012) No evidence of telomere length attrition in newborns from high level natural background radiation areas in Kerala coast, south west India, *Int J Radiat Biol 88*, 642-647.
49. Ahmad, S., Koya, P. K., and Seshadri, M. (2013) Effects of chronic low level radiation in the population residing in the high level natural radiation area in Kerala, India: employing heritable DNA mutation studies, *Mutat Res 751*, 91-95.
50. Das, B., Ghosh, A., Ahmad, S., Saini, D., Chauhan, P. S., and Seshadri, M. (2010) Germline mutation rates in families residing in high level natural radiation areas of Kerala coast in south west India., *Proceedings of 7th international conference on high level natural radiation and radon areas.* , 214-215.
51. Kumar, P. R., Cheriyan, V. D., and Seshadri, M. (2012) Evaluation of spontaneous DNA damage in lymphocytes of healthy adult individuals from high-level natural radiation areas of Kerala in India, *Radiat Res 177*, 643-650.
52. Brenner, D. J. (2009) Extrapolating radiation-induced cancer risks from low doses to very low doses, *Health Phys 97*, 505-509.
53. Eccles, L. J., O'Neill, P., and Lomax, M. E. (2011) Delayed repair of radiation induced clustered DNA damage: friend or foe?, *Mutat Res 711*, 134-141.
54. Goodhead, D. T. (1994) Initial events in the cellular effects of ionizing radiations: clustered damage in DNA, *Int J Radiat Biol 65*, 7-17.
55. Sutherland, B. M., Bennett, P. V., Sidorkina, O., and Laval, J. (2000) Clustered DNA damages induced in isolated DNA and in human cells by low doses of ionizing radiation, *Proc Natl Acad Sci U S A 97*, 103-108.
56. Cucinotta, F. A., Pluth, J. M., Anderson, J. A., Harper, J. V., and O'Neill, P. (2008) Biochemical kinetics model of DSB repair and induction of gamma-H2AX foci by non-homologous end joining, *Radiat Res 169*, 214-222.
57. Gulston, M., de Lara, C., Jenner, T., Davis, E., and O'Neill, P. (2004) Processing of clustered DNA damage generates additional double-strand breaks in mammalian cells post-irradiation, *Nucleic Acids Res 32*, 1602-1609.
58. Gulston, M., Fulford, J., Jenner, T., de Lara, C., and O'Neill, P. (2002) Clustered DNA damage induced by gamma radiation in human fibroblasts (HF19), hamster (V79-4) cells

and plasmid DNA is revealed as Fpg and Nth sensitive sites, *Nucleic Acids Res 30*, 3464-3472.

59. Iliakis, G., Wang, H., Perrault, A. R., Boecker, W., Rosidi, B., Windhofer, F., Wu, W., Guan, J., Terzoudi, G., and Pantelias, G. (2004) Mechanisms of DNA double strand break repair and chromosome aberration formation, *Cytogenet Genome Res 104*, 14-20.
60. Lomax, M. E., Gulston, M. K., and O'Neill, P. (2002) Chemical aspects of clustered DNA damage induction by ionising radiation, *Radiat Prot Dosimetry 99*, 63-68.
61. Sutherland, B. M., Bennett, P. V., Cintron-Torres, N., Hada, M., Trunk, J., Monteleone, D., Sutherland, J. C., Laval, J., Stanislaus, M., and Gewirtz, A. (2002) Clustered DNA damages induced in human hematopoietic cells by low doses of ionizing radiation, *J Radiat Res 43 Suppl*, S149-152.
62. Sutherland, B. M., Bennett, P. V., Sidorkina, O., and Laval, J. (2000) Clustered damages and total lesions induced in DNA by ionizing radiation: oxidized bases and strand breaks, *Biochemistry 39*, 8026-8031.
63. Sutherland, B. M., Bennett, P. V., Sutherland, J. C., and Laval, J. (2002) Clustered DNA damages induced by x rays in human cells, *Radiat Res 157*, 611-616.
64. Georgakilas, A. G. (2008) Processing of DNA damage clusters in human cells: current status of knowledge, *Mol Biosyst 4*, 30-35.
65. Peddi, P., Francisco, D. C., Cecil, A. M., Hair, J. M., Panayiotidis, M. I., and Georgakilas, A. G. (2008) Processing of clustered DNA damage in human breast cancer cells MCF-7 with partial DNA-PKcs deficiency, *Cancer Lett 269*, 174-183.
66. Lomax, M. E., Folkes, L. K., and O'Neill, P. (2013) Biological consequences of radiation-induced DNA damage: relevance to radiotherapy, *Clin Oncol (R Coll Radiol) 25*, 578-585.
67. Ding, L. H., Shingyoji, M., Chen, F., Hwang, J. J., Burma, S., Lee, C., Cheng, J. F., and Chen, D. J. (2005) Gene expression profiles of normal human fibroblasts after exposure to ionizing radiation: a comparative study of low and high doses, *Radiat Res 164*, 17-26.
68. Amundson, S. A., Bittner, M., Meltzer, P., Trent, J., and Fornace, A. J., Jr. (2001) Induction of gene expression as a monitor of exposure to ionizing radiation, *Radiat Res 156*, 657-661.

69. Amundson, S. A., Grace, M. B., McLeland, C. B., Epperly, M. W., Yeager, A., Zhan, Q., Greenberger, J. S., and Fornace, A. J., Jr. (2004) Human in vivo radiation-induced biomarkers: gene expression changes in radiotherapy patients, *Cancer Res 64*, 6368-6371.
70. Berglund, S. R., Rocke, D. M., Dai, J., Schwietert, C. W., Santana, A., Stern, R. L., Lehmann, J., Hartmann Siantar, C. L., and Goldberg, Z. (2008) Transient genome-wide transcriptional response to low-dose ionizing radiation in vivo in humans, *Int J Radiat Oncol Biol Phys 70*, 229-234.
71. Wang, J. Y. (2001) DNA damage and apoptosis, *Cell Death Differ 8*, 1047-1048.
72. Xie, S., Wu, H., Wang, Q., Cogswell, J. P., Husain, I., Conn, C., Stambrook, P., Jhanwar-Uniyal, M., and Dai, W. (2001) Plk3 functionally links DNA damage to cell cycle arrest and apoptosis at least in part via the p53 pathway, *J Biol Chem 276*, 43305-43312.
73. Jeggo, P., and Lobrich, M. (2006) Radiation-induced DNA damage responses, *Radiat Prot Dosimetry 122*, 124-127.
74. Misri, S., Pandita, S., and Pandita, T. K. (2009) Detecting ATM-dependent chromatin modification in DNA damage and heat shock response, *Methods Mol Biol 523*, 395-410.
75. Pandita, T. K., and Richardson, C. (2009) Chromatin remodeling finds its place in the DNA double-strand break response, *Nucleic Acids Res 37*, 1363-1377.
76. Kumar, R., Horikoshi, N., Singh, M., Gupta, A., Misra, H. S., Albuquerque, K., Hunt, C. R., and Pandita, T. K. (2012) Chromatin modifications and the DNA damage response to ionizing radiation, *Front Oncol 2*, 214.
77. van Attikum, H., Fritsch, O., Hohn, B., and Gasser, S. M. (2004) Recruitment of the INO80 complex by H2A phosphorylation links ATP-dependent chromatin remodeling with DNA double-strand break repair, *Cell 119*, 777-788.
78. Downs, J. A., Nussenzweig, M. C., and Nussenzweig, A. (2007) Chromatin dynamics and the preservation of genetic information, *Nature 447*, 951-958.
79. Cortez, D., Wang, Y., Qin, J., and Elledge, S. J. (1999) Requirement of ATM-dependent phosphorylation of brca1 in the DNA damage response to double-strand breaks, *Science 286*, 1162-1166.

80. Stewart, G. S., Wang, B., Bignell, C. R., Taylor, A. M., and Elledge, S. J. (2003) MDC1 is a mediator of the mammalian DNA damage checkpoint, *Nature 421*, 961-966.
81. Cui, X., Yu, Y., Gupta, S., Cho, Y. M., Lees-Miller, S. P., and Meek, K. (2005) Autophosphorylation of DNA-dependent protein kinase regulates DNA end processing and may also alter double-strand break repair pathway choice, *Mol Cell Biol 25*, 10842-10852.
82. Iyama, T., and Wilson, D. M., 3rd. (2013) DNA repair mechanisms in dividing and non-dividing cells, *DNA Repair (Amst) 12*, 620-636.
83. Mladenov, E., and Iliakis, G. (2011) Induction and repair of DNA double strand breaks: the increasing spectrum of non-homologous end joining pathways, *Mutat Res 711*, 61-72.
84. Riballo, E., Kuhne, M., Rief, N., Doherty, A., Smith, G. C., Recio, M. J., Reis, C., Dahm, K., Fricke, A., Krempler, A., Parker, A. R., Jackson, S. P., Gennery, A., Jeggo, P. A., and Lobrich, M. (2004) A pathway of double-strand break rejoining dependent upon ATM, Artemis, and proteins locating to gamma-H2AX foci, *Mol Cell 16*, 715-724.
85. Richardson, C., and Jasin, M. (2000) Coupled homologous and nonhomologous repair of a double-strand break preserves genomic integrity in mammalian cells, *Mol Cell Biol 20*, 9068-9075.
86. Rich, T., Allen, R. L., and Wyllie, A. H. (2000) Defying death after DNA damage, *Nature 407*, 777-783.
87. Frosina, G., Fortini, P., Rossi, O., Carrozzino, F., Raspaglio, G., Cox, L. S., Lane, D. P., Abbondandolo, A., and Dogliotti, E. (1996) Two pathways for base excision repair in mammalian cells, *J Biol Chem 271*, 9573-9578.
88. Matsumoto, Y., Kim, K., and Bogenhagen, D. F. (1994) Proliferating cell nuclear antigen-dependent abasic site repair in Xenopus laevis oocytes: an alternative pathway of base excision DNA repair, *Mol Cell Biol 14*, 6187-6197.
89. Christmann, M., Tomicic, M. T., Roos, W. P., and Kaina, B. (2003) Mechanisms of human DNA repair: an update, *Toxicology 193*, 3-34.
90. Christmann, M., and Kaina, B. (2013) Transcriptional regulation of human DNA repair genes following genotoxic stress: trigger mechanisms, inducible responses and genotoxic adaptation, *Nucleic Acids Res 41*, 8403-8420.

91. Hess, M. T., Schwitter, U., Petretta, M., Giese, B., and Naegeli, H. (1997) Bipartite substrate discrimination by human nucleotide excision repair, *Proc Natl Acad Sci U S A 94*, 6664-6669.
92. Batty, D. P., and Wood, R. D. (2000) Damage recognition in nucleotide excision repair of DNA, *Gene 241*, 193-204.
93. Volker, M., Mone, M. J., Karmakar, P., van Hoffen, A., Schul, W., Vermeulen, W., Hoeijmakers, J. H., van Driel, R., van Zeeland, A. A., and Mullenders, L. H. (2001) Sequential assembly of the nucleotide excision repair factors in vivo, *Mol Cell 8*, 213-224.
94. Sugasawa, K., Shimizu, Y., Iwai, S., and Hanaoka, F. (2002) A molecular mechanism for DNA damage recognition by the xeroderma pigmentosum group C protein complex, *DNA Repair (Amst) 1*, 95-107.
95. Wood, R. D., Araujo, S. J., Ariza, R. R., Batty, D. P., Biggerstaff, M., Evans, E., Gaillard, P. H., Gunz, D., Koberle, B., Kuraoka, I., Moggs, J. G., Sandall, J. K., and Shivji, M. K. (2000) DNA damage recognition and nucleotide excision repair in mammalian cells, *Cold Spring Harb Symp Quant Biol 65*, 173-182.
96. Yan, T., Schupp, J. E., Hwang, H. S., Wagner, M. W., Berry, S. E., Strickfaden, S., Veigl, M. L., Sedwick, W. D., Boothman, D. A., and Kinsella, T. J. (2001) Loss of DNA mismatch repair imparts defective cdc2 signaling and G(2) arrest responses without altering survival after ionizing radiation, *Cancer Res 61*, 8290-8297.
97. Martin, L. M., Marples, B., Coffey, M., Lawler, M., Lynch, T. H., Hollywood, D., and Marignol, L. (2010) DNA mismatch repair and the DNA damage response to ionizing radiation: making sense of apparently conflicting data, *Cancer Treat Rev 36*, 518-527.
98. Young, L. C., Hays, J. B., Tron, V. A., and Andrew, S. E. (2003) DNA mismatch repair proteins: potential guardians against genomic instability and tumorigenesis induced by ultraviolet photoproducts, *J Invest Dermatol 121*, 435-440.
99. Modrich, P. (2006) Mechanisms in eukaryotic mismatch repair, *J Biol Chem 281*, 30305-30309.
100. Genschel, J., and Modrich, P. (2006) Analysis of the excision step in human DNA mismatch repair, *Methods Enzymol 408*, 273-284.

101. Genschel, J., Bazemore, L. R., and Modrich, P. (2002) Human exonuclease I is required for 5' and 3' mismatch repair, *J Biol Chem 277*, 13302-13311.
102. Genschel, J., Littman, S. J., Drummond, J. T., and Modrich, P. (1998) Isolation of MutSbeta from human cells and comparison of the mismatch repair specificities of MutSbeta and MutSalpha, *J Biol Chem 273*, 19895-19901.
103. Sung, P. (1994) Catalysis of ATP-dependent homologous DNA pairing and strand exchange by yeast RAD51 protein, *Science 265*, 1241-1243.
104. Sonoda, E., Takata, M., Yamashita, Y. M., Morrison, C., and Takeda, S. (2001) Homologous DNA recombination in vertebrate cells, *Proc Natl Acad Sci U S A 98*, 8388-8394.
105. Takata, M., Sasaki, M. S., Sonoda, E., Morrison, C., Hashimoto, M., Utsumi, H., Yamaguchi-Iwai, Y., Shinohara, A., and Takeda, S. (1998) Homologous recombination and non-homologous end-joining pathways of DNA double-strand break repair have overlapping roles in the maintenance of chromosomal integrity in vertebrate cells, *EMBO J 17*, 5497-5508.
106. Jeggo, P. A., Geuting, V., and Lobrich, M. (2011) The role of homologous recombination in radiation-induced double-strand break repair, *Radiother Oncol 101*, 7-12.
107. Lieber, M. R., and Wilson, T. E. (2010) SnapShot: Nonhomologous DNA end joining (NHEJ), *Cell 142*, 496-496 e491.
108. Lieber, M. R., Gu, J., Lu, H., Shimazaki, N., and Tsai, A. G. (2010) Nonhomologous DNA end joining (NHEJ) and chromosomal translocations in humans, *Subcell Biochem 50*, 279-296.
109. Rothkamm, K., Kruger, I., Thompson, L. H., and Lobrich, M. (2003) Pathways of DNA double-strand break repair during the mammalian cell cycle, *Mol Cell Biol 23*, 5706-5715.
110. Shelke, S., and Das, B. (2015) Dose response and adaptive response of non-homologous end joining repair genes and proteins in resting human peripheral blood mononuclear cells exposed to gamma radiation, *Mutagenesis 30*, 365-379.

111. Amundson, S. A., Lee, R. A., Koch-Paiz, C. A., Bittner, M. L., Meltzer, P., Trent, J. M., and Fornace, A. J., Jr. (2003) Differential responses of stress genes to low dose-rate gamma irradiation, *Mol Cancer Res 1*, 445-452.
112. Kruhlak, M. J., Celeste, A., Dellaire, G., Fernandez-Capetillo, O., Muller, W. G., McNally, J. G., Bazett-Jones, D. P., and Nussenzweig, A. (2006) Changes in chromatin structure and mobility in living cells at sites of DNA double-strand breaks, *J Cell Biol 172*, 823-834.
113. Rogakou, E. P., Boon, C., Redon, C., and Bonner, W. M. (1999) Megabase chromatin domains involved in DNA double-strand breaks in vivo, *J Cell Biol 146*, 905-916.
114. Lydall, D., and Whitehall, S. (2005) Chromatin and the DNA damage response, *DNA Repair (Amst) 4*, 1195-1207.
115. Li, B., Carey, M., and Workman, J. L. (2007) The role of chromatin during transcription, *Cell 128*, 707-719.
116. Falk, M., Lukasova, E., Gabrielova, B., Ondrej, V., and Kozubek, S. (2007) Chromatin dynamics during DSB repair, *Biochim Biophys Acta 1773*, 1534-1545.
117. Falk, M., Lukasova, E., and Kozubek, S. (2008) Chromatin structure influences the sensitivity of DNA to gamma-radiation, *Biochim Biophys Acta 1783*, 2398-2414.
118. Falk, M., Lukasova, E., and Kozubek, S. (2010) Higher-order chromatin structure in DSB induction, repair and misrepair, *Mutat Res 704*, 88-100.
119. Hittelman, W. N., and Pollard, M. (1984) Visualization of chromatin events associated with repair of ultraviolet light-induced damage by premature chromosome condensation, *Carcinogenesis 5*, 1277-1285.
120. Belyaev, I. Y., Czene, S., and Harms-Ringdahl, M. (2001) Changes in chromatin conformation during radiation-induced apoptosis in human lymphocytes, *Radiat Res 156*, 355-364.
121. Dinant, C., Houtsmuller, A. B., and Vermeulen, W. (2008) Chromatin structure and DNA damage repair, *Epigenetics Chromatin 1*, 9.
122. Jezkova, L., Falk, M., Falkova, I., Davidkova, M., Bacikova, A., Stefancikova, L., Vachelova, J., Michaelidesova, A., Lukasova, E., Boreyko, A., Krasavin, E., and Kozubek, S. (2014) Function of chromatin structure and dynamics in DNA damage,

repair and misrepair: gamma-rays and protons in action, *Appl Radiat Isot 83 Pt B*, 128-136.

123. Corpet, A., and Almouzni, G. (2009) A histone code for the DNA damage response in mammalian cells?, *EMBO J 28*, 1828-1830.
124. Ljungman, M. (1989) Pretreatment with UV light renders the chromatin in human fibroblasts more susceptible to the DNA-damaging agents bleomycin, gamma radiation and 8-methoxypsoralen, *Carcinogenesis 10*, 447-451.
125. Bloomfield, V. A. (1981) Quasi-elastic light scattering applications in biochemistry and biology, *Annu Rev Biophys Bioeng 10*, 421-450.
126. Lee, K. S., Mandelkern, M., and Crothers, D. M. (1981) Solution structural studies of chromatin fibers, *Biochemistry 20*, 1438-1445.
127. Holde, K. V., Leuda, S. H., and Zlatanova, J. (1998) Physical approaches to the study of chromatin fibers, *Gene. ther. Molec. Biol. 1*.
128. Berne, B. J., and Pecora, R. (2000) Dynamic Light Scattering: With application to chemistry, biology and physics. *, 3rd edition, NewYork : Dover publications.*
129. Hanlon, A. D., Larkin, M. I., and Reddick, R. M. (2010) Free-solution, label-free protein-protein interactions characterized by dynamic light scattering, *Biophys J 98*, 297-304.
130. Campbell, A. M., Cotter, R. I., and Pardon, J. F. (1978) Light scattering measurements supporting helical structures for chromatin in solution, *Nucleic Acids Res 5*, 1571-1580.
131. Schmitz, K. S., and Shaw, B. R. (1977) Hydrodynamic evidence in support of spacer regions in chromatin, *Science 197*, 661-663.
132. Roche, J., Girardet, J. L., Gorka, C., and Lawrence, J. J. (1985) The involvement of histone H1[0] in chromatin structure, *Nucleic Acids Res 13*, 2843-2853.
133. Eisenberg, H., Borochov, N., Kam, Z., and Voordouw, G. (1979) Conformation of plasmid DNA and of DNA-histone chromatin like complexes by laser light scattering., *Philosoph Transact Royal Soc London 293*, 303-313.
134. Dimitrov, S., Makarov, V., Apostolova, T., and Pashev, I. (1986) Structure of hyperacetylated chromatin: Light scattering and flow dichroism study., *Fed Eur Biochem Soc Lett 197*, 217-220.

135. Dimitrov, S. I., Apostolova, T. M., Makarov, V. L., and Pashev, I. G. (1986) Chromatin superstructure - a study with an immobilized trypsin., *Fed Eur Biochem Soc Lett 200*, 322-326.

136. Greulich, K. O., Ausio, J., Seger, D., Wachtel, E., and Eisenberg, H. (1986) Chromatin folding into higher order structure, *Biophys J 49*, 7-8.

137. Makarov, V., Smirnov, I., and Dimitrov, S. I. (1987) Higher order folding of chromatin is induced in different ways by monovalent and by divalent cations., *Fed Eur Biochem Soc Lett 212*, 263-266.

138. Selvi, B. R., Pradhan, S. K., Shandilya, J., Das, C., Sailaja, B. S., Shankar, G. N., Gadad, S. S., Reddy, A., Dasgupta, D., and Kundu, T. K. (2009) Sanguinarine interacts with chromatin, modulates epigenetic modifications, and transcription in the context of chromatin, *Chem Biol 16*, 203-216.

139. Majumder, P., and Dasgupta, D. (2011) Effect of DNA groove binder distamycin A upon chromatin structure, *PLoS One 6*, e26486.

140. Lobrich, M., Shibata, A., Beucher, A., Fisher, A., Ensminger, M., Goodarzi, A. A., Barton, O., and Jeggo, P. A. (2010) gammaH2AX foci analysis for monitoring DNA double-strand break repair: strengths, limitations and optimization, *Cell Cycle 9*, 662-669.

141. Olive, P. L., and Banath, J. P. (2004) Phosphorylation of histone H2AX as a measure of radiosensitivity, *Int J Radiat Oncol Biol Phys 58*, 331-335.

142. Redon, C. E., Dickey, J. S., Bonner, W. M., and Sedelnikova, O. A. (2009) gamma-H2AX as a biomarker of DNA damage induced by ionizing radiation in human peripheral blood lymphocytes and artificial skin, *Adv Space Res 43*, 1171-1178.

143. Rogakou, E. P., Pilch, D. R., Orr, A. H., Ivanova, V. S., and Bonner, W. M. (1998) DNA double-stranded breaks induce histone H2AX phosphorylation on serine 139, *J Biol Chem 273*, 5858-5868.

144. Rothkamm, K., Barnard, S., Moquet, J., Ellender, M., Rana, Z., and Burdak-Rothkamm, S. (2015) DNA damage foci: Meaning and significance, *Environ Mol Mutagen 56*, 491-504.

145. Horn, S., Barnard, S., and Rothkamm, K. (2011) Gamma-H2AX-based dose estimation for whole and partial body radiation exposure, *PLoS One 6*, e25113.

146. Kinner, A., Wu, W., Staudt, C., and Iliakis, G. (2008) Gamma-H2AX in recognition and signaling of DNA double-strand breaks in the context of chromatin, *Nucleic Acids Res 36*, 5678-5694.

147. Fernandez-Capetillo, O., Celeste, A., and Nussenzweig, A. (2003) Focusing on foci: H2AX and the recruitment of DNA-damage response factors, *Cell Cycle 2*, 426-427.

148. Fernandez-Capetillo, O., Lee, A., Nussenzweig, M., and Nussenzweig, A. (2004) H2AX: the histone guardian of the genome, *DNA Repair (Amst) 3*, 959-967.

149. Valdiglesias, V., Giunta, S., Fenech, M., Neri, M., and Bonassi, S. (2013) γH2AX as a marker of DNA double strand breaks and genomic instability in human population studies., *Mutation Research 753*, 24-40.

150. Vandevoorde, C., Franck, C., Bacher, K., Breysem, L., Smet, M. H., Ernst, C., De Backer, A., Van De Moortele, K., Smeets, P., and Thierens, H. (2015) gamma-H2AX foci as in vivo effect biomarker in children emphasize the importance to minimize x-ray doses in paediatric CT imaging, *Eur Radiol 25*, 800-811.

151. Neumaier, T., Swenson, J., Pham, C., Polyzos, A., Lo, A. T., Yang, P., Dyball, J., Asaithamby, A., Chen, D. J., Bissell, M. J., Thalhammer, S., and Costes, S. V. (2012) Evidence for formation of DNA repair centers and dose-response nonlinearity in human cells, *Proc Natl Acad Sci U S A 109*, 443-448.

152. Lobrich, M., Rief, N., Kuhne, M., Heckmann, M., Fleckenstein, J., Rube, C., and Uder, M. (2005) In vivo formation and repair of DNA double-strand breaks after computed tomography examinations, *Proc Natl Acad Sci U S A 102*, 8984-8989.

153. Olive, P. L. (2004) Detection of DNA damage in individual cells by analysis of histone H2AX phosphorylation, *Methods Cell Biol 75*, 355-373.

154. Rothkamm, K., Balroop, S., Shekhdar, J., Fernie, P., and Goh, V. (2007) Leukocyte DNA damage after multi-detector row CT: a quantitative biomarker of low-level radiation exposure, *Radiology 242*, 244-251.

155. Asaithamby, A., and Chen, D. J. (2009) Cellular responses to DNA double-strand breaks after low-dose gamma-irradiation, *Nucleic Acids Res 37*, 3912-3923.

156. Andrievski, A., and Wilkins, R. C. (2009) The response of gamma-H2AX in human lymphocytes and lymphocytes subsets measured in whole blood cultures, *Int J Radiat Biol 85*, 369-376.
157. Moquet, J., Barnard, S., and Rothkamm, K. (2014) Gamma-H2AX biodosimetry for use in large scale radiation incidents: comparison of a rapid '96 well lyse/fix' protocol with a routine method, *PeerJ 2*, e282.
158. Roch-Lefevre, S., Mandina, T., Voisin, P., Gaetan, G., Mesa, J. E., Valente, M., Bonnesoeur, P., Garcia, O., and Roy, L. (2010) Quantification of gamma-H2AX foci in human lymphocytes: a method for biological dosimetry after ionizing radiation exposure, *Radiat Res 174*, 185-194.
159. Ismail, I. H., Wadhra, T. I., and Hammarsten, O. (2007) An optimized method for detecting gamma-H2AX in blood cells reveals a significant interindividual variation in the gamma-H2AX response among humans, *Nucleic Acids Res 35*, e36.
160. Kuo, L. J., and Yang, L. X. (2008) Gamma-H2AX - a novel biomarker for DNA double-strand breaks, *In Vivo 22*, 305-309.
161. Beels, L., Werbrouck, J., and Thierens, H. (2010) Dose response and repair kinetics of gamma-H2AX foci induced by in vitro irradiation of whole blood and T-lymphocytes with X- and gamma-radiation, *Int J Radiat Biol 86*, 760-768.
162. Halm, B. M., Franke, A. A., Lai, J. F., Turner, H. C., Brenner, D. J., Zohrabian, V. M., and DiMauro, R. (2014) gamma-H2AX foci are increased in lymphocytes in vivo in young children 1 h after very low-dose X-irradiation: a pilot study, *Pediatr Radiol 44*, 1310-1317.
163. Antonelli, F., Campa, A., Esposito, G., Giardullo, P., Belli, M., Dini, V., Meschini, S., Simone, G., Sorrentino, E., Gerardi, S., Cirrone, G. A., and Tabocchini, M. A. (2015) Induction and Repair of DNA DSB as Revealed by H2AX Phosphorylation Foci in Human Fibroblasts Exposed to Low- and High-LET Radiation: Relationship with Early and Delayed Reproductive Cell Death, *Radiat Res 183*, 417-431.
164. Asaithamby, A., Uematsu, N., Chatterjee, A., Story, M. D., Burma, S., and Chen, D. J. (2008) Repair of HZE-particle-induced DNA double-strand breaks in normal human fibroblasts, *Radiat Res 169*, 437-446.

165. Lassmann, M., Hanscheid, H., Gassen, D., Biko, J., Meineke, V., Reiners, C., and Scherthan, H. (2010) In vivo formation of gamma-H2AX and 53BP1 DNA repair foci in blood cells after radioiodine therapy of differentiated thyroid cancer, *J Nucl Med 51*, 1318-1325.

166. Leatherbarrow, E. L., Harper, J. V., Cucinotta, F. A., and O'Neill, P. (2006) Induction and quantification of gamma-H2AX foci following low and high LET-irradiation, *Int J Radiat Biol 82*, 111-118.

167. Sedelnikova, O. A., Rogakou, E. P., Panyutin, I. G., and Bonner, W. M. (2002) Quantitative detection of (125)IdU-induced DNA double-strand breaks with gamma-H2AX antibody, *Radiat Res 158*, 486-492.

168. May, M. S., Brand, M., Wuest, W., Anders, K., Kuwert, T., Prante, O., Schmidt, D., Maschauer, S., Semelka, R. C., Uder, M., and Kuefner, M. A. (2012) Induction and repair of DNA double-strand breaks in blood lymphocytes of patients undergoing (1)(8)F-FDG PET/CT examinations, *Eur J Nucl Med Mol Imaging 39*, 1712-1719.

169. Zahnreich, S., Ebersberger, A., Kaina, B., and Schmidberger, H. (2015) Biodosimetry Based on gamma-H2AX Quantification and Cytogenetics after Partial- and Total-Body Irradiation during Fractionated Radiotherapy, *Radiat Res 183*, 432-446.

170. Gentile, M., Latonen, L., and Laiho, M. (2003) Cell cycle arrest and apoptosis provoked by UV radiation-induced DNA damage are transcriptionally highly divergent responses, *Nucleic Acids Res 31*, 4779-4790.

171. Amundson, S. A., and Fornace, A. J., Jr. (2001) Gene expression profiles for monitoring radiation exposure, *Radiat Prot Dosimetry 97*, 11-16.

172. Amundson, S. A., and Fornace, A. J., Jr. (2003) Monitoring human radiation exposure by gene expression profiling: possibilities and pitfalls, *Health Phys 85*, 36-42.

173. Brengues, M., Paap, B., Bittner, M., Amundson, S., Seligmann, B., Korn, R., Lenigk, R., and Zenhausern, F. (2010) Biodosimetry on small blood volume using gene expression assay, *Health Phys 98*, 179-185.

174. Fornace, A. J., Jr., Amundson, S. A., Do, K. T., Meltzer, P., Trent, J., and Bittner, M. (2002) Stress-gene induction by low-dose gamma irradiation, *Mil Med 167*, 13-15.

175. Huang, T. C., Paul, S., Gong, P., Levicky, R., Kymissis, J., Amundson, S. A., and Shepard, K. L. (2011) Gene expression analysis with an integrated CMOS microarray by time-resolved fluorescence detection, *Biosens Bioelectron 26*, 2660-2665.

176. Ivanov, V. N., Ghandhi, S. A., Zhou, H., Huang, S. X., Chai, Y., Amundson, S. A., and Hei, T. K. (2011) Radiation response and regulation of apoptosis induced by a combination of TRAIL and CHX in cells lacking mitochondrial DNA: a role for NF-kappaB-STAT3-directed gene expression, *Exp Cell Res 317*, 1548-1566.

177. Lu, T. P., Hsu, Y. Y., Lai, L. C., Tsai, M. H., and Chuang, E. Y. (2014) Identification of gene expression biomarkers for predicting radiation exposure, *Sci Rep 4*, 6293.

178. Paul, S., and Amundson, S. A. (2008) Development of gene expression signatures for practical radiation biodosimetry, *Int J Radiat Oncol Biol Phys 71*, 1236-1244.

179. Paul, S., and Amundson, S. A. (2011) Gene expression signatures of radiation exposure in peripheral white blood cells of smokers and non-smokers, *Int J Radiat Biol 87*, 791-801.

180. Paul, S., Barker, C. A., Turner, H. C., McLane, A., Wolden, S. L., and Amundson, S. A. (2011) Prediction of in vivo radiation dose status in radiotherapy patients using ex vivo and in vivo gene expression signatures, *Radiat Res 175*, 257-265.

181. Uehara, Y., Ito, Y., Taki, K., Nenoi, M., Ichinohe, K., Nakamura, S., Tanaka, S., Oghiso, Y., Tanaka, K., Matsumoto, T., Paunesku, T., Woloschak, G. E., and Ono, T. (2010) Gene expression profiles in mouse liver after long-term low-dose-rate irradiation with gamma rays, *Radiat Res 174*, 611-617.

182. Ghandhi, S. A., Smilenov, L. B., Elliston, C. D., Chowdhury, M., and Amundson, S. A. (2015) Radiation dose-rate effects on gene expression for human biodosimetry, *BMC Med Genomics 8*, 22.

183. Paul, S., Smilenov, L. B., Elliston, C. D., and Amundson, S. A. (2015) Radiation Dose-Rate Effects on Gene Expression in a Mouse Biodosimetry Model, *Radiat Res 184*, 24-32.

184. Amundson, S. A., Do, K. T., Vinikoor, L. C., Lee, R. A., Koch-Paiz, C. A., Ahn, J., Reimers, M., Chen, Y., Scudiero, D. A., Weinstein, J. N., Trent, J. M., Bittner, M. L., Meltzer, P. S., and Fornace, A. J., Jr. (2008) Integrating global gene expression and

radiation survival parameters across the 60 cell lines of the National Cancer Institute Anticancer Drug Screen, *Cancer Res 68*, 415-424.

185. Amundson, S. A., and Fornace, A. J., Jr. (2003) Microarray approaches for analysis of tumor suppressor gene function, *Methods Mol Biol 223*, 141-154.
186. Ghandhi, S. A., Yaghoubian, B., and Amundson, S. A. (2008) Global gene expression analyses of bystander and alpha particle irradiated normal human lung fibroblasts: synchronous and differential responses, *BMC Med Genomics 1*, 63.
187. Amundson, S. A., Do, K. T., and Fornace, A. J., Jr. (1999) Induction of stress genes by low doses of gamma rays, *Radiat Res 152*, 225-231.
188. Franco, N., Lamartine, J., Frouin, V., Le Minter, P., Petat, C., Leplat, J. J., Libert, F., Gidrol, X., and Martin, M. T. (2005) Low-dose exposure to gamma rays induces specific gene regulations in normal human keratinocytes, *Radiat Res 163*, 623-635.
189. Warters, R. L., Packard, A. T., Kramer, G. F., Gaffney, D. K., and Moos, P. J. (2009) Differential gene expression in primary human skin keratinocytes and fibroblasts in response to ionizing radiation, *Radiat Res 172*, 82-95.
190. Fachin, A. L., Mello, S. S., Sandrin-Garcia, P., Junta, C. M., Ghilardi-Netto, T., Donadi, E. A., Passos, G. A., and Sakamoto-Hojo, E. T. (2009) Gene expression profiles in radiation workers occupationally exposed to ionizing radiation, *J Radiat Res 50*, 61-71.
191. Morandi, E., Severini, C., Quercioli, D., Perdichizzi, S., Mascolo, M. G., Horn, W., Vaccari, M., Nucci, M. C., Lodi, V., Violante, F. S., Bolognesi, C., Grilli, S., Silingardi, P., and Colacci, A. (2009) Gene expression changes in medical workers exposed to radiation., *Radiation Research 172*, 500-508.
192. Albanese, J., Martens, K., Karanitsa, L. V., Schreyer, S. K., and Dainiak, N. (2007) Multivariate analysis of low-dose radiation-associated changes in cytokine gene expression profiles using microarray technology, *Exp Hematol 35*, 47-54.
193. Fachin, A. L., Mello, S. S., Sandrin-Garcia, P., Junta, C. M., Donadi, E. A., Passos, G. A., and Sakamoto-Hojo, E. T. (2007) Gene expression profiles in human lymphocytes irradiated in vitro with low doses of gamma rays, *Radiat Res 168*, 650-665.

194. Lee, K. F., Weng, J. T., Hsu, P. W., Chi, Y. H., Chen, C. K., Liu, I. Y., Chen, Y. C., and Wu, L. S. (2014) Gene expression profiling of biological pathway alterations by radiation exposure, *Biomed Res Int 2014*, 834087.

195. Lanza, V., Pretazzoli, V., Olivieri, G., Pascarella, G., Panconesi, A., and Negri, R. (2005) Transcriptional response of human umbilical vein endothelial cells to low doses of ionizing radiation, *J Radiat Res 46*, 265-276.

196. Wyrobek, A. J., Manohar, C. F., Krishnan, V. V., Nelson, D. O., Furtado, M. R., Bhattacharya, M. S., Marchetti, F., and Coleman, M. A. (2011) Low dose radiation response curves, networks and pathways in human lymphoblastoid cells exposed from 1 to 10cGy of acute gamma radiation, *Mutat Res 722*, 119-130.

197. Long, X. H., Zhao, Z. Q., He, X. P., Wang, H. P., Xu, Q. Z., An, J., Bai, B., Sui, J. L., and Zhou, P. K. (2007) Dose-dependent expression changes of early response genes to ionizing radiation in human lymphoblastoid cells, *Int J Mol Med 19*, 607-615.

198. Sokolov, M., and Neumann, R. (2014) Effects of low doses of ionizing radiation exposures on stress-responsive gene expression in human embryonic stem cells, *Int J Mol Sci 15*, 588-604.

199. Fujimori, A., Okayasu, R., Ishihara, H., Yoshida, S., Eguchi-Kasai, K., Nojima, K., Ebisawa, S., and Takahashi, S. (2005) Extremely low dose ionizing radiation up-regulates CXC chemokines in normal human fibroblasts, *Cancer Res 65*, 10159-10163.

200. Yin, E., Nelson, D. O., Coleman, M. A., Peterson, L. E., and Wyrobek, A. J. (2003) Gene expression changes in mouse brain after exposure to low-dose ionizing radiation, *Int J Radiat Biol 79*, 759-775.

201. Luckey, T. D. (2006) Radiation hormesis: the good, the bad, and the ugly, *Dose Response 4*, 169-190.

202. Doss, M. (2013) Linear No-Threshold Model VS. Radiation Hormesis, *Dose Response 11*, 480-497.

203. Nenoi, M., Wang, B., and Vares, G. (2015) In vivo radioadaptive response: a review of studies relevant to radiation-induced cancer risk, *Hum Exp Toxicol 34*, 272-283.

204. Mine, M., Okumura, Y., Ichimaru, M., Nakamura, T., and Kondo, S. (1990) Apparently beneficial effect of low to intermediate doses of A-bomb radiation on human lifespan, *Int J Radiat Biol 58*, 1035-1043.

205. Aurengo, A., Averbeck, D., Bonnin, A., LeGuen, B., Masse, R., Monier, R., Tubiana, M., Valleron, A. J., and de Vathaire, F. (2005) Dose-effect relationships and estimation of the carcinogenic eff ects of low doses of ionizing radiation . *Paris: Academies of Sciences and Medicine.*

206. Thayer, K. A., Melnick, R., Burns, K., Davis, D., and Huff, J. (2005) Fundamental flaws of hormesis for public health decisions, *Environ Health Perspect 113*, 1271-1276.

207. Szumiel, I. (2012) Radiation hormesis: Autophagy and other cellular mechanisms, *Int J Radiat Biol 88*, 619-628.

208. Liu, S. Z. (1989) Radiation hormesis. A new concept in radiological science, *Chin Med J (Engl) 102*, 750-755.

209. Liu, S. Z., Liu, W. H., and Sun, J. B. (1987) Radiation hormesis: its expression in the immune system, *Health Phys 52*, 579-583.

210. Liu, S. Z. (2003) On radiation hormesis expressed in the immune system, *Crit Rev Toxicol 33*, 431-441.

211. Liu, S. Z. (2004) Radiation-induced change in lymphocyte proliferation and its neuroendocrine regulation: dose-response relationship and pathophysiological implications, *Nonlinearity Biol Toxicol Med 2*, 233-243.

212. Joiner, M. C., Lambin, P., and Marples, B. (1999) Adaptive response and induced resistance, *C R Acad Sci III 322*, 167-175.

213. Liang, X., So, Y. H., Cui, J., Ma, K., Xu, X., Zhao, Y., Cai, L., and Li, W. (2011) The low-dose ionizing radiation stimulates cell proliferation via activation of the MAPK/ERK pathway in rat cultured mesenchymal stem cells, *J Radiat Res 52*, 380-386.

214. Parsons, W. B., Jr., Watkins, C. H., Pease, G. L., and Childs, D. S., Jr. (1954) Changes in sternal marrow following roentgen-ray therapy to the spleen in chronic granulocytic leukemia, *Cancer 7*, 179-189.

215. Nagasawa, H., and Little, J. B. (1992) Induction of sister chromatid exchanges by extremely low doses of alpha-particles, *Cancer Res 52*, 6394-6396.

216. Chai, Y., and Hei, T. K. (2008) Radiation Induced Bystander Effect in vivo, *Acta Med Nagasaki 53*, S65-S69.
217. Azzam, E. I., De Toledo, S. M., Spitz, D. R., and Little, J. B. (2002) Oxidative metabolism modulates signal transduction and micronucleus formation in bystander cells from alpha-particle-irradiated normal human fibroblast cultures, *Cancer Res 62*, 5436-5442.
218. Deshpande, A., Goodwin, E. H., Bailey, S. M., Marrone, B. L., and Lehnert, B. E. (1996) Alpha-particle-induced sister chromatid exchange in normal human lung fibroblasts: evidence for an extranuclear target, *Radiat Res 145*, 260-267.
219. Mothersill, C., and Seymour, C. B. (2002) Bystander and delayed effects after fractionated radiation exposure, *Radiat Res 158*, 626-633.
220. Hu, B., Wu, L., Han, W., Zhang, L., Chen, S., Xu, A., Hei, T. K., and Yu, Z. (2006) The time and spatial effects of bystander response in mammalian cells induced by low dose radiation, *Carcinogenesis 27*, 245-251.
221. Lyng, F. M., Maguire, P., McClean, B., Seymour, C., and Mothersill, C. (2006) The involvement of calcium and MAP kinase signaling pathways in the production of radiation-induced bystander effects, *Radiat Res 165*, 400-409.
222. Zhou, H., Ivanov, V. N., Gillespie, J., Geard, C. R., Amundson, S. A., Brenner, D. J., Yu, Z., Lieberman, H. B., and Hei, T. K. (2005) Mechanism of radiation-induced bystander effect: role of the cyclooxygenase-2 signaling pathway, *Proc Natl Acad Sci U S A 102*, 14641-14646.
223. Albanese, J., and Dainiak, N. (2000) Ionizing radiation alters Fas antigen ligand at the cell surface and on exfoliated plasma membrane-derived vesicles: implications for apoptosis and intercellular signaling, *Radiat Res 153*, 49-61.
224. Brooks, A. L., Retherford, J. C., and McClellan, R. O. (1974) Effect of 239PuO2 particle number and size on the frequency and distribution of chromosome aberrations in the liver of the Chinese hamster, *Radiat Res 59*, 693-709.
225. Khan, M. A., Hill, R. P., and Van Dyk, J. (1998) Partial volume rat lung irradiation: an evaluation of early DNA damage, *Int J Radiat Oncol Biol Phys 40*, 467-476.

226. Brooks, A. L. (2004) Evidence for 'bystander effects' in vivo, *Hum Exp Toxicol 23*, 67-70.

227. Rockett, J. C., Burczynski, M. E., Fornace, A. J., Herrmann, P. C., Krawetz, S. A., and Dix, D. J. (2004) Surrogate tissue analysis: monitoring toxicant exposure and health status of inaccessible tissues through the analysis of accessible tissues and cells, *Toxicol Appl Pharmacol 194*, 189-199.

228. Pool-Zobel, B. L., Dornacher, I., Lambertz, R., Knoll, M., and Seitz, H. K. (2004) Genetic damage and repair in human rectal cells for biomonitoring: sex differences, effects of alcohol exposure, and susceptibilities in comparison to peripheral blood lymphocytes, *Mutat Res 551*, 127-134.

229. ICRP report. (1991) 1990 recommendations of the International Commission on Radiological Protection. Ann ICRP, *21*, 1-3.

230. Nair, R. R. K., Akiba, S., Binu, V. S., Jayalekshmi, P., Gangadharan, P., and Nair, M. K. (2005) Individual dose estimation—our experience with the Karunagapally study in Kerala, India. Internatinal Congress Series., *1276*, 41-45.

231. Huang, X., and Darzynkiewicz, Z. (2006) Cytometric assessment of histone H2AX phosphorylation: a reporter of DNA damage, *Methods Mol Biol 314*, 73-80.

232. Das, C., Hizume, K., Batta, K., Kumar, B. R., Gadad, S. S., Ganguly, S., Lorain, S., Verreault, A., Sadhale, P. P., Takeyasu, K., and Kundu, T. K. (2006) Transcriptional coactivator PC4, a chromatin-associated protein, induces chromatin condensation, *Mol Cell Biol 26*, 8303-8315.

233. Vrijheid, M., Cardis, E., Ashmore, P., Auvinen, A., Bae, J. M., Engels, H., Gilbert, E., Gulis, G., Habib, R., Howe, G., Kurtinaitis, J., Malker, H., Muirhead, C., Richardson, D., Rodriguez-Artalejo, F., Rogel, A., Schubauer-Berigan, M., Tardy, H., Telle-Lamberton, M., Usel, M., and Veress, K. (2007) Mortality from diseases other than cancer following low doses of ionizing radiation: results from the 15-Country Study of nuclear industry workers, *Int J Epidemiol 36*, 1126-1135.

234. Zielinski, J. M., Ashmore, P. J., Band, P. R., Jiang, H., Shilnikova, N. S., Tait, V. K., and Krewski, D. (2009) Low dose ionizing radiation exposure and cardiovascular disease

mortality: cohort study based on Canadian national dose registry of radiation workers, *Int J Occup Med Environ Health 22*, 27-33.

235. Stoilov, L. M., Mullenders, L. H., Darroudi, F., and Natarajan, A. T. (2007) Adaptive response to DNA and chromosomal damage induced by X-rays in human blood lymphocytes, *Mutagenesis 22*, 117-122.

236. Sykes, P. J., Day, T. K., Swinburne, S. J., Lane, J. M., Morley, A. A., Hooker, A. M., and Bhat, M. (2006) In vivo mutagenic effect of very low dose radiation, *Dose Response 4*, 309-316.

237. Anderson, R. E., Tokuda, S., Williams, W. L., and Warner, N. L. (1982) Radiation-induced augmentation of the response of A/J mice to SaI tumor cells, *Am J Pathol 108*, 24-38.

238. Djuzenova, C. S., Elsner, I., Katzer, A., Worschech, E., Distel, L. V., Flentje, M., and Polat, B. (2013) Radiosensitivity in breast cancer assessed by the histone gamma-H2AX and 53BP1 foci, *Radiat Oncol 8*, 98.

239. Sedelnikova, O. A., Horikawa, I., Redon, C., Nakamura, A., Zimonjic, D. B., Popescu, N. C., and Bonner, W. M. (2008) Delayed kinetics of DNA double-strand break processing in normal and pathological aging, *Aging Cell 7*, 89-100.

240. Sharma, P. M., Ponnaiya, B., Taveras, M., Shuryak, I., Turner, H., and Brenner, D. J. (2015) High throughput measurement of gammaH2AX DSB repair kinetics in a healthy human population, *PLoS One 10*, e0121083.

241. Ward, J. F. (1994) The complexity of DNA damage: relevance to biological consequences, *Int J Radiat Biol 66*, 427-432.

242. Schmid, T. E., Dollinger, G., Beisker, W., Hable, V., Greubel, C., Auer, S., Mittag, A., Tarnok, A., Friedl, A. A., Molls, M., and Roper, B. (2010) Differences in the kinetics of gamma-H2AX fluorescence decay after exposure to low and high LET radiation, *Int J Radiat Biol 86*, 682-691.

243. Strande, N. T., Waters, C. A., and Ramsden, D. A. (2012) Resolution of complex ends by Nonhomologous end joining - better to be lucky than good?, *Genome Integr 3*, 10.

244. Goodarzi, A. A., Jeggo, P., and Lobrich, M. (2010) The influence of heterochromatin on DNA double strand break repair: Getting the strong, silent type to relax, *DNA Repair (Amst) 9*, 1273-1282.

245. Lemaitre, C., Grabarz, A., Tsouroula, K., Andronov, L., Furst, A., Pankotai, T., Heyer, V., Rogier, M., Attwood, K. M., Kessler, P., Dellaire, G., Klaholz, B., Reina-San-Martin, B., and Soutoglou, E. (2014) Nuclear position dictates DNA repair pathway choice, *Genes Dev 28*, 2450-2463.

246. Lorat, Y., Schanz, S., Schuler, N., Wennemuth, G., Rube, C., and Rube, C. E. (2012) Beyond repair foci: DNA double-strand break repair in euchromatic and heterochromatic compartments analyzed by transmission electron microscopy, *PLoS One 7*, e38165.

247. Akerman, G. S., Rosenzweig, B. A., Domon, O. E., Tsai, C. A., Bishop, M. E., McGarrity, L. J., Macgregor, J. T., Sistare, F. D., Chen, J. J., and Morris, S. M. (2005) Alterations in gene expression profiles and the DNA-damage response in ionizing radiation-exposed TK6 cells, *Environ Mol Mutagen 45*, 188-205.

248. Takahashi, A., Su, X., Suzuki, H., Omori, K., Seki, M., Hashizume, T., Shimazu, T., Ishioka, N., Iwasaki, T., and Ohnishi, T. (2010) p53-dependent adaptive responses in human cells exposed to space radiations, *Int J Radiat Oncol Biol Phys 78*, 1171-1176.

249. Shimizu, T., Kato, T., Jr., Tachibana, A., and Sasaki, M. S. (1999) Coordinated regulation of radioadaptive response by protein kinase C and p38 mitogen-activated protein kinase, *Exp Cell Res 251*, 424-432.

250. Ishii, K., and Watanabe, M. (1996) Participation of gap-junctional cell communication on the adaptive response in human cells induced by low dose of X-rays, *Int J Radiat Biol 69*, 291-299.

251. Hayakawa, J., Mittal, S., Wang, Y., Korkmaz, K. S., Adamson, E., English, C., Ohmichi, M., McClelland, M., and Mercola, D. (2004) Identification of promoters bound by c-Jun/ATF2 during rapid large-scale gene activation following genotoxic stress, *Mol Cell 16*, 521-535.

252. Bhoumik, A., Takahashi, S., Breitweiser, W., Shiloh, Y., Jones, N., and Ronai, Z. (2005) ATM-dependent phosphorylation of ATF2 is required for the DNA damage response, *Mol Cell 18*, 577-587.

253. Malewicz, M., Kadkhodaei, B., Kee, N., Volakakis, N., Hellman, U., Viktorsson, K., Leung, C. Y., Chen, B., Lewensohn, R., van Gent, D. C., Chen, D. J., and Perlmann, T. (2011) Essential role for DNA-PK-mediated phosphorylation of NR4A nuclear orphan receptors in DNA double-strand break repair, *Genes Dev 25*, 2031-2040.

254. Jagirdar, K., Yin, K., Harrison, M., Lim, W., Muscat, G. E., Sturm, R. A., and Smith, A. G. (2013) The NR4A2 nuclear receptor is recruited to novel nuclear foci in response to UV irradiation and participates in nucleotide excision repair, *PLoS One 8*, e78075.

255. Mezentsev, A., and Amundson, S. A. (2011) Global gene expression responses to low- or high-dose radiation in a human three-dimensional tissue model, *Radiat Res 175*, 677-688.

256. Manning, G., Kabacik, S., Finnon, P., and Badie, C. (2011) Assessing a new gene expression analysis technique for radiation biodosimetry applications, *Radiation Measurements 46*, 1014-1018.

257. Tucker, J. D., Joiner, M. C., Thomas, R. A., Grever, W. E., Bakhmutsky, M. V., Chinkhota, C. N., Smolinski, J. M., Divine, G. W., and Auner, G. W. (2014) Accurate gene expression-based biodosimetry using a minimal set of human gene transcripts, *Int J Radiat Oncol Biol Phys 88*, 933-939.

258. Knops, K., Boldt, S., Wolkenhauer, O., and Kriehuber, R. (2012) Gene expression in low- and high-dose-irradiated human peripheral blood lymphocytes: possible applications for biodosimetry, *Radiat Res 178*, 304-312.

259. Riecke, A., Rufa, C. G., Cordes, M., Hartmann, J., Meineke, V., and Abend, M. (2012) Gene expression comparisons performed for biodosimetry purposes on in vitro peripheral blood cellular subsets and irradiated individuals, *Radiat Res 178*, 234-243.

260. Turtoi, A., Brown, I., Oskamp, D., and Schneeweiss, F. H. (2008) Early gene expression in human lymphocytes after gamma-irradiation-a genetic pattern with potential for biodosimetry, *Int J Radiat Biol 84*, 375-387.

261. Grace, M. B., McLeland, C. B., and Blakely, W. F. (2002) Real-time quantitative RT-PCR assay of GADD45 gene expression changes as a biomarker for radiation biodosimetry, *Int J Radiat Biol 78*, 1011-1021.

262. Goodarzi, A. A., Noon, A. T., and Jeggo, P. A. (2009) The impact of heterochromatin on DSB repair, *Biochem Soc Trans 37*, 569-576.

Publications

Mutation Research xxx (2016) xxx–xxx

Contents lists available at ScienceDirect

Mutation Research/Fundamental and Molecular Mechanisms of Mutagenesis

journal homepage: www.elsevier.com/locate/molmut
Community address: www.elsevier.com/locate/mutres

Lack of increased DNA double-strand breaks in peripheral blood mononuclear cells of individuals from high level natural radiation areas of Kerala coast in India

Vinay Jain[a,b], P.R. Vivek Kumar[a], P.K.M. Koya[a], G. Jaikrishan[a], Birajalaxmi Das[a,*]

[a] Low Level Radiation Research Section, Radiation Biology and Health Sciences Division, Bio-Science Group, Bhabha Atomic Research Centre, Trombay, Mumbai 400 085, India
[b] Homi Bhabha National Institute, Anushakti Nagar, Mumbai 400 094, India

ARTICLE INFO

Article history:
Received 19 August 2015
Received in revised form 14 February 2016
Accepted 24 March 2016
Available online xxx

Keywords:
Peripheral blood mononuclear cells
DNA double strand breaks
Gamma-H2AX foci
Chronic exposure
Normal level natural radiation area
High level natural radiation area

ABSTRACT

The high level natural radiation area (HLNRA) of Kerala is a 55 km long and 0.5 km wide strip in south west coast of India. The level of background radiation in this area varies from <1.0 mGy/year to 45.0 mGy/year. It offers unique opportunity to study the effect of chronic low dose/low dose-rate radiation directly on human population. Spontaneous level of DNA double strand breaks (DSBs) was quantified in peripheral blood mononuclear cells of 91 random individuals from HLNRA (N = 61, mean age: 36.1 ± 7.43 years) and normal level natural radiation area (NLNRA) (N = 30, mean age: 35.5 ± 6.35 years) using gamma-H2AX as a marker. The mean annual dose received by NLNRA and HLNRA individuals was 1.28 ± 0.086 mGy/year and 8.28 ± 4.96 mGy/year, respectively. The spontaneous frequency of DSBs in terms of gamma-H2AX foci among NLNRA and HLNRA individuals were 0.095 ± 0.009 and 0.084 ± 0.004 per cell (P = 0.22). The individuals from HLNRA were further classified as low dose group (LDG, 1.51–5.0 mGy/year, mean dose: 2.63 ± 0.76 mGy/year) and high dose group (HDG, >5.0 mGy/year, mean dose: 11.04 ± 3.57 mGy/year). The spontaneous frequency of gamma-H2AX foci per cell in NLNRA, LDG and HDG was observed to be 0.095 ± 0.009, 0.096 ± 0.008 and 0.078 ± 0.004 respectively. Individuals belonging to HDG of HLNRA showed marginally lower frequency of DSBs as compared to NLNRA and LDG of HLNRA. This could be suggestive of either lower induction or better repair of DSBs in individuals from HDG of HLNRA. The present study indicated that 5.0 mGy/year could be a possible threshold dose for DSB induction at chronic low-dose radiation exposure *in vivo*. However, further studies on DNA damage induction and repair kinetics are required to draw firm conclusions.

1. Introduction

Exposure of low level ionizing radiation (IR) to humans comes from both natural as well as man-made sources. These include exposures from high level natural radiation areas (HLNRAs), medical exposures (radio-therapeutic and diagnostic), occupational exposures and accidental exposures like Chernobyl and Fukushima Daiichi nuclear disasters. There are several places in the world where the background radiation is high due to radioactive mineral in the beach sand or radioactive contents in the hot springs. Prominent among them are Guarapari in Brazil, Yangjiang in China, Kerala in southwest India and Ramsar in Iran. HLNRAs provide unique opportunity to understand the biological effects of low dose/dose-rate radiation directly on humans at all stages of development [1]. Several epidemiological studies are conducted worldwide on human population residing in HLNRAs, occupational radiation workers and population exposed to nuclear disasters like Chernobyl and Fukushima Daiichi to find out health effects, if any, due to low dose radiation exposure [2–7].

Although there is no concrete evidence of adverse effects due to low dose radiation exposure, the public health concern still remains. Studies pertaining to the effects of low doses of radiation below 100 mSv (equivalent dose) or 100 mGy (absorbed dose for low LET radiation) are highly relevant for radiation protection science. Hence, efforts are made worldwide to study the biological and health effects of low dose and low dose-rate ionizing radiation in humans [8]. Linear no threshold hypothesis (LNT) is well debated and lacks scientific evidence, as it involves extrapolation of data at

* Corresponding author at: Low Level Radiation Research Section, Radiation Biology and Health Sciences Division, Bio-Science Group, Bhabha Atomic Research Centre, Trombay, Mumbai 400085, India.
E-mail addresses: birajalaxmi@yahoo.co.in, biraj@barc.gov.in (B. Das).

http://dx.doi.org/10.1016/j.mrfmmm.2016.03.002
0027-5107/

high acute dose exposures to low dose exposures [8,9]. Apart from health effects, the mechanism of carcinogenesis and the underlying mechanisms such as adaptive response, bystander effects, genome instability and abscopal effects are not yet clearly understood at low doses.

The interaction of IR with human cell is complex. At high doses, human cells are typically hit by many tracks of radiation, but at low doses most cells are typically hit by a single track of radiation. At very low doses, proportionately fewer cells are hit, mostly by single track of radiation [10]. Several studies have shown that the cellular responses to low and high doses of radiation exposure are quantitatively and qualitatively different [11–13]. Hence, the experimental evidence at very low doses and the mechanistic studies at high doses vs. low doses might throw some insights for risk estimation.

IR induces a variety of DNA lesions including double strand breaks (DSBs), which are considered to be highly deleterious. If DSBs are mis-repaired or un-repaired it may lead to increased frequency of chromosomal aberrations, mutations and carcinogenesis. DNA damage end points such as dicentrics, micronuclei etc. are good indicators of radiation induced damage and are useful for biological dosimetry, radio-therapeutic, diagnostic and population monitoring studies [14]. DSBs can be measured by comet assay, pulse field gel electrophoresis (PFGE) and immunofluorescence based gamma-H2AX assay. Comet assay detects both single strand breaks and DSBs. But immunofluorescence based gamma-H2AX assay is specific for DSBs and each focus represents one DSB [15–17]. This method is very sensitive and around 100 times more sensitive to detect DNA damage as compared to comet assay and allows scoring of foci in single intact cells [18].

Gamma-H2AX foci are formed at the site of DNA DSBs. One of the earliest events in cellular response to DSBs is the phosphorylation of H2AX protein at Ser139, which is referred to as gamma-H2AX. H2AX is a variant of the H2A protein family and constitutes around 10% of nucleosomal H2A histone protein in human cells. Gamma-H2AX foci formation occurs rapidly at the DSB sites and plays an important role in DNA damage response (DDR) signaling cascade. It recruits other DSB signaling and repair factors such as MDC1, 53BP1 etc., to form ionizing radiation induced foci (IRIF) or DNA repair foci [15,17,19–24]. There are reports, showing that gamma-H2AX is phosphorylated by members of phosphatidylinositol 3-kinase-related kinase family (PI3KK) such as ataxia telangiectasia mutated (ATM), ATM-Rad3-related (ATR) kinases and DNA-dependent protein kinase, catalytic subunit (DNA-PKcs) which helps in recruitment of DNA repair proteins at the site of DSBs [15].

Gamma-H2AX is considered as a surrogate marker for DSBs and is widely used for quantitative evaluation of DSB formation and repair in human lymphocytes and cell lines exposed to IR [13,16,17,22,25–29]. Several studies have been conducted, where gamma-H2AX foci was used to quantify the effect of partial or total body exposures during fractionated and mixed radio-therapeutic applications, CT/PET scans, X-rays, radio-iodine therapy etc. [17,25,28,30–36]. The level of gamma-H2AX foci, measured in human cells exposed to both low and high LET radiations such as gamma rays, protons, carbon ions and alpha particles clearly indicated the influences of track structure and fluence in the induction of foci [27,37,38].

The monazite bearing Kerala coastal belt is a 55 km long and 0.5 km wide strip extending from Neendakara (Kollam district) in the south to Purakkadu (Alappuzha district) in the north. The level of background radiation varies from <1.0 mGy/year to 45.0 mGy/year with an average dose of ~4.0 mGy/year. The population size in this area is approximately 400,000. The radioactive beach sand contains 8–10% thorium (^{232}Th) which is highest in the world. Due to patchy distribution of monazite in the beach sand, the level of radiation vary from place to place and therefore the population from this area offers opportunity to conduct dose response studies on *in vivo* exposure. For the past few decades, several investigations have been conducted in this area, which include screening of newborns for congenital malformations, case-control study on selected malformations, chromosome aberration analysis including dicentrics, translocations and inversions, micronuclei formation, quantification of DNA strand breaks using comet assay and measurement of telomere length in newborns as well as adults [39–47]. None of the above studies have shown any adverse effects of natural chronic radiation exposure on human population residing in this area. Interestingly, DNA damage and repair kinetics study using comet assay in peripheral blood mononuclear cells (PBMCs) of individuals from this area indicated fast and efficient repair of DNA strand breaks at an early time point in HLNRA individuals as compared to NLNRA [48].

In the present study, we have employed gamma-H2AX assay to estimate the basal level/spontaneous frequency of DNA DSBs in PBMCs of individuals from different background dose groups from the Kerala coast.

2. Materials and methods

2.1. Sample collection and ethics statement

Venous blood samples were collected from 91 random volunteers with written informed consent, which was approved by the Medical Ethics Committee, Bhabha Atomic Research Centre, Mumbai, India. A detailed questionnaire was used to obtain information on age, lifestyle and smoking habit.

2.2. Individual dosimetric information

Individual dose was calculated for all the volunteers. Dosimetry was carried out to measure the external gamma radiation levels in each donor's house by using a halogen quenched Geiger Muller (GM) tube-based survey meter consisting of a GM tube and a microprocessor-based digital display (Type ER-709, Nucleonix Systems, India). Both inside house as well as outside house measurements were done. Measurement was done at a height of 1 m inside and outside of each house. The mean of three readings was taken for each measurement. The survey meter readings measured absorbed doses in air (μR/h) due to gamma rays and were converted to annual dose (mGy/year) using a conversion factor of 0.0765 ($= 0.873 \times 24\,h \times 365\,days \times 10^{-5}$) [6]. The individual dose contributed by the gamma rays was derived as sum of 0.5 (occupancy factor) × the annual indoor dose and 0.5 (occupancy factor) × the annual outdoor dose. The occupancy factor taken for the calculation of individual dose was based on the sex and age specific occupancy factors estimated in a previous study conducted by Nair et al. [49]. Individuals receiving a dose of ≤1.5 mGy/year were considered as NLNRA individuals, whereas individuals receiving >1.5 mGy/year were considered as HLNRA individuals.

2.3. Isolation of peripheral blood mononuclear cells from human blood

Approximately 3.0 ml of blood samples were collected and PBMCs were separated by density gradient centrifugation using Histopaque 1077^{TM} (Sigma Aldrich, St. Louis, MO, USA) solution. Histopaque solution was transferred carefully to 15 ml sterile polypropylene centrifuge tubes and overlaid with equal volume of whole blood. Centrifugation was done at 400*g* for 30 min at room temperature. Interface opaque layer containing PBMCs was carefully aspirated and transferred to fresh sterile centrifuge tube, washed with chilled isotonic phosphate-buffered saline (PBS) and

Please cite this article in press as: V. Jain, et al., Lack of increased DNA double-strand breaks in peripheral blood mononuclear cells of individuals from high level natural radiation areas of Kerala coast in India, Mutat. Res.: Fundam. Mol. Mech. Mutagen. (2016), http://dx.doi.org/10.1016/j.mrfmmm.2016.03.002

Table 1
Distribution of gamma-H2AX foci per cell with respect to age and background dose level among HLNRA and NLNRA individuals. HLNRA: High Level Natural Radiation area, NLNRA: Normal Level Natural Radiation area. LDG: Low Dose group, HDG: High dose group. S. D: standard deviation.

Area	Background dose groups (mGy/year)	Number of individuals studied	Mean Age ± S.D (Age range in years)	Mean background dose ± S.D (dose range in mGy/year)	Frequency of gamma-H2AX foci ± S.E. (range)
NLNRA	≤1.50	30	35.5 ± 6.35 (25–50)	1.28 ± 0.086 (1.1–1.50)	0.095 ± 0.009 (0.01–0.28)
HLNRA	LDG (1.51–5.0)	20	34.2 ± 5.7 (25–44)	2.63 ± 0.76 (1.57–4.64)	0.096 ± 0.008 (0.05–0.17)
	HDG (>5.00–21.6)	41	37.1 ± 8.03 (18–59)	11.04 ± 3.57 (5.53–21.60)	0.078 ± 0.004 (0.02–0.14)
HLNRA (Total)	>1.50	61	36.1 ± 7.43 (18–59)	8.28 ± 4.96 (1.57–21.60)	0.084 ± 0.004 (0.02–0.17)

centrifuged at 250*g* for 10 min. The pellet was washed twice with isotonic PBS and kept for further use.

2.4. Immunofluorescence staining

Sample preparation for immunofluorescence staining was done as described elsewhere with slight modifications [50,51]. Briefly, PBMCs were transferred into a sterile 15 ml centrifuge tube containing freshly prepared chilled 1% formaldehyde (Sigma Aldrich, St. Louis, MO, USA) for fixation on ice for 15 min. After fixation, tubes were centrifuged at 250*g* for 15 min at room temperature. Cells were washed with PBS (pH 7.4) and transferred to 1.5 ml sterile centrifuge tubes. PBMCs were re-suspended in 70% freshly prepared ethanol. The cells were stored at −20 °C until further processing. The tubes were centrifuged, the pellets (PBMCs) were transferred to fresh 1.5 ml tubes and permeabilized with 0.2% Triton-X-100 solution (Sigma Aldrich, St. Louis, MO, USA) for 5 min at room temperature. Blocking was done with 1% bovine serum albumin (Sigma Aldrich, St. Louis, MO, USA) and cells were incubated overnight at 4 °C in 1:100 (10 μg/ml) concentration of anti-phospho-histone H2AX (Ser139), antibody (Upstate-Millipore 05-636, CA, USA). After overnight incubation, cells were washed in 1% blocking solution and labeled with Alexafluor- 488 conjugated rabbit anti-mouse antibody (Molecular probes A-11059, Eugene, USA) for 1 h at room temperature. After secondary antibody incubation, cells were washed with PBS and diluted to a concentration of approximately 1×10^6 cells/ml. Cell suspension (100 μl) was layered onto poly-l-lysine coated coverslips (BD BioCoat™ 354085, USA) and kept for 30 min at room temperature for adherence. It was then washed with PBS and mounted onto glass slides using prolong gold antifade DAPI reagent (Molecular Probes P 36931, USA).

2.5. Acquisition and analysis of images

The slides were examined at 40x magnification using fluorescence microscope (Carl Zeiss Microscopy GmbH, Germany). All the slides were blind coded and identity of individuals was not disclosed during the preparation and scoring of the slides. Two slides were prepared for each sample. Around 20–25 random images with ~8 to 10 well spreaded independent cells were captured from both the slides. An average of 250 cells was scored manually for gamma-H2AX foci for each individual. Scoring was carried out manually from the merged image obtained from DAPI and alexafluor filters using Zen 2012 SP2 software (Carl Zeiss Microscopy GmbH, Germany). The number of gamma-H2AX foci observed in each cell was recorded. The information about the multiple foci observed in the cells was also recorded for further analysis. To maintain the sensitivity of each focus observed, all the images were processed with the same detection parameters of object size and contrast. Scoring was done blindly without knowing the sample information by two independent scientists. Thereafter, the samples were classified according to the background dose and further analysis was carried out.

2.6. Statistical analysis

Statistical analysis was performed using STATISTICA version 9.1 [StatSoft, Inc. (2010) www.statsoft.com].The level of signif-

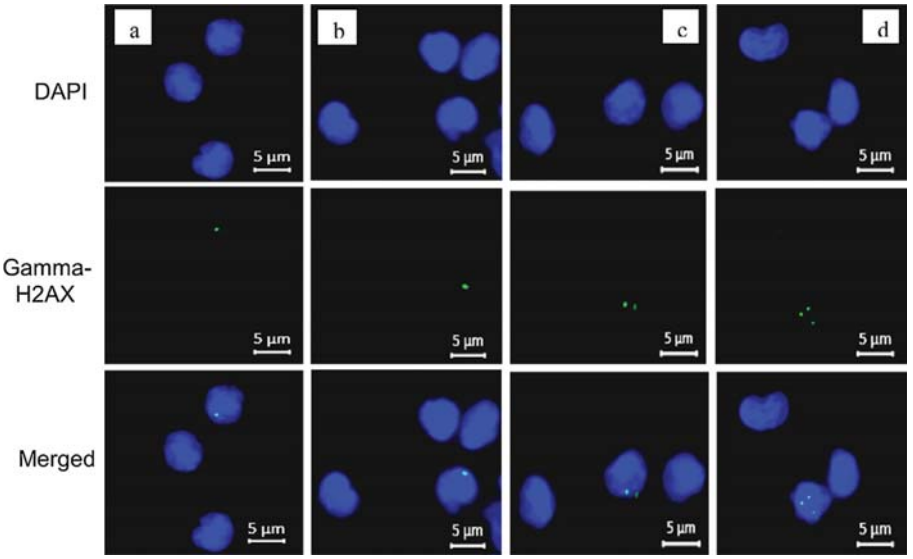

Fig. 1. Representative fluorescence microscopy images showing gamma-H2AX foci in PBMCs counterstained with DAPI. Panel 1 shows DAPI staining, Panel 2 shows gamma-H2AX antibody staining and Panel 3 shows merged images. Scoring was carried out in merged images. In the panel 2 and 3, the columns (a) and (b) single focus per cell, (c) two foci/cell, (d) three foci/cell.

Please cite this article in press as: V. Jain, et al., Lack of increased DNA double-strand breaks in peripheral blood mononuclear cells of individuals from high level natural radiation areas of Kerala coast in India, Mutat. Res.: Fundam. Mol. Mech. Mutagen. (2016), http://dx.doi.org/10.1016/j.mrfmmm.2016.03.002

icance was set at $p \leq 0.05$ for all statistical analysis. The mean frequency of foci was calculated by dividing the total number of foci observed by total number of cells scored for each sample. Student *t*-test was employed for comparison of mean foci/cell between two subgroups, and ANOVA, for comparison across more than two subgroups. Regression analysis was carried out to study influence of background dose and age on spontaneous frequency of gamma-H2AX foci. Coefficient of variation (CV) which represents the variability in relation to the mean was calculated by taking the ratio of standard deviation and mean (CV = standard deviation/mean × 100).

3. Results

The spontaneous frequency of DNA DSBs was estimated using gamma-H2AX marker among 91 random, healthy male donors (NLNRA, N = 30, and HLNRA, N = 61) in the study population. The mean background dose, mean age and frequency of gamma-H2AX foci per cell are given in Table 1. The mean background dose of the individuals from NLNRA was 1.28 ± 0.086 (range 1.1–1.5 mGy/year) and the mean background dose of individuals from HLNRA was 8.28 ± 4.96 mGy/year (range 1.57–21.60 mGy/year). The mean age of NLNRA and HLNRA individuals was 35.5 ± 6.35 years and 36.1 ± 7.43 years, respectively with an average of 35.9 ± 7.9 years among the 91 individuals studied. No statistically significant difference (P = 0.3) was observed between individuals from NLNRA and HLNRA with respect to age.

The mean spontaneous frequency of gamma-H2AX foci among the NLNRA individuals was 0.095 ± 0.009 per cell and ranged between 0.01–0.28 foci per cell. The mean frequency of gamma-H2AX foci among HLNRA individuals was 0.084 ± 0.004 per cell with a range between 0.02–0.17 foci per cell, which was not significantly (P = 0.2) different from the frequency observed among NLNRA individuals. Smoking did not influence the frequency of foci among individuals from NLNRA (P = 0.43) and HLNRA (P = 0.57). The overall CV of gamma-H2AX foci among these 91 individuals was observed to be approximately 44% (NLNRA = 54% and HLNRA = 37%). The representative fluorescence microscopy image given in Fig. 1 shows the distribution of one, two, three gamma-H2AX focus/foci in PBMCs counterstained with DAPI.

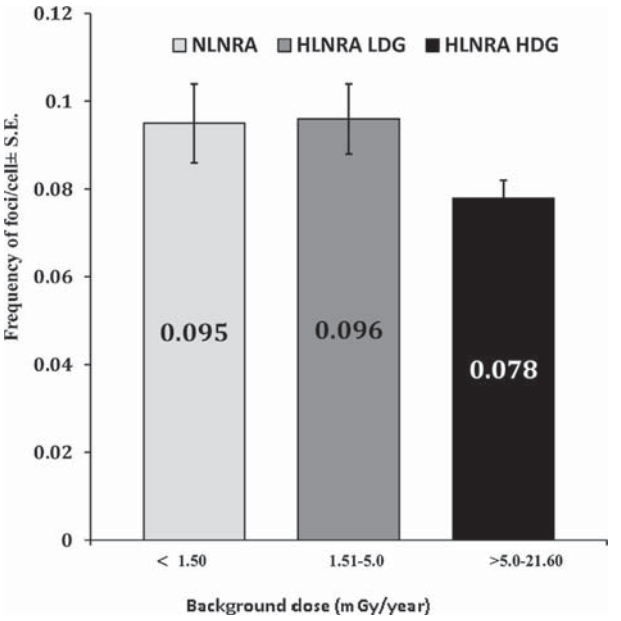

Fig. 2. Mean frequency of gamma-H2AX foci/cell observed in individuals from NLNRA (≤1.50 mGy/year), low dose group (LDG, 1.51–5.0 mGy/year) and high dose group (HDG, >5.0 mGy/year) of HLNRA. NLNRA: Normal level natural radiation area, HLNRA: High level natural radiation area. S.E: Standard error.

Analysis was carried out in three groups: NLNRA and two HLNRA groups: Low dose group (LDG, 1.51–5.0 mGy/year, mean dose: 2.63 ± 0.76 mGy/year) and High dose group (HDG, >5.0 mGy/year, mean dose: 11.04 ± 3.57mGy/year). The mean age among NLNRA, LDG and HDG individuals were 35.5 ± 6.35, 34.2 ± 5.7 and 37.05 ± 8.03 years, respectively, which were not statistically different. The three groups were also similar with respect to proportion

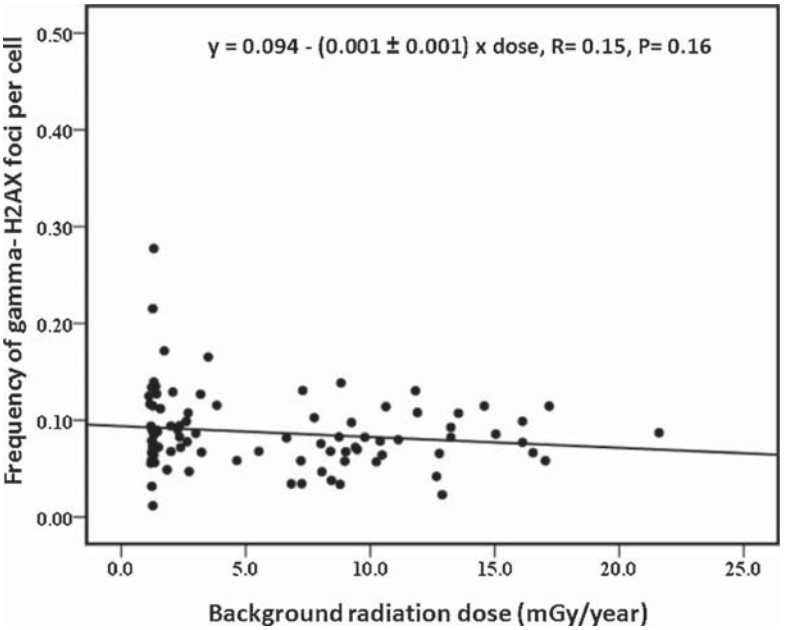

Fig. 3. Distribution of gamma-H2AX foci with respect to the background radiation dose (mGy/year). Each dot represents the frequency of gamma-H2AX foci/cell observed for each individual studied.

Please cite this article in press as: V. Jain, et al., Lack of increased DNA double-strand breaks in peripheral blood mononuclear cells of individuals from high level natural radiation areas of Kerala coast in India, Mutat. Res.: Fundam. Mol. Mech. Mutagen. (2016), http://dx.doi.org/10.1016/j.mrfmmm.2016.03.002

of smokers. The frequency of gamma-H2AX foci in NLNRA, LDG and HDG was observed to be 0.095 ± 0.009, 0.096 ± 0.008 and 0.078 ± 0.004 per cell respectively (as shown in Table 1 and Fig. 2). A marginal reduction in frequency of gamma-H2AX foci was observed in the HDG individuals as compared to the LDG of HLNRA and NLNRA individuals. ANOVA was carried out to compare the means among the groups and the difference was observed to be non-significant ($F_{(2,88)} = 2.22$, $P = 0.12$).

The distribution of gamma-H2AX foci was also assessed among the 91 individuals studied in terms of number of foci/cell as shown in Fig. 1 and Table 2. The percentage of gamma-H2AX positive cells (cells containing gamma-H2AX foci) in NLNRA and HLNRA individuals were 8.85% and 7.61% respectively. The percentage of gamma- H2AX positive cells in LDG and HDG was 8.44% and 7.22% respectively. As shown in Table 2, around 90% of the positive cells in all the three dose groups had only single gamma-H2AX focus [NLNRA = 95.44%, LDG (HLNRA) = 89.9%, HDG (HLNRA) = 93.17%]. However, the percentage of positive cells in NLNRA, LDG and HDG individuals with two foci was 3.56%, 8.76% and 5.28%, respectively. Approximately 2% cells had more than two foci. A marginal reduction ($P = 0.06$) in positive cells was observed in HDG individuals as compared to the LDG and NLNRA individuals.

The spontaneous frequency of gamma-H2AX foci/cell with respect to background dose levels is shown in Fig. 3. The regression analysis did not reveal any significant correlation with respect to the background dose levels ($y = 0.094–0.001 \times$ dose, $R = 0.15$, $P = 0.16$). However, a marginal positive correlation was observed ($y = 0.048 + 0.001 \times$ age, $R = 0.2$, $p = 0.06$) between the frequency of gamma-H2AX foci and age of the individuals as shown in Fig. 4A. Further, in sub group analysis, a significant positive influence of age on the frequency gamma-H2AX foci was found in individuals from NLNRA ($R = 0.37$, $p = 0.04$). However, no significant influence of age ($R = 0.11$, $P = 0.39$) was observed in individuals from HLNRA (Fig. 4B). No dose response was observed in terms of frequency of gamma-H2AX foci/cell with respect to background dose.

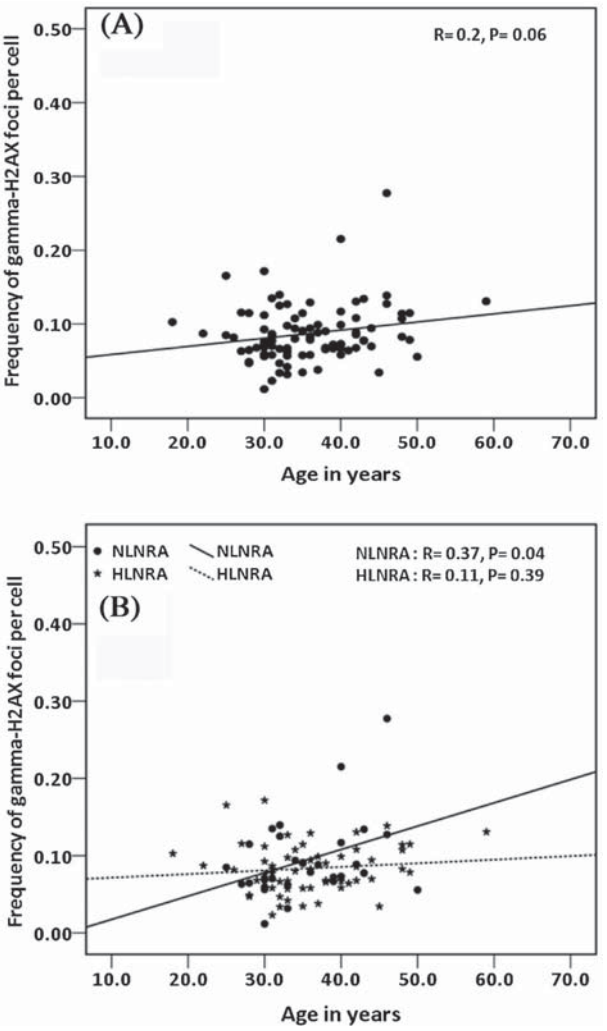

Fig. 4. Distribution of the frequency of gamma-H2AX foci/cell in individuals from HLNRA (>1.5 mGy/year) and NLNRA (<1.5 mGy/year) with respect to age. (A) Regression analysis to study the influence of age in all the 91 individuals. Each dot represents the frequency of gamma H2AX foci/cell for each individual studied. (B) Regression analysis was carried out in HLNRA and NLNRA individuals separately. HLNRA: high level natural radiation area, NLNRA: normal level natural radiation area. X-axis represents the age in years for the individuals studied.

4. Discussion

Quantification of radiation induced DNA damage at very low doses is important for risk estimation. So far, there is no conclusive evidence regarding the adverse effects of low dose radiation below 100 mSv. Risk estimation at low doses of radiation has been extrapolated from epidemiological data obtained at high acute doses of radiation. But recent reports indicated that biological effects of IR at low and high doses of exposure in human cells are qualitatively and quantitatively different at the level of DNA damage and gene expression [11–13]. Several end points have been analyzed in human cells after exposure to low dose radiation including chromosomal aberrations, micronuclei, mutation induction, gamma-H2AX foci, and apoptosis [8]. In addition, experimental evidences at low doses are essential to understand the mechanism occurring at cellular and molecular level.

The focus of the present study was to estimate and compare the baseline frequency of DSBs in PBMCs of individuals from different background dose groups from the Kerala coast. Extensive studies have been undertaken in this area in newborns as well as in adults using various biological end points [1,8,39–48]. So far, no dose response has been observed at any of the above end points studied. In the present study, attempt has been made to measure the basal level of DSBs in terms of gamma-H2AX foci, which are formed due to cellular response at the site of DNA damage. As shown in Table 1, no significant difference in the mean basal level frequency of gamma-H2AX foci was observed between HLNRA (>1.50 mGy/year) and NLNRA (≤1.50 mGy/year) individuals. Interestingly, the stratification of the samples into three different dose groups (≤1.5 mGy/year (NLNRA), two HLNRA groups [1.51–5.0 mGy/year (LDG) and >5.0 mGy/year (HDG)], showed a marginal reduction of DSBs in the HDG (HLNRA) as compared to NLNRA and LDG (HLNRA). This data might indicate that the individuals from HDG (HLNRA) have lower basal levels of DSBs as compared to NLNRA. The possible explanations could be as follows: Firstly, it could be due to active repair of DSBs occurring in human cells in HDG (HLNRA) individuals. Secondly, there could be elimination of damaged cells that might lead to lower frequency of basal level of DSBs. Thirdly, reduction of basal level of DSBs could be due to a better antioxidant defense mechanism in HDG (HLNRA) as compared to LDG (HLNRA) and NLNRA.

The present data on the baseline frequency of DSBs in terms of gamma-H2AX foci is supportive of the view that cell signaling does not occur in response to DNA damage at low dose exposures below 5.0 mSv [52]. Possibly, this is one of the reasons because of which we did not observe increase in gamma-H2AX foci in LDG (HLNRA) as compared to NLNRA. Another important noteworthy aspect is that the basal levels of radiation induced DNA damage due to very

Please cite this article in press as: V. Jain, et al., Lack of increased DNA double-strand breaks in peripheral blood mononuclear cells of individuals from high level natural radiation areas of Kerala coast in India, Mutat. Res.: Fundam. Mol. Mech. Mutagen. (2016), http://dx.doi.org/10.1016/j.mrfmmm.2016.03.002

Table 2
Distribution of gamma-H2AX focus/foci in peripheral blood mononuclear cells of individuals in different background dose groups. Numbers in parantheses show the percentage of positive cells having 1, 2, 3 or 4 focus/foci in different background dose groups. HLNRA: High Level Natural Radiation area, NLNRA: Normal Level Natural Radiation area. LDG: Low Dose group, HDG: High dose group.

Area	Background dose groups (mGy/year)	No. of cells scored	Total number of cells with gamma-H2AX foci (%)	Distribution of gamma-H2AX foci/cell			
				1 focus	2 foci	3 foci	4 foci
NLNRA	≤1.50	7935	702 (8.84%)	670 (8.44%)	25 (0.31%)	6 (0.08%)	1 (0.01%)
HLNRA	LDG (1.51–5.0)	5145	434 (8.44%)	390 (7.58%)	38 (0.74%)	5 (0.10%)	1 (0.02%)
	HDG (>5.0–21.6)	10752	776 (7.21%)	723 (6.72%)	41 (0.38%)	11 (0.10%)	1 (0.01%)
HLNRA (Total)	>1.50	15897	1210 (7.61%)	1113 (7.00%)	79 (0.50%)	16 (0.10%)	2 (0.01%)

low dose exposure are underestimated by higher levels of endogenous damage. As compared to the increased levels of endogenous damages (about ~50,000 lesions per day), the radiation induced damage in human cells is low [53].

It has also been reported that DNA repair processes are activated at doses more than 5.0 mGy [25,52].The same might be reflected in the present study. The basal level of DSBs in individuals belonging to HDG of HLNRA, which received an average background dose of 11.04 ± 3.57 mGy/year is 0.078 ± 0.004 foci/cell as compared to 0.096 ± 0.008 foci/cell in LDG of HLNRA (average dose: 2.63 ± 0.76 mGy/year). The reduction observed in DSB frequency in individuals belonging to HDG of HLNRA is clearly suggestive of active DNA repair process in human cells occurring at low chronic dose exposures. From the data obtained in the present study, it can reasonably be concluded that 5.0 mGy/year in HLNRA could be a threshold dose for DSB induction to *in vivo* chronic radiation exposures, below which the induction of DSBs may be similar to NLNRA. DNA repair study carried out in primary human fibroblast cells demonstrated that gamma-H2AX foci are substantially reduced in terms of DSB repair at low doses. It has been observed in cultures of non-dividing primary human fibroblasts that DSBs induced at very low radiation doses such as 1 mGy and 2.5 mGy do not show any foci loss (remains unrepaired) for many days. At the same time, at higher dose exposures, efficient DSB repair in terms of reduction of foci has been observed [13,16]. This again supports high sensitivity of gamma-H2AX foci for detection of DSBs at very low doses. Another aspect is that, there could be a minimum threshold level of damage, which is essential for cellular response to activate DNA repair machinery [13].

Since immuno-fluorescence detection of gamma-H2AX foci represents the DSBs in a 1:1 manner [15,16], this assay has advantage over other DSB detection methods such as Pulsed field gel electrophoresis and neutral comet assay [18,19,22,29,54]. Its increasing importance is reflected from its increasing use in various applications such as biological dosimetry, radio-therapeutic and diagnostic applications [22,36,55–58].

There are several studies, where baseline frequency of gamma-H2AX foci has been measured. For instance, Roch-Lefevre et al. [22] reported 0.09 ± 0.05 foci/per cell among 21 individuals from French population and 0.07 ± 0.05 foci/cell in six Cuban individuals. Rothkamm et al. [28] reported the base line value of 0.06 ± 0.02 foci/cell, whereas Djuzenova et al. [26] reported 0.12 ± 0.10 foci/cell among 12 individuals. In the present study, comparatively a larger number of samples (91 individuals) were analyzed and the overall baseline frequency of gamma-H2AX foci was observed to be 0.087 ± 0.039, which is comparable to the above published reports.

The data was analyzed in terms of distribution of foci per cell to understand whether the ionization process has traversed single or multiple tracks at such low dose exposures. The spatial distribution of radiation-induced DNA breaks within the cell nucleus depends on radiation quality in terms of energy deposition pattern [38]. However, several studies at low LET radiation, below 100 mGy, have not shown linearity, in contrary to the LNT hypothesis. A cell nucleus exposed to 100 mGy is traversed by ~100 electron tracks. But for natural background levels, each cell nucleus is possibly traversed by only on the order of 1 track per year. Therefore, excluding a threshold dose and extrapolating the linear dose-response relationship to such chronic low dose exposures where the induction of damage is occurring in single track is difficult [59]. A minimum threshold level of damage is essential for cellular response to activate DNA repair machinery to repair the damage [13]. There are studies which show linear increase in number or frequency of gamma-H2AX foci in human PBMCs [34]. Non linearity has also been observed in cell line [60]. However, our present study did not show any linear dose response in terms of gamma-H2AX foci.

In the present study, we have observed more than 90% gamma-H2AX positive cells had only single focus as shown in Table 2. However, only small percentage of cells (3% to 6%) had two foci per cell and approximately 2% cells had more than two foci (either three or four). Above findings indicate that very few percentage of cells have been hit by low dose radiation and most of the positive cells have been hit by single track of low LET ionizing radiation. Interestingly, only 7.22% cells are gamma-H2AX positive in HDG which is marginally lower (P = 0.06) as compared to NLNRA and LDG, where the frequencies are 8.85% and 8.44%. The above results also suggest similar pattern of distribution of foci in all the three groups. The average annual dose is almost 10 times higher in HDG individuals than NLNRA individuals. Therefore the data supports an existence of a threshold dose of 5mGy/year for DSBs on *in vivo* chronic low dose exposure, where the damage is similar to NLNRA and repair process does not seem to occur.

Another interesting fact is that, a dose of 10 mGy which is similar to radio-therapeutic or CT scan dose of low LET radiation has been shown to increase the number of gamma-H2AX foci in PBMCs [25,28]. HDG individuals have been exposed to an average dose of 11.04 ± 3.57 mGy/year, but we observed lower DSBs in HDG as compared to LDG and NLNRA. It is indicative of natural chronic low dose radiation induced adaptation in individuals from HLNRA. These findings are also supported by our recently published data on repair kinetics of DNA damage using alkaline comet assay, where we have observed efficient repair of DNA strand breaks in HLNRA [48].

We have also analyzed our data considering confounding factors such as influence of age and smoking habits on the basal level frequency of DSBs. We have observed a positive correlation (P = 0.04, R = 0.37) between age and DSB frequency in terms of gamma-H2AX foci in NLNRA individuals whereas no age related increase in gamma-H2AX foci was observed among HLNRA individuals (P = 0.39, R = 0.11). A previous study using alkaline comet assay reported a significant increase in basal DNA damage with age in NLNRA individuals. However, a significant negative correlation was observed between age and basal DNA damage in HLNRA individuals [47].

IR is known to induce various cellular responses including DNA damage response (DDR), DNA repair and apoptosis. It may also affect immune system which leads to induction of inflammatory

Please cite this article in press as: V. Jain, et al., Lack of increased DNA double-strand breaks in peripheral blood mononuclear cells of individuals from high level natural radiation areas of Kerala coast in India, Mutat. Res.: Fundam. Mol. Mech. Mutagen. (2016), http://dx.doi.org/10.1016/j.mrfmmm.2016.03.002

responses [61]. DDR leads to the activation of cell cycle check point and cell cycle arrest which allows the cells to repair the damage by activating various DNA repair pathways. Involvement of DSB repair pathways in PBMCs at G0/G1 cells using end points such as gene, protein and miRNA expression might give some clue to understand the role of DNA repair after low dose exposures. Our studies on radio-adaptive response at acute dose exposures have shown involvement of base excision and non-homologous end joining pathways in resting PBMCs [62–66]. In addition, our study demonstrated changes in chromatin fibers in response to radiation induced DNA damage at low doses [51]. Hence, further studies on DNA repair kinetics, radio-adaptive response of genes involved in DNA repair pathways and chromatin modification are required to understand the underlying mechanisms active in HLNRA.

In conclusion, the present study revealed that the basal levels of DSBs are similar in NLNRA and LDG (≤5.0 mGy/year). A marginal reduction of DSBs, observed among the individuals belonging to HDG (>5.0 mGy/year) of HLNRA plausibly due to better adaptation or active DNA repair process in HLNRA individuals. The absence of increased DSBs in NLNRA and LDG of HLNRA indicated that perhaps a threshold dose of 5 mGy/year exists in human cells for *in vivo* chronic exposures.

Conflicts of interest

All the authors declare that there are no conflicts of interest.

Acknowledgements

We profusely thank the volunteers who have willingly participated in the study. We are also thankful to all the staff members of LLRRL Kollam and LLRRS, Mumbai for extending co-operation at various stages of the experiment.

References

[1] B. Das, Genetic studies on human population residing in High Level Natural Radiation Areas of Kerala coast, BARC News Lett. (2010) 28–37.
[2] E. Cardis, M. Hatch, The Chernobyl accident–an epidemiological perspective, Clin. Oncol. (R. Coll. Radiol.) 23 (2011) 251–260.
[3] E. Cardis, M. Vrijheid, M. Blettner, E. Gilbert, M. Hakama, C. Hill, G. Howe, J. Kaldor, C.R. Muirhead, M. Schubauer-Berigan, T. Yoshimura, F. Bermann, G. Cowper, J. Fix, C. Hacker, B. Heinmiller, M. Marshall, I. Thierry-Chef, D. Utterback, Y.O. Ahn, E. Amoros, P. Ashmore, A. Auvinen, J.M. Bae, J.B. Solano, A. Biau, E. Combalot, P. Deboodt, A. Diez Sacristan, M. Eklof, H. Engels, G. Engholm, G. Gulis, R. Habib, K. Holan, H. Hyvonen, A. Kerekes, J. Kurtinaitis, H. Malker, M. Martuzzi, A. Mastauskas, A. Monnet, M. Moser, M.S. Pearce, D.B. Richardson, F. Rodriguez-Artalejo, A. Rogel, H. Tardy, M. Telle-Lamberton, I. Turai, M. Usel, K. Veress, Risk of cancer after low doses of ionising radiation: retrospective cohort study in 15 countries, BMJ 331 (2005) 77.
[4] G. Smith, UNSCEAR 2013 Report. Volume I: report to the General Assembly, Annex A: levels and effects of radiation exposure due to the nuclear accident after the 2011 great east-Japan earthquake and tsunami, J. Radiol. Prot. 34 (2014) 725–727.
[5] J.D. Boice Jr., J.H. Hendry, N. Nakamura, O. Niwa, S. Nakamura, K. Yoshida, Low-dose-rate epidemiology of high background radiation areas, Radiat. Res. 173 (2010) 849–854.
[6] R.R. Nair, B. Rajan, S. Akiba, P. Jayalekshmi, M.K. Nair, P. Gangadharan, T. Koga, H. Morishima, S. Nakamura, T. Sugahara, Background radiation and cancer incidence in Kerala, India-Karanagappally cohort study, Health Phys. 96 (2009) 55–66.
[7] Z. Tao, Y. Zha, S. Akiba, Q. Sun, J. Zou, J. Li, Y. Liu, H. Kato, T. Sugahara, L. Wei, Cancer mortality in the high background radiation areas of Yangjiang, China during the period between 1979 and 1995, J. Radiat. Res. 41 (Suppl) (2000) 31–41.
[8] W.F. Morgan, W.J. Bair, Issues in low dose radiation biology: the controversy continues. A perspective, Radiat. Res. 179 (2013) 501–510.
[9] P.C. Kesavan, Linear, no threshold response at low doses of ionizing radiation: ideology, prejudice and science, Curr. Sci. 107 (2014) 46–53.
[10] D.J. Brenner, Extrapolating radiation-induced cancer risks from low doses to very low doses, Health Phys. 97 (2009) 505–509.
[11] S.A. Amundson, R.A. Lee, C.A. Koch-Paiz, M.L. Bittner, P. Meltzer, J.M. Trent, A.J. Fornace Jr., Differential responses of stress genes to low dose-rate gamma irradiation, Mol. Cancer Res. 1 (2003) 445–452.
[12] L.H. Ding, M. Shingyoji, F. Chen, J.J. Hwang, S. Burma, C. Lee, J.F. Cheng, D.J. Chen, Gene expression profiles of normal human fibroblasts after exposure to ionizing radiation: a comparative study of low and high doses, Radiat. Res. 164 (2005) 17–26.
[13] S. Grudzenski, A. Raths, S. Conrad, C.E. Rube, M. Lobrich, Inducible response required for repair of low-dose radiation damage in human fibroblasts, Proc. Natl. Acad. Sci. U. S. A. 107 (2010) 14205–14210.
[14] S.M. Miller, C.L. Ferrarotto, S. Vlahovich, R.C. Wilkins, D.R. Boreham, J.A. Dolling, Canadian Cytogenetic Emergency network (CEN) for biological dosimetry following radiological/nuclear accidents, Int. J. Radiat. Biol. 83 (2007) 471–477.
[15] L.J. Kuo, L.X. Yang, Gamma-H2AX—a novel biomarker for DNA double-strand breaks, In Vivo 22 (2008) 305–309.
[16] K. Rothkamm, M. Lobrich, Evidence for a lack of DNA double-strand break repair in human cells exposed to very low x-ray doses, Proc. Natl. Acad. Sci. U. S. A. 100 (2003) 5057–5062.
[17] M. Lobrich, A. Shibata, A. Beucher, A. Fisher, M. Ensminger, A.A. Goodarzi, O. Barton, P.A. Jeggo, GammaH2AX foci analysis for monitoring DNA double-strand break repair: strengths, limitations and optimization, Cell Cycle 9 (2010) 662–669.
[18] I.H. Ismail, T.I. Wadhra, O. Hammarsten, An optimized method for detecting gamma-H2AX in blood cells reveals a significant interindividual variation in the gamma-H2AX response among humans, Nucleic Acids Res. 35 (2007) e36.
[19] E.P. Rogakou, D.R. Pilch, A.H. Orr, V.S. Ivanova, W.M. Bonner, DNA double-stranded breaks induce histone H2AX phosphorylation on serine 139, J. Biol. Chem. 273 (1998) 5858–5868.
[20] S. Panier, S.J. Boulton, Double-strand break repair: 53BP1 comes into focus, Nat. Rev. Mol. Cell Biol. 15 (2014) 7–18.
[21] K. Rothkamm, S. Barnard, J. Moquet, M. Ellender, Z. Rana, S. Burdak-Rothkamm, DNA damage foci: meaning and significance, Environ. Mol. Mutagen. 56 (2015) 491–504.
[22] S. Roch-Lefevre, T. Mandina, P. Voisin, G. Gaetan, J.E. Mesa, M. Valente, P. Bonnesoeur, O. Garcia, L. Roy, Quantification of gamma-H2AX foci in human lymphocytes: a method for biological dosimetry after ionizing radiation exposure, Radiat. Res. 174 (2010) 185–194.
[23] A. Kinner, W. Wu, C. Staudt, G. Iliakis, Gamma-H2AX in recognition and signaling of DNA double-strand breaks in the context of chromatin, Nucleic Acids Res. 36 (2008) 5678–5694.
[24] T.T. Paull, E.P. Rogakou, V. Yamazaki, C.U. Kirchgessner, M. Gellert, W.M. Bonner, A critical role for histone H2AX in recruitment of repair factors to nuclear foci after DNA damage, Curr. Biol. 10 (2000) 886–895.
[25] M. Lobrich, N. Rief, M. Kuhne, M. Heckmann, J. Fleckenstein, C. Rube, M. Uder, In vivo formation and repair of DNA double-strand breaks after computed tomography examinations, Proc. Natl. Acad. Sci. U. S. A. 102 (2005) 8984–8989.
[26] C.S. Djuzenova, I. Elsner, A. Katzer, E. Worschech, L.V. Distel, M. Flentje, B. Polat, Radiosensitivity in breast cancer assessed by the histone gamma-H2AX and 53BP1 foci, Radiat. Oncol. 8 (2013) 98.
[27] E.L. Leatherbarrow, J.V. Harper, F.A. Cucinotta, P. O'Neill, Induction and quantification of gamma-H2AX foci following low and high LET-irradiation, Int. J. Radiat. Biol. 82 (2006) 111–118.
[28] K. Rothkamm, S. Balroop, J. Shekhdar, P. Fernie, V. Goh, Leukocyte DNA damage after multi-detector row CT: a quantitative biomarker of low-level radiation exposure, Radiology 242 (2007) 244–251.
[29] V. Valdiglesias, S. Giunta, M. Fenech, M. Neri, S. Bonassi, γH2AX as a marker of DNA double strand breaks and genomic instability in human population studies, Mutat. Res. 753 (2013) 24–40.
[30] O.A. Sedelnikova, E.P. Rogakou, I.G. Panyutin, W.M. Bonner, Quantitative detection of (125)IdU-induced DNA double-strand breaks with gamma-H2AX antibody, Radiat. Res. 158 (2002) 486–492.
[31] L. Beels, J. Werbrouck, H. Thierens, Dose response and repair kinetics of gamma-H2AX foci induced by in vitro irradiation of whole blood and T-lymphocytes with X- and gamma-radiation, Int. J. Radiat. Biol. 86 (2010) 760–768.
[32] M. Lassmann, H. Hanscheid, D. Gassen, J. Biko, V. Meineke, C. Reiners, H. Scherthan, In vivo formation of gamma-H2AX and 53BP1 DNA repair foci in blood cells after radioiodine therapy of differentiated thyroid cancer, J. Nucl. Med. 51 (2010) 1318–1325.
[33] M.S. May, M. Brand, W. Wuest, K. Anders, T. Kuwert, O. Prante, D. Schmidt, S. Maschauer, R.C. Semelka, M. Uder, M.A. Kuefner, Induction and repair of DNA double-strand breaks in blood lymphocytes of patients undergoing (1)(8)F-FDG PET/CT examinations, Eur. J. Nucl. Med. Mol. Imaging 39 (2012) 1712–1719.
[34] B.M. Halm, A.A. Franke, J.F. Lai, H.C. Turner, D.J. Brenner, V.M. Zohrabian, R. DiMauro, Gamma-H2AX foci are increased in lymphocytes in vivo in young children 1 h after very low-dose X-irradiation: a pilot study, Pediatr. Radiol. 44 (2014) 1310–1317.
[35] S. Zahnreich, A. Ebersberger, B. Kaina, H. Schmidberger, Biodosimetry based on gamma-H2AX quantification and cytogenetics after partial- and total-body irradiation during fractionated radiotherapy, Radiat. Res. 183 (2015) 432–446.
[36] S. Horn, S. Barnard, K. Rothkamm, Gamma-H2AX-based dose estimation for whole and partial body radiation exposure, PLoS One 6 (2011) e25113.
[37] A. Asaithamby, N. Uematsu, A. Chatterjee, M.D. Story, S. Burma, D.J. Chen, Repair of HZE-particle-induced DNA double-strand breaks in normal human fibroblasts, Radiat. Res. 169 (2008) 437–446.

Please cite this article in press as: V. Jain, et al., Lack of increased DNA double-strand breaks in peripheral blood mononuclear cells of individuals from high level natural radiation areas of Kerala coast in India, Mutat. Res.: Fundam. Mol. Mech. Mutagen. (2016), http://dx.doi.org/10.1016/j.mrfmmm.2016.03.002

[38] F. Antonelli, A. Campa, G. Esposito, P. Giardullo, M. Belli, V. Dini, S. Meschini, G. Simone, E. Sorrentino, S. Gerardi, G.A. Cirrone, M.A. Tabocchini, Induction and repair of DNA DSB as revealed by H2AX phosphorylation foci in human fibroblasts exposed to low- and high-LET radiation: relationship with early and delayed reproductive cell death, Radiat. Res. 183 (2015) 417–431.
[39] G. Jaikrishan, V.J. Andrews, M.V. Thampi, P.K. Koya, V.K. Rajan, P.S. Chauhan, Genetic monitoring of the human population from high-level natural radiation areas of Kerala on the southwest coast of India. I. Prevalence of congenital malformations in newborns, Radiat. Res. 152 (1999) S149–153.
[40] G. Jaikrishan, K.R. Sudheer, V.J. Andrews, P.K. Koya, M. Madhusoodhanan, C.K. Jagadeesan, M. Seshadri, Study of stillbirth and major congenital anomaly among newborns in the high-level natural radiation areas of Kerala, India, J. Community Genet. 4 (2013) 21–31.
[41] P.K. Koya, M.P. Chougaonkar, P. Predeep, P.J. Jojo, V.D. Cheriyan, Y.S. Mayya, M. Seshadri, Effect of low and chronic radiation exposure: a case-control study of mental retardation and cleft lip/palate in the monazite-bearing coastal areas of southern Kerala, Radiat. Res. 177 (2012) 109–116.
[42] V.D. Cheriyan, C.J. Kurien, B. Das, E.N. Ramachandran, C.V. Karuppasamy, M.V. Thampi, K.P. George, P.C. Kesavan, P.K. Koya, P.S. Chauhan, Genetic monitoring of the human population from high-level natural radiation areas of Kerala on the southwest coast of India. II. Incidence of numerical and structural chromosomal aberrations in the lymphocytes of newborns, Radiat. Res. 152 (1999) S154–158.
[43] E.N. Ramachandran, C.V. Karuppasamy, V.D. Cheriyan, D.C. Soren, B. Das, V. Anilkumar, P.K. Koya, M. Seshadri, Cytogenetic studies on newborns from high and normal level natural radiation areas of Kerala in southwest coast of India, Int. J. Radiat. Biol. 89 (2013) 259–267.
[44] B. Das, C.V. Karuppasamy, Spontaneous frequency of micronuclei among the newborns from high level natural radiation areas of Kerala in the southwest coast of India, Int. J. Radiat. Biol. 85 (2009) 272–280.
[45] B. Das, D. Saini, M. Seshadri, Telomere length in human adults and high level natural background radiation, PLoS One 4 (2009) e8440.
[46] B. Das, D. Saini, M. Seshadri, No evidence of telomere length attrition in newborns from high level natural background radiation areas in Kerala coast, south west India, Int. J. Radiat. Biol. 88 (2012) 642–647.
[47] P.R. Kumar, V.D. Cheriyan, M. Seshadri, Evaluation of spontaneous DNA damage in lymphocytes of healthy adult individuals from high-level natural radiation areas of Kerala in India, Radiat. Res. 177 (2012) 643–650.
[48] P.R. Kumar, M. Seshadri, G. Jaikrishan, B. Das, Effect of chronic low dose natural radiation in human peripheral blood mononuclear cells: evaluation of DNA damage and repair using the alkaline comet assay, Mutat. Res. 775 (2015) 59–65.
[49] R.R.K. Nair, S. Akiba, V.S. Binu, P. Jayalekshmi, P. Gangadharan, M.K. Nair, B. Rajan, Individual dose estimation-our experience with the Karunagapally studyin Kerala, India, Int. Congr. Ser. 1276 (2005) 41–45.
[50] X. Huang, Z. Darzynkiewicz, Cytometric assessment of histone H2AX phosphorylation: a reporter of DNA damage, Methods Mol. Biol. 314 (2006) 73–80.
[51] V. Jain, P.A. Hassan, B. Das, Radiation-induced conformational changes in chromatin structure in resting human peripheral blood mononuclear cells, Int. J. Radiat. Biol. 90 (2014) 1143–1151.
[52] M. Tubiana, L.E. Feinendegen, C. Yang, J.M. Kaminski, The linear no-threshold relationship is inconsistent with radiation biologic and experimental data, Radiology 251 (2009) 13–22.
[53] M.E. Lomax, L.K. Folkes, P. O'Neill, Biological consequences of radiation-induced DNA damage: relevance to radiotherapy, Clin. Oncol. (R. Coll. Radiol.) 25 (2013) 578–585.
[54] W.M. Bonner, C.E. Redon, J.S. Dickey, A.J. Nakamura, O.A. Sedelnikova, S. Solier, Y. Pommier, GammaH2AX and cancer, Nat. Rev. Cancer 8 (2008) 957–967.
[55] A. Ivashkevich, C.E. Redon, A.J. Nakamura, R.F. Martin, O.A. Martin, Use of the gamma-H2AX assay to monitor DNA damage and repair in translational cancer research, Cancer Lett. 327 (2012) 123–133.
[56] J. Moquet, S. Barnard, K. Rothkamm, Gamma-H2AX biodosimetry for use in large scale radiation incidents: comparison of a rapid '96 well lyse/fix' protocol with a routine method, PeerJ 2 (2014) e282.
[57] C. Vandevoorde, M. Gomolka, U. Roessler, D. Samaga, C. Lindholm, M. Fernet, J. Hall, E. Pernot, H. El-Saghire, S. Baatout, A. Kesminiene, H. Thierens, EPI-CT: in vitro assessment of the applicability of the gamma-H2AX-foci assay as cellular biomarker for exposure in a multicentre study of children in diagnostic radiology, Int. J. Radiat. Biol. (2015) 1–11.
[58] C. Vandevoorde, C. Franck, K. Bacher, L. Breysem, M.H. Smet, C. Ernst, A. De Backer, K. Van De Moortele, P. Smeets, H. Thierens, gamma-H2AX foci as in vivo effect biomarker in children emphasize the importance to minimize x-ray doses in paediatric CT imaging, Eur. Radiol. 25 (2015) 800–811.
[59] J.S. Puskin, Perspective on the use of LNT for radiation protection and risk assessment by the U.S. Environmental Protection Agency, Dose Response 7 (2009) 284–291.
[60] T. Neumaier, J. Swenson, C. Pham, A. Polyzos, A.T. Lo, P. Yang, J. Dyball, A. Asaithamby, D.J. Chene, M.J. Bisselld, S. Thalhammera, S.V. Costes, Evidence for formation of DNA repair centers and dose-response nonlinearity in human cells, PNAS 109 (2012) 443–448.
[61] A.G. Georgakilas, A. Pavlopoulou, M. Louka, Z. Nikitaki, C.E. Vorgias, P.G. Bagos, I. Michalopoulos, Emerging molecular networks common in ionizing radiation, immune and inflammatory responses by employing bioinformatics approaches, Cancer Lett. (2015), http://dx.doi.org/10.1016/j.canlet.2015.03.021.
[62] D. Saini, S. Shelke, A. Mani Vannan, S. Toprani, V. Jain, B. Das, M. Seshadri, Transcription profile of DNA damage response genes at G(0) lymphocytes exposed to gamma radiation, Mol. Cell. Biochem. 364 (2012) 271–281.
[63] S. Shelke, B. Das, Dose response and adaptive response of non-homologous end joining repair genes and proteins in resting human peripheral blood mononuclear cells exposed to gamma radiation, Mutagenesis 30 (2015) 365–379.
[64] S.M. Toprani, B. Das, Role of base excision repair genes and proteins in gamma-irradiated resting human peripheral blood mononuclear cells, Mutagenesis 30 (2015) 247–261.
[65] V. Jain, B. Das, M. Seshadri, Transcriptional expression of H2B, CTP synthase and PLK3 genes in whole blood exposed to 60Co gamma radiation, Int. J. Low Radiat. 8 (2011) 55–65.
[66] S.M. Toprani, B. Das, Radio-adaptive response of base excision repair genes and proteins in human peripheral blood mononuclear cells exposed to gamma radiation, Mutagenesis 30 (2015) 663–676.

Please cite this article in press as: V. Jain, et al., Lack of increased DNA double-strand breaks in peripheral blood mononuclear cells of individuals from high level natural radiation areas of Kerala coast in India, Mutat. Res.: Fundam. Mol. Mech. Mutagen. (2016), http://dx.doi.org/10.1016/j.mrfmmm.2016.03.002

International Journal of Radiation Biology, December 2014; 90(12): 1143–1151

ISSN 0955-3002 print / ISSN 1362-3095 online
DOI: 10.3109/09553002.2014.925605

informa
healthcare

Radiation-induced conformational changes in chromatin structure in resting human peripheral blood mononuclear cells

Vinay Jain[1], P. A. Hassan[2] & Birajalaxmi Das[1]

[1]*Low Level Radiation Research Section, Radiation Biology and Health Sciences Division, Bio Science Group, and* [2]*Chemistry Division, Bhabha Atomic Research Centre, Trombay, Mumbai-400 085, India*

Abstract

Background: **Ionizing radiation induces a plethora of DNA damage including double-strand breaks (DSB) that may trigger a series of events such as transcription, DNA repair and alteration in the conformation of chromatin structure in human cells. We have made an attempt to study the conformational changes in chromatin fibers in irradiated human peripheral blood mononuclear cells (PBMC) using Dynamic Light Scattering (DLS) as a new tool.**

Materials and methods**: Venous blood samples were collected from 10 random, healthy individuals with written informed consent, approved by institutional ethics committee. PBMC were separated from blood, irradiated with different doses of gamma radiation from 0.25–1.0 Gy. Native chromatin was isolated from irradiated PBMC and changes in the hydrodynamic diameter of the chromatin fiber were measured using DLS. Both dose response and time kinetics was studied in order to see the chromatin changes. Radiation-induced DNA double-strand breaks were measured using gamma-H2AX (histone 2A member X) as a biomarker using flow cytometry and foci were visualized in confocal microscopy.**

Results: **A significant alteration in hydrodynamic diameter of the chromatin fiber was observed at lower doses (0.25 and 0.50 Gy), whereas at higher dose (1.0 Gy), the size of the chromatin fiber was comparable to unirradiated control. Among the 10 individuals studied, five individuals showed significant increase ($p \leq 0.002$) in hydrodynamic size at 0.25 Gy whereas four individuals showed significant decrease ($p \leq 0.009$) at 0.25 Gy. One individual did not show any significant difference as compared to control. However, dose-dependent increase in gamma-H2AX fluorescence signals as well as foci number was observed. Increased fragmentation of chromatin fiber was also observed using Atomic Force Microscopy at higher doses.**

Conclusion: **Radiation-induced DNA damage response can lead to individual specific conformational changes in chromatin structure at lower doses (0.25 Gy and 0.50 Gy) which can be detected using dynamic light scattering method in resting human PBMC.**

Keywords: Ionizing radiation, peripheral blood mono-nuclear cells (PBMC), DNA damage response, chromatin fiber conformational changes, Dynamic Light Scattering

Introduction

Ionizing radiation induces a variety of isolated and clustered DNA damage including double-strand breaks (DSB). However, the efficient DNA repair machinery in human cells maintains a balance between repair and cell death. DSB are complex damages, which may lead to consequences like lethal mutations, genome instability and carcinogenesis (Sutherland et al. 2000, Rydberg 2001). DNA damage response comprises of a series of events which may trigger changes at the level of transcription, histone modification and protein expression (Sutherland et al. 2000, Amundson et al. 2004, Corpet and Almouzni 2009, Horn et al. 2011, Jain et al. 2011, Polo and Jackson 2011, Saini et al. 2012). However, the packaging of human DNA is complex and the accessibility to damage sites for repair process to occur depends upon many factors including modifications and rearrangements in chromatin structure. Human genomic DNA is packaged into nucleosomes which are composed of a histone octamer consisting of four types of histone proteins (H2A, H2B, H3 and H4), wrapped by ~ 146 base pairs of double-stranded DNA. Dynamic packaging of DNA results in different levels of chromatin compaction from 10 nm fiber to higher order structures (Naumova et al. 2013) and plays a central role in DNA damage response. It may thereby affect several cellular processes like transcription, replication and repair (Rogakou et al. 1999, Lydall and Whitehall 2005, Kruhlak et al. 2006, Bing et al. 2007,

Correspondence: Dr. Birajalaxmi Das, MPhil, PhD, Head, Low Level Radiation Research Section, Radiation Biology and Health Sciences Division, Bio Science Group, Bhabha Atomic Research Centre, Trombay, Mumbai 400 085. India. Tel: + 91 022 2559 5047/25590422. E-mail: birajalaxmi@yahoo.co.in, biraj@barc.gov.in

(Received 13 December 2013; revised 4 May 2014; accepted 14 May 2014)

Downs et al. 2007, Falk et al. 2007, Groth et al. 2007, Pandita and Richardson 2009).

Several studies have shown changes in the chromatin dynamics in response to radiation induced DNA double-strand breaks (Hittelman and Pollard 1984, Ljungman 1989, Belyaev et al. 2001, Attikum et al. 2004, Falk et al. 2007, Dinant et al. 2008, Kovalchuk and Baulch 2008, Pandita and Richardson 2009, Falk et al. 2010). DNA damage induces various post-translational modifications such as phosphorylation, acetylation etc., in histone proteins that alters chromatin structure (Corpet and Almouzni 2009). Phosphorylation at Ser 139 residue of H2A.X (histone 2A member X) is one of the initial signals of DNA double-strand breaks (Rogakou et al. 1998, Rothkamm and Löbrich 2003, Horn et al. 2011). Phosphorylated H2AX or gamma-H2AX triggers the accumulation of a various DNA damage signaling, chromatin modifying and DNA repair proteins at DSB site and form discrete nuclear foci termed as ionizing radiation-induced foci (IRIF) (Paull et al. 2000, Fernandez-Capetillo et al. 2003, 2004, Kinner et al. 2008, Neumaier et al. 2012). It is surmised that DNA damage response may be different at low and high doses of radiation. Hence, low dose radiation-induced chromatin dynamics may have implications in the formation of IRIF cluster formation (Falk et al 2007).

There are various methods to detect changes in chromatin due to stress including ionizing radiation. Dynamic Light Scattering (DLS) is a technique, which allows studying the internal dynamics of biological macromolecules in solution. It is a non-invasive technique which has an advantage over scanning techniques like Atomic Force Microscopy (AFM) and Scanning Electron Microscopy (SEM), where fixation of biomolecules is required. DLS has been used to study protein-protein interactions, DNA-protein interactions and protein aggregation (Bloomfield 1981, Lee et al. 1981, Holde et al. 1998, Berne and Pecora 2000, Hanlon et al. 2010). Light scattering techniques have been used in studying helical structures of chromatin in solution (Campbell et al. 1978), finding linker/spacer regions in chromatin (Schmitz and Shaw 1977, Roche et al. 1985) and in understanding the higher order chromatin structure (Eisenberg et al. 1979, Dimitrov et al. 1986a, 1986b, Greulich et al. 1986, Makarov et al. 1987). Most recently, DLS has also been used to study the effect of drug binding on chromatin structure (Selvi et al. 2009, Majumdar and Dasgupta 2011). However, its application in studying radiation-induced changes in chromatin structure has not been explored yet. Human peripheral blood mononuclear cells (PBMC) are most radiosensitive and are ideal to study the radiation-induced changes at the level of chromatin in vitro. In the present study, we made an attempt to evaluate chromatin conformational changes in irradiated PBMC using DLS as a tool. The level of damage or fragmentation in the chromatin fiber was assessed using AFM. DNA damage quantitation was performed using gamma-H2AX as a marker. DNA double-strand break-specific foci in irradiated PBMC were visualized using confocal microscopy and the fluorescence positive cells were quantitated using flow cytometry (Huang and Darzynkiewicz 2006, Ismail et al. 2007).

Materials and methods

Ethics statement

Venous blood samples were collected from 10 random healthy volunteers with written informed consent, which was approved by Medical Ethics Committee, Bhabha Atomic Research Centre, Trombay, Mumbai, India.

Isolation and irradiation of PBMC from human blood

Approximately, 12 ml of venous blood samples were collected from these individuals (Age range: 25–35 years) in Ethylenediaminetetraacetic acid (EDTA) containing Vacutainers® (BD, New Jersey, USA). All the individuals were non-smokers and without any history of chronic illness. PBMC were separated from blood by Ficoll-paque density gradient centrifugation (Bøyum 1968) using Histopaque® 1077 (Sigma, St Louis, MO, USA) and irradiated with different doses of gamma radiation using ^{60}Co source (Bhabhatron II, Panacea Medical Technologies, Bangalore, India) at a dose rate of 1.0 Gy/min. Native chromatin was isolated from irradiated cells exposed to 0.25, 0.5 and 1.0 Gy along with sham-irradiated controls. For time kinetics experiment, PBMC were irradiated at 1.0 Gy and hydrodynamic diameter of chromatin was estimated using DLS at 15 min, 45 min, and 90 min and 120 min post-irradiation.

Chromatin isolation

Isolation of native chromatin from irradiated PBMC was carried out using the protocol described elsewhere (Lee et al. 1981, Das et al. 2006) with a few modifications. The protocol in brief is as follows: PBMC were incubated in hypotonic buffer [0.25 M Sucrose, 10 mM Tris-HCl, pH 7.4, 10 mM KCl, 1.5 mM $MgCl_2$, 0.1 mM Phenylmethylsulfonyl fluoride (PMSF), Sigma] and were kept on ice for 30 min. Cell lysates were centrifuged at 2200 *g* for 10 min to obtain nuclear pellets which was resuspended in MNase digestion buffer (50 mM Tris-HCl, 1 mM $CaCl_2$, 25 mM NaCl, 3 mM $MgCl_2$, 0.2 mM PMSF) and partial digestion of nuclei was done with 0.00125 U of MNase enzyme (Sigma) for 1 min at room temperature to obtain long and intact chromatin fibers. The digestion of nuclei was stopped with 10 mM EDTA and the tubes were kept on ice for 30 min to obtain chromatin fragments in solution. Nuclear debris was removed by centrifugation at 6500 *g* for 10 min and chromatin fragments were dialyzed against 10 mM Tris-HCl (pH 7.4) buffer.

Dynamic Light Scattering analysis

Dynamic light scattering experiments were performed using a Malvern 4800 Autosizer (Malvern Instruments Ltd, Malvern, Worcestershire, UK) employing 7132 digital correlator. Dialyzed chromatin at a concentration of 4 μg/ml was taken for DLS measurements. The light source was an Ar-ion laser operated at 514.5 nm with maximum power output of 2 W. DLS measures time dependent fluctuations in the scattering intensity and uses this to determine the diffusion coefficient 'D' of the sample by means of its inbuilt autocorrelator. Size of the particle (Hydrodynamic diameter) is calculated using Stokes-Einstein equation,

$$D_h = \frac{kT}{f} = \frac{kT}{3\pi\eta D} \quad (1)$$

where D_h is the hydrodynamic diameter, k is the Bolzmann constant, f is particle frictional coefficient, η is solvent viscosity (here, we have given the viscosity of water as the solvent viscosity), T is the absolute temperature and D is the diffusion coefficient. The distribution in diffusion coefficient was obtained by an Inverse Laplace Transformation algorithm 'CONTIN' supplied by instrument manufacturer. Multiple readings were taken for each sample and mean and standard deviation was calculated and used for further analysis.

Analysis of damage in the chromatin fiber using Atomic Force Microscopy

The level of fragmentation of chromatin fibers was studied using AFM. For that purpose, native chromatin was isolated from irradiated PBMC at 5.0 Gy along with sham irradiated control and freshly prepared chromatin fragments were fixed with 0.1% glutaraldehyde and incubated overnight at 4°C. After fixation, the samples were spread onto a freshly cleaved mica substrate and kept at room temperature for 15 min. AFM imaging was carried out on mica sheet and the measurements were taken in contact mode using a scanning probe microscope (SPM-Solver P47, NT-MDT, Moscow, Russia). Rectangular cantilevers of silicon nitride having force constant of 3 N/m were employed for measurement.

Quantitation and visualization of DNA double-strand breaks using gamma-H2AX

DNA damage quantitation was done in flow cytometer (Partec Cyflow, Munster, Germany) using phosphorylated H2AX (gamma-H2AX) as a biomarker. The visualization of gamma-H2AX foci was done using confocal microscopy.

(a) Flow cytometric analysis. Peripheral blood mononuclear cells were irradiated with different doses between 0.25 Gy and 2.0 Gy along with sham-irradiated control. The sample preparation for flow cytometry was carried out according to the protocol described elsewhere (Huang and Darzynkiewicz 2006) with a few modifications. Briefly, cells were incubated at 37°C for 30 min and fixed with 1% formaldehyde for 15 min on ice. After fixation, cells were washed with phosphate buffered saline (pH 7.5) and then resuspended in 70% alcohol and incubated at −20°C for 2 h. Cells were permeabilized with 0.2% Triton- X- 100 solution for 5 min at room temperature. Blocking was done with 1% bovine serum albumin (Sigma) and cells were incubated overnight at 4°C in 1:100 concentration of anti-phospho-histone H2AX (Ser139), antibody (Upstate-Millipore 05-636, Billerica, MA, USA). After overnight incubation, cells were washed in blocking solution and labeled with AlexaFluor 488-conjugated rabbit anti-mouse antibody (Molecular probes A-11059, Eugene, USA). Cells were counter-stained with 4′,6-diamidino-2-phenylindole (DAPI, Sigma) (5 µg/ml) for 20 min at room temperature and taken for flow cytometric analysis. Approximately 50,000 cells were analyzed for each dose point studied. Gating was done in order to include singlet cells with good DAPI staining for analysis.

(b) Visualization of gamma-H2AX by confocal microscopy. The method for fixation and labeling of PBMC for confocal microscopy is the same as used for flow cytometry experiments. Labeled PBMC were diluted to a concentration of 1×10^6 cells / ml and 100 µl of cell suspension was layered onto poly-l-lysine coated coverslips (Becton Dickinson BioCoat™ 354085, NJ, USA). Coverslips were kept for 30 min at room temperature for adherence, washed with phosphate buffered saline and mounted on glass slides using Prolong Gold Antifade DAPI reagent (Molecular Probes P 36931, USA). Imaging was done using laser scanning microscope (Carl Zeiss, Model - LSM 510 Meta, Gottingen, Germany).

Time kinetics

Human PBMC were irradiated with 1.0 Gy of dose and were incubated for different time intervals such as 15 min, 45 min, 90 min, and 120 min. Native chromatin was isolated at the above time intervals and hydrodynamic measurements were carried out using dynamic light scattering.

Results

We studied radiation-induced dynamics of chromatin fibers in human PBMC of 10 individuals using DLS where hydrodynamic diameter of chromatin fibers was measured. Hydrodynamic diameter measured in DLS is the size of the sphere that has the same translational diffusion coefficient as the particle being measured. The translational diffusion coefficient depends on the size, shape, and the surface charge of the particle in solution and hence provides information about the conformational changes taking place in chromatin structure following DNA damage. Figure 1 shows a representative pattern of autocorrelation function and intensity size distribution from DLS instrument. Our data did not reveal any significant change in the average values of hydrodynamic diameter (D_h, nm) of chromatin fibers of 10 individuals after exposure of their PBMC to 0.25, 0.5 and 1.0 Gy as compared to unirradiated control. The average hydrodynamic diameter for chromatin fibers from 10 individuals was observed to be 193.2 ± 22.4 nm, 196.7 ± 29.4 nm, 195.9 ± 32.1 nm and 194.2 ± 24.2 nm at 0.0 Gy (unirradiated control), 0.25, 0.50 and 1.0 Gy, respectively. Inter-individual variation in the hydrodynamic size was clearly observed. Among the 10 individuals studied, significant changes were observed in the chromatin fibers among nine individuals at 0.25 Gy. Only one individual did not show any significant difference as compared to control.

As shown in Table I, chromatin fibers of six individuals showed changes both at 0.25 Gy and 0.50 Gy and only two individuals showed changes at 1.0 Gy. Further, we observed two different patterns of change in hydrodynamic diameter (increase or decrease in size) at 0.25 Gy among nine individuals (Figure 2). Chromatin fibers from five individuals showed significant increase ($p \leq 0.002$) in the average hydrodynamic diameter of the chromatin fibers at 0.25 Gy (Trend A) whereas significant decrease ($p \leq 0.009$) was observed in

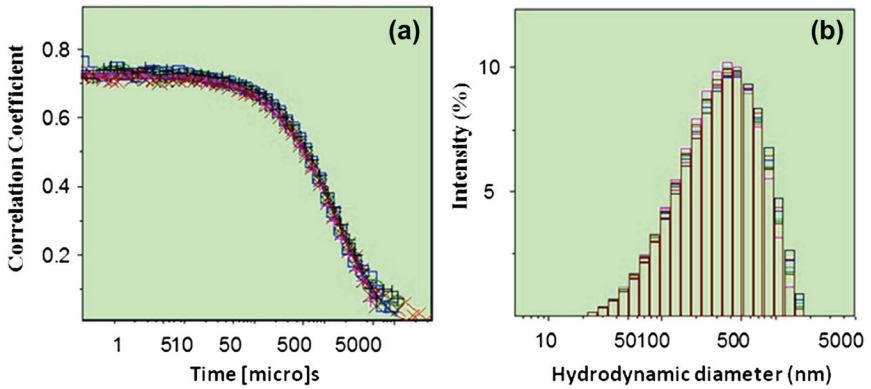

Figure 1. Representative images showing (a) autocorrelation of scattered light intensity with time. The autocorrelation function is used to obtain hydrodynamic diameter of chromatin fibers. (b) Intensity weighted hydrodynamic diameter distribution of chromatin fibers. Each colour represents DLS readings obtained for each data point. This Figure is reproduced in color in the online version of the *International Journal of Radiation Biology*.

the chromatin from four individuals (Trend B) (Figure 3). The average hydrodynamic diameter in trend A and trend B at 0.25 Gy was observed to be 216.66 ± 16.8 nm and 173.95 ± 28.98 nm, respectively. In summary, significant changes at the chromatin level were observed at lower dose points (0.25 Gy and 0.50 Gy) which recovered to its unirradiated state at higher dose points (1.0 Gy).

Since, chromatin from majority of individuals did not show significant difference in hydrodynamic diameter at 1.0 Gy, we carried out time kinetics experiments at 15, 45, 90 and 120 min at 1 Gy post-irradiation in chromatin from six individuals (three individuals from trend A and three from trend B). Interestingly, we observed significant changes in average hydrodynamic diameter at 45 min and 90 min ($p \leq 0.05$) time intervals, but at 120 min we have observed recovery of the size of the chromatin fiber, which was comparable with that of unirradiated control cells (Figure 4). The AFM image revealed that at 5.0 Gy, the chromatin fibers were fragmented and diffused as compared to the unirradiated ones where the chromatin fibers were intact (Figure 5).

DNA damage response and alteration of chromatin conformation complement each other. DSB were estimated in terms of increase in gamma-H2AX positive cells after irradiation with doses ranging from 0.25–2.0 Gy. The average percentage of gamma-H2AX positive cells in the 10 individuals is shown in Figure 6. Representative profile of gamma-H2AX fluorescence in PBMC of an individual is shown in Figure 7. The average number of gamma-H2AX positive cells increased from 6.5% in unirradiated cells to 74.8% after 2.0 Gy of irradiation. A dose-dependent increase in the number of gamma-H2AX foci was also visualized in these individuals using confocal microscopy (Figure 8).

Discussion

The organization of the human genome is very complex and dynamic. Chromatin reorganization plays an important role in DNA damage response by making damaged sites more accessible to damage sensor and repair proteins. Ionizing radiations induce DNA lesions which alter conformation of the chromatin in the vicinity of lesion. Complex damages like DNA double-strand breaks and non-DSB clusters are difficult to repair (Sutherland et al. 2000) and their misrepair may lead to genome instability, apoptosis and carcinogenesis. There are reports (Lorat et al. 2012) suggesting that after exposure to ionizing radiation nearly all DSB in human are efficiently rejoined, sometimes resulting in rearrangement of DNA and chromatin. In contrast, at very low doses (<10 mGy) it has been reported that DSB were not repaired efficiently and therefore residual damage was seen in G_0/G_1 cells (Rothkamm and Löbrich 2003, Grudzenski et al. 2010, Horn et al. 2011). Also, low dose-specific signatures have been reported at gene expression level (Ding et al. 2005). The above findings indicate that cellular responses following low-dose radiation may be different from those subsequent to high-dose exposures.

In the present study, we observed that at lower doses, the conformational changes in chromatin structure were detectable as compared to higher doses. This might be due to the fact that at low doses induction of single-strand breaks (SSB) and base damages are higher as compared double-strand breaks. The yield of double-strand breaks upon 1.0 Gy irradiation is estimated to be 40 as compared with about 1000 single-strand breaks and 2000 oxidized bases that are likely to be part for most of the non-DSB clustered

Table I. Hydrodynamic diameter (nm) of the chromatin fibers obtained using DLS at different radiation doses in 10 random donors.

Dose (Gy)	Donor 1	Donor 2	Donor 3	Donor 4	Donor 5	Donor 6	Donor 7	Donor 8	Donor 9	Donor 10
0.0	184.2 ± 5.5	208.3 ± 5.9	203.0 ± 7.7	195.9 ± 9.7	244.4 ± 7.7	159.4 ± 7.5	186.2 ± 6.8	183.3 ± 6.9	182.2 ± 6.2	185 ± 4.4
0.25	213.6 ± 7.3*	231 ± 7.0*	235.1 ± 6.1*	173.9 ± 2.8*	212.5 ± 8.9*	142.6 ± 5.0*	188.0 ± 6.3	166.8 ± 6.4*	193.6 ± 5.4*	210 ± 8.9*
0.50	205.7 ± 6.9*	224.3 ± 5.2*	252.4 ± 7.6*	209.2 ± 7.1	211.1 ± 8.7*	135.9 ± 3.2*	184.0 ± 4.3	188.1 ± 7.2	179.1 ± 9.3	169.2 ± 2.2*
1.0	187.2 ± 7.5	211.5 ± 7.5	226.4 ± 8.1*	205.2 ± 6.6	220.9 ± 8.6*	148.7 ± 6.6	205.5 ± 4.6	176.1 ± 7.1	187.8 ± 8.5	172.6 ± 6.3

*denotes significant value at $p \leq 0.05$, mean $\pm$ standard deviation.

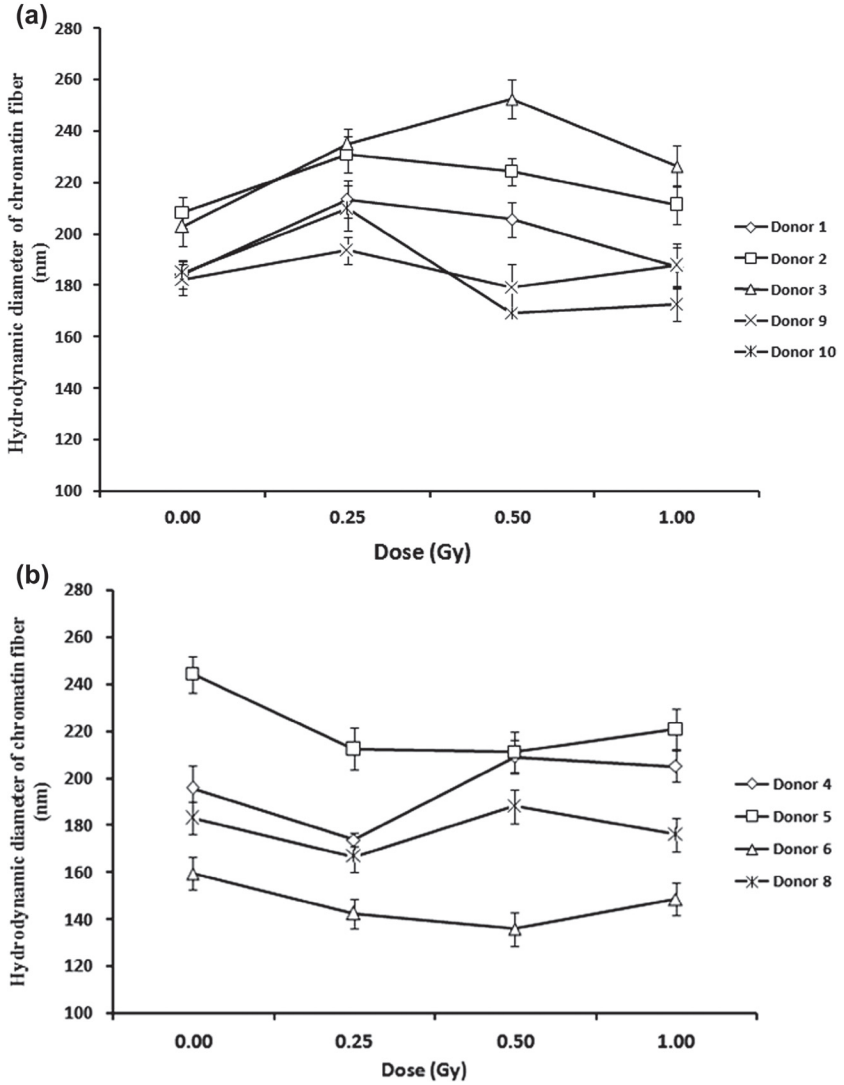

Figure 2. Dose-dependence of hydrodynamic diameter (D_h) of chromatin fiber in irradiated PBMC of nine donors. (a) Significant increase ($p \leq 0.05$) in hydrodynamic diameter of chromatin fibers of five donors after exposure to 0.25 Gy (b) Significant decrease ($p \leq 0.05$) in hydrodynamic diameter of chromatin fiber of four donors after exposure to 0.25 Gy. Error bars represent standard deviation which is calculated from 10 DLS measurements obtained at each dose point from each donor.

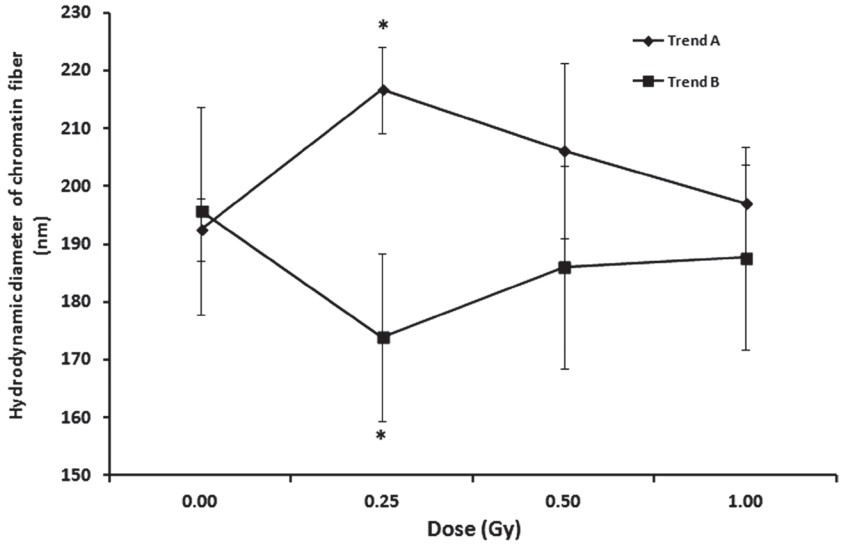

Figure 3. Average hydrodynamic diameter of chromatin fiber from PBMC of nine donors after exposure to different doses of radiation. (a) Trend A: Average hydrodynamic diameter of five donors showing significant increase ($^*p \leq 0.002$) at 0.25 Gy. (b) Trend B: Average hydrodynamic diameter of four donors showing significant decrease ($^*p \leq 0.009$) at 0.25 Gy. The standard error of the mean is calculated from the average values obtained from the donors in each group.

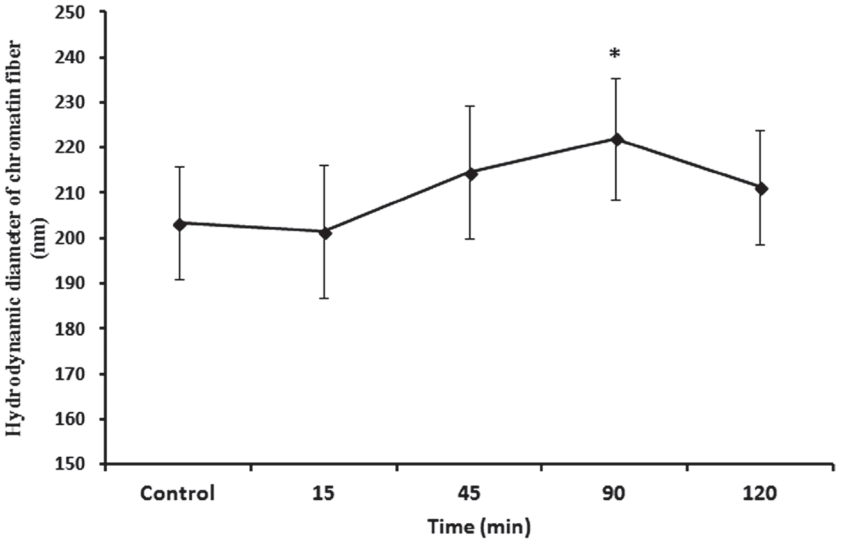

Figure 4. Time point changes in the average hydrodynamic diameter of chromatin fibers in PBMC of six donors exposed to 1.0 Gy of radiation. The error bar represents the standard error of the mean which is calculated from average values of six donors. * denotes $p \leq 0.05$.

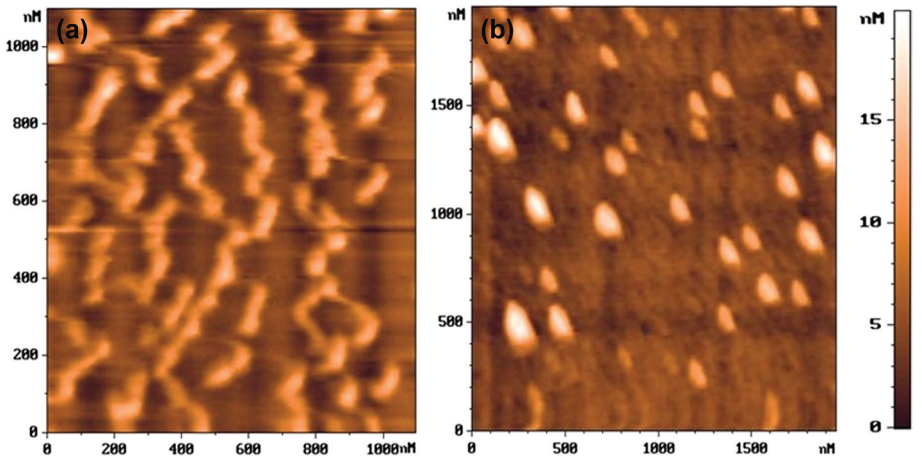

Figure 5. AFM image showing chromatin structure in human PBMC. (a) Intact chromatin fragments in unirradiated PBMC; (b) fragmented and diffused chromatin fragments after 5.0 Gy. Depth indicator reflects the thickness/height of chromatin fibers (in nm) present on the surface scanned by AFM. Dark to light shade indicates increase in size (nm) of chromatin fiber. This Figure is reproduced in color in the online version of the *International Journal of Radiation Biology*.

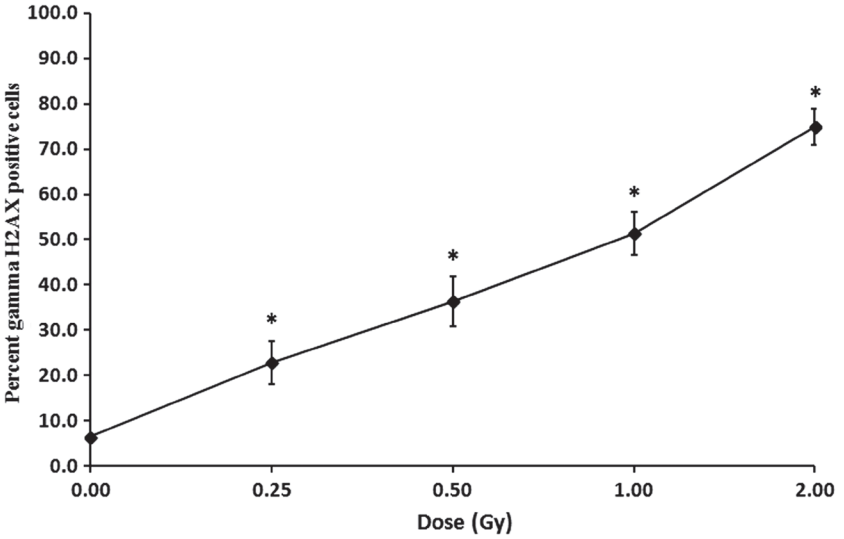

Figure 6. Percentage increase in gamma-H2AX positive cells in PBMC on exposure to different doses of gamma radiation ($n = 10$). Error bars represents the standard error of the mean which is calculated from mean values obtained from 10 donors (biological replicates). N is number of donors. * denotes $p \leq 0.05$.

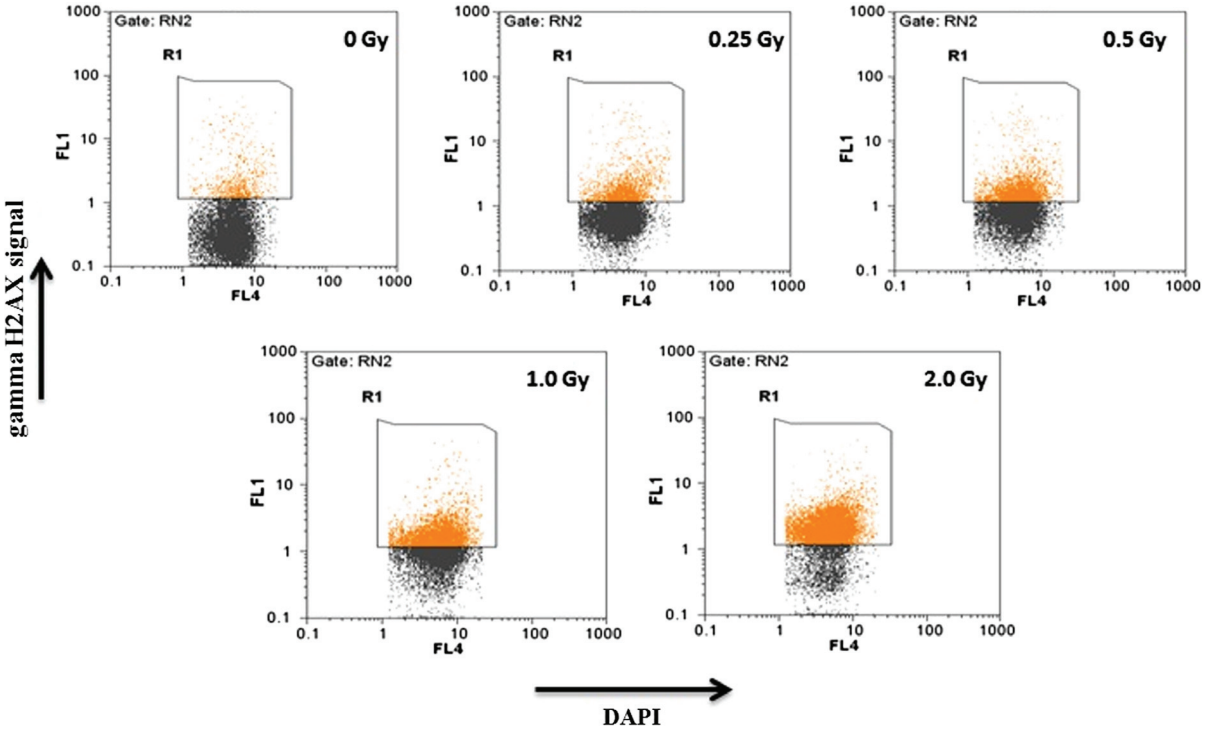

Figure 7. Representative flow cytometric profile of gamma-H2AX positive cells in PBMC from one donor exposed to different doses of radiation. Gate R1 (Rectangular Gate 1) represents DAPI stained gamma-H2AX positive cells at different doses [0 Gy (unirradiated control), 0.25, 0.50, 1.0 and 2.0 Gy]. This Figure is reproduced in color in the online version of the *International Journal of Radiation Biology*.

lesions. There are reports which supports that the SSB and oxidized bases produced through the oxidative metabolism is at least 10-fold higher as compared to DSB and clustered damage (Sutherland et al. 2000, Hada and Sutherland 2006, Hada and Georgakilas 2008). Perhaps, the changes of hydrodynamic size were detectable at lower doses, because the severity of damage was less. Thus, changes at chromatin level were prominent, which was not observed at higher doses (1.0 Gy).

The spatial organization of chromatin in the nucleus reflects another aspect of its dynamic nature. There is emerging evidence that chromatin is organized in functional compartments, such as transcription factories and repair centers (Misteli and Soutoglou 2009, Bekker-Jensen and Mailand

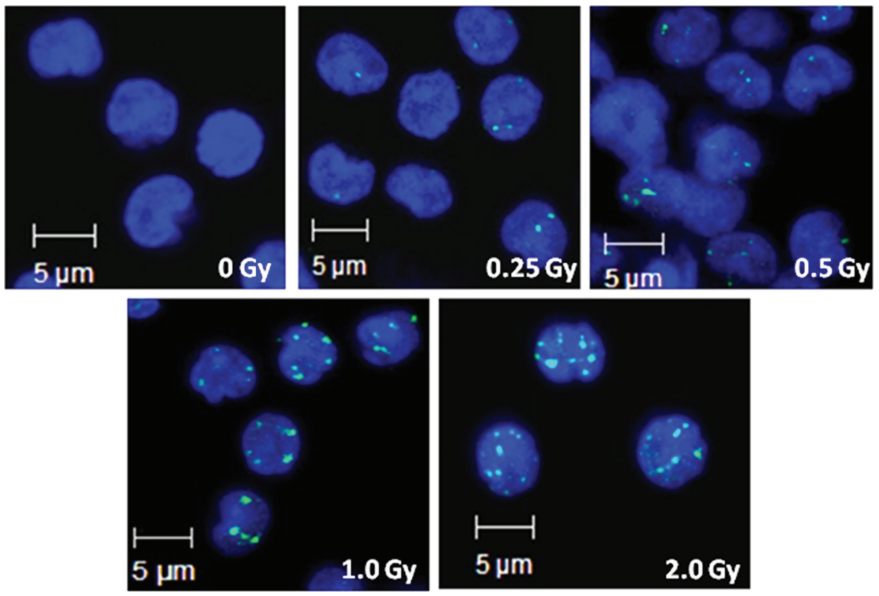

Figure 8. Confocal microscopy image showing dose-dependent increase in the number of gamma- H2AX foci in PBMC of an individual. Cell nuclei (chromatin) were counterstained with DAPI. Images were captured after manual focusing at 100 × objective with 2 × scanning zoom. This Figure is reproduced in color in the online version of the *International Journal of Radiation Biology*.

2010). It has also been reported (Lorat et al. 2012) that DNA strand breaks are more complex in heterochromatin and their processing is slower in heterochromatin as compared to euchromatin compartment (Goodarzi et al. 2009, 2010, Kakarougkas and Jeggo 2014). The two trends observed at 0.25 Gy might be explained on the basis of the random distribution of DNA strand breaks between different chromatin compartments, i.e., heterochromatin and euchromatin. Since, induction of DNA strand breaks by ionizing radiation is a random phenomenon so distribution of DNA strand breaks between chromatin compartments might influence the overall dynamics of chromatin especially at low doses as at higher doses number of DSB is comparatively higher and thus minute conformational changes are not detectable.

Phosphorylated H2AX foci serve as platform for the recruitment of DNA repair and chromatin remodeling factors at damage sites. Phosphorylated H2AX foci are detectable after low dose radiation exposures (Rothkamm and Löbrich 2003, Leatherbarrow et al. 2006, Asaithamby and Chen 2009, Beels et al. 2010). In the present study, a dose-dependent increase in gamma-H2AX positive cells and number of foci was observed in the individuals studied. As shown in Figure 8, clustered foci were observed above 1.0 Gy at 30 min post-irradiation, perhaps indicating accumulation of DSB and non-DSB clustered lesions in human PBMC. The AFM image indicated that at higher radiation dose exposures the chromatin fibers get fragmented and diffused.

Human peripheral blood mononuclear cells are most radiosensitive and are ideal to study the radiation-induced changes at the level of chromatin in vitro. Chromatin changes occurring at such low-dose exposures in resting PBMC has important implications for existing exposure situations such as high level natural radiation areas (HLNRA) where people can accumulate a dose of more than 500 mGy (0.5 Gy) during their life spans. So far, genetic studies carried out in high level natural radiation areas of Kerala coast did not reveal any significant difference in the incidence of congenital malformations and the frequency of gross chromosomal aberrations (including dicentrics, transloactions and inversions), micronuclei and telomere length (Cheriyan et al. 1999, Das and Karuppasamy 2009, Das et al. 2009, 2012, Ramachandran et al. 2013, Jaikrishan et al. 2013). It will be ideal to employ new techniques to find out chronic low-dose radiation-induced changes if any, at molecular level. The present study offers DLS as a novel technique to study radiation-induced changes of chromatin dynamics at such low-dose radiation exposures.

Acknowledgements

We thank all the volunteers, who have participated and donated blood samples for our study. We are thankful to Ms Prabhu J. A. and Mr Sangram Kamble for helping us in collecting the blood samples from BARC dispensary, Modular Laboratories, Trombay, Mumbai. We acknowledge Mr Prayag Amin for his excellent technical assistance, while acquiring the samples in Flow Cytometry experiments. We thank Dr (Mrs) Bhavani Shankar for the inputs during flow cytometry experiment. We also acknowledge Ms Vasumathy and Shri Manzoor Ali for helping us during confocal microscopy. We are thankful to Dr (Mrs) Shilpa Sawant for helping us during AFM experiments. We express our sincere thanks to Dr M. Seshadri, Former Head, Radiation Biology and Health Sciences Division for useful discussion during the experiments. We profusely thank Dr K. B. Sainis, former Director, Biomedical Group, for critical evaluation and useful discussions during the preparation of the manuscript. We also thank Dr J. R. Bandekar, Head, Radiation Biology and Health Sciences Division, for his useful discussions.

Declaration of interest

The authors report no conflicts of interest. The authors alone are responsible for the content and writing of the paper.

References

Amundson SA, Grace MB, McLeland CB, Epperly MW, Yeager A, Zhang Q, Greenberger JS, Furnace AJ Jr. 2004. Human in vivo radiation induced biomarkers: Gene expression changes in radiotherapy patients. Cancer Res 64:6368–6371.

Asaithamby A, Chen DJ. 2009. Cellular responses to DNA double-strand breaks after low-dose γ-irradiation. Nucleic Acids Res 37:3912–3923.

Attikum HV, Fritsch O, Hohn B, Gasser SM. 2004. Recruitment of the INO80 complex by H2A phosphorylation links ATP dependent chromatin remodeling with DNA double strand break repair. Cell 119:777–788.

Beels L, Werbrouck J, Thierens H. 2010. Dose response and repair kinetics of γ-H2AX foci induced by in vitro irradiation of whole blood and T-lymphocytes with X and γ- radiation. Int J Radiat Biol 86:760–768.

Bekker-Jensen S, Mailand N. 2010. Assembly and function of DNA double-strand break repair foci in mammalian cells. DNA Rep 9:1219–1228.

Belyaev IY, Czene S, Harms-Ringdahl M. 2001. Changes in chromatin conformation during radiation induced apoptosis in human lymphocytes. Radiat Res 156:355–364.

Berne BJ, Pecora R. 2000. Dynamic Light Scattering: With application to chemistry, biology and physics. 3rd ed. New York: Dover Publications.

Bing L, Carey M, Workman J. 2007. The role of chromatin during transcription. Cell 128:707–719.

Bloomfield VA. 1981. Quasi-elastic light scattering applications in biochemistry and biology. Ann Rev Biophys Bioengineer 10: 421–450.

Bøyum A. 1968. Isolation of mononuclear cells and granulocytes from human blood. Scand J Clin Lab Investigat 21:77–89.

Campbell AM, Cotter RI, Pardon JF. 1978. Light scattering measurements supporting helical structures for chromatin in solution. Nucleic Acid Res 5:1571–1580.

Cheriyan VD, Kurien CJ, Das B, Ramachandran EN, Karuppasamy CV, Thampi MV, George KP, Kesavan PC, Koya PKM, Chauhan PS. 1999. Genetic monitoring of the human population from high level natural radiation areas of Kerala on the southwest coast of India. Incidence of numerical and structural chromosomal aberrations in the lymphocytes of newborn. Radiat Res 152:154–158.

Corpet A, Almouzni G. 2009. A histone code for the DNA damage response in mammalian cells. Eur Molec Biol Organizat J 28: 1828–1830.

Das B, Karuppasamy CV. 2009. Spontaneous frequency of micronuclei among newborn from high level natural radiation areas of Kerala in southwest coast of India. Int J Radiat Biol 85:272–280.

Das B, Divyalakshmi Saini, Seshadri M. 2009. Telomere length in human adults and high level natural background radiation. Public Library Sci One 4(12):e8440.

Das B, Divyalakshmi Saini, Seshadri M. 2012. No evidence of telomere length attrition in newborns exposed to high level natural background radiation in Kerala coast, south west India. Int J Radiat Biol 88:642–647.

Das C, Hizume K, Batta K, Kumar BRP, Gadad SS, Ganguly S, Lorain S, Verreault A, Sadhale PP, Takeyasu K, Kundu TK. 2006. Transcriptional co-activator PC4, a chromatin associated protein induces chromatin condensation. Molec Cell Biol 26:8303–8315.

Dimitrov S, Makarov V, Apostolova T, Pashev I. 1986a. Structure of hyperacetylated chromatin: Light scattering and flow dichroism study. Fed Eur Biochem Soc Lett 197:217–220.
Dimitrov SI, Apostolova TM, Makarov VL, Pashev IG. 1986b. Chromatin superstructure – a study with an immobilized trypsin. Fed Eur Biochem Soc Lett 200:322–326.
Dinant C, Houtsmuller AB, Vermeulen W. 2008. Chromatin structure and DNA damage repair. Epigenetics Chromatin 1(1):9.
Ding LH, Shingyoji M, Chen F, Hwang JJ, Burma S, Lee C Cheng JF, Chen DJ. 2005. Gene expression profiles of normal human fibroblasts after exposure to ionizing radiation: A comparative study of low and high doses. Radiat Res 164:17–26.
Downs JA, Nussenzweig MC, Nussenzweig A. 2007. Chromatin dynamics and the preservation of genetic information. Nature 447: 951–958.
Eisenberg H, Borochov N, Kam Z, Voordouw G. 1979. Conformation of plasmid DNA and of DNA-histone chromatin like complexes by laser light scattering. Philosoph Transact Royal Soc London 293:303–313.
Falk M, Lukasova E, Gabeielova B, Ondrej V, Kozubek S. 2007. Chromatin dynamics during DSB repair. Biochim Biophys Acta 1773:1534–1545.
Falk M, Lukasova E, Kozubek S. 2010. Higher-order chromatin structure in DSB induction, repair and misrepair. Mutat Res 704:88–100.
Fernandez-Capetillo O, Celeste A, Nussenzweig A. 2003. Focusing on foci: H2AX and the recruitment of DNA-damage response factors. Cell Cycle 2:426–427.
Fernandez-Capetillo O, Lee A, Nussenzweig M, Nussenzweig A. 2004. H2AX: The histone guardian of the genome. DNA Rep 3:959–967.
Goodarzi AA, Noon AT, Jeggo A. 2009. The impact of heterochromatin on DSB repair. Biochem Soc Transact 37:569–576.
Goodarzi AA, Jeggo A, Löbrich M. 2010. The influence of heterochromatin on DNA double strand break repair: Getting the strong, silent type to relax. DNA Rep 9(12):1273–1282.
Greulich KO, Ausio J, Seger D, Wachtel E. Eisenberg H. 1986. Chromatin folding into higher order structure. Biophys J 49:7–8.
Groth A, Rocha W, Verreault A, Almouzni G. 2007. Chromatin challenges during DNA replication and repair. Cell 128:721–733.
Grudzenski S, Raths A, Conrad S, Rube CE, Löbrich M. 2010. Inducible response required for repair of low dose radiation damage in human fibroblasts. Proc Natl Acad Sci USA 107:14205–14210.
Hada M, Sutherland B. 2006. Spectrum of complex DNA damages depends on the incident radiation. Radiat Res 165(2):223–230.
Hada M, Georgakilas AG. 2008. Formation of clustered DNA damage after high LET irradiation: A review. J Radiat Res 49(3):203–210.
Hanlon AD, Larkin ML, Reddick RM. 2010. Free-solution, label-free protein-protein interactions characterized by Dynamic Light Scattering. Biophys J 98:297–304.
Hittelman WN, Pollard M. 1984. Visualization of chromatin events associated with repair of ultraviolet light-induced damage by premature chromosome condensation. Carcinogenesis 5:1277–1285.
Holde KV, Leuba SH, Zlatanova J. 1998. Physical approaches to the study of chromatin fibers. Gene Ther Molec Biol 1:475–482.
Horn S, Barnard S, Rothkamm K. 2011. Gamma-H2AX-based dose estimation for whole and partial body radiation exposure. Public Library Sci One 6:e25113.
Huang X, Darzynkiewicz Z. 2006. Cytometric assessment of histone H2AX phosphorylation: A reporter of DNA damage. Meth Molec Biol 314:73–80.
Ismail IH, Wadhra TI, Hammarsten O. 2007. An optimized method for detecting gamma-H2AX in blood cells reveals a significant interindividual variation in the gamma-H2AX response among humans. Nucleic Acids Res 35:1–10.
Jaikrishan G, Sudheer KR, Andrews VJ, Koya PKM, Madhusoodhanan M, Jagadeesan CK, Seshadri M. 2013. Study of stillbirth and major congenital anomaly among newborns in the high level natural radiation areas of Kerala, India. J Community Genet 4:21–31.
Jain V, Das B, Seshadri M. 2011. Transcriptional expression of H2B, CTP synthase and PLK3 genes in whole blood exposed to ^{60}Co gamma radiation. Int J Low Radiat 8:55–65.
Kakarougkas A, Jeggo PA. 2014. DNA DSB repair pathway choice: An orchestrated handover mechanism. Br J Radiol 87:20130685.
Kinner A, Wu W, Staudt C, Iliakis G. 2008. γ-H2AX in recognition and signaling of DNA double strand breaks in the context of chromatin. Nucleic Acids Res 36:5678–5694.
Kovalchuk O, Baulch JE. 2008. Epigenetic changes and non-targeted radiation effects – is there a link. Environ Molec Mutagenesis 49:16–25.
Kruhlak MJ, Celeste A, Dellaire G, Capetillo OF, Muller WG, McNally JG, Bazett-Jones DP, Nussenzweig A. 2006. Changes in chromatin structure and mobility in living cells at sites of DNA double strand breaks. J Cell Biol 172:823–834.
Leatherbarrow EL, Harper JV, Cucinotta FA, O'Neill P. 2006. Induction and quantification of γ-H2AX foci following low and high LET-irradiation. Int J Radiat Biol 82:111–118.
Lee KS, Mandelkern M, Crothers DM. 1981. Solution structural studies of chromatin fibers. Biochemistry 20:1438–1445.
Ljungman M. 1989. Pretreatment with UV light renders the chromatin in human fibroblasts more susceptible to the DNA damaging agents bleomycin, gamma radiation and 8-methoxypsoralen. Carcinogenesis 10:447–451.
Lorat Y, Schanz S, Schuler N, Wennemuth G, Rübe C, Rübe CB. 2012. Beyond repair foci: DNA double strand break repair in euchromatic and heterochromatic compartments analyzed by transmission electron microscopy. Public Library Sci One 7:e38165.
Lydall D, Whitehall S. 2005. Chromatin and the DNA damage response. DNA Rep 4:1195–1207.
Majumdar P, Dasgupta D. 2011. Effect of DNA groove binder distamycin A upon chromatin structure. Public Library Sci One 6:e26486.
Makarov VL, Smirnov I, Dimitrov SI. 1987. Higher order folding of chromatin is induced in different ways by monovalent and by divalent cations. Fed Eur Biochem Soc Lett 212:263–266.
Misteli T, Soutoglou E. 2009. The emerging role of nuclear architecture in DNA repair and genome maintenance. Nature Rev Molec Cell Biol 10:243–254.
Naumova N, Imakaev M, Fudenberg G, Zhan Y, Lajole BR, Mirny LA, Dekkar J. 2013. Organization of the mitotic chromosome. Science 342:948–953.
Neumaier T, Swenson J, Pham C, Polyzos A, Lo AT, Yang PoAn, Dyball J, Asaithamby A, Chen DJ, Bissell MJ, Thalhammer S, Costes SV. 2012. Evidence for formation of DNA repair centers and dose response nonlinearity in human cells. Proc Natl Acad Sci USA 109:443–448.
Pandita TK, Richardson C. 2009. Chromatin remodeling finds its place in the DNA double strand break response. Nucleic Acids Res 37:1363–1377.
Paull TT, Rogakou EP, Yamazaki V, Kirchgessner CU, Gellert M, Bonner WM. 2000. A critical role for histone H2AX in recruitment of repair factors to nuclear foci after DNA damage. Curr Biol 10:886–895.
Polo SE, Jackson SP. 2011. Dynamics of DNA damage response proteins at DNA breaks: A focus on protein modifications. Genes Develop 25:409–433.
Ramachandran EN, Karuppasamy CV, Cheriyan VD, Soren DC, Das B, Anilkumar V, Koya PKM, Seshadri M. 2013. Cytogenetic studies on newborns from high and normal level natural radiation areas of Kerala in southwest coast of India. Int J Radiat Biol 89:259–267.
Roche J, Girardet JL, Gorka C, Lawrence JJ. 1985. The involvement of histone H1 in chromatin structure. Nucleic Acids Res 13:2843–2853.
Rogakou EP, Boon C, Redon C, Bonner WM. 1999. Megabase chromatin domains involved in DNA double strand breaks in vivo. J Cell Biol 146:905–915.
Rogakou EP, Pilch DR, Orr AH, Ivanova VS, Bonner WM. 1998. DNA double-stranded breaks induce histone H2AX phosphorylation on serine 139. J Biolog Chem 273:5858–5868.
Rothkamm K, Löbrich M. 2003. Evidence of a lack of DNA double-strand break repair in human cells exposed to very low X-ray doses. Proc Natl Acad Sci USA 100:5057–5062.
Rydberg B. 2001. Radiation induced DNA damage and chromatin structure. Acta Oncolog 40:682–685.
Saini D, Shelke S, Manivannan A, Toprani S, Jain V, Das B, Seshadri M. 2012. Transcription profile of DNA damage response genes at G_0 lymphocytes exposed to gamma radiation. Molec Cellular Biochem 364:271–281.
Schmitz KS, Shaw BR. 1977. Hydrodynamic evidence in support of spacer regions in chromatin. Science 197:661–662.
Selvi BR, Pradhan SK, Shandilya J, Das Chandrima, Sailaja BD, Shankar GN, Gadad SS, Reddy A, Dasgupta D, Kundu TK. 2009. Sanguinarine interacts with chromatin modulates epigenetic modifications, and transcription in the context of chromatin. Chem Biol 16:203–216.
Sutherland BM, Bennett PV, Sidorkina O, Laval J. 2000. Clustered DNA damages induced in isolated DNA and in human cells by low doses of ionizing radiation. Proc Natl Acad Sci USA 97:103–108.

Mol Cell Biochem
DOI 10.1007/s11010-012-1227-9

Transcription profile of DNA damage response genes at G_0 lymphocytes exposed to gamma radiation

Divyalakshmi Saini · Shridevi Shelke · A. Mani Vannan · Sneh Toprani · Vinay Jain · Birajalaxmi Das · M. Seshadri

Received: 18 September 2011 / Accepted: 4 January 2012

Abstract Ionizing radiation induces a plethora of DNA damages in human cells which may alter the level of mRNA expression. We have analyzed mRNA expression profile of DNA damage response genes involved in G_0/G_1 check point pathway in whole blood to assess their radio-adaptive response, if any, to gamma radiation. Blood samples were collected from twenty-five random, normal, and healthy male donors with written informed consent and irradiated at doses between 0.1 and 2.0 Gy (0.7 Gy/min). DNA strand breaks were studied using comet assay, whereas DNA double-strand breaks were visualized using γH2AX as a biomarker. Dose response if any, at transcriptional level was studied for all these dose groups at 1 and 5-h post-irradiation. Adaptive response at transcriptional level was studied at three different priming doses (0.1, 0.3, and 0.6 Gy) separately followed by a challenging dose of 2.0 Gy after 4 h. For both the experiments, total RNA was isolated from PBMCs obtained from irradiated whole blood and reverse transcribed to cDNA. The level of mRNA expression of ATM, ATR, GADD45A, CDKN1A, P53, CDK2, MDM2, and Cyclin E was studied using real-time quantitative PCR. A significant dose-dependant increase in the percentage of DNA damage in tail was observed using comet assay. Similarly, increased number of foci was observed at γH2AX with increasing dose. At transcriptional level, a significant dose-dependent up-regulation at GADD45A, CDKN1A, and P53 genes up to 1.0 Gy was observed at 5-h post-irradiation ($P \leq 0.05$). Radio-adaptive response at mRNA expression level was observed at CDK2, Cyclin E, and P53, whereas ATM, ATR, GADD45A, MDM2, ATM, and ATR have not shown any radio-adaptive changes in the expression profile. DNA damage response genes involved in G_0/G_1 checkpoint pathway has important implications in terms of radiosensitivity in vivo and changes in the transcriptional profile might throw some new insights to understand the mechanism of adaptive response.

Keywords Human peripheral blood mononuclear cells (PBMC) · mRNA expression · Relative quantitation · Real-time q-PCR · Gamma irradiation

Introduction

Environmental mutagens including ionizing radiation exposure is known to challenge normal cellular functions in human. Ionizing radiation induces a spectrum of DNA lesions including single and double strand breaks, DNA crosslinks, isolated and clustered DNA lesions [1–4] in human cells. Double-strand breaks (DSB) and clustered DNA damages are highly deleterious and sometimes mis-repaired DNA lesions may lead to chromosomal abnormalities as well as gene mutations [5, 6]. However, efficient DNA repair machinery in human cells maintain genome integrity by modulating various cellular and molecular mechanisms. Human population exposed to high level natural background radiation exposures or individuals with occupational exposures are monitored using biomarkers, such as chromosomal aberrations (especially dicentrics) or micronuclei [7, 8]. In recent years, efforts have been made to establish molecular biomarkers for identifying the radiation signatures. Adaptive response

D. Saini · S. Shelke · A. Mani Vannan · S. Toprani · V. Jain · B. Das (✉) · M. Seshadri
Low Level Radiation Studies Section, Radiation Biology and Health Sciences Division, Bio-Medical Group, Bhabha Atomic Research Centre, Trombay, Mumbai 400 085, India
e-mail: birajalaxmi@yahoo.co.in; biraj@barc.gov.in

Published online: 19 January 2012

study using these biomarkers might help in identifying radiosensitive and radio-resistant individuals from human population exposed to ionizing radiation.

Cellular response to ionizing radiation is mediated through a number of genes which controls complex regulatory pathways. These pathways may result in cell cycle delays, apoptosis, and DNA repair [9]. Alteration of gene expression in response to ionizing radiation is one of the indicators of DNA damage. Although several investigators have studied the expression pattern of these DNA damage response genes exposed to radiation [10, 11], most of the studies have been explored in different cell lines, normal human fibroblasts, and skin biopsies [12–14].

Human peripheral blood mononuclear cells (PBMCs) are ideal choice to conduct ex vivo studies. Little is known about the transcriptional expression pattern of these DNA damage response genes in resting lymphocytes (G_0). In dividing cells, ionizing radiation induces DNA damage and regulates the response to DNA damage through ataxia telangiectasia, mutated (ATM) and ATR (ATM and Rad3-related) protein kinases belonging to serine–threonine kinases [15]. After the activation of ATM/ATR, phosphorylation of p53 takes place, which upon activation induces GADD45A and CDKN1A (p21) leading to G_1 arrest [16]. In this process, other genes involved are MDM2, CDK2, Cyclin E which may have important role for G_1 check point arrest [17]. In this article, we have studied the transcriptional status of these genes in resting lymphocytes. The characteristics of the genes studied are as follows: cyclin-dependent kinase inhibitor 1a (CDKN1A) is also referred as p21 and inhibits cyclin-kinase activity which is tightly regulated at the transcriptional level by p53 [18]. Growth arrest and DNA damage-inducible gene (GADD45A) is the only member of the GADD group that is frequently inducible by ionizing radiation and is involved in DNA repair, maintenance of genomic stability, cell cycle control, and apoptosis [19, 20]. p53 (also known as TP53) regulates cell cycle, DNA repair, and apoptosis [21]. Although in normal cells, p53 protein level is low, DNA damage response may increase the level of p53 proteins. ATM and ATR are two signalling molecules which get recruited at DNA damage sites in response to ionizing radiation through the phosphorylation of specific sets of target proteins on serine or threonine residues [22–24]. Cdks (cyclin-dependent kinases) are heteromeric serine/threonine kinases that control progression through the cell cycle with the help of cyclins. The Cyclin E/CDK2 complex phosphorylates p27 (an inhibitor of cyclin D), tagging it for degradation [25]. MDM2 is an important negative regulator of the p53. Following DNA damage, phosphorylation of MDM2 leads to stabilize p53 [25].

The objective of the study was to assess dose response if any, at mRNA expression level of DNA damage response genes involved in G_0/G_1 checkpoint pathway. In addition, we have tried to evaluate whether there exists any adaptive response at the transcriptional pattern of these genes in human blood at resting stage (G_0) in response to radiation. To address these queries, DNA damage quantitation in terms of DNA strand breaks was studied in PBMCs using alkaline comet assay. As several post-translational modifications of histone proteins, especially phosphorylation of Ser 139 residue H2AX is implicated in DNA damage response, we also have made an attempt to see whether DNA DSB were formed or visualized in PBMCs using γH2AX as a biomarker. Finally, dose response as well as adaptive response study at the transcriptional level was studied in PBMCs exposed to various doses of gamma radiation.

Materials and methods

Collection of blood samples and ethics statement

Venous blood samples were collected in sterile vacutainers containing EDTA from twenty-five random, healthy male donors (non smokers) with an age group between 25 and 40 years. All the donors gave written consent and the experiment was approved by Medical ethic Committee, Bhabha Atomic Research Centre (BARC), Trombay, Mumbai. Both dose response and adaptive response experiments were performed.

Sample irradiation and isolation of PBMCs from blood

For DNA damage experiments, blood samples were irradiated at five dose groups 0.1, 0.3, 0.6, 1.0, and 2.0 Gy at a dose rate of 70 cGy/min using a ^{60}CO source in Blood irradiator 2000 (Board of Radiation and Isotope Technology, Mumbai, India) along with sham irradiated control. PBMCs were isolated from irradiated whole blood through gradient centrifugation using Histopaque® 1077 (Sigma Aldrich, St Louis, USA) according to the manufacturer's protocol.

DNA damage quantitation

We have performed alkaline comet assay to quantitate DNA strand breaks at the dose groups mentioned above. Dose response experiment was also performed using γH2AX, a biomarker specific to DSB.

Measurement of DNA strand breaks using Comet assay

Alkaline comet assay was used for quantitating DNA strand breaks. The protocol used for this assay is as follows: Melted agarose (1%) was layered onto the frosted slide to prepare a basal layer. It was covered with coverslip

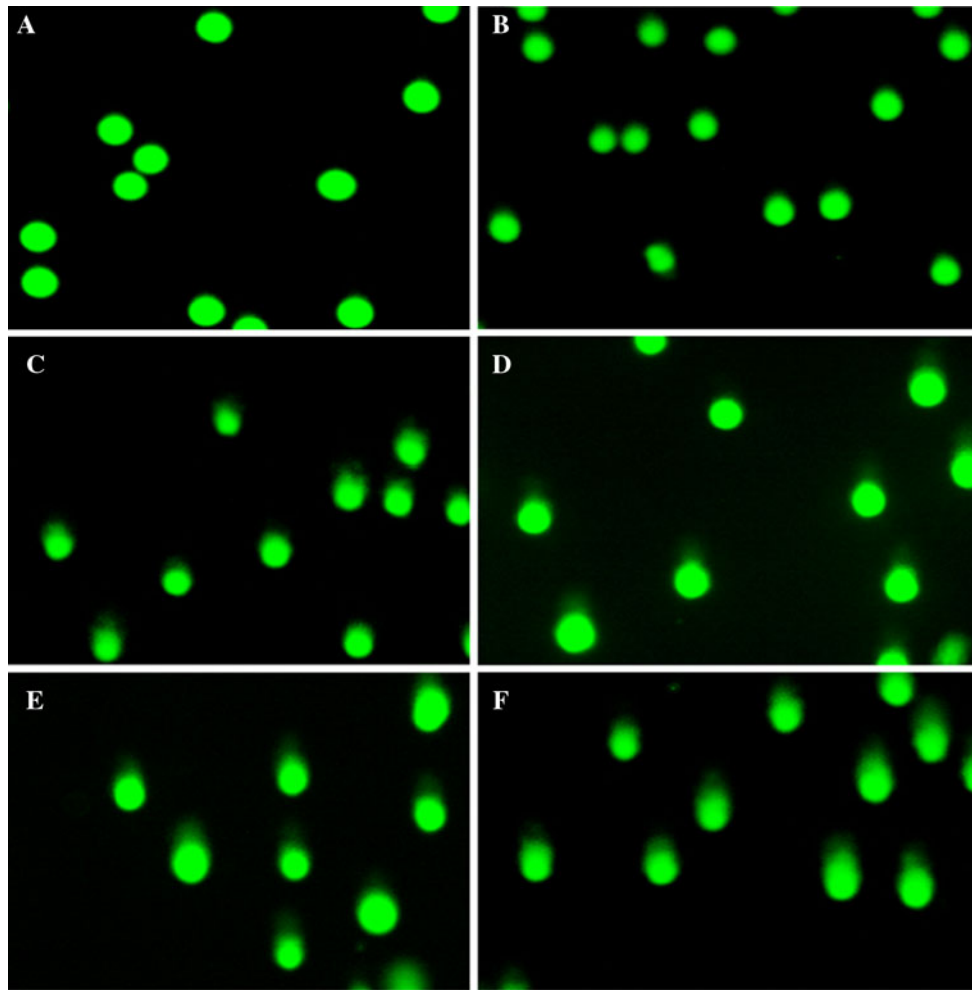

Fig. 1 Images showing DNA damage using comet assay at various dose groups. **a** 0.0Gy, **b** 0.1 Gy, **c** 0.3 Gy, **d** 0.6 Gy, **e** 1.0 Gy, and **f** 2.0 Gy

and kept at 4°C until it solidifies. PBMCs (1×10^5/ml cells/ml) were mixed gently with 0.5% molten agarose (low melting, Sigma Aldrich, USA) at 37°C at a ratio of 1:10 (v/v). The mixture of cells in the molten agarose (250 µl) was spread onto the frosted slide after the basal layer was solidified. Care was taken to spread the samples onto the basal layer of agarose area in the frosted slide. The slides were kept in a flat surface at 4°C in dark for 30 min to improve adherence of samples. Soon after the agarose containing cell layer solidifies, the cover slip was removed and lysis step was performed. The slides were immersed in freshly prepared pre-chilled lysis solution (2.5 M NaCl, 100 mM EDTA, 10 mM Trizma base, 10% DMSO, and 1% Triton-X-100, pH 10.0) and kept at 4°C for 20 min. After lysis step is over, the excess buffer was removed from the slide and immersed in freshly prepared alkaline solution, pH > 13.0 containing 0.6 g NaOH pellets and 20 mM EDTA for 30 min at room temperature in dark. The slides were finally transferred from alkaline solution to a horizontal electrophoresis apparatus, where slides were placed flat onto a gel tray and were alligned equidistant from the electrodes. Alkaline electrophoresis solution (pH > 13) containing 12 g of NaOH pellets and 500 mM EDTA (pH 8.0) was poured carefully into the electrophoresis buffer tank until the level of the solution covers the sample slides. Electrophoresis was carried out for 20 min at 25 volts, 300 mAmps. After electrophoresis, the slides were rinsed in neutralization buffer (0.4 M Tris–HCl, pH 7.5) for 5 min. The slides were fixed in 70% ethanol for 5 min, air dried, and stained with 1× SyBr green dye. Observations were made in dark at 20× magnification using a epifluorescent microscope (Nikon Eclipse Ti-U inverted microscope, Japan). About 100 cells (50 from each slide) were randomly selected and quantified with TriTek Comet Score TM Version 1.5. The images at various dose groups are shown in Fig. 1. Quantitation of DNA damage in tail (%) in different dose groups was represented in the histogram as shown in Fig. 2.

Detection of DNA damage using phosphorylated-H2AX

We have used confocal microscopy to detect DNA DSB using phosphorylated H2AX, as a biomarker. The methodology to detect γH2AX foci is as per the protocol described below. Venous blood samples were collected from random and healthy individuals, irradiated with 0.1, 0.3, 0.6, 1.0, and 2.0 Gy along with sham irradiated control. In brief, the protocol is as follows: PBMCs were separated from irradiated whole blood, incubated at 37°C for 30-min post-irradiation, and then fixed with 1% formaldehyde for 15 min on ice followed by incubation in 70% ethanol for 2 h. For permeabilization, cells were also incubated in 1% BSA–Triton-X-100–PBS solution (mixture of bovine serum albumin and Triton-X-100 in phosphate buffered saline. Cells were incubated overnight at 4°C in Anti-phospho-Histone H2AX (Ser139) antibody, 05-636 (Millipore, Temecula, CA, USA) in 1% BSA–Triton-X-100–PBS solution (BSA–T–PBS) at a concentration of 10 µg/ml. After overnight incubation, cells were washed with 1% BSA–T–PBS solution containing 0.05% Tween 20 and incubated with Alexa Fluor 488 labeled Rabbit Anti-mouse antibody, A-11059 Molecular probes (Invitrogen, Eugene, Oregon, USA). The labeled cells were diluted to a concentration of 1× ($\sim 10^6$ cells/ml) and a suspension of 100 µl was layered onto Poly-L-Lysine coated coverslips (BioCoat™354085, BD Biosciences, India) for 30 min at room temperature in dark. After proper adherence of the cells, the coverslip was washed twice with BSA–T–PBS–Tween 20 solution. The coverslips were mounted onto glass slides using Prolong Gold Antifade DAPI reagent with DAPI, P-36935, Molecular Probes (Invitrogen, Eugene, Oregon, USA) and visualized in confocal microscope (Carl Zeiss, Model-LSM 510 Meta, Germany). The dose related increase in γH2AX foci formation is shown in Fig. 2.

Total RNA isolation and cDNA preparation and analysis of mRNA expression

Total RNA isolation from PBMCs

Gene expression profile of DNA damage response genes was studied at dose groups such as 0.1, 0.3, 0.6, 1.0, and 2.0 Gy (dose rate of 70 cGy/min). Total RNA was isolated using Hipura RNA isolation Kit (Himedia Laboratory Pvt. Ltd. Mumbai, India) from PBMCs separated from irradiated whole blood at 1 and 5 h. (As separation of PBMCs from whole blood took an hour, gene expression profile observed at 0 and 4 h incubation were considered as expression as 1 and 5 h.) In addition, adaptive response study on these genes was carried out, where whole blood was irradiated separately with three different priming doses

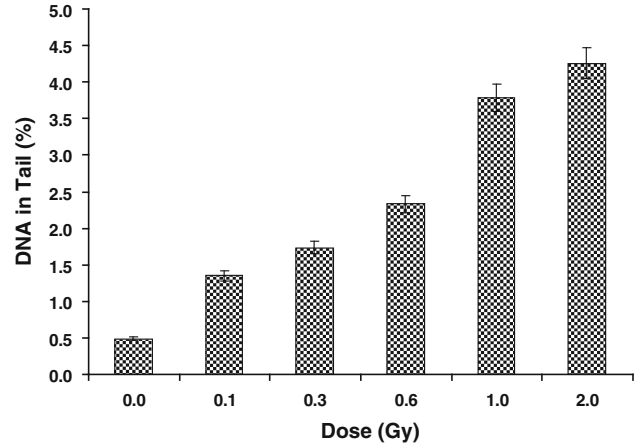

Fig. 2 Average DNA damage (% of DNA in tail) using alkaline comet assay

(0.1, 0.3, and 0.6 Gy) followed by a challenging dose of 2.0 Gy after 4 h. Total RNA was isolated separately from each blood samples which were given priming doses followed by challenging dose after 4 h. RNA was quantified using picodrop Microlitre spectrophotometer and the purity was checked by taking 260/280 nm ratio. Integrity of RNA was checked on 0.8% agarose gel, stained with ethidium bromide. RNA samples with clear-cut 28S and 18S bands were used for cDNA synthesis.

cDNA synthesis and real-time quantitative PCR (RT-qPCR)

For each aliquot of samples, total RNA (250 ng) was reverse transcribed to cDNA using transcriptor high fidelity cDNA synthesis kit (Roche Diagnostics, GmbH, Germany). RT-qPCR was performed to quantitate the level of mRNA expression of selected genes (ATM, ATR, CDKN1A, GADD45A, P53, MDM2, CDK2, and Cyclin E). RT-qPCR was performed on 96-multiwell plates using LC 480 real time PCR machine (Roche Diagnostics, GmbH, Germany). All the reactions were carried out in duplicates and were normalized against B-Actin and B2M. No significant changes were observed in the baseline expression. Therefore, beta actin was used for relative quantitation for all the genes. All the primer sets were procured from Sigma-Aldrich, USA. Primer sequences used in the study are given in Table 1. Each RT-qPCR reaction was performed in a total volume of 25 µl containing 0.25 mM of each dNTPs (Roche diagnostics Pvt. Ltd. GmbH, Germany), 0.5 U of Fast Taq DNA polymerase (Roche Diagnostics Pvt. Ltd. GmbH, Germany), 5.0 pmols of both forward and reverse primers, and 0.3× of SYBR green (Sigma Aldrich, USA). A total of 40 cycles of real-time q-PCR was carried out for all the genes with the following PCR steps : a pre-incubation step at 95°C for

Table 1 Primer sequences

Name of the primer	Primer sequences
ATM PR1 (forward)	5′-CCA GGC AGG AAT CAT TCA G-3′
ATM PR2 (reverse)	5′-CAA TCC TTT TAA ATA GAC GGA AAG AA-3′
ATR PR1 (forward)	5′-GAC ATT GGG CCT ATA TTG CAG-3′
ATR PR2 (reverse)	5′-TGG TTT CTG AAG AGA AGC AAG A-3′
P53 PR1 (forward)	5′-GTC CAA TGG AGG AGG AGA GCT GGT TTA-3′
P53 PR2 (reverse)	5′-CTG ATG AAC AAC CCA GCC ATT GTC-3′
CDKN1A PR1 (forward)	5′-AAG ACC ATG TGG ACC TGT-3′
CDKN1A PR2 (reverse)	5′-GGC TTC CTC TTG GAG-3′
GADD45A PR1 (forward)	5′-AGA GCA GAA GAC CGA AAG GAT GG-3′
GADD45A PR2 (reverse)	5′-GAA CCC ATT GAT CCA TGT AGC G-3′
MDM2 PR1 (forward)	5′-TGC AGA AAA TTT GCA TCA GC-3′
MDM2 PR2 (reverse)	5′-GGA TCT TTG TCA GAA AGC AAC A-3′
CDK2 PR1 (forward)	5′-GGG CTC GAA ATA TTA TTC CAC A-3′
CDK2 PR2 (reverse)	5′-CAG AAT CTC CAG GGA ACA GG-3′
Cyclin E PR1 (forward)	5′-GGC CAA AAT CGA CAG GAC-3′
Cyclin E PR2 (reverse)	5′-GGG TCT GCA CAG ACT GCA T-3′
B-Actin PR1 (forward)	5′-ATA CCC CTC GTA GAT GGG CAC-3′
B-Actin PR2 (reverse)	5′-GAG AAA ATC TGG CAC CAC ACC-3′
B2M PR1 (forward)	5′-TGC TGT CTC CAT GTT TGA TGT ATC T-3′
B2M PR2 (reverse)	5′-TCT CTG CTC CCC ACC TCT AAG T-3′

5 min followed by denaturation at 95°C 10 s, annealing 59°C for 30 s, and extension at 72°C for 30 s. Melting curve analysis was done in three steps: melting at 95°C for 5 min followed by an annealing step at 59°C for 1 min and an extension at 72°C followed by a final step at 40°C for 10 s. Melting curve analysis was also done to ensure that the amplified DNA is the product of interest. Relative quantification was performed by using the LC480 software version 1.1. The results are expressed in normalized ratio as described by Pfaffle [26].

$$\text{Normalized ratio} = (\text{conc. target}/\text{conc. reference})_{\text{sample}} : (\text{conc. target}/\text{conc. reference})_{\text{calibrator}}.$$

Statistical analysis

Paired *t* test was performed between the average expression levels of control and irradiated samples. Regression analysis was performed to see the correlation between the level of mRNA expression at 1 and 5 h in irradiated blood samples at all the eight genes. Statistical analysis was performed using Sigma Stat software [27].

Results

DNA damage and the level of mRNA expression pattern was studied in irradiated whole blood which were exposed to dose groups between 0.1 and 2.0 Gy along with sham-irradiated control. Quantitation DNA strand breaks especially percentage of DNA in tail was done in these individuals using single cell gel electrophoresis (comet assay). As shown in Fig. 2, there is a clear-cut dose response observed with the dose points used in DNA damage observed in tail. It was well complemented with γH2AX foci formation with increasing dose as shown in Fig. 3.

The transcriptional expression pattern of eight DNA damage response genes was studied in irradiated whole blood in the same dose groups at 1 and 5 h. The relative quantitation of ATM, ATR, CDKN1A, GADD45A, P53, MDM2, CDK2, and Cyclin E were normalized with respect to beta actin gene. The average relative expression of these genes at 1 and 5-h post-irradiation was compared and represented in the histogram (Fig. 4a–h). Our results have shown a clear-cut radiation dose response at 5 h for GADD45, CDKN1A, and P53 up to 1.0 Gy, with a decline in the level of expression at 2.0 Gy as compared to 1 h.

Paired *t* test was carried out to see the significance between the level of expression at 1 and 5 h. ATM has shown a marginal increase in the expression profile at 0.3, 0.6, and 1.0 Gy ($P = 0.04$), but no significant change in the level of expression was observed at 2.0 Gy. The transcriptional profile of ATR did not show any increased response up to 1.0 Gy, but significantly up regulated at 2.0 Gy for 5 h. At MDM2, significant transcriptional changes observed at 0.3–2.0 Gy at 5 h ($P = 0.03$). At CDK2, there is a marginal increase in the level of

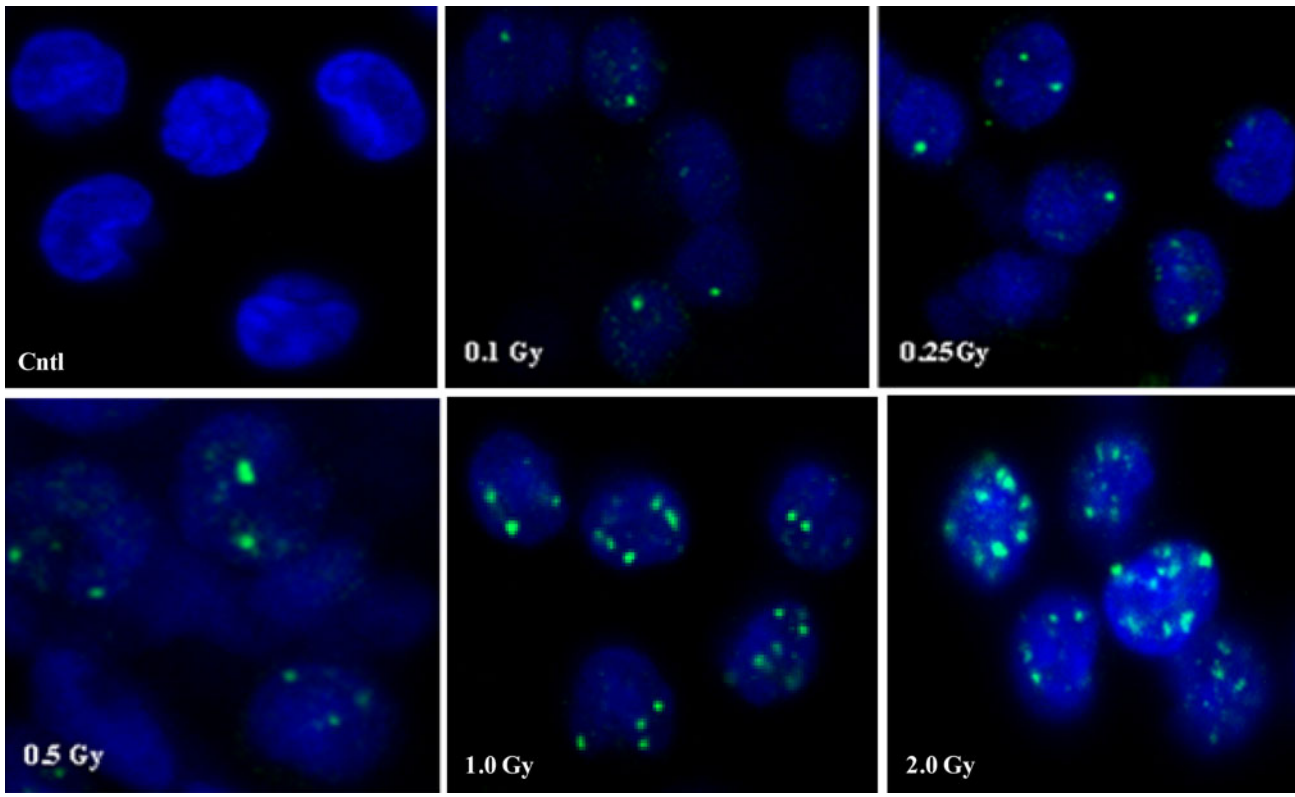

Fig. 3 Images showing γH2AX foci at various dose groups in human peripheral blood lymphocytes using confocal microscopy

expression at all the dose groups, though not significant. Cyclin E has shown significant up-regulation at all the dose groups ($P = 0.02$) at 5 h but no significant trend was observed as compared to 1 h. Out of eight genes, three genes (GADD45A, CDKN1A, and P53) have shown a significant increasing trend in the expression level up to 1.0 Gy ($P < 0.05$). We have performed regression analysis to find out the correlation between the expression pattern observed at 1 and 5 h. Trend test has shown significant differences in the expression profile for ATR ($R = 0.956$, $P = 0.03$), CDK2 ($R = 0.953$, $P = 0.03$), and CDKN1A ($R = 0.995$, $P = 0.001$).

Adaptive response study

Analysis of gene expression was carried out separately with the samples which were administered with priming doses: 0.1, 0.3, and 0.6 Gy, followed by a challenging dose of 2.0 Gy to assess adaptive response, if any, as shown in Fig. 5a, b. In this study, it was observed that at priming doses of 0.1, 0.3, and 0.6 Gy, no adaptive response was observed for ATM, ATR, MDM2, GADD45A, and CDKN1A. However, Cyclin E, CDK2, and P53 have shown adaptive response ($P < 0.05$). ATM has shown adaptive response though not significant at 0.1 and 0.3 Gy of prime doses followed by a challenging dose of 2.0 Gy. At a prime dose of 0.3 Gy, ATR has shown similar expression similar to the expression observed at 2.0 Gy. Interestingly, although CDKN1A has shown dose-dependent increase in the expression profile, no adaptive response was observed for any of the three priming doses. Similarly, GADD45A has shown increased up-regulation in the expression profile between 0.1 and 2.0 Gy. But no adaptive response was observed at any of the three priming doses. P53 has also shown increased up-regulation at all the dose groups, but showed adaptive response only at a priming dose of 0.1 Gy. CDK2 has shown adaptive response at 0.3 and 0.6 Gy. But at a priming dose of 0.1 Gy, it showed similar expression as shown at 2.0 Gy. Cyclin E has shown steady adaptive response at all the three priming doses. MDM2 has not shown adaptive response at all.

Discussion

Mammalian cells possess complex molecular responses to physiological and genotoxic stresses including ionizing radiation. Many such responses are mediated through alterations in gene expression [28, 29]. Majority of early

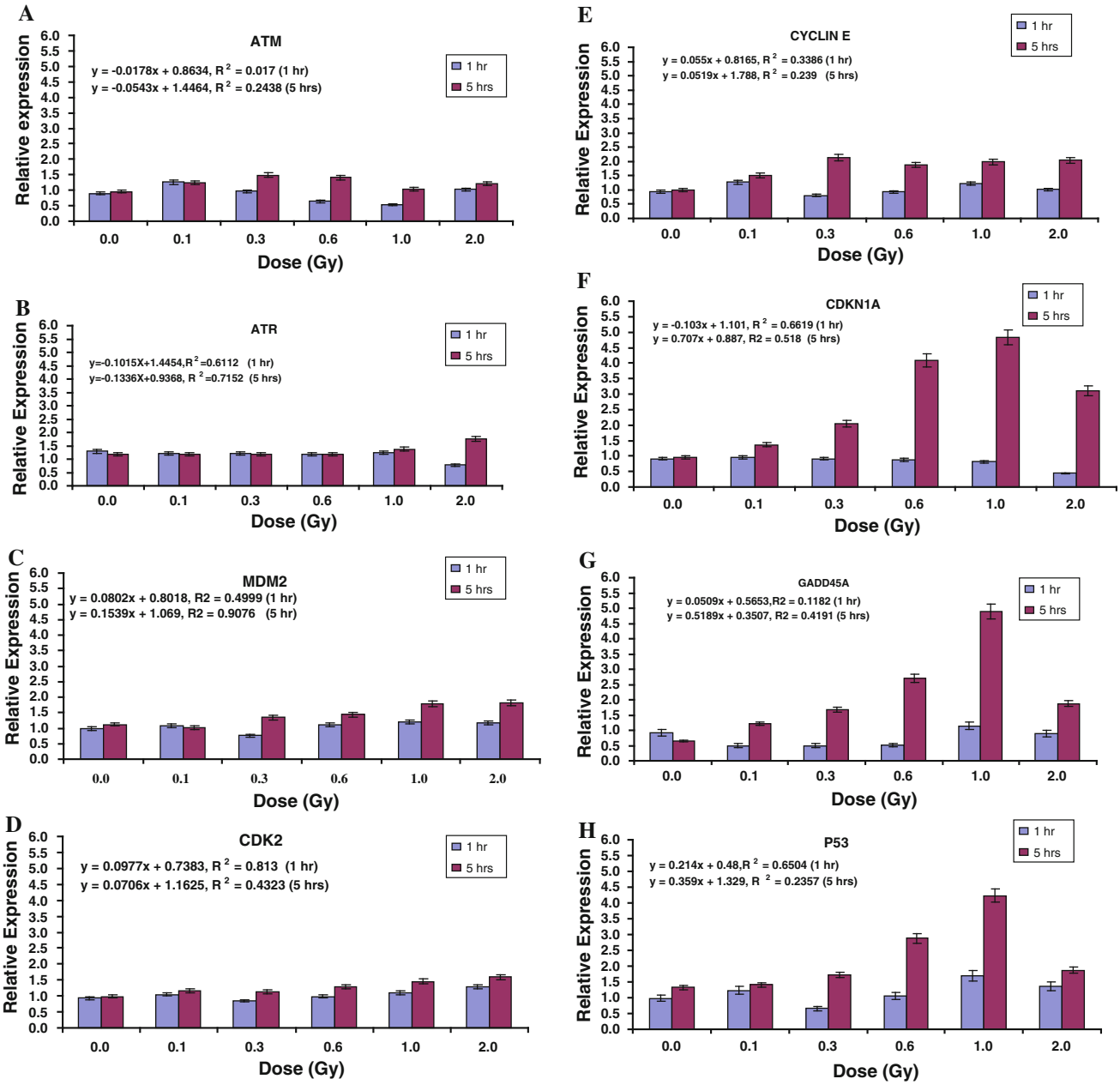

Fig. 4 **a**–**h** Gene expression pattern of DNA damage response genes involved in G_0/G_1 checkpoint pathway in irradiated whole blood. **a** ATM, **b** ATR, **c** MDM2, **d** CDK2, **e** Cyclin E, **f** CDKN1A, **g** GADD45A, and **h** P53

study on the regulation of gene expression in response to radiation was carried out using high dose exposures, but data from low dose exposures are relevant in the perspective of therapeutic or environmental doses [30].

DNA damage-related expression profile at mRNA level to assess individual sensitivity to ionizing radiation is important for population monitoring, occupational, and radiotherapy-exposed individuals [31, 32]. Studies have demonstrated that there is extensive variation in the baseline expression level of radiation responsive genes among normal individuals. The variation could be attributed toward radio-sensitive and radio-resistant individuals in a population. Ionizing radiation induces a spectrum of DNA damages in human cells. Both low and high LET radiation can induce isolated and clustered DNA damages which are more complex. Cluster damages can either DSB or non-DSB oxidative clustered DNA lesions, which can be induced at very low doses [4–6]. However, these complex damages are very difficult to repair. In addition, processing of clustered DNA damages at such exposures may generate DSBs [5, 6]. The consequences of these damages are not known at the level of expression. Non-DSB lesions can be

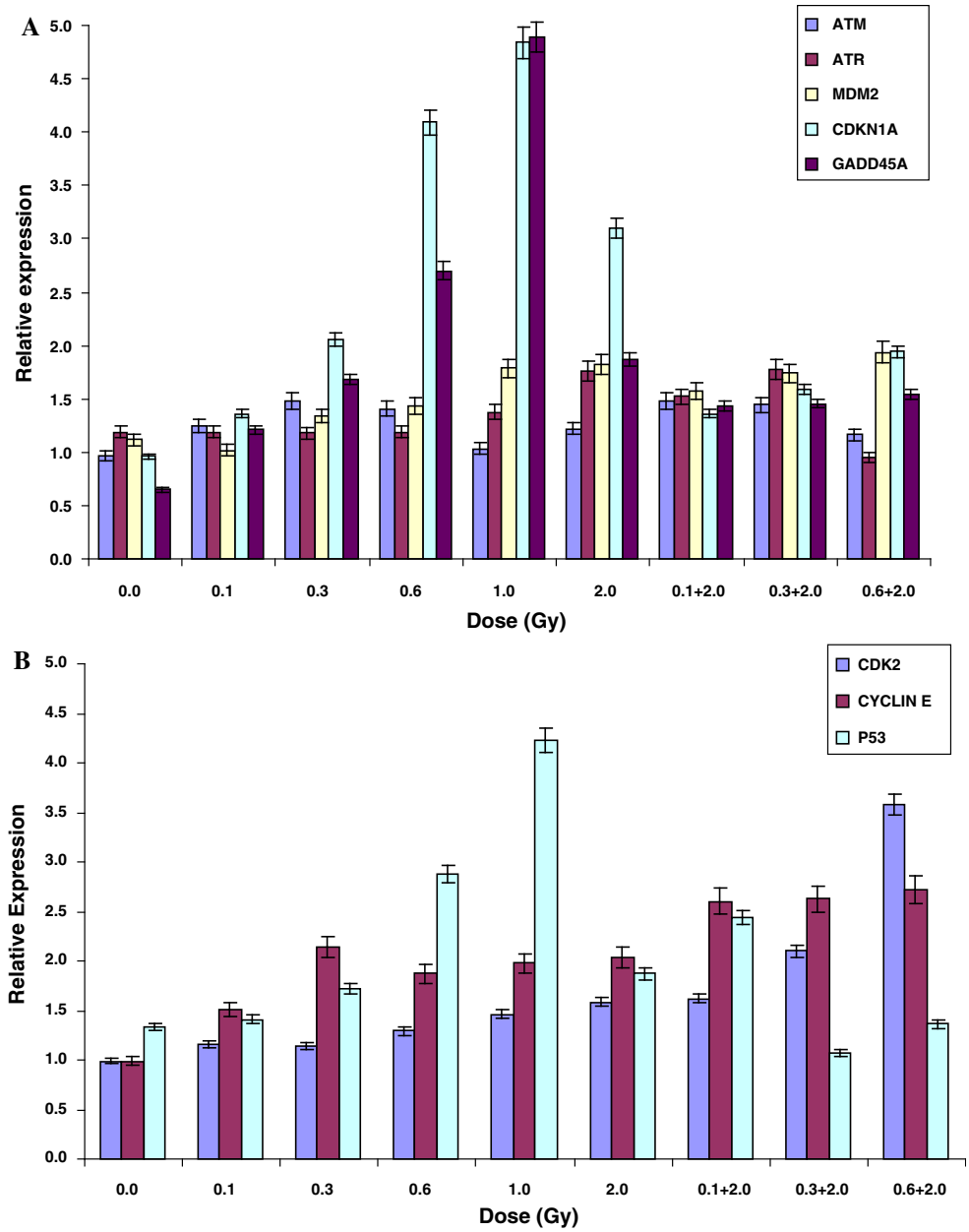

Fig. 5 **a** Transcriptional pattern of genes (ATM, ATR, MDM2, CDKN1A, and GADD45A) not showing adaptive response in irradiated whole blood. **b** Transcriptional pattern of genes (CDK2, Cyclin E, and P53) showing adaptive response in irradiated whole blood

measured by alkaline comet assay; whereas, DSBs can be measured by using pulsed field electrophoresis and neutral comet assay. Limited data is available on PBMCs and we, therefore, have made an attempt to see whether strand breaks and DSBs are detectable and induced at such exposures. By using comet assay and γH2AX biomarker, we have observed that DNA strand breaks in terms of percentage of DNA in tail which increases with increasing dose. Similarly, we have observed γH2AX foci formation was increased with dose. In response to DNA damage, we have observed increased level of mRNA expression in normal individuals exposed to acute doses of gamma radiation, after 5-h post-irradiation. We have also demonstrated the radio-adaptive response of CDK2, Cyclin E, and P53 irrespective of their mRNA expression level.

Cellular responses to ionizing radiation is mediated through genes that control multifaceted regulatory pathways including growth factors, cytokines, oncogenes, and genes involved in cell cycle, apoptosis, and DNA repair [33, 34]. Transcriptional response to radiation has been reported in human PBMCs at important genes like p53, p21, DDB2, cyclinG1, GADD45 and some apoptotic genes like BAX, Bcl-2, etc. The transcriptional regulation of cell cycle regulated genes is closely related to checkpoint

functions upon DNA damage and changes in gene expression may be a mechanism for initiation of cell cycle arrest [35].

In this study, we have shown that, mRNA expression level at P53, CDKN1A (p21), GADD45A, CDK2, and Cyclin E are significantly up regulated after exposures between 0.1 and 1.0 Gy of gamma radiation. It is to be pointed out here that the PBMCs used here are not proliferated cells. Several reports have shown adaptive response in mammalian cells to radiation exposure using end points, such as mutation, survival and chromosomal damage [36–41]. Olivieri et al. [42] have reported adaptive response in human lymphocytes exposed in vitro to low level of radiation [42]. However, adaptive response at the transcriptional expression level of these genes is not known. Adaptive response in ex vivo studies of blood cells has important implications to human health. It generates a strong cellular defense mechanism thereby activating or strengthening the DNA repair system. Although after the discovery of radio-adaptive response a lot of cellular studies have been carried out in vitro in human cell lines, limited information is available on PBMCs.

In this study, we have studied dose response relationship as well as its radio-adaptive nature if any, at three separate priming doses such as 0.1, 0.3, and 0.6 Gy. In general, ATM and ATR are DNA damage sensors [25, 43], which are activated by DNA damage and takes part in signal transduction cascades associated with cell cycle checkpoints and DNA repair through activation of a number of transcription factors, including TP53 [44]. Similarly, GADD45 have also shown to be induced by gamma rays and X-rays [30, 45] have demonstrated a dose response relationship of five genes, i.e., CDKN1A, GADD45, MDM2, ATF3, and BAX in response to acute gamma-ray exposures between 2 and 50 cGy and they found out that both GADD45A and CDKN1A genes were induced to lesser levels by irradiation at decreasing dose rates. Interestingly, ATM and ATR did not show any changes in the level of expression. The reason is not clear yet. It needs to be further explored by proliferating lymphocytes. We have demonstrated that in vivo exposures to radiation ranging between 0.1 and 2.0 Gy in human blood can induce mRNA expression level at DNA damage response genes involved in G_0/G_1 check point pathway. Our data was complemented by DNA damage study using single cell electrophoresis and γH2AX. There is a dose-dependent increase in DNA damage in tail as shown in Fig. 2. In this study, significant up-regulation of GADD45A, CDKN1A, and P53 at 1- and 5-h post-irradiation has indicated the implications of induction of mRNA expression level.

CDKN1A, GADD45, and P53 are promising biomarkers for ex vivo radiation–response studies despite the existence of inter-individual differences [46, 47]. In this study, we have observed that P53, GADD45A, and CDKN1A have shown dose-dependant increase between 0.1 and 1.0 Gy. However, the response was different in adaptive response study where separate priming doses such as 0.1, 0.3, or 0.6 Gy was given followed by challenging dose of 2.0 Gy after 4 h. Interestingly, CDKN1A, GADD45A, and P53 have shown adaptive response at transcriptional level. At the same time, adaptive response study did not reveal any significant change in the pattern of transcriptional expression was for ATM, ATR, MDM2, CDK2, and Cyclin E. Interestingly, significant up-regulation was observed at Cyclin E, CDK2, MDM2 with priming doses of 0.1, 0.3, or at 0.6 Gy. At the same time, P53 has shown adaptive response at 0.1 Gy only.

In summary, our results have indicated the role of Cyclin E, CDK2, MDM2, and p53 in regulating the G_0 check point pathway in PBMCs. The up-regulation of these genes can be attributed toward a radio resistance of PBMCs after exposure to a priming dose of 0.1, 0.3, or 0.6 Gy. The mechanism of adaptive response observed at the level of transcriptional profile is not yet known. Therefore, further research on proliferated PBMCs may provide better understanding of the transcriptional profile of these genes. Adaptive response at the transcriptional profile is a novel phenomenon and can further be investigated. DNA damage response leading to efficient DNA repair and the role of transcriptional up-regulation of Cyclin E, MDM2, CDK2, and P53 in regulating the G_1 check point in PBMCs samples can throw new insights to in vivo response. It is also evident from our data that alteration in the transcription profile varies from gene to gene depending upon their function.

In conclusion, our data on dose response and adaptive response study at these important DNA damage response genes of G_0/G_1 checkpoint pathway has important implications in identifying radiosensitive and radioresistant individuals in vivo. These data would be helpful in defining the extent and nature of the normal variability in gene expression in human blood. It may contribute to understand the inter-individual variation seen among healthy individuals. It provides strong support for the feasibility of using gene expression patterns in peripheral blood as a basis for radiation signature. However, further data on this aspect would be required for studying the mechanism of adaptive response and its relationship with transcription profile.

Acknowledgments We are very much thankful to the volunteers who have participated in the study. We also profusely thank Ms. Prabhu J. A and Mr. Sangram Kamble for helping us in collecting the blood samples from BARC dispensary, Trombay, Mumbai.

Conflict of interest The authors declare there is no conflict of interest.

References

1. O'Neill P, Fielden EM (1993) Primary free radical processes in DNA. Adv Radiat Biol 17:53–120
2. Nakajima M, Takenchi T, Takeshita T, Morimoto K (1996) 8-Hydroxydeoxyguanosine in human leukocyte DNA and daily health practice factors: effects of individual alcohol sensitivity Environ. Health Perspect 104:1336–1338
3. von Sonntag C (1987) The chemical basis of radiation biology. Taylor and Francis, London
4. Sutherland BM, Bennett PV, Sidorkina O, Laval J (2000) Clustered DNA damages induced in isolated DNA and in human cells by low doses of ionizing radiation. Proc Natl Acad Sci USA 97:103–108
5. Hada M, Georgakilas AG (2008) Formation of clustered DNA damage after high-LET irradiation: a review. J Radiat Res 49:203–210
6. Georgakilas AG (2008) Processing of DNA damage clusters in human cells: current status of knowledge. Mol Biosyst 4:30–35
7. IAEA (2001) Cytogenetic analysis for radiation dose assessment: a manual. Technical Report series No. 405, p 127
8. Léonard A, Rueff J, Gerber GB, Léonard ED (2005) Usefulness and limits of biological dosimetry based on cytogenetic methods. Radiat Prot Dosim 115:448–454
9. Iliakis G, Wang Y, Guan J, Wang H (2003) DNA damage checkpoint control in cells exposed to ionizing radiation. Oncogene 22:5834–5847
10. Weichselbaum RR, Hallahan D, Fuks Z, Kufe D (1994) Radiation induction of immediate early genes: effectors of the radiation-stress response. Int J Radiat Oncol Biol Phys 30:229–234
11. Amundson SA, Bittner M, Meltzer P, Trent J, Fornace AJ Jr (2001) Induction of gene expression as a monitor of exposure to ionizing radiation. Radiat Res 156(5):657–661
12. Goldberg Z, Schwietert CW, Lehnert B, Stern R, Nami I (2004) Effects of low dose ionizing radiation on gene expression in human skin biopsies. Int J Radiat Oncol 58(2):567–574
13. Tachiiri S, Katagiri T, Tsunoda T, Oya N, Hiraoka M, Nakamura Y (2006) Analysis of gene expression profiles after gamma irradiation of normal human fibroblasts. Int J Radiat Oncol 64(1):272–279
14. Chaudhry MA (2008) Analysis of gene expression in normal and cancer cells expose to γ-radiation. J Biomed Biotechnol. ID 541678
15. Sen CK, Sies H, Baeuerle PA (2000) Antioxidant and redox regulation of genes. Academic Press, San Diego, CA, p 562
16. Canman CE, Lim D, Cimprich KA, Taya Y, Tamai K, Sakaguchi K, Appella E, Kastan MB, Siliciano JD (1998) Activation of the ATM kinase by ionizing radiation and phosphorylation of p53. Science 281(5383):1677–1679
17. Khanna KK, Shiloh Y (2010) The DNA damage response: implications on cancer formation and treatment. Springer, New York, p 449
18. Harper JW, Adami GR, Wei N, Keyomarsi K, Elledge SJ (1993) The p21 Cdk-interacting protein Cip1 is a potent inhibitor of G_1 cyclin-dependent kinases. Cell 75(4):805–816
19. Carrier FP, George T, Pourquier P, Blake M, Kontny HU, Antinore MJ, Gariboldi M, Myers TG, Weinstein JN, Pommier Y, Fornace AJ Jr (1999) GADD45, a p53-responsive stress protein, modifies DNA accessibility on damaged chromatin. Mol Cell Biol 19(3):1673–1685
20. Daino K, Ichimura S, Mitsuru N (2002) Early induction of CDKN1A (p21) and GADD45 mRNA by a low dose of ionizing radiation is due to their dose-dependent post-transcriptional regulation. Radiat Res 157(4):478–482
21. Adimoolam S, James M, Ford JM (2003) p53 and regulation of DNA damage recognition during nucleotide excision repair. DNA Repair 2:947–954
22. Shiloh Y (2002) ATM and ATR: networking cellular responses to DNA damage. Curr Opin Genet Dev 11(1):71–77
23. Abraham RT (2001) Cell cycle checkpoint signaling through the ATM and ATR kinases. Genes Dev 15:2177–2196
24. Shiloh Y (2001) ATM and related protein kinases: safeguarding genome integrity. Nat Rev Cancer 3:155–168
25. Iliakis G, Wang Y, Guan J, Wang H (2003) DNA damage checkpoint control in cells exposed to ionizing radiation. Oncogene 22(37):5834–5847
26. Pfaffle MW (2001) A new mathematical model for relative quantification in real time RT-PCR. Nucleic Acid Res 29:2002–2007
27. SIGMASTAT software version 3.5 (2006) http://www.systat.com
28. Amundson SA, Fornace AJ Jr (2001) Gene expression profiles for monitoring radiation exposure. Radiat Prot Dosim 97:11–16
29. Grace MB, Blakely WF (2007) Transcription of five p53- and Stat 3-inducible genes after ionizing radiation. Radiat Meas 42:1147–1151
30. Moustacchi E (2007) DNA damage and repair: consequences on dose-responses. Mutat Res 464(1):35–40
31. Amundson SA, Fornace AJ Jr, Amundson SA (2003) Microarray approaches for analysis of tumor suppressor gene function. Methods Mol Biol 223:141–154
32. Bishey K, Ory K, Oliver M, Lebeau J, Levalas C, Chevillard S (2001) DNA damage related RNA expression to assess individual sensitivity to ionizing radiation. Carcinogenesis 22(8):1179–1183
33. Chaudhry MA, Lewis A, Chodosh W, McKenna G, Muschel RJ (2003) Gene expression profile of human cells irradiated in G_1 and G_2 phases of cell cycle. Cancer Lett 195:221–233
34. Sakamoto-Hojo ET, Mello SS, Pereira E, Fachin AL, Cardoso RS, Junta CM, Garcia PS, Donadi EA, Passos GAS (2003) Gene expression profiles in human cells submitted to genotoxic stress. Mutat Res 544:403–413
35. Zhou T, Chou JW, Simpson DA, Zhou Y, Mullen TE, Medeiros M, Bushel PR, Paules RS, Yang X, Hurban P, Lobenhofer EK, Kaufmann WK (2006) Profiles of global gene expression in ionizing-radiation-damaged human diploid fibroblasts reveal synchronization behind the G_1 checkpoint in a G_0-like state of quiescence. Environ Health Perspect 114(4):553–559
36. Raaphorst GP, Boyden S (1999) Adaptive response and its variation in human normal and tumour cells. Int J Radiat Biol 75(7):865–873
37. Rigaud O, Mouslacchi E (1994) Radioadaptation to the mutagenic effect of ionizing radiation in human lymphoblasts. Molecular analysis of HPRT mutants. Cancer Res 54:1924–1928
38. Marples B, Joiner MC (1995) The elimination of low dose hypersensitivity in Chinese hamster V79–379A cells by pretreatment with X-rays or hydrogen peroxide. Radiat Res 141:160–169
39. Alsbeih G, Arlette FB, Malaise EP (1996) High split-dose recovery in hypersensitive human fibroblasts: a case of induced radiation resistance. Int J Radiat Biol 69:225–239
40. Seong J, Suh CO, Kim GE (1995) Adaptive response to ionizing radiation induced by low doses of gamma rays in human cell lines. Int J Radiat Oncol 33:869–874
41. Shadely JD, Dai G (1992) Cytogenetic and survival adaptive response in G_1 phase human lymphocytes. Mutat Res 265:273–281
42. Olivieri P, Bodycote J, Wilff S (1984) Adaptive response of human lymphocytes to low concentration of radioactive thymidine. Science 223:594–597

43. Sancar A, Laura A, Ünsal-Kaçmaz LK, Linn S (2004) Molecular mechanisms of mammalian DNA repair and the DNA damage checkpoints. Annu Rev Biochem 73:39–85
44. Jen KY, Cheung VG (2005) Identification of novel p53 target genes in ionizing radiation response. Cancer Res 65:7666–7673
45. Hildesheim J, Fornace AJ Jr (2002) Gadd45A: an elusive yet attractive candidate gene in pancreatic cancer. Clin Cancer Res 8(8):2475–2479
46. Sudo HA (2007) Loss of function screen identifies nine new radiation Susceptibility genes. Biophys Biochem Res Commun 364:695–701
47. Amundson SA, Grace MB, McLeland CB, Epperly MW, Yeager A, Zhang Q, Greenberger JS, Furnace AJ Jr (2004) Human in vivo radiation induced biomarkers: gene expression changes in radiotherapy patients. Cancer Res 64:6368–6371

Transcriptional expression of *H2B*, *CTP synthase* and *PLK3* genes in whole blood exposed to ^{60}Co gamma radiation

Vinay Jain, Birajalaxmi Das* and M. Seshadri

Low Level Radiation Studies Section,
Radiation Biology and Health Sciences Division,
Bhabha Atomic Research Centre,
Mumbai 400 085, India
Email: vinayj@barc.gov.in
Email: biraj@barc.gov.in
Email: msesh@barc.gov.in
*Corresponding author

Abstract: Ionising radiation induces complex molecular responses in human cells resulting in changes at mRNA and protein expression. Limited data is available on the transcriptional status of functional genes in response to ionising radiation using peripheral blood mononuclear cells (PBMCs). In the present study, transcriptional profiles of *Histone 2B*, *CTP synthase* and *PLK3* were studied. Blood samples were collected from ten random healthy males with informed consent. Whole blood irradiation was done at four different dose groups (0.3, 0.6, 1.0 and 2.0 Gy) at a dose rate of 0.68 Gy/minute. PBMCs were separated immediately as well as 4 hours post-irradiation. Total RNA was isolated, transcribed to cDNA and real-time quantitative PCR was performed. Our results revealed a dose-dependent significant upregulation at *H2B* and *CTP synthase* at 4 hours post-irradiation. At *PLK3* significant upregulation was observed at 2.0 Gy (P = 0.007). In conclusion, these genes can be used for population monitoring programme.

Keywords: whole blood irradiation; transcriptional profile; RT-q-PCR; *H2B*; *CTP synthase*; *PLK3*.

Reference to this paper should be made as follows: Jain, V., Das, B. and Seshadri, M. (2011) 'Transcriptional expression of *H2B*, *CTP synthase* and *PLK3* genes in whole blood exposed to ^{60}Co gamma radiation', *Int. J. Low Radiation*, Vol. 8, No. 1, pp.55–65.

Biographical notes: Vinay Jain is a scientific officer in Low Level Radiation Studies Section, Radiation Biology and Health Sciences Division, Bio-Medical Group of Bhabha Atomic research Centre, Trombay, Mumbai. He obtained his MSc degree in Biomedical Sciences. Presently he is pursuing his research career in the field of Radiation Biology.

Birajalaxmi Das is a senior scientific Officer, working in Low Level Radiation Studies Section, Radiation Biology and Health Sciences Division, Bio-Medical Group, Bhabha Atomic research Centre, Mumbai. She is actively involved in investigating the biological and health effects of chronic natural background radiation on human population living in High Level Natural Radiation Areas of Kerala coast in South West India. She has contributed substantially in cytogenetic

investigation of newborns, germinal mutation analysis in the families using autosomal and Y chromosomal markers and trancriptome analysis. She did her post-doctoral research on clustered DNA damage and repair in Biology Department, Brookhaven National Laboratory, Upton, NY, USA.

M. Seshadri is the Head, Radiation Biology and Health Sciences Division, Bio-Medical group, Bhabha Atomic research Centre, Mumbai. He has contributed substantially in the field of immunology, human genetics, radiation biology. He is involved in investigating the biological and health effects of natural background radiation on human population living in Kerala coast, South West India. He is a renowned scientist in different capacities in India. He has contributed substantially in studying germinal mutation analysis in families from Kerala coast and trancriptome analysis on adults.

1 Introduction

Ionising radiations induce various types of DNA lesions such as single-strand breaks, Double-Strand Breaks (DSBs) and oxidative base damage in human cells. These damages can be deleterious if not repaired and may lead to chromosomal aberrations, micronuclei formation, mutations, etc. As a serious consequence, the stability and integrity of the genome is affected leading to cancer (Jessica et al., 2007). One of the early responses to radiation stress in human cells is alteration of the transcriptional profile of the active genes. Alteration in both protein and mRNA level allows a cell to maintain its homeostasis following exposure to genotoxic agents including ionising radiations (Whitehead et al., 2006). Human cell possesses surveillance systems to monitor and maintain the integrity of the genome which is collectively termed as DNA-Damage Response (DDR). It regulates a complex network of cellular and molecular events that occurs at both protein and RNA levels to minimise the damage by activating cell cycle checkpoints, DNA repair and apoptosis (Gentile et al., 2003; Jan and Cheung, 2005; Shimada et al., 2008).

A number of studies have been undertaken dealing with radiation-induced changes at the transcriptional level in human cells especially using in vitro cell culture assays or on animal models exposed to relatively higher doses (Yin et al., 2003; Ding et al., 2005). However, limited in vivo studies are available in humans dealing with life time exposure to ionising radiation (Amundson et al., 2000; Kang et al., 2003; Berglund et al., 2008; Gruel et al., 2008; Turtoi et al., 2008; Morandi et al., 2009). DNA damage may lead to alterations in the level of mRNA expression. It is important to study changes in the transcription of genes on exposure at different doses/dose rates in order to find out the radiation sensitivity of an individual.

In the present study, we have made an attempt to understand the transcriptional changes at three target genes such as *H2B*, *CTP synthase* and *PLK3* in whole blood after low-dose exposure to ^{60}Co gamma radiation. Since alteration in the expression profile is one of the indications of DDR, we have chosen to study the transcriptions profile of three genes in irradiated whole blood. All these three genes are functionally important and thus play an important role in DNA damage repair, apoptosis and cell cycle. For instance, *H2B* is an integral part of nucleosome core which packages eukaryotic DNA into chromatin. Chromatin plays a crucial role in DDR by initiating DNA repair and inducing several

damage response genes (Gabler et al., 2004; van Attikum and Gasser, 2005; Jessica et al., 2007; Shimada et al., 2008; Morandi et al., 2009). *PLK3* is another crucial DDR gene which is involved in regulating a variety of molecular and cellular events including DDRs and cell cycle control. It also contributes to the regulation of M phase of cell cycle and functionally links DNA damage to cell cycle arrest and apoptosis (Conn et al., 2000; Xie et al., 2001; Bahassi et al., 2002; Winkles and Alberts, 2005; Zhou et al., 2006). *CTP synthase* gene is involved in the regulation of DNA synthesis, through de-novo synthesis of nucleotides in response to DNA damage (Rieger and Chu, 2004; Whitehead et al., 2006).

2 Materials and methods

2.1 Sample collection

Approximately 12 ml of venous blood samples were collected in EDTA vacutainers from ten random healthy male individuals of age between 23 and 27 years. All the individuals studied were non-smokers and are volunteers without any chronic illness. All the samples were collected with written informed consent which was approved by Medical Ethic Committee, Bhabha Atomic Research Centre, Trombay, Mumbai, India.

2.2 Irradiation

Blood samples were aliquoted into 1 ml volume for each dose group and irradiation was done in room temperature at dose rate of 0.68 Gy/minute using Blood Irradiator 2000 (BRIT, Mumbai) containing ^{60}Co gamma source. Samples were divided into two sets: one set for 0 hour and the other set for 4 hours post-irradiation. Each group consisted of four dose groups 0.3, 0.6, 1.0 and 2.0 Gy and a sham irradiated control. Both the sets were irradiated together except the controls. One set was immediately processed for 0-hour experiment and the second set was incubated for 4 hours at 37°C.

2.3 Isolation of Peripheral Blood Mononuclear Cells (PBMCs)

Immediately after irradiation Peripheral Blood Mononuclear Cells (PBMCs) were separated from the first set (0-hour experiment) of whole blood samples through gradient centrifugation using Histopaque® 1077 (Sigma Aldrich, St Louis, USA) according to the manufacturer's protocol. An equal volume of blood was overlaid on Histopaque in 1:1 ratio and centrifuged at 400x g for 30 minutes at 25°C. The PBMC population was collected from the interface and washed with Phosphate Buffered Saline (PBS) twice to remove plasma and Histopaque.

2.4 RNA isolation

Total RNA was isolated from approximately 1.5 to 2.0 × 10^6 cells separated from 1 ml of aliquot of blood. Each sample was processed for RNA isolation using Hipura RNA isolation kit (Himedia Laboratory Pvt. Ltd., Mumbai, India) according to manufacturer's protocol. RNA was quantified using Picodrop Microlitre Spectrophotometer and the

purity was checked by taking 260/280 nm ratio. RNA bands were visualised on 0.8% agarose gel, which was stained with ethidium bromide. RNA samples with clear-cut 28S and 18S bands were used for cDNA synthesis (Figure 1). The RNA samples with double the intensity of 28S bands as compared to 18S were taken for cDNA synthesis.

Figure 1 Gel image showing three clear bands (28S, 18S and 5S) of RNA

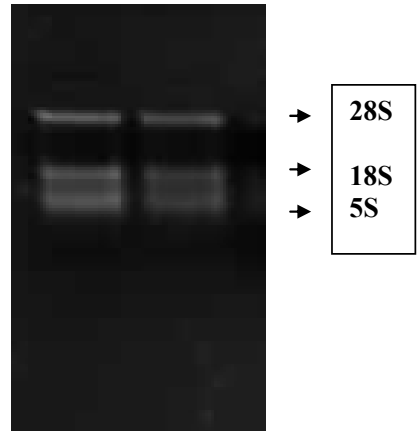

2.5 Synthesis of cDNA and Real-Time quantitative PCR (RT-qPCR)

Total RNA was isolated from each aliquot and 250 ng of RNA was reverse transcribed to cDNA using transcriptor high fidelity cDNA synthesis kit (Roche Diagnostics, GmbH, Germany). Real-Time quantitative Polymerase Chain Reaction (RT-qPCR) was performed to quantitate mRNA levels expression of selected genes (*H2B*, *CTP synthase* and *PLK3*). RT-qPCR reactions were performed on 96 multiwell plates using LC 480 Real-time PCR machine (Roche Diagnostics, GmbH, Germany). All the reactions were carried out in duplicates and were normalised against *β-actin* gene. All the primer sets were procured from Sigma Aldrich, USA. Primer sequences used in the study are given in Table 1 (Glaser et al., 2003). Each RT-qPCR reaction was performed in a total volume of 25 µl containing 0.25 mM of each dNTPs (Roche Diagnostics Pvt. Ltd., GmbH, Germany), 1.0 U of Fast Taq DNA polymerase (Roche Diagnostics Pvt. Ltd., GmbH, Germany), 10 pmols of both forward and reverse primers and 0.3X of SYBR green (Sigma Aldrich, USA). A total of 45 cycles of real-time q-PCR was carried out for *H2B*, *CTP synthase* and *PLK3* genes with the following PCR steps: a pre-incubation step at 95°C for 5 minutes followed by denaturation at 95°C for 10 seconds, annealing 59°C for 30 seconds and extension at 72°C for 30 seconds. Melting curve analysis was done in three steps: melting at 95°C for 5 minutes followed by an annealing step at 59°C for 1 minute and an extension at 72°C followed by a final step at 40°C for 10 seconds. Melting curve analysis was also done to ensure that the amplified DNA is the product of interest. After the real-time q-PCR is over, all the PCR products were run in 10% Poly Acrylamide Gel Electrophoresis (PAGE) followed by silver staining. The PCR product size of each gene is given in Figure 2. The amplification and melting curves for three

gene and beta-actin are shown in Figures 3(a) and 3(b), respectively. Relative quantification was performed by using the LC480 software version 1.1. The results are expressed in normalised ratio as described by Pfaffl (2001).

Normalised ratio = (conc. target/conc. reference)$_{sample}$: (conc. target/conc. reference)$_{calibrator}$.

Table 1 Primer sequences

Gene name	*Primer sequence*	*Base pairs*
Histone H2B forward	5′ TGT GAC CAA GGC GCA GAA G 3′	19
Histone H2B reverse	5′ ACA CGG AGT AGC TCT CCT TAC GA 3′	23
CTP synthetase forward	5′ GTG GTC GTA GAC ATG CCA GAA C 3′	22
CTP synthetase reverse	5′ TTG CCC AGC CTC ATG GTT 3′	18
PLK 3 forward	5′ CTA CAT GGA GCA GCA CCT CA 3′	20
PLK 3 reverse	5′ GTG GTC CCC GTA GAA GTT CA 3′	20
Beta-actin forward	5′ ATA CCC CTC GTA GAT GGG CAC 3′	21
Beta-actin reverse	5′ GAG AAA ATC TGG CAC CAC ACC 3′	21

Figure 2 Silver stained gel showing RT-qPCR product for *beta-actin*, *H2B*, *CTP synthase* and *PLK3* (see online version for colours)

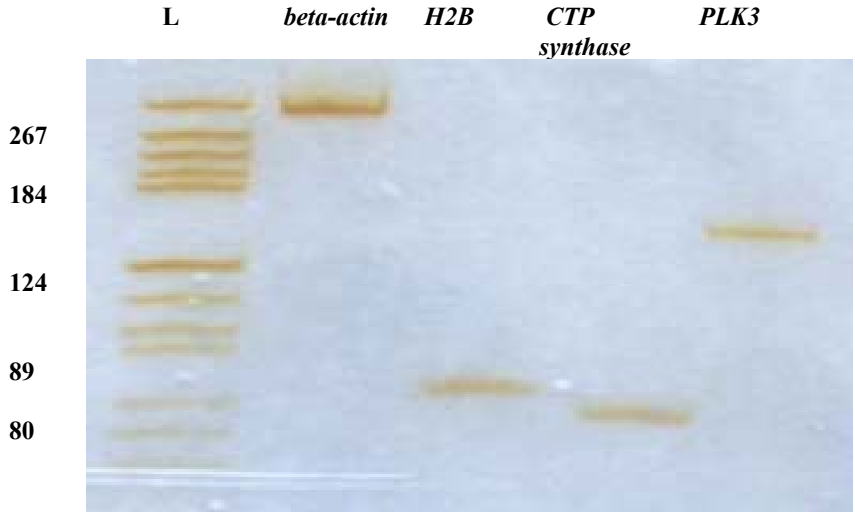

2.6 Statistical analysis

Paired *t*-test was performed between the level of expression of control and irradiated samples at using the software Sigma Stat ver 11.0 (SIGMASTAT software version 3.5). The statistical significance between the level of expression at 0 hour and 4 hours was performed.

Figure 3 (a) Amplification curves and (b) melting curves for *beta-actin*, *PLK3*, *H2B* and *CTP synthase* (see online version for colours)

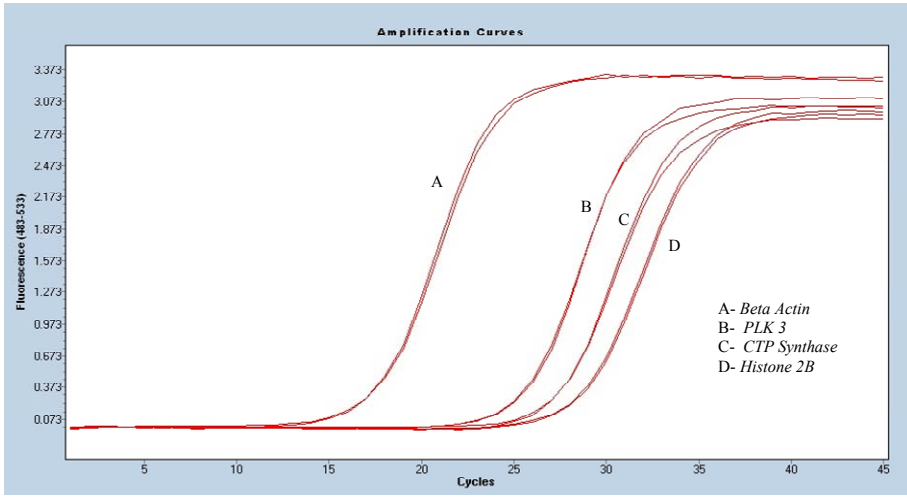

(a)

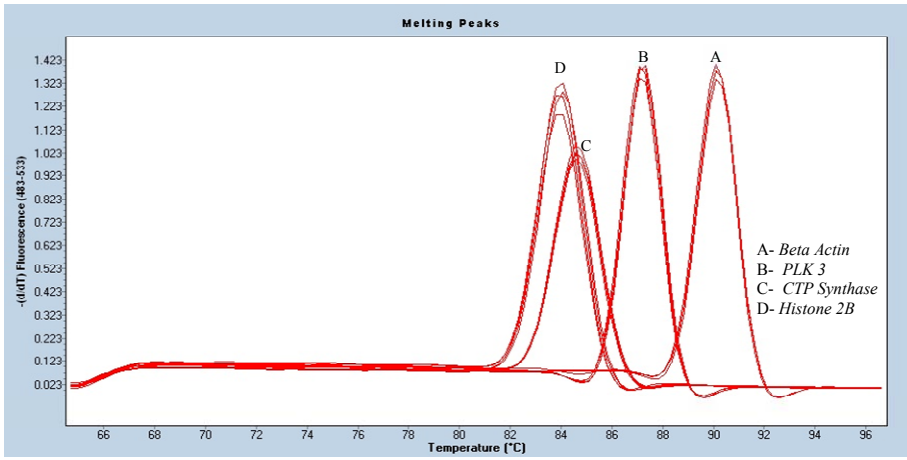

(b)

3 Results

In the present study, we have studied the gene expression pattern of three genes (*H2B*, *CTP synthase* and *PLK3*) in whole blood samples immediately and 4 hours after irradiation. At 0 hours the basal level expression was studied for all the three genes and compared to the expression pattern observed after 4 hours post-irradiation.

The baseline expression level immediately after irradiation (0 hour) did not show significant changes at all the dose groups studied (0.0, 0.3, 0.6, 1.0 and 2.0 Gy). The response in the level of expression at all these three genes at 4 hours post-irradiation was different. However, there was an overall trend of upregulation observed at all the three genes studied. As compared to 0 hours significant upregulation at 4 hours was observed at *H2B* (p = 0.006) and *CTP synthase* (p = 0.008). Similarly significant (p = 0.014)

upregulation was observed at *PLK3* in 4 hours as compared to 0 hour. At *H2B*, the maximum upregulation was observed at 0.6 Gy; whereas for *CTP synthase* and *PLK3*, maximum expression was 1.0 Gy and 2.0 Gy, respectively, at 4 hours post-irradiation (Figure 4).

Figure 4 Relative ratio at three genes at various doses of gamma irradiation: (a) *H2B*, (b) *CTP synthase*, (c) *PLK3*

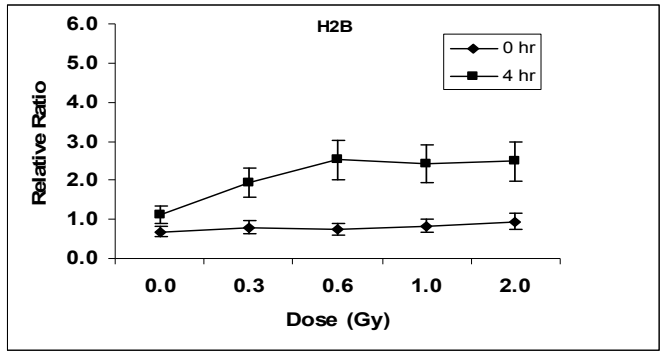

(a)

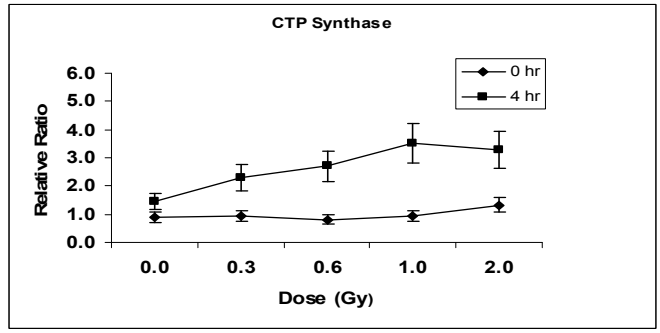

(b)

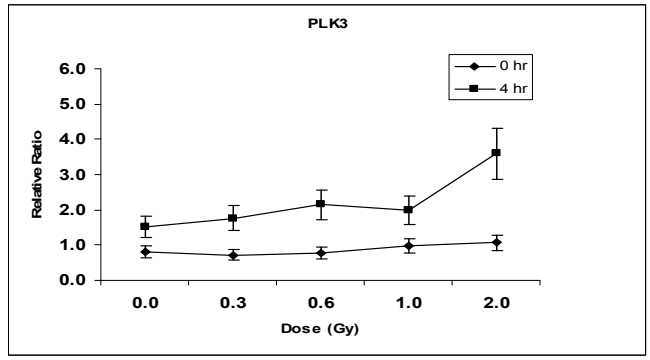

(c)

There was a great deal of variation in the pattern of expression in all the dose groups studied at 4 hours post-irradiation. At *H2B*, we observed a significantly increasing trend up to 0.6 Gy and thereafter it remained almost same for 1.0 and 2.0 Gy. For *CTP*

synthase, there was a significant increase in the level of expression up to 1.0 Gy and decreased at 2.0 Gy. In contrast, at *PLK3*, no significant change in the expression was observed up to 1.0 Gy; however, at 2.0 Gy, a significant upregulation was observed in 4 hours as compared to 0 hour. As compared to 0 hour, a maximum increase of threefold changes in the expression was observed at 0.6 Gy for *H2B*, approximately fourfold increases at 1.0 Gy for *CTP synthase* and fourfold increases at 2.0 Gy for *PLK3*.

4 Discussion

In the present study, we have studied in vivo response of low-dose ionising radiation in whole blood where the cells are in resting phase of the cell cycle (G_0) at the three selected genes. The involvement of these genes (*H2B*, *CTP synthase* and *PLK3*) represents three important functions like DNA repair, cell cycle checkpoint and apoptosis. Cellular response to ionising radiations is very complex. As a consequence, a plethora of DNA damage lesions is induced during this process. Upon induction of DNA damage, alteration of mRNA expression level takes place in various genes resulting up/downregulation. The response is not always uniform as it depends on the type of radiation, dose and dose rate given. Also, the level of expression in response to radiation varies in different cell types as well as and phase of the cell cycle.

One of the consequences of DNA damage produced by ionising radiations is the condensation of the chromatin at the sites of DSBs which is accompanied by phosphorylation of H2AX (ser-139) and *H2B* (ser-14) to form a Irradiation-Induced Foci (IRIF) that concentrates various DNA repair factors at the site (de la Barre et al., 2001; Cheung et al., 2003; Fernandez-Capetillo et al., 2004). *H2B* is known to form foci and its role in damage response has been established. Numerous studies have already shown that the synthesis of core histones is closely coupled with the replication of DNA during S phase of cell cycle (Sittman et al., 1983; Osley, 1991; Zheng et al., 2003). But there are few reports available dealing with transcription profile of histone genes (*H2B*) in PBMCs/whole blood (Waithe et al., 1983). In the present study, we have studied the mRNA expression status of *H2B* immediately after irradiation and after an incubation of 4 hours in whole blood. The significant changes at 4 hours suggest the interaction of DNA damage and the changes in the chromatin core proteins. Our results have shown that ionising radiation increases the mRNA levels of *H2B* gene in whole blood in vivo. Most of the studies reported so far were on actively dividing cultured cells and have shown a DNA synthesis dependent reduction in histone levels. No studies have been carried out so far to see the *H2B* expression levels in response to radiation exposure in whole human blood. Our data have shown that this increase is dose dependent as we observed significant increase at all the four doses studied with maximum increase observed at 0.6 Gy and thereafter remained same in 1.0 and 2.0 Gy.

CTP synthase is a key enzyme which is involved in de-novo synthesis of cytidine triphosphate, an important component of all nucleic acids. Studies have shown that upregulation of nucleotide biogenesis genes occurs in response to DNA damage in mammalian cells (Rieger and Chu, 2004; Whitehead et al., 2006). Upregulation of mRNA expression level of *CTP synthase* gene in normal human blood has been studied (Verschuur et al., 1999). However, no data are available on the transcriptional changes of *CTP synthase* gene after exposure to low doses of ionising radiation in whole blood. In

the present study, we have analysed changes in the mRNA levels of *CTP synthase* gene on exposure to different doses of ionising radiation in whole blood. Our results have shown a significant increase in the mRNA transcript of *CTP synthase* gene at doses as low as 30 cGy and the upregulation continued further up to 2.0 Gy at 4 hours post-irradiation. Reports suggest that upregulation of this gene can be indicative of increased de-novo synthesis of nucleotides, which may be necessary to accommodate increases in transcription and DNA repair in response to radiation-induced DNA damage (Whitehead et al., 2006).

PLK3 is a multifunctional protein that links DNA damage to cell cycle arrest and apoptosis (Xie et al., 2001; Zhou et al., 2006). Cell cycle regulation and programmed cell death play a critical role in DDR. As a consequence, alteration or changes in the expression pattern can be observed at various molecules involved in cell cycle progression, DNA repair and apoptosis. Previous reports have shown that *PLK3* is involved in DNA damage checkpoint response through regulation of the activation of p53 in mammalian cells. Reports have also linked to over expression of *PLK3* with chromatin condensation and DNA fragmentation (Conn et al., 2000; Bahassi et al., 2002). There are also reports showing increase in levels of *PLK3* during transition from G1 to S phase and in G2 phase in mammalian cells (Chase et al., 1998). However, no information is available on the transcription status of *PLK3* in whole blood (G_0 cells), especially in response to radiation damage. Our results have shown a significant increase in the mRNA levels of *PLK3* gene post-irradiation at 2.0 Gy at 4 hours post-irradiation.

Understanding the biological changes occurring in human cells in response to low-dose ionising radiation is a thrust area of research in radiation biology. The changes at cellular and molecular levels would contribute substantially to understand the effect of ionising radiation on living cell. A number of studies are available on DNA damage and its response to repair processes in human cells, especially at considerably higher doses of radiation. It is, therefore, essential to delineate the biological effects of radiation at low doses of radiation. The kinetics and the quality of response towards exposure to ionising radiation also vary in different genetic backgrounds among different individuals. Hence, it is interesting to study the transcription profile at different dose groups for human subjects. The data obtained from this study would provide useful information on transcriptional patterns of radiation response genes involved in various pathways. This might also provide important information in the regulation of these genes in response to gamma radiation. Finally, our data suggest that these genes could be used as potential biomarkers for radiation therapy or population biomonitoring programme. However, further research on protein expression profile is required to support these data.

Acknowledgements

We are thankful to all the donors who have volunteered to donate blood samples for this study. We thank Ms. Prabhu of BARC Modular Laboratory Dispensary for helping us in blood sample collection. We are thankful to Dr. Anu Ghosh and Mrs. Divya Saini for their help during the experiment.

References

Amundson, S.A., Do, K.T., Shahab, S., Bittner, M., Meltzer, P., Trent, J. and Fornace, A.J., Jr. (2000) 'Identification of potential mRNA biomarkers in peripheral blood lymphocytes for human exposure to ionizing radiation', *Radiation Research*, Vol. 154, No. 3, pp.342–346.

Bahassi, E.M., Conn, C.W., Myer, D.L., Hennigan, R.F., McGowan, C.H., Sanchez, Y. and Stambrook, P.J. (2002) 'Mammalian polo-like kinase 3 (PlK3) is a multifunctional protein involved in stress response pathways', *Oncogene*, Vol. 21, No. 43, pp.6633–6640.

Berglund, S.R., Rocke, D.M., Dai, J., Schwietert, C.W., Santana, A., Stern, R.L., Lehmann, J., Siantar, C.L.H. and Goldberg, Z. (2008) 'Transient genome wide transcriptional response to low dose ionizing radiation in vivo in humans', *International Journal of Radiation Oncology, Biology, Physics*, Vol. 70, No. 1, pp.229–234.

Chase, D., Feng, Y., Hanshew, B., Winkles, J.A., Longo, D.L. and Ferris, D.K. (1998) 'Expression and phosphorylation of fibroblast-growth-factor-inducible kinase (Fnk) during cell-cycle progression', *Journal of Biochemistry*, Vol. 333, pp.655–660.

Cheung, W.L., Ajiro, K., Samejima, K., Kloc, M., Heung, P., Mizzen, C.A., Beeser, A., Etkin, L.D., Chernoff, J., Earnshaw, W.C. and Allis, D. (2003) 'Apoptotic phosphorylation of histone H2B is mediated by mammalian sterile twenty kinase', *Cell*, Vol. 113, pp.507–517.

Conn, C.W., Hennigan, R.F., Dai, W., Sanchez, Y. and Stambrook, P.J. (2000) 'Incomplete cytokinesis and induction of apoptosis by over expression of the mammalian polo-like kinase, Plk3', *Cancer Research*, Vol. 60, pp.6826–6831.

Ding, L.H., Shingyoji, M., Chen, F., Hwang, J., Burma, S., Lee, C., Cheng, J. and Chen, D.J. (2005) 'Gene expression profiles of normal human fibroblasts after exposure to ionizing radiation: a comparative study of low and high doses', *Radiation Research*, Vol. 164, pp.17–26.

de la Barre, A.E., Angelov, D., Molla, A. and Dimitrov, S. (2001) 'The N-terminus of histone H2B, but not that of histone H3 or its phosphorylation, is essential for chromosome condensation', *European Molecular Biology Organization*, Vol. 20, pp.6383–6393.

Fernandez-Capetillo, O., Allis, C.D. and Nussenzweig, A. (2004) 'Phosphorylation of histone H2B at DNA double strand breaks', *Journal of Experimental Medicine*, Vol. 199, pp.1671–1677.

Gabler, C., Blank, N., Hieronymus, T., Schiller, M., Berden, J.M.H., Kalden, J.R. and Lorenz, H-M. (2004) 'Extranuclear detection of histones and nucleosomes in activated human lymphoblasts as an early event in apoptosis', *Annals of the Rheumatic Diseases*, Vol. 63, pp.1135–1144.

Gentile, M., Latonen, L. and Laiho, M. (2003) 'Cell cycle arrest and apoptosis provoked by UV radiation induced DNA damage are transcriptionally highly divergent responses', *Nucleic Acids Research*, Vol. 31, No. 16, pp.4779–4790.

Glaser, K.B., Staver, M.J., Waring, J.F., Stender, J., Ulrich, R.G. and Davidsen, S.K. (2003) 'Gene expression profiling of multiple histone deacetylase (HDAC) inhibitors: defining a common gene set produced by HDAC inhibition in T24 and MDA carcinoma cell lines', *Molecular Cancer Therapeutics*, Vol. 151, No. 2, pp.151–163.

Gruel, G., Voisin, P., Vaurijoux, A., Roch-Lefevre, S., Grégoire, E., Maltere, P., Petat, C., Gidrol, X., Voisin, P. and Roy, L. (2008) 'Broad modulation of gene expression in CD4 + lymphocyte subpopulations in response to low doses of ionizing radiation', *Radiation Research*, Vol. 170, pp.335–344.

Jessica, A.D., Michel, C.N. and Andre, N. (2007) 'Chromatin dynamics and the preservation of genetic information', *Nature*, Vol. 447, pp.951–958.

Kang, C., Park, K.P., Song, J.E., Jeoung, D., Cho, C., Kim, T., Bae, S., Lee, S. and Lee, Y. (2003) 'Possible biomarkers for ionizing radiation exposure in human peripheral blood lymphocytes', *Radiation Research*, Vol. 159, pp.312–319.

Jan, K-Y. and Cheung, V.G. (2005) 'Identification of novel p53 target genes in ionizing radiation response', *Cancer Research*, Vol. 65, pp.7666–7673.

Morandi, E., Severini, C., Quercioli, D., Perdichizzi, S., Mascolo, M.G., Horn, W., Vaccari, M., Nucci, M.C., Lodi, V., Violante, F.S., Bolognesi, C., Grilli, S., Silingardi, P. and Colacci, A. (2009) 'Gene expression changes in medical workers exposed to radiation', *Radiation Research*, Vol. 172, No. 4, pp.500–508.

Osley, M.A. (1991) 'The regulation of histone synthesis in the cell cycle', *Annual Review of Biochemistry*, Vol. 60, pp.827–861.

Pfaffl, M.F. (2001) 'A new mathematical model for relative quantification in real time RT-PCR', *Nucleic Acids Research*, Vol. 29, pp.2002–2007.

Rieger, K.E. and Chu, G. (2004) 'Portrait of transcriptional responses to ultraviolet and ionizing radiation in human cells', *Nucleic Acids Research*, Vol. 32, No. 16, pp.4786–4803.

SIGMASTAT software version 3.5 (2006) Available online at: http://www.systat.com

Sittman, D.B., Graves, R.A. and Marzluff, W.F. (1983) 'Histone mRNA concentrations are regulated at the level of transcription and mRNA degradation', *Proceedings of the National Academy of Sciences*, Vol. 80, pp.1849–1853.

Shimada, M., Niida, H., Zineldeen, D.H., Tagami, H., Tanaka, M., Saito, H. and Nakanishi, M. (2008) 'Chk1 is a histone H3 threonine 11 Kinase that regulates DNA damage induced transcriptional repression', *Cell*, Vol. 132, pp.221–232.

Turtoi, A., Brown, I., Oskamp, D. and Schneeweiss, F.H.A. (2008) 'Early gene expression in human lymphocytes after γ-irradiation – a genetic pattern with potential for biodosimetry', *International Journal of Radiation Biology*, Vol. 84, pp.375–387.

van Attikum, H. and Gasser, S.M. (2005) 'The histone code at DNA breaks: a guide to repair', *Nature Reviews*, Vol. 6, pp.757–765.

Verschuur, A.C., Van Gennip, A.H., Muller, E.J., Voute, P.A., Vreken, P. and Van Kuilenburg, A.B. (1999) 'Cytidine triphosphate synthase activity and mRNA expression in normal human blood cells', *Biological Chemistry*, Vol. 380, No. 1, pp.41–46.

Waithe, W.I., Renaud, J., Nadeau, P. and Pallotta, D. (1983) 'Histone synthesis by lymphocytes in G0 and G1', *Biochemistry*, Vol. 22, No. 8, pp.1778–1783.

Winkles, J.A. and Alberts, G.F. (2005) 'Differential regulation of polo-like kinase 1, 2 ,3 and 4 gene expression in mammalian cells and tissues', *Oncogene*, Vol. 24, pp.260–266.

Xie, S., Wu, H., Wang, Q., Cogswell, J.P., Husain, I., Conn, C., Stambrook, P., Jhanwar-Uniyal, M. and Dai, W. (2001) 'Plk3 functionally links DNA damage to cell cycle arrest and apoptosis at least in part via the p53 pathway', *The Journal of Biological Chemistry*, Vol. 276, No. 46, pp.43305–43312.

Yin, E., Nelson, D.O., Coleman, M.A., Peterson, L.E. and Wyrobek, A.J. (2003) 'Gene expression changes in mouse brain after exposure to low dose ionizing radiation', *International Journal of Radiation Biology*, Vol. 79, pp.759–775.

Zheng, L., Roeder, R.G. and Luo, S.Y. (2003) 'Phase activation of the histone H2B promoter by OCA-S, a coactivator complex that contains GAPDH as a key component', *Cell*, Vol. 114, No. 2, pp.255–266.

Zhou, T., Chou, J.W., Simpson, D.A., Zhou, Y., Mullen, T.E., Medeiros, M., Bushel, P.R., Paules, R.S., Yang, X., Hurban, P., Lobenhofer, E.K. and Kaufmann, W.K. (2006) 'Profiles of global gene expression in ionizing radiation damaged human diploid fibroblasts reveal synchronization behind the G_1checkpoint in a G_0-like state of quiescence', *Environmental Health Perspectives*, Vol. 114, No. 4, pp.553–559.